AN INVESTIGATION OF THE PHOTOCHEMISTRY OF ORGANOMETALLIC METAL CARBONYL COMPOUNDS BY TRANSIENT SPECTROSCOPIC TECHNIQUES

A thesis presented for the degree of Doctor of Philosophy

by

Irene Mc Grath B. Sc.

under the supervision of Dr. Conor Long

at

DUBLIN CITY UNIVERSITY

School of Chemical Sciences

AUGUST 1993

Declaration

I hereby certify that this material, which I now submit for assessment on the programme of study leading to the award of Ph. D. is entirely my own work and has not been taken from the work of others save and to the extent that such work has been cited and acknowledged within the text of my work.

Signed: Irene Mc Grath Date: 30/9/1993.

Irene Mc Grath

Dedication

To Joe, Evelyn and Siobhan.

Acknowledgements

Above all I would sincerely like to thank my supervisor, Dr. Conor Long, for his encouragement and guidance throughout this research. The success of my experimental work at Nottingham University is attributed to the assistance of Dr. Michael George, Dr. James Turner and Dr Martyn Poliakoff, for which I am truly grateful. Financially, the understanding of Co. Kildare V.E.C. during my empoverished days was greatly appreciated.

Finally, the support of my friends and family during the preparation of this manuscript is gratefully acknowledged; especially Siobhan, Paul, Teri, Maureen and Dave.

Table of Contents

Aims and Objectives

The goals of this study were as follows

(i) to synthesise a range of (η^6-arene)$Cr(CO)_3$ complexes

(ii) to characterise the primary and secondary photoproducts of these systems in alkane solution at ambient temperature and obtain kinetic data for their reactions with CO and other potential ligands

(iii) to measure the effect of the substituent on the reactivity of the photoproducts

(iv) to relate the experimental findings to the photochemistry of "half-sandwich" compounds and the isoelectronic (η^5-C_5R_5)$Mn(CO)_3$ system (R = H, Me, or Et)

(v) to study the photochemistry of $Mn(CO)_4$-η^3-C_3H_4-C_6H_5 in alkane solution at ambient temperature, characterise the photoproducts and obtain kinetic data for the reaction of these species with CO and other potential ligands

(vi) to study the photochemistry of the heterobimetallic dinuclear complex $Mn(CO)_4$-η^3-C_3H_4-η^6-C_6H_5-$Cr(CO)_3$ and relate it to the photochemistry of the uncomplexed $Mn(CO)_4$-η^3-C_3H_4-C_6H_5 and (η^6-benzene)$Cr(CO)_3$ compounds

(vii) to study the effect of complexation upon the UV/vis absorption spectra of the individual component complexes comprising this dinuclear species

(viii) to study the photochemistry of (η^5-C_5H_5)$V(CO)_4$ in cyclohexane solution at room temperature utilising different laser excitation wavelengths in order to investigate the reported wavelength dependancy

(ix) to investigate the reported experimental irreproducibility on photochemistry of (η^5-C_5H_5)$V(CO)_4$ in alkane solution

Abstract

(η^6-benzene)$Cr(CO)_2$(S) was unequivocally identified as an intermediate in the flash photolysis of (η^6-benzene)$Cr(CO)_3$ in alkane solution by a combination of UV/vis and TRIR studies A range of substituted (η^6-arene)$Cr(CO)_3$ complexes was synthesised, where arene = toluene, p-xylene, 1,3,5-mesitylene or C_6Me_6, and the effect of increased methylation of the arene ring upon the reactivity of the (η^6-arene)$Cr(CO)_2$(S) intermediate was investigated The rate of reaction of this species with CO increased upon methyl substitution of the arene and upon changing the solvent from cyclohexane to alkane The enthalpies of activation for this reaction were constant at 25 ± 2 kJ mol^{-1} while the entropy of activation increased with increased methyl substitution The rate of reaction of this species with parent to produce the dinuclear complex (η^6-arene)$Cr(CO)_2(\mu CO)Cr(CO)_2(\eta^6$-arene) was noted in the benzene case Complexes attributed to the binding of solvent impurities were ascribed to some of the primary and secondary photochemistry observed.

The heterobimetallic dinuclear complex $Mn(CO)_4$-η^3-C_3H_4-η^6-C_6H_5-$Cr(CO)_3$ and its substituent $Mn(CO)_4$-η^3-C_3H_4-C_6H_5 were investigated by laser flash photolysis. The formation of an acyclic pentadienyl complex is proposed in both cases, by means of a facile η^3 to η^5 hapticity change of the allyl group In the dinuclear complex this reaction occurs independently of both parent and CO concentration

The laser flash photolysis of (η^5-C_5H_5)$V(CO)_4$ was studied at excitation wavelengths of 266nm and 355nm The experimental results were extremely irreproducible The observation of both (η^5-C_5H_5)$V(CO)_3$(S) and (η^3-C_5H_5)$V(CO)_5$ was suggested The observation of a long-lived product in solution

was attributed to the formation of $(\eta^5\text{-}C_5H_5)_2V_2(CO)_5$ The results did not permit the proposal of a reaction scheme

Chapter 1

Introduction

1.1 Introduction

The past 20 years have seen the emergence of a variety of novel, useful and important homogeneous catalyst systems, and this rapid enrichment seems to be only the beginning of further growth of this field[1] The development of coordination chemistry has greatly aided the understanding of these metal based catalysts and has intensified the search for catalytically active metal systems employing novel and unique ligands The use of heterogeneous catalysts in industry far outweighs the use of homogeneous catalysts because they are more easily removed from the reaction medium. However, homogeneous catalysts have emerged as the method of choice in many cases, operating under milder conditions and providing a greater degree of selectivity for many synthetic applications Certain chemicals are almost exclusively produced using homogeneous catalysts One such process is the Wacker process for the production of ethanal by the palladium catalysed oxidation of ethene. Homogeneous catalysts are used to effect highly specific organic transformations; industrially, this selectivity is exploited in the production of polymers and pharmaceuticals One such example is in the synthesis of L-DOPA, used in the treatment of Parkinson's disease, where the asymmetric hydrogenation of acetamidocinnamic acid is effectively accomplished using a soluble rhodium(1) complex bearing optically active tertiary phosphine ligands[2] Clearly, homogeneous and heterogeneous systems are closely related in that they both involve reactions occurring at metal centres, and frequently insight obtained from studying homogeneous catalysis has aided in explaining results obtained with heterogeneous systems

The photochemistry of metal carbonyl complexes has become of increasing importance in recent times The potential uses of these compounds in synthetic and catalytic applications has been known for many years Although most industrial catalytic processes occur thermally, it has been shown that the intermediates in a particular organometallic reaction are often identical whether generated photochemically or thermally[3] The use of photochemical methods to study these catalytic processes can therefore provide valuable information about the nature of these reactions Certain carbonyl complexes are used industrially as homogeneous catalysts, an example being the 'oxo' process for the hydroformylation of ethene, in the presence of synthesis gas (a CO/H_2 mixture), by the complex $Co_2(CO)_8$[4]. Moreover, photosubstitution reactions have provided a valuable synthetic route to substituted derivatives of thermally inert complexes This is particularly true for metal carbonyl compounds[5] The photosubstituted products can be generated at low enough temperatures to be isolable, whereas attempts to generate them at elevated temperatures could result in further decomposition of the products. One example is the photosubstitution of $Fe(CO)_5$ by pyridine to yield $Fe(CO)_4$(pyridine) at 298K[6] whereas thermal reaction at higher temperatures yields disproportionation of the $Fe(CO)_5$ complex[7] The stereochemistry of photosubstitution is also potentially different from the thermal reactivity and does not merely represent an acceleration of thermal reactions Hence, reactions can be promoted photochemically which are not accessible by thermal means, a typical example is the loss of SO_3^{2-} from *trans*-$Co(CN)_4(SO_3)(OH_2)^{3-}$ which is a reaction which does not occur thermally[8] In a similar way C_2H_4 in $PtCl_3(C_2H_4)^-$ is substantially inert thermally, but can be

substituted photochemically[9]. Such great diversity in the behaviour of transition metal coordination compounds suggests a continuing and expanding interest in these systems from both applied and fundamental viewpoints.

Although exact mechanisms of many reactions involving metal carbonyl complexes are still unknown, the initial steps would seem to be the generation of a vacant site at the metal centre, which can then initiate further reactions. A site of coordinative unsaturation is perhaps the single most important property of a homogeneous catalyst [10]. While thermal displacement of the carbonyl ligand is often difficult, photochemical decarbonylation can proceed with quantum yields approaching 1[11]. In general the primary photoinduced reaction of metal carbonyls involves the monodecarbonylation process, as shown in reaction 1.1.1.

$$M(CO)_x \xrightarrow{h\nu} M(CO)_{x-1} + CO \qquad (1.1.1)$$

Important features of this reaction are its high quantum efficiency and the reactive nature of the decarbonylated product. Both these features are readily explained by examining the molecular orbital diagram of the bonding between the CO ligand and the metal. Figure 1.1.1 exhibits the molecular orbital diagram for the group 6 hexacarbonyls[12]. The highest occupied molecular orbitals are the metal based orbitals of t_{2g} symmetry, which are involved in π-bonding between the metal and the carbonyl ligand; while the lowest unoccupied orbitals are the orbitals of e_g symmetry, which are strongly antibonding with respect to the σ-interaction of the carbonyls. On photochemical excitation the relative population of these orbitals is altered as an electron is promoted from the t_{2g} orbital sub-set to the σ^*-orbital. This transition

involves the removal of electron density from orbitals contributing to the back-bonding interaction and the population of an orbital that is strongly antibonding with respect to the carbonyl σ-interaction. The result is a greatly weakened metal-ligand bond in the excited state which ultimately leads to the labilisation of the carbonyl ligand.

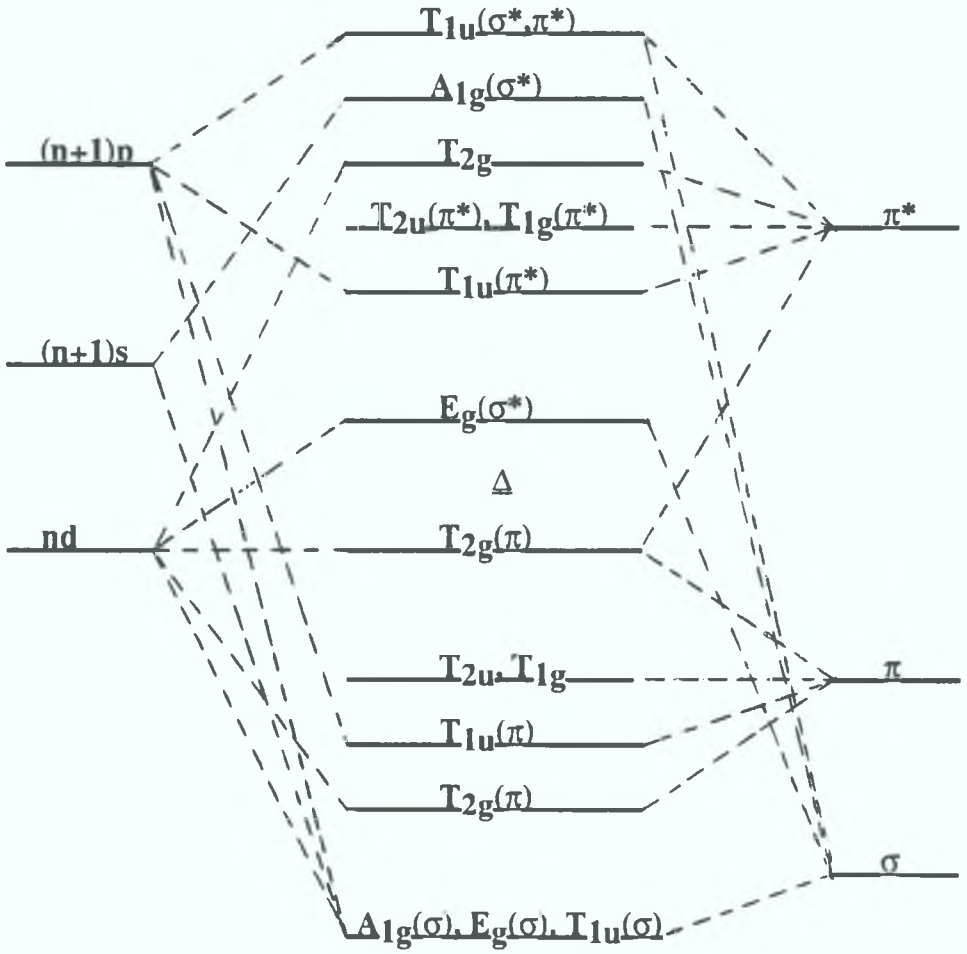

Figure 1.1.1 The molecular orbital diagram for the group 6 hexacarbonyls[12].

The photochemical generation of vacant coordination sites on metal carbonyl complexes and the investigation of the subsequent reactions at these sites is the basis of this work.

A knowledge of the reactivity of coordinatively unsaturated complexes is of primary importance in understanding the mechanisms of many catalytic systems. Initial studies into these reactions were based on the analysis of isolated products. These were unsuccessful as it became clear that the complexes isolated were the end-products of a series of chemical reactions. In many cases the photochemical products are suggestive of at least some of the features of the photochemical mechanism. However, because of the long time span between the initiation of a photochemical event and the appearance of a photoproduct, there is no guarantee that the nature of the final products provides a valid picture of the total sequence of events which constitute the photochemical mechanism. The coordinatively unsaturated intermediates formed during reactions involving organometallic compounds often have lifetimes in the picosecond to millisecond range. Most of the conventional techniques for the elucidation of molecular structure are inapplicable to the characterisation of these intermediates. These problems associated with time scale can be addressed by using transient spectroscopic techniques; which include laser flash photolysis with UV/vis monitoring, and, more recently, time-resolved infrared (TRIR) spectroscopy. Alternatively, cryoscopic techniques may be employed; these include low temperature matrix isolation studies and studies in liquified noble gases. A brief outline of each technique is now presented, particular attention being paid to their uses in the photochemical study of metal carbonyl species.

1.1.1 Matrix Isolation

Matrix isolation is a technique which utilises noble gases, solid at liquid helium temperatures, as media for stabilising reactive chemical species for the purpose of spectroscopic study. The modern practice of matrix isolation, involving the use of monatomic rare gases (e.g. Ar, Kr, Xe) as matrix materials in the temperature range 4-20K, was pioneered by Pimentel *et al.*[13] in the early 1950's. These materials offer the advantages of transparency over a range from the far infrared to the vacuum ultraviolet, of chemical inertness, and of rigidity at suitably low temperatures. Typically, the experimental technique involves condensation of gaseous atomic or molecular species together with a large excess of an inert gas matrix on a suitable substrate at cryogenic temperatures. The photoproducts generated within the matrix, by UV irradiation of stable precursor molecules, may then be studied by a variety of spectroscopic methods; including IR, UV/vis, vacuum UV (VUV), Raman, Mössbauer, UV/vis emission, laser-induced fluorescence, ESR spectroscopy and magnetic circular dichroism. One of the great strengths of matrix isolation is the wide range of spectroscopic techniques that can be applied to to the characterisation of photofragments.

An attractive feature of this method is that normally unstable or highly reactive species may be isolated for long periods of time, allowing leisurely spectroscopic examination. Thermal excitation of low-lying excited electronic states is usually quenched at cryogenic temperatures, thereby simplifying the absorption spectra by effectively trapping the reactive intermediates, even if they have a low barrier to further reaction. If energy is then supplied to the trapped intermediate,

either by warming the matrix (annealing) or by irradiation, the energy barrier can be surmounted and the reaction can go to completion. The randomly orientated, rigidly held fragments also permit the exploitation of photoselection techniques and polarisation spectroscopy, which are valuable for identification purposes. Isotopic enrichment is now being widely applied to metal carbonyl fragments in matrices; partial ^{13}CO enrichment combined with IR spectroscopy has been extremely successful in determining the structures of fragments.

Perutz and Turner[14] have shown that visible absorption spectra generated on photolysis of group 6 metal hexacarbonyls in rigid matrices are sensitive to the nature of the matrix medium. Mixed matrix experiments and comparison with spectra of stable species revealed that the shifts in spectra are due to spectroscopic interactions between the $M(CO)_5$ photofragment and the matrix species occupying the sixth coordination site. The shifts in visible bands were interpreted in terms of a weak metal-matrix bond and the small change in the axial-radial bond angle determined by the matrix species in the sixth coordination site. This study also provided evidence for the existence of $Cr(CO)_5(Ar)$, where an inert noble gas is coordinated by the unsaturated photofragment - demonstrating the extreme reactivity of these coordinatively unsaturated intermediates. Subsequent studies have provided evidence for the formation of $Cr(CO)_5(N_2)$[15] and $Mn(CO)_5(Kr)$[16], however in the majority of cases no interaction is observed between the reactive intermediates and the matrix.

The major limitation of the matrix isolation technique lies in the requirement that the species itself or a suitable photolytic precursor be produced initially in the

gaseous state[17]. It cannot easily be used for charged species and kinetic studies are difficult because of the restricted temperature range and limited diffusion of the reactive species The sort of reactions that may occur in these low temperature matrices are substantially limited by the restrictions of the so-called 'cage effect'; it is generally difficult to produce main group species by an *in situ* photolysis in inert matrices at 20K by photoejection of a second row or larger atom because the atom is too large to diffuse through the lattice interstices and away from the newly formed unstable species Thus the two fragments held together inside the matrix cage recombine to reform the parent molecule In matrix experiments finer details of spectroscopic structure can be lost due to inhomogeneous broadening and perturbations induced by the matrix host. Splitting of spectral lines can arise from a myriad of solid state and electronic effects, the most commonly encountered being multiple trapping sites, low site symmetries, metal isotopes in natural abundance and extraneous impurity centres In CH_4 matrices, absorptions of the uncoordinated CH_4 dominate the infrared spectrum and obscure bands due to the bonding of the M-CH_4 matrix species, as in the case of $Fe(CO)_4(CH_4)$[18]

1.1.2 Supercritical Fluid Techniques

One of the obstacles to comparison of matrix and solution studies has been the complete lack of inert and transparent cryogenic solvents[19]. By using quite modest pressures (<15 atm.) and a range of mixtures of N_2, Ar, Kr, and Xe, a full liquid range from 77 to 230K can be obtained The range can be extended to 289K if a pressure of 58 atm can be tolerated A particular advantage of these liquified gases as solvents is their total lack of IR bands, which, when combined with Fourier transform

infrared (FTIR) allows weak absorptions due to coordinated ligands to be detected. Using a high-pressure IR cell Turner *et al* have obtained solution spectra of the metal carbonyl dinitrogen species previously observed in matrices[20-22] These workers have also observed $Cr(CO)_5(H_2)$ in liquid xenon, the H-H stretching vibration of coordinated dihydrogen is too weak to be observed in matrices[23] Since these solvents have no absorptions long path lengths and low concentrations can be employed This steady-state method should be appropriate to many of the more stable species observed in matrices, which are nevertheless too reactive to be observed by more conventional means Liquified noble gases also offer a great advantage over matrix isolation techniques in that they allow kinetic studies and the determination of the activation parameters for the reaction of metal carbonyl fragments

1.1.3 Laser Flash Photolysis

Flash photolysis was pioneered by Norrish and Porter[24] for which they recieved the Nobel prize Advances in instrumentation over the years mean that transient intermediates can now be detected on a femtosecond timescale, corresponding to the fastest chemical processes possible Laser flash photolysis has been used extensively to provide information about primary photochemical processes occuring in metal carbonyl chemistry [25-29]

The principle of flash photolysis involves the generation of a high concentration of a short-lived intermediate by excitation of the sample with a high intensity pulse of very short duration The sample is analysed at a short time interval after the pulse by examining the intermediate's absorption or emission characteristics In practice there are two variants of the flash photolysis technique, the spectrographic

and the kinetic methods, with the latter being the most commonly used. In the spectrographic method the complete absorption spectrum of the transient is recorded with a spectrograph or a photographic plate at a fixed time after the flash The decay of the excited molecule can then be observed by recording spectra at different time intervals after excitation The kinetic method measures primarily the decay of the excited state absorption as a function of time at a particular wavelength using a photomultiplier coupled to an oscilloscope with a time-based sweep The signal obtained may be analysed to obtain the lifetime of photofragments If the measurement is repeated at different monitoring wavelengths a UV/vis spectrum of the transient can be constructed 'point by point' by plotting the absorbance at any fixed time after excitation at different wavelengths In general a 'difference spectrum' is obtained, in which only changes in absorption are displayed, thus, bands due to parent compounds destroyed by the flash appear as negative absorptions while bands due to photoproducts appear as positive absorptions. Intermediates can be identified by a combination of their reaction kinetics and by comparison with UV/vis data from matrix isolation experiments

The polychromatic nature of the radiation from conventional discharge tubes creates the possibility of generating more than one exciting or absorbing species in solution This problem is minimised by using the monochromatic radiation of lasers. However, the most important advantage in using lasers lies in the reproducibility with which a pulse of very short duration can be produced by means of Q-switching; greatly enhancing the resolution of the experiment in the time-domain. The excitation wavelength is not limited to the fundamental output wavelength of the laser, as

frequency doubling, tripling and quadrupling can be used to increase the range of wavelengths available.

Generally, the fragments produced from 18-electron metal carbonyl species are quite easy to detect by flash photolysis techniques as their UV/vis spectra often vary greatly from that of the parent compound Transition metal carbonyls have reasonably intense UV/vis absorptions and quantum yields for their formation are high Reaction rates are fast, and therefore good time resolution is required Most solvents have no absorptions in the visible region, and reactions (e.g bimolecular radical recombination) can often be slowed down by dilution and a corresponding path length increase without adversely affecting the signal-to-noise ratio of the spectrum or the intensity of the transient absorption Although UV/vis spectroscopy is now routinely used for detecting intermediates generated by flash photolysis and has been found effective in establishing the broad outlines of the photochemistry of many metal carbonyl compounds, it also has severe limitations These limitations arise from the general broadness and lack of resolvable fine structure in the electronic absorptions Thus, flash photolysis has produced evidence for the existence of intermediates but rarely provides much structural information about transient metal fragments. This has proved to be a severe restriction on the technique and most studies have been limited to relatively simple systems where the number of possible intermediates was small.

1.1.4 Time Resolved Infrared (TRIR) Spectroscopy

Pimentel was the first to develop a viable technique for the measurement of infrared spectra of transient species[30] In the last ten years or so there have been

major advances in fast IR spectroscopy It is now possible to detect metal carbonyl intermediates at room temperature in both solution and gas phase reactions. Vibrational spectra have more accessible structural information than similar spectra in the UV or visible regions because of the finite spectral shifts associated with even minor structural changes in molecules The infrared spectrum of a metal carbonyl provides important information on the nature of the carbonyl groups present as the number and intensity of infrared bands is dependant on the molecular symmetry For example, a single carbonyl absorption is observed in the infrared spectrum of a $M(CO)_6$ complex, attributed to the T_{1u} band of O_h symmetry, whereas three ν_{CO} are expected for a $M(CO)_5$ complex of C_{4v} symmetry, attributed to the A_1, E, and A_1 bands In the case of some metal carbonyl species TRIR can even provide accurate estimates of bond angles involving ν_{CO} In principle, UV flash photolysis, usually by laser, is combined with IR monitoring at a single IR wavelength By repeating the measurement at a series of different IR wavelengths data are accumulated across the spectral region of interest These data can then be used to construct 'point-by point' spectra corresponding to any particular time delay after the flash, i e a time-resolved IR (TRIR) spectrum. As with flash photolysis UV/vis spectra, this TRIR spectrum is a difference spectrum

Already a considerable number of transient organometallic species have been characterised by IR kinetic spectroscopy [27,31-34] It is now possible to obtain IR spectra and reaction kinetics of metal carbonyl intermediates in solution on a 1μs timescale TRIR spectroscopy is a valuable addition to the techniques available for studying the kinetics and mechanisms of reactions in solution As solvent absorption

is a serious problem for IR measurements, even for the ν_{CO} region of the spectrum, typically IR solution cells are limited to <5mm pathlength for most applications. These shorter pathlengths make it more difficult to build time-resolved IR apparatus which are optically as efficient as the equivalent UV/vis equipment This restricts the technique to the detection of metal carbonyl fragments by virtue of the intensity of their infrared carbonyl absorptions In addition, faster transient absorptions can be detected in UV/vis measurements due to the faster risetimes of the detectors used.

1.2 Studies on (η^6-arene)Cr(CO)$_3$ Systems

Complexes of (η^6-arene)chromium tricarbonyl have been known as selective hydrogenation catalysts in solution since 1968[35] Experimental studies have revealed a dramatic difference in the stereochemistry of photosubstitution and thermal reactivity of these complexes, providing an apparent example of a system with a large difference in excited state and ground state reactivity. In general, photosubstitution leads to dissociative loss of a carbonyl moiety, while thermally the arene group is labilised. Recent papers on the mechanism of arene exchange processes have renewed interest in the study of this class of complexes, particularly on account of the importance that formation and displacement of transition-metal π-bonds display in catalysis. For clarity, the experimental findings are subdivided into thermal and photochemical studies respectively

1.2.1 Thermal Studies on (η^6-arene)Cr(CO)$_3$ Complexes

Strohmeier *et al* carried out a series of high temperature (413-453K) exchange reactions between ^{14}C-labelled benzene and η^6-benzenetricarbonyl metal

complexes of Cr, Mo and W[36] Kinetic data was presented for arene exchange between the free arene and the arene metal complex in a non-coordinating solvent. The derived rate expression for these reactions was of the form;

Rate $=k_2[ArCr(CO)_3]^2 + k_2'[ArCr(CO)_3][Ar^*]$ (1 2 1.1)

where the rate of exchange is second order in $ArM(CO)_3$ and about one-third order in ^{14}C-labelled arene The mechanistic conclusion drawn from these kinetic studies was that two different mechanisms were operative, Schemes 1.2.1.1 and 1 2 1 2. Both proposed mechanisms have been criticised on general mechanistic and energetic grounds by subsequent workers in this area[37]

SCHEME 1.2.1.1

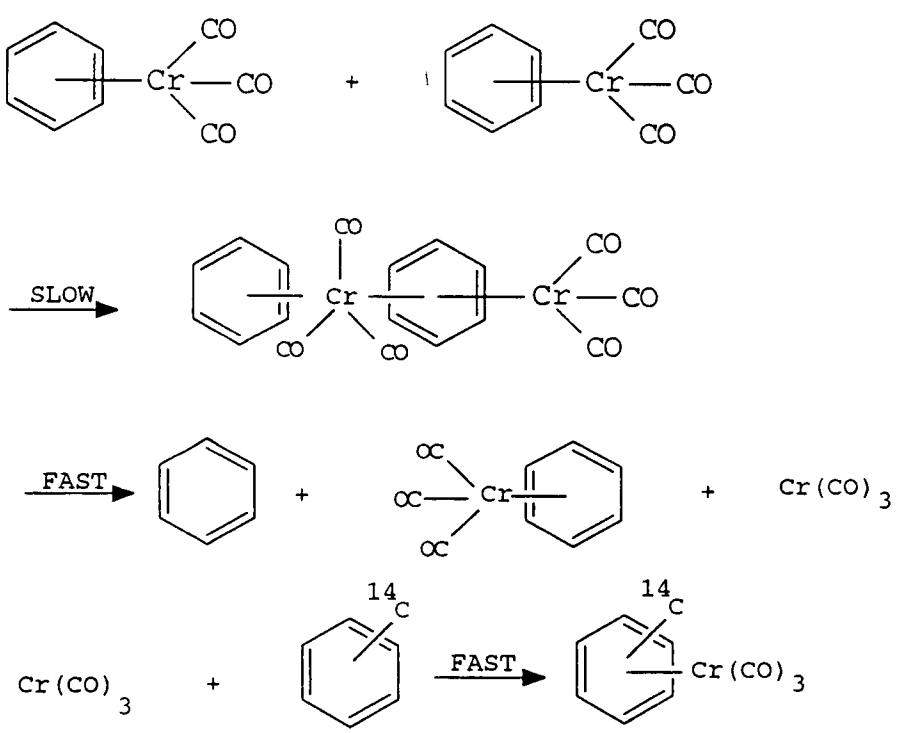

SCHEME 1 2.1 2

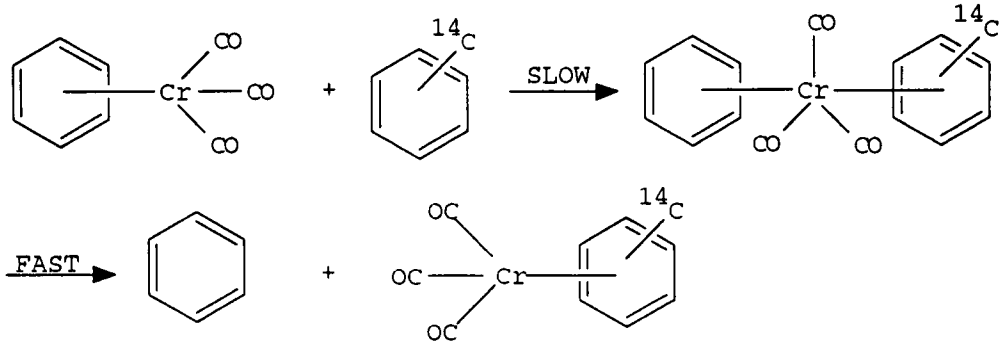

Catalysis of arene exchange by donor solvents was demonstrated in the η^6-benzenetricarbonyl chromium system by Mahaffy and Pauson[38] The stabilities of η^6-arene tricarbonyl chromium complexes were found to decrease in the order Me_6C_6 > mesitylene> xylene > toluene/benzene > chlorobenzene >> naphthalene. These results agree with microcalorimetric studies which indicated the total arene-metal bond strengths to be 174 ± 13 and 178 ± 13 kJ mol^{-1} for toluene and benzene respectively[39] They suggested the alternative mechanism of reaction 1 2.1.2 where either intermediate could lead to exchange The uncatalysed reaction for which Strohmeier proposed Schemes 1 2 1 1 and 1 2 1 2 was not studied

$$2ArCr(CO)_3 \text{ ----------> } ArCr(CO)_2 + (\eta^4\text{-}Ar)Cr(CO)_4 \qquad (1.2.1\ 2)$$

Zimmerman *et al* [40] determined the rates of exchange of arene ligands with hexamethylbenzene in cyclohexanone solution at several temperatures in the range 353-413K according to the following reaction,

$$ArCr(CO)_3 + C_6Me_6 \text{ ----------> } C_6Me_6Cr(CO)_3 + Ar \qquad (1\ 2\ 1\ 3)$$

In all cases the reactions were first order in the complex and independent of the concentration of hexamethylbenzene The data were consistent with a simple reversible dissociation process giving the free arene and a tricarbonylchromium fragment, presumably solvent stabilised, which can then react with hexamethylbenzene to give the final product.

$$ArHCr(CO)_3 \overset{S}{\rightleftharpoons} ArH + Cr(CO)_3S_x \qquad (1.2.1.4)$$

$$Cr(CO)_3S_x + C_6Me_6 \text{ ----------> } C_6Me_6Cr(CO)_3 + S \qquad (1.2.1\ 5)$$

(where S = solvent)

Recent investigations into the mechanism of thermally induced arene exchange were performed by Traylor *et al* [41] in order to confirm and expand upon earlier work by Strohmeier *et al* [36] The reactions of $Ar'Cr(CO)_3$ (Ar'=benzene or substituted benzene) with various substituted arene ligands were performed at high temperatures (443K) in vacuum sealed NMR tubes, the disappearence of complex as well as the appearance of product were followed by ^1H NMR The series of experiments indicated that the single elementary step of the proposed mechanism for arene exchange, with any of the ligands investigated, was a reduction in coordination of the arene ligand (η^6 to η^4) resulting in a simple stepwise displacement of the arene (Scheme 1.2 1 3, L is a catalytic ligand which can be any two-electron Lewis base including ketones, nitriles, carbonyl groups or even another arene)

SCHEME 1 2.1.3

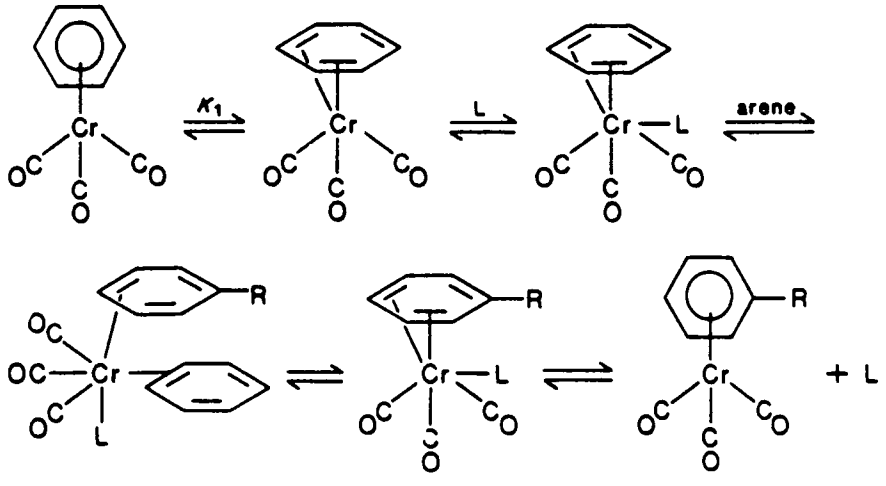

The arene-exchange reaction in naphthalene and pyrene-$Cr(CO)_3$ was studied by Howell *et al* [42] in hydrocarbon solvents A two-term rate law was established of the form

$$-d[S]/dt = k_a[S] + k_b[S][arene'] \qquad (1.2\ 1.6)$$

where S is the (arene)$Cr(CO)_3$ substrate and toluene was used as the external (arene') ligand. Activation parameters were determined for both reactions It was suggested that the arene-independent path in the above rate law proceeds *via* an (η^y-arene)$Cr(CO)_3$ intermediate and the arene-dependant path through an (η^x-arene)$Cr(CO)_3$ intermediate with $y<x$ Molecular orbital calculations at the extended Huckel level were used to construct full potential energy surfaces for ring-slippage in benzene, naphthalene, and (pyrene)$Cr(CO)_3$. An η^6 to η^4 path was found to be most

favorable for the naphthalene system, whereas an η^6 to η^1 path required the least energy for pyrene. In (benzene)$Cr(CO)_3$ both paths were found to be comparable in energy The calculations correctly predict arene lability to be in the order benzene<<naphthalene<<pyrene No evidence for a discrete η^4 intermediate was found for the arene-independent route

1.2.2 Photochemistry of (η^6-arene)$Cr(CO)_3$ Systems

The earliest observations of the photoreactions of (η^6-arene)$Cr(CO)_3$ complexes were made by Strohmeier and Von Hobe[43] who proposed the following reactions,

$$ArCr(CO)_3 + {}^{14}CO \xrightarrow{h\nu} ArCr(CO)_2({}^{14}CO) + (CO)_{solv.} \qquad (1.2.2.1)$$

$$ArCr(CO)_3 + Ar^* \xrightarrow{h\nu} Ar^*Cr(CO)_3 + Ar \qquad (1.2.2.2)$$

It was found that, upon irradiation with λ=254nm irradiation $ArCr(CO)_3$ will undergo carbon monoxide or benzene exchange processes (reactions 1.2 2.1 and 1.2.2.2). These conclusions were based on experiments in which the complexes were irradiated in the presence of either ^{14}CO or ^{14}C-labelled arene, in both cases incorporation of the labelled species was noted.

Yavorskii *et al* [44] and Trembovler *et al* [45] described electronic absorption spectral changes which occur during irradiation of (η^6-arene)$Cr(CO)_3$ in cyclohexane solution These compounds were shown to interact with visible light and the observed photodecay was described by first order kinetics It was concluded that the spectral

data are compatible with the formation of arene and chromium hexacarbonyl during the reaction Further, Trembovler *et al* [45] determined the quantum yield of photodecomposition as a function of light intensity and proposed the simultaneous occurance of three decay processes with different dependancies on light intensity. No conclusions about the detailed photolytic reactions were drawn, however.

Nasielski and Denisoff[46] performed a quantitative study of the photosubstitution of CO in (η^6-mesitylene)$Cr(CO)_3$ by N-dodecylmaleimide In cyclohexane solution the study was hampered by the photo-instability of the reactants and products, whereas in benzene solution the reaction was clean and the quantum yield was calculated as 0 90+/-0 09 at 313nm No detectable level of mesitylene-benzene exchange was observed

Wrighton and Haverty[47] examined the photosubstitution of $ArCr(CO)_3$ according to equation 1 2 2.3, in which Ar=benzene or mesitylene, and X=pyridine.

$$ArCr(CO)_3 + X \xrightarrow{h\nu} ArCr(CO)_2X + CO \qquad (1.2.2\ 3)$$

The chemistry observed was consistent with dissociative loss of CO as the primary excited state process The quantum yield for formation of $ArCr(CO)_2$(pyridine) was found to be 0 72+/-0 07, independent of wavelength (313, 366, 436nm), solvent, arene and light intensity Arene exchange was found to be insignificant under the conditions used

Gilbert *et al* [48] studied photoinduced CO exchange of $ArCr(CO)_3$ (Ar= η^6-benzene) and obtained a quantum yield in accordance with that reported by Wrighton

and Haverty (0 72), the efficiency of arene exchange was given as approximately one-sixth of this value. It was evident that arene exchange was strongly suppressed by the presence in solution of free carbon monoxide, whereas carbon monoxide exchange was relatively unaffected by the presence of free benzene It was concluded that photochemical arene and carbon monoxide exchange proceed *via* a common intermediate which was suggested to be the $ArCr(CO)_2$ UV/vis monitored flash photolysis of $ArCr(CO)_3$ in cyclohexane solution revealed the formation of a weakly absorbing transient species which reacted further (within 1ms) to form a second transient species which absorbed throughout the visible spectrum (λ_{max} 500nm). Both species were strongly quenched if the solution was saturated under one atmosphere of CO It was considered that the first species observed was $ArCr(CO)_2$ and that exchange with benzene involves this intermediate and does not occur through a one-step dissociation of the excited molecule to give $Cr(CO)_3$ and benzene.

Bamford *et al* [49] examined the course and kinetics of the photolyses of $ArCr(CO)_3$ (Ar = η^6-benzene and η^6-toluene) in hydrocarbon and monomer solutions, together with a study of the kinetics of polymerisation photoinitiated by (η^6-benzene)$Cr(CO)_3$ Scission of carbon monoxide was found to be the main route of photodecomposition, as proposed by previous workers [44, 45, 47]. The resulting $ArCr(CO)_2$ fragment decomposed to yield arene The course of the reaction appeared to be greatly modified when carried out in methyl methacrylate solution

The photochemistry of (η^6-benzene)$Cr(CO)_3$ in inert (argon or CH_4) and reactive (N_2) matrices at 12K was investigated by Rest *et al* [50] Photolysis of $ArCr(CO)_3$ in argon and methane matrices gave rise to bands in the infrared spectrum

attributed to photochemically generated 'free' carbon monoxide and the unsaturated $ArCr(CO)_2$(matrix species) On photolysis of the tricarbonyl compound in a N_2 matrix, bands assignable to $ArCr(CO)_2(N_2)$ could be identified. However, unlike the analogous compound $(\eta^4\text{-}C_4H_4)Fe(CO)_2(N_2)$, which underwent rapid photoconversion to $(\eta^4\text{-}C_4H_4)Fe(CO)_3$ on irradiation at lower wavelengths, the dinitrogen complex $ArCr(CO)_2(N_2)$ did not undergo photoreversal No evidence was obtained in this study for the photo-ejection of the arene ligand to give $Cr(CO)_3$; even when the complexes were photolysed in CO matrices

Black *et al* briefly reported the photochemistry of $ArCr(CO)_3$ in methyl-THF glasses at 77K Photolysis gave rise to two pairs of bands, of which the higher frequency pair was less intense and disappeared on annealing Similar behaviour was observed in several other systems of the type $M(C_nH_n)(CO_2)(ROR')$ The bands were attributed to the creation by photolysis of two distinct families of rotamers depending on the arrangement of solvent molecules around the photolysed molecule No evidence for the displacement of benzene by solvent (mTHF) was found

An extensive range of carbonyl substituted compounds can be conveniently synthesised by UV irradiation of $ArCr(CO)_3$ complexes in hydrocarbon solvents in the presence of substituting nucleophilic ligands[52-54] Both the arene and carbonyl ligands can be replaced by nucleophiles, although thermal conditions generally favour arene exchange, while photolysis usually leads to CO loss

Hill and Wrighton[55] investigated the oxidative addition of trisubstituted silanes to the photochemically generated coordinatively unsaturated $(\eta^4\text{-}C_4H_4)Fe(CO)_2$, $(\eta^5\text{-}C_5H_5)Mn(CO)_2$, $(\eta^5\text{-}C_5Me_5)Mn(CO)_2$, $(\eta^5\text{-}C_5H_5)Re(CO)_2$,

and $(\eta^6\text{-}C_6H_6)Cr(CO)_2$ species Irradiation of the parent tricarbonyl at low temperatures (85-157K) in inert organic solvents resulted in dissociative CO loss to generate the sixteen valence electron dicarbonyl species which was spectroscopically characterised by means of IR On melting the frozen glasses doped with trisubstituted silane, the dicarbonyl reacted to form the oxidative addition product of the formula $(R)M(CO)_2H(SiR_3)$ The reactivity of the Cr species with Et_3SiH was higher than any of the other 16 electron compounds studied, as under the conditions used, the barrier to reaction between CO or Et_3SiH and $ArCr(CO)_2$ was sufficiently low that no unsaturated species was detected

Bitterwolf *et al* [56] photolysed four half-sandwich compounds, including $(\eta^6\text{-}C_6H_6)Cr(CO)_3$ in nujol at 77K Photolysis was found to form the corresponding dicarbonyl products and 'free' CO, these reactions were photochemically reversible $(\eta^6C_6H_6)\text{-}Cr(CO)_3$ was found to produce small amounts of a previously unobserved dinuclear species $(\eta^6\text{-}C_6H_6)_2Cr_2(CO)_5$ directly upon photolysis This compound is the chromium analogue of the isolable rhenium dinuclear compound $(\eta^5\text{-}C_5H_5)_2Re_2(CO)_5$[57]. The bands associated with the dinuclear compound increased somewhat during annealing In order to confirm the assignment of a dinuclear species, a sample of ^{13}CO-labelled $(\eta^6\text{-}C_6H_6)Cr(CO)_3$ was prepared. The appearance of only two bands in the bridging carbonyl regions of the isotopically mixed sample permitted the conclusion that the dinuclear photoproduct has only one bridging carbonyl group This product was thought to result from reactions of dicarbonyl photoproducts with parent tricarbonyl complexes, Scheme 1 2.2 1.

SCHEME 1 2.2 1

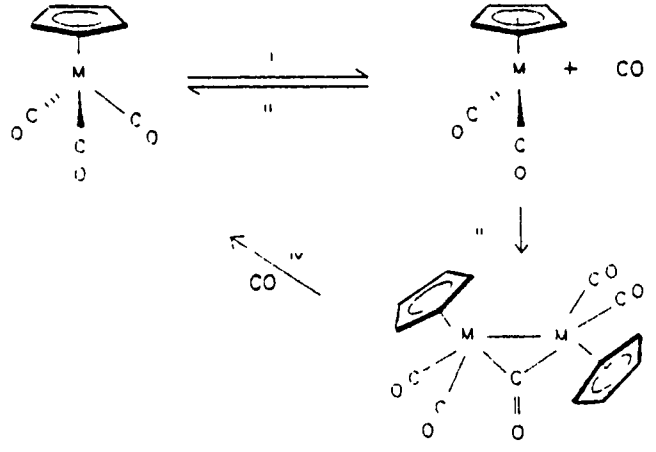

Wang *et al* [58] studied the photochemistry of $(\eta^6\text{-}C_6H_6)Cr(CO)_3$ in the gas phase by time-resolved infrared absorption spectroscopy The photofragments produced upon 355nm and 266nm photolyses were identified. $(\eta^6\text{-}C_6H_6)Cr(CO)_2$ was found to be the predominant photoproduct upon 355nm photolysis while both $(\eta^6\text{-}C_6H_6)Cr(CO)_2$ and $(\eta^6\text{-}C_6H_6)Cr(CO)$ were produced upon 266nm photolysis in a ratio of about 2 5 The reaction rates of the coordinatively unsaturated species with CO were determined to be in the order of picoseconds

1.3 Photochemistry of (π-allyl)Mn(CO)$_4$

There has been much interest in η^3-allyl organometallic complexes since it was first demonstrated in the late 1950's that $(C_4H_7)Co(CO)_3$ has a η^3-bonding configuration[59]. The allyl group is a commonly encountered ligand in organometallic reactions[60] and catalytic processes[61] The ligand is of particular interest because it can engage in either η^1 or η^3 bonding to a transition metal; that is it can be either σ-bonded (η^1) or σ- and π-bonded (η^3) Allyl-bridged complexes

have also been identified[62] While allyl complexes of the first-row transition metals have been prepared, the most stable examples, of Cr and Ni, still decompose at room temperature Despite, and in fact because of, this much lower thermal stability, metal-allyl compounds have been utilised in a number of synthetic and catalytic applications[63] In general, the η^1-allyl complexes are thermally less stable than their corresponding η^3-allyl compounds and may decompose to form η^3-allyl complexes[64,65] A σ to π rearrangement is an intramolecular reaction in which an organic group σ-bonded (η^1) to a metal becomes π-bonded (η^n), and this process is often reversible Such σ to π rearrangements are important in organic syntheses and homogeneous catalytic processes[66] Interesting consequences of CO dissociation from substituted allyl complexes, e g $Fe(\eta^5\text{-}C_5H_5)(CO)_2(\eta^1\text{-}C_3H_4R)$ include *syn-* and *anti*-conformations of the R-group after σ to π rearrangement[67], reaction 1 3 1

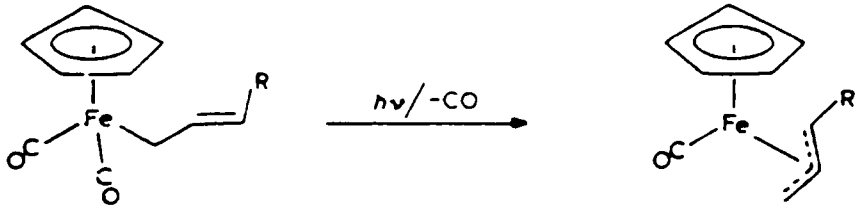

(1.3.1)

In most cases the thermal and photochemical σ to π rearrangements are irreversible, e.g reaction 1 3 2, but in principle the process should be reversible

$$(\eta^1\text{-}C_3H_5)Mn(CO)_5 \underset{}{\overset{h\nu}{\rightleftharpoons}} (\eta^3\text{-}C_3H_5)Mn(CO)_4 + CO \qquad (1\,3\,2)$$

Paz-Sandoval *et al* [68] investigated the addition and substitution reactions of the pentadienyl complex $(\eta^5\text{-}C_5H_7)Mn(CO)_3$. It was found that reaction of strong σ-donor phosphites (L=PMe_3, PMe_2Ph or P-n-Bu_3) with $(\eta^5\text{-}C_5H_7)Mn(CO)_3$ in cyclohexane at room temperature afforded the η^3-pentadienyl adducts $(\eta^3\text{-}C_5H_7)Mn(CO)_3L$, *via* an associative ligand substitution involving η^3 to η^5 interconversion The vinyl substituent was shown to be in the *anti*-position, reaction 1.3 3.

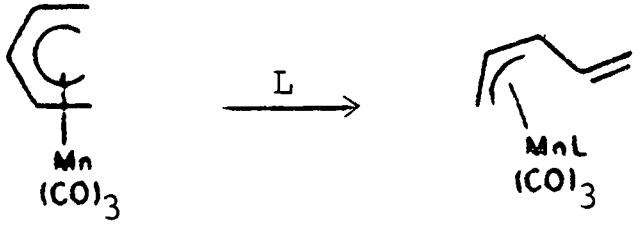

(1.3 3)

Preliminary photochemical studies in frozen gas matrices at 20K were also presented. Three-hour photolysis of $(\eta^5\text{-}C_5H_7)Mn(CO)_3$ in CO matrices gave rise to bands attributed to formation of $(\eta^3\text{-}C_5H_7)Mn(CO)_4$ The spectra showed complete consumption of the starting material and conversion into essentially only one product. Bands assignable to $(\eta^3\text{-}C_5H_7)Mn(CO)_3(N_2)$ were identified on photolysis of the pentacarbonyl in a N_2 matrix This work showed the expected propensity of the π-pentadienyl ligand to readily undergo η^5 to η^3 conversion. A subsequent investigation of the chemical properties of the $Mn(\eta^5\text{-}C_3H_5)(CO)_3$ complex in the presence of secondary amines has led to the development of a general route for the synthesis of nitrogen donor $(\eta^5$-pentenyl)manganese complexes which have not been previously reported[69].

The kinetics and mechanism of CO substitution reactions of $(\eta^3$-$C_3H_4X)Mn(CO)_4$ compounds was explored by Palmer and Bosolo[70], where X is H, Me, Ph, t-Bu, or Cl in the 1- or 2-position of the allyl ligand, reaction 1 3.4

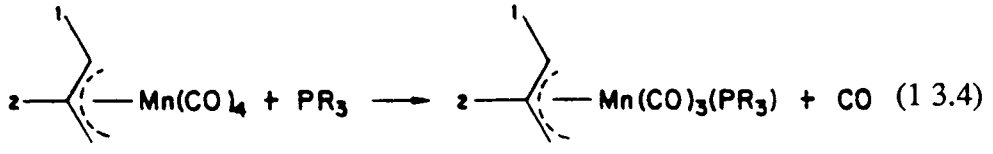

(1 3.4)

Studies on the decarbonylation reactions of $(\eta^1$-$C_3H_4)Mn(CO)_4L$ ruled out an η^3 to η^1 to η^3 mechanism It was concluded that CO substitution takes place by a dissociation (S_N1) process Substituents on the 1-position of the allyl group had a small retardation effect on the rates of CO substitution Substitution on the 2-position enhanced the rate of reaction, furthermore, this enhancement increased with increasing bulkiness of the substituent

The photochemistry of $(\eta^1$-$C_3H_5)Mn(CO)_5$ isolated at high dilution in frozen gas matrices at *ca* 12K was investigated by Hitam *et al* [71]. UV irradiation in inert CH_4 and Ar matrices resulted in the photoejection of a CO ligand with concomitant σ to π rearrangement to afford $(\eta^3$-$C_3H_5)Mn(CO)_4$, which lost a further CO reversibly to yield the 16-electron species $(\eta^3$-$C_3H_5)Mn(CO)_3$ In N_2 matrices the unsaturated species reacted with a N_2 ligand to yield $(\eta^3$-$C_3H_5)Mn(CO)_3(N_2)$, while in CO matrices it's reaction with CO was so facile that no $(\eta^3$-$C_3H_5)Mn(CO)_3$ could be detected even after prolonged irradiation In a CO matrix no evidence was found for the reverse reaction, reaction 1 3 5

$$(\eta^3\text{-}C_3H_5)Mn(CO)_3 + CO \xrightarrow{h\nu} (\eta^1\text{-}C_3H_5)Mn(CO)_5 \qquad (1.3\ 5)$$

It was concluded that η^1 to η^3-allyl rearrangements in general proceed in solution by a two step reactions, even when the intermediate stages cannot be observed. The observation of a η^1 to η^3 conversion in all matrices (CH_4, Ar, N_2, CO) suggests that it is a very facile process It also suggests that manganese has a preference for an η^3-allyl ligand and that η^1 to η^3 rearrangement is irreversible in this case This is in contrast to an earlier study on the photochemistry of $(\eta^3\text{-allyl})Co(CO)_3$ isolated in a CO matrix where η^3 to σ rearrangement was found to be reversible, reaction 1 3.6[72]

$$(\eta^3\text{-allyl})Co(CO)_3 + CO \underset{}{\overset{h\nu}{\rightleftharpoons}} (\sigma\text{-allyl})Co(CO)_4 \qquad (1\ 3\ 6)$$

Lee *et al* [73] reported the synthesis of $(\eta^1$-2,4-pentadienyl)$Mn(CO)_5$, which undergoes photo-induced conversion to (*syn*-η^3-2,4,-pentadienyl)$Mn(CO)_4$ and thermal conversion to $(\eta^5$-pentadienyl)$Mn(CO)_3$ in a η^1 to *syn*-η^3 to η^5 transformation, Scheme 1 3 2.

SCHEME 1 3.2

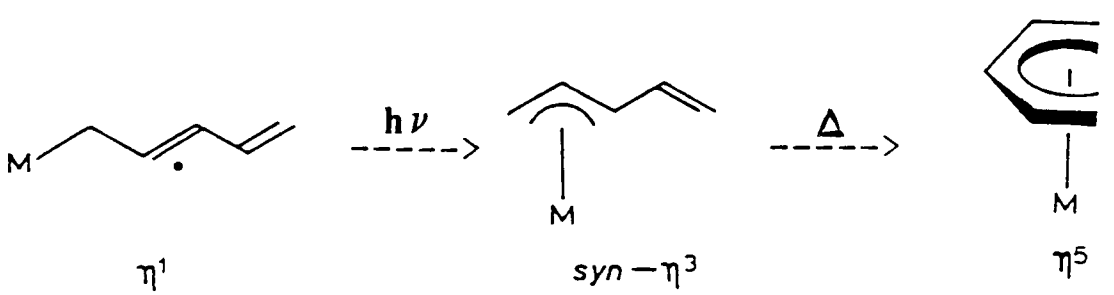

A recent investigation by Young and Wrighton[74] studied the photochemistry of $(\eta^1\text{-}C_6H_5CH_2)Mn(CO)_5$ in alkane glasses at 95K. CO loss was the only detectable photoprocess to form the ring-slipped product $(\eta^3\text{-}C_6H_5CH_2)Mn(CO)_4$ The identity of the η^3-intermediate was established by spectroscopic means and by chemical-trapping experiments The photoproduced $(\eta^3\text{-}C_6H_5CH_2)Mn(CO)_4$ was relatively inert thermally and photochemically with respect to CO loss and was generated essentially quantitatively with no detectable secondary CO loss chemistry The ratio of CO loss to Mn-R bond homolysis was found to be wavelength dependent on irradiation at 200K, R = $CH_2\text{-}C_6H_5$. The $(\eta^3\text{-}C_6H_5CH_2)Mn(CO)_4$ produced by 254nm irradiation of the $(\eta^1\text{-}C_6H_5CH_2)Mn(CO)_5$ in argon deoxygenated methylcyclohexane (MCH) at 200K was detected by ^1H NMR It was concluded that the η^3-aryl tetracarbonyl is fluxional at 200K, i e. the two compounds shown in reaction 1.3 7 are rapidly interconverting Room-temperature irradiation of $(\eta^1\text{-}C_6H_5CH_2)Mn(CO)_5$ yielded both CO loss and Mn-R bond cleavage, giving $Mn(CO)_5$ and R radicals. The relative importance of these two competitive primary photoprocesses was shown to be wavelength dependent.

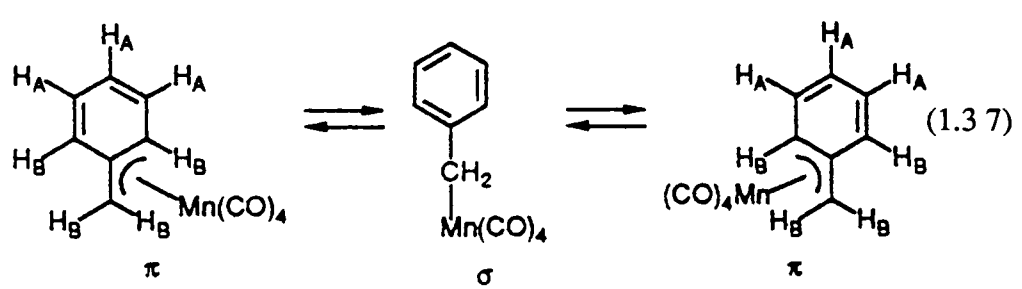

(1.3 7)

1.4 Photochemistry of Dinuclear (π-allyl)manganese Compounds

Various studies have shown that irradiation of $Mn_2(CO)_{10}$[75], $Re_2(CO)_{10}$[76,77] or $MnRe(CO)_{10}$[78] leads to loss of CO as the only detectable photoreaction in a low-temperature rigid medium Oyer and Wrighton[78] studied the photochemistry of the heterodinuclear complex $MnRe(CO)_{10}$; they established that the Mn-centre is the source of the photoejected CO on near-UV irradiation in MCH glass containing PPh_3 at 77K On warming the sample to 298K, PPh_3 reacted with the coordinatively unsaturated $MnRe(CO)_9$ to yield exclusively the Mn-substituted species $Mn(CO)_4(PPh_3)Re(CO)_5$ Reaction of PPh_3 with photogenerated $MnRe(CO)_9$, to give $Mn(CO)_4(PPh_3)Re(CO)_5$, is consistent with a $MnRe(CO)_9$ structure formed by loss of CO from the Mn centre, yielding a species with a semi-bridged CO that then reacts selectively at Mn, reaction 1 4.1 It was concluded that Mn is the more thermally labile centre and that net substitution occurs at the site from which CO was extruded in the primary photoprocess

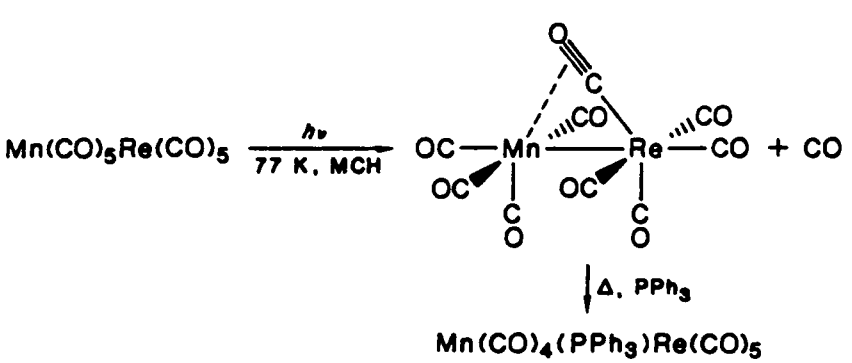

(1 4 1)

Sullivan and Brown[79] presented evidence that the photochemical reaction of dinuclear manganese carbonyl compounds with tributyltin hydride or triethylsilane occurs *via* oxidative addition to the primary photochemical product resulting from CO loss; reactions 1 4 2 and 1 4 3 where L=CO, PMe_3, $P(n\text{-}Bu)_3$, $P(i\text{-}Pr)_3$.

$$Mn_2(CO)_8L_2 \xrightarrow{h\nu} Mn_2(CO)_7L_2 + CO \qquad (1\,4\,2)$$

$$Mn_2(CO)_7L_2 + HMR_3 \longrightarrow (CO)_3L(H)(MR_3)Mn\text{-}Mn(CO)_4L \qquad (1.4\,3)$$

Following the oxidative addition step reductive elimation and uptake of CO leads to $HMn(CO)_4L$ and $R_3MMn(CO)_4L$ The rate of oxidative addition decreased as the steric requirements of L increased, also the lifetime of the intermediate product $Mn_2(CO)_7L_2$, resulting from the initial addition, varied greatly with L It was concluded that a complete model for the reaction systems must take account of the CO-loss product as the prevalent species in a non-coordinating solvent; formation of the semi-bridging form from the open form appeared to have a significant energy barrier

There are many examples in the literature of organometallic complexes with two metal atoms, at least one of which is a second- or third-row element. Almost all of these have the two metal atoms directly bonded, such as $MnRe(CO)_{10}$[78] or joined by simple bridging groups such as hydrido and alkenyl[80], or pyrazine[81]. None of these compounds have extended bridging ligands; particularly extended π-systems as in π-allyl The most extensive series of complexes with two or more π-donor sites reported so far have been (η^5-aroylcyclopentadienyl)rhenium tricarbonyls and their (η^6-arene)$Cr(CO)_3$ complexes[82], a series of these complexes has been

prepared for the purpose of studying through-ligand metal-metal interaction The carbonyl stretching frequencies of the $Re(CO)_3$ group and the cyclopentadienyl proton resonances indicated π-electron delocalisation through the ligand system by the $Cr(CO)_3$ group More recently a series of heterobimetallic complexes of chromium and manganese with bridging σ,π benzene and benzoyl ligands have been prepared by Lotz *et al* [83], this synthesis and structural analysis represents the first reported example of manganese σ-bonded to a π-coordinated benzene of (η^6-arene)$Cr(CO)_3$ No photolytic studies have been performed on these complexes to date

1.5 Photochemistry of (η^5-C_5H_5)$V(CO)_4$

The chemistry of the monocyclopentadienyl complex of vanadium, (η^5-C_5H_5)$V(CO)_4$, is currently limited to the photosubstitution of one or two carbonyls by ligands such as phosphines, hydrazines[84], arsines[85], aromatic alkynes[86] and nitric oxide[87] which are able to resist the harsh photochemical conditions These reactions employ the photolability of (η^5-C_5H_5)$V(CO)_4$ in preparing a variety of (η^5-C_5H_5)$V(CO)_{4-m}L_m$ complexes by irradiating (η^5-C_5H_5)$V(CO)_4$ in the presence of L, reaction 1 5 1

$$CpV(CO)_4 + mL \xrightarrow{h\nu} CpV(CO)_{4-m}L_m + mCO \qquad (1\,5.1)$$

(where $Cp = \eta^5$-C_5H_5)

In the case of the monodentate ligands, e.g. L = diene[5], PPh_3[86,88,89], P(n-Bu)$_3$[90], or PH_3[91], the products are monosubstituted derivatives of the type (η^5-

$C_5H_5)V(CO)_3L$. Photoreactions with bidentate phosphines (L-L), e.g. L-L = $Ph_2P(CH_2)_nPPh_2$ (n = 1, 2, 4)[92] or $PhP(CH_2CH_2PPh_2)_2$[93], gave substituted complexes of the type *cis*-$CpV(CO)_2(L\text{-}L)$

The complex $(\eta^5\text{-}C_5H_5)V(CO)_3(THF)$, THF = tetrahydrofuran, analagous to the well-known $(\eta^5\text{-}C_5H_5)Mn(CO)_3(THF)$, has been obtained by low temperature irradiation of dilute solutions of $(\eta^5\text{-}C_5H_5)V(CO)_4$, any attempt to isolate this species affording $(\eta^5\text{-}C_5H_5)_2V_2(CO)_5$ in quite low yield[94-97] Similarly, irradiation in tetrahydrothiophene (THT) affords the complex $(\eta^5\text{-}C_5H_5)V(CO)_3(THT)$[98] The utilisation of tetrahydrothiophene, instead of the isostructural tetrahydrofuran, provides a milder synthetic pathway to the preparation of $(\eta^5\text{-}C_5H_5)V(CO)_4$ derivatives $(\eta^5\text{-}C_5H_5)V(CO)_3(THT)$ reacts readily with several ligands, e g 2,2'-bipyridine (bpy) or pyrrolidine (pyrr) to produce the derivatives *cis*-$CpV(CO)_2(bpy)$ and $(\eta^5\text{-}C_5H_5)V(CO)_3(pyrr)$[98]. A disubstitution product $(\eta^5\text{-}C_5H_5)V(CO)_2(NN^*)$ is formed on irradiation of a bidentate amine ligand NN* with $(\eta^5\text{-}C_5H_5)V(CO)_4$ in THF The ligands used (1,2-diaminopropane, 1,2-diaminocyclohexane, and a Schiff base) were chelated in a bidentate manner[99]. Other synthetic reactions include the irradiation of $(\eta^5\text{-}C_5H_5)V(CO)_4$ in the presence of acetylenes (RC=CR'), e g R=H and R'=H, n-Bu, n-Pr, or CMe_3[89] and R=R'=Ph[100-102] or C_6F_5[101] to afford the acetylene complexes $(\eta^5\text{-}C_5H_5)V(CO)_2(RC{=}CR')$

Haward *et al* [103] recently prepared the complex $(\eta^5\text{-}C_5H_5)V(CO)_3(\eta^2\text{-}H_2)$, in which the H_2 is coordinated in a 'non-classical' manner This product was formed by UV photolysis of $(\eta^5\text{-}C_5H_5)V(CO)_4$ and H_2 in n-heptane solution at room

temperature and in liquid xenon solution at -78°C. A combination of FTIR and TRIR was used to characterise this novel synthetic product.

Kinetic studies of the thermal substitution reactions of $(\eta^5\text{-}C_5H_5)V(CO)_4$ with a variety of phosphines and phosphites have suggested that the reactions proceed by dissociative paths in which loss of a CO-ligand is the rate-determining step[104]. Although the quantum yield data for the photochemical reaction of $(\eta^5\text{-}C_5H_5)V(CO)_4$ with PPh_3 was consistent with an associative path, this was ruled out because it seemed unlikely that a sterically crowded 20-electron intermediate, $(\eta^5\text{-}C_5H_5)V(CO)_4(PPh_3)$, could be formed[88]. Instead, the photosubstitution reactions of $(\eta^5\text{-}C_5H_5)V(CO)_4$ have been proposed to involve dissociative loss of CO, i.e. reactions 1.5.2 to 1.5.4 , where the asterisk (*) denotes an excited-state species.

$$CpV(CO)_4 \xrightarrow{h\nu} CpV(CO)_4^* \qquad (1.5.2)$$

$$CpV(CO)_4^* \longrightarrow CpV(CO)_3 + CO \qquad (1.5.3)$$

$$CpV(CO)_3 + PPh_3 \longrightarrow CpV(CO)_3(PPh_3) \qquad (1.5.4)$$

In the case of reactions carried out in THF/THT, which are coordinating solvents, the CO-loss product is trapped as a solvated species before the THF/THT is displaced by the entering ligand, reactions 1.5.5 and 1.5.6.

$$CpV(CO)_3 + THF \xrightarrow{THF} CpV(CO)_3(THF) \qquad (1.5.5)$$

$$CpV(CO)_3(THF) + L \longrightarrow CpV(CO)_3(L) + THF \qquad (1.5.6)$$

Early attempts to isolate $(\eta^5\text{-}C_5H_5)V(CO)_3(THF)$ afforded $(\eta^5\text{-}C_5H_5)_2V_2(CO)_5$ in quite low yield[94-97]. Recently, however, both $(\eta^5\text{-}C_5H_5)V(CO)_3(THF)$[95,105] and $(\eta^5\text{-}C_5H_5)V(CO)_3(THT)$[98] have been isolated, providing strong evidence for the dissociative path in the thermal substitution of $(\eta^5\text{-}C_5H_5)V(CO)_4$. The use of THF as a solvent serves as the most general synthetic method for photosubstitution of $CpV(CO)_4$.

Recently, Hitam and Rest[106] investigated the photochemistry of $(\eta^5\text{-}C_5H_5)V(CO)_4$. Infrared spectroscopic evidence, including ^{13}C-labelling, was presented showing that the irradiation of $(\eta^5\text{-}C_5H_5)V(CO)_4$ at high dilution in frozen gas matrices at *ca.* 12K results in two types of reversible process. One process (Ar, CH_4 matrices) is ejection of CO to yield the species $(\eta^5\text{-}C_5H_5)V(CO)_n$ (n=1-3), by means of a dissociative pathway. The second process is proposed to involve a change in the ring hapticity with the formation $(\eta^3\text{-}C_5H_5)V(CO)_4$ and probably $(\eta^3\text{-}C_5H_5)V(CO)_5$ in CO matrices. The detection of these ring dechelation species suggests that the contribution of a S_N2 pathway to the solution substitution pathways should be reevaluated. In reactive and doped matrices (N_2, C_2H_4, doped CH_4) irradiation yielded $(\eta^5\text{-}C_5H_5)V(CO)_3(N_2)$, $(\eta^5\text{-}C_5H_5)V(CO)_3(C_2H_4)$ and *trans*-$(\eta^5\text{-}C_5H_5)V(CO)_2(C_2H_4)_2$ species.

1.6 References

1. A. Nakamura and M. Tsutsui; *Principles and Applications of Homogeneous Catalysis*,Wiley-Interscience, New York, 1980.
2. G.W. Parshall; *Homogeneous Catalysis*, Wiley-Interscience, New York, 1980.
3. G.R. Dobson, I. Bernal, M.G. Reisner, C.B. Dobson, and S.E. Mansour, *J. Am. Chem. Soc.*, 1985, **107**, 525.
4. C. Masters; *Homogeneous Transition-metal Catalysis*, Science Paperbacks, Chapman and Hall, 1981.
5. M. Wrighton, *Chem. Rev.*,1974, **74**, 401.
6. E.H. Schubert and R.K. Sheline, *Inorg. Chem.*, 1966, **5**, 1071.
7. M.S. Wrighton, *Fortschr. Chem. Forsch.*, 1976, **65**, 37.
8. M.S. Wrighton, H.B. Gray, G.S. Hammond, and V.M. Miskowski, *Inorg. Chem.*, 1973, **12**, 740.
9. P. Natarjan and A.W. Adamson, *J. Am. Chem. Soc.*, 1971, **93**, 5599.
10. J.P. Collman, *Acc. Chem. Res.*, 1968, 136.
11. W. Strohmeier, *Angew. Chem. Int. Ed.*, 1964, **3(11)**, 730.
12. (a) H.B. Gray and N.A. Beach, *J. Am. Chem. Soc.*, 1963, **85**, 2922.
    (b) N.A. Beach and H.B. Gray, *J. Am. Chem. Soc.*, 1968, **90**, 5713.
13. (a) E. Whittle, D.A. Dows, and G.C. Pimentel, *J. Phys. Chem.*, 1954, **22**, 1943.
    (b) G.C. Pimentel, *Angew. Chem. Int. Ed. Engl.*, 1975, **14**, 199.
14. R.N. Perutz and J.J. Turner, *J. Am. Chem. Soc.*, 1975, **97**, 4791.

15. J.K. Burdett, A.J. Downs, G.P. Gaskill, M.A. Graham, J.J. Turner, and R.F. Turner, *Inorg. Chem.*, 1978, **17**, 523.

16. S.A. Fairhurst, J.R. Morton, R.N. Perutz, and K.F. Preston, *Organometallics*, 1984, **3**, 1389.

17. G.A. Ozin and S.A. Mitchell, *Angew. Chem. Int. Ed. Engl.*, 1983, **22**, 674.

18. M. Poliakoff and E. Weitz, *Acc. Chem. Res.*, 1987, **20**, 408.

19. R.N. Perutz, *Chem. Rev.*, 1985, **85**, 97.

20. W.B. Maier, M. Poliakoff, M.B. Simpson, and J.J. Turner, *J. Chem. Soc., Chem. Commun.*, 1980, 587.

21. J.J. Turner, M.B. Simpson, M. Poliakoff, and W.B. Maier, *J. Am. Chem. Soc.*, 1983, **105**, 3898.

22. J.J. Turner, M.B. Simpson, M. Poliakoff, W.B. Maier, and M.A. Graham, *Inorg. Chem.*, 1983, **22**, 911.

23. M.B. Simpson, M. Poliakoff, J.J. Turner, W.B. Maier, and J.G. Mc Laughlin, *J. Chem. Soc., Chem. Commun.*, 1983, 1355.

24. (a) R.G.W. Norrish and G. Porter, *Nature*, 1949, **164**, 685.
(b) R.W. Norrish and B.A. Thrush, *Q. Rev. Chem. Soc.*, 1956, **10**, 149.

25. J. Nasielski and A. Colas, *J. Organomet. Chem.*, 1975, **101**, 215.

26. G.K. Yang, K.S. Peters, and V. Vaida, *J. Am. Chem. Soc.*, 1986, **108**, 2511.

27. T.A. Seder, S.P. Church, A.J. Ouderkirk, and E. Weitz, *J. Am. Chem. Soc.*, 1985, **107**, 1432.

28. B.S. Creaven, A.J. Dixon, J.M. Kelly, C. Long, and M. Poliakoff, *Organometallics*, 1987, **6**, 2600.

29. (a) J.M. Kelly, D.V. Bent, H. Hermann, D. Schulte-Frohlinde, and E. Koerner von Gustorf, *J. Organomet. Chem.*, 1974, **69**, 259.

(b) R. Bonneau and J.M. Kelly, *J. Am. Chem. Soc.*, 1980, **102**, 1220.

(c) J.M. Kelly, C. Long, and R. Bonneau, *J. Phys. Chem.*, 1983, **87**, 3344.

30. (a) A.S. Lefohn and G.C. Pimentel, *J. Chem. Phys.*, 1971, **55**, 1213.

(b) L.Y. Tan, A.M. Winter, and G.C. Pimentel, *J. Chem. Phys.*, 1972, **57**, 4028.

31. S.D. Church, F.W. Grevels, H. Hermann, and K. Schaffner, *Inorg. Chem.*, 1984, **23**, 3830.

32. T.R. Fletcher and R.N. Rosenfeld, *J. Am. Chem. Soc.*, 1985, **107**, 2203.

33. S.P. Church, F.W. Grevels, H. Herrman, and K. Schaffner, *Inorg. Chem.*, 1985, **24**, 418.

34. S.P. Church, F.W. Grevels, H. Herrman, and K. Schaffner, *J. Chem. Soc., Chem. Commun.*, 1985, 30.

35. (a) M. Cais, E.N. Frankel, and A. Rejoan, *Tetrahedron Lett.*, 1968, 1919

(b) E.N. Frankel, E. Selke, and C.A. Glass, *J. Am. Chem. Soc.*, 1968, **90**, 2446.

36. (a) W. Strohmeier and E.H. Staricco, *Z. Phys. Chem.*, 1963, **38**, 315.

(b) W. Strohmeier and H. Mittnacht, *Z. Phys. Chem.*, 1961, **29**, 339.

(c) W. Strohmeier and M. Müller, *Z. Phys. Chem.*, 1964, **40**, 85.

37. E.L. Muetterties, J.R. Bleeke and A.C. Sievert, *J. Organomet. Chem.*, 1979, **178**, 197.

38. C.A.L. Mahaffy and P.L. Pauson, *J. Chem. Res., Synop.*, 1979, 126; *J. Chem. Res., Miniprint*, 1979, 1752.

39. (a) F.A. Adeji, D.L.S. Brown, J.A. Connor, M.L. Leung, I.M. Paz-Andrade, and H.A. Skinner, *J. Organomet. Chem.*, 1975, **97**, 221.

(b) D.L.S. Brown, J.A. Connor, C.P. Demain, M.L. Leung, J.A. Marinho-Simoes, H.A. Skinner, and M.T. Zafarani Moattar, *J. Organomet. Chem.*, 1977, **142**, 321.

40. C.L. Zimmerman, S.L. Shaner, S.A. Roth, and B.R. Willeford, *J. Chem. Res., Synop.*, 1980, 108; *J. Chem. Res., Miniprint*, 1980, 1289.

41. (a) T.G. Traylor and K. Stewart, *Organometallics*, 1984, **3**, 325.

(b) T.G. Traylor, K. Stewart, and M.J. Goldberg, *J. Am. Chem. Soc.*, 1984, **106**, 4445.

(c) T.G. Traylor, K. Stewart, and M.J. Goldberg, *Organometallics*, 1986, **5**, 2062.

(d) T.G. Traylor and K. Stewart, *J. Am. Chem. Soc.*, 1986, **108**, 6977.

(e) T.G. Traylor and M.J. Goldberg, *Organometallics*, 1987, **6**, 2531.

(f) T.G. Traylor and M.J. Goldberg, *J. Am. Chem. Soc.*, 1987, **109**, 3968.

42. J.A.S. Howell, N.F. Ashford, D.T. Dixon, J.C. Kola, T.A. Albright, and S.K. Kang, *Organometallics*, 1991, **10**, 1852.

43. (a) W. Strohmeier and D. Von Hobe., *Z. Naturforsch.*, 1963, **18b**, 770.

(b) W. Strohmeier and D. Von Hobe., *Z. Naturforsch.*, 1963, **18b**, 981.

(c) W. Strohmeier, *Angew. Chem. Int. Ed.*, 1963, **2**, 270.

44. (a) B M Yavorskıı, N K. Baranetskaya, V.N Trembovler, and V N. Setkına, *Doklady Akad Nauk S S R* , 1972, **207**, 1147

(b) B M Yavorskıı, V N Trembovler, V.N Setkına, N.K Baranetskaya, G.B Zaslavskaya, and M.G. Evdokımora, *Russ J Phys Chem* , 1974, **3**, 1231.

(c) B M Yavorskıı, V N Trembovler, V N. Setkına, N.K Baranetskaya, and G B Zaslavskaya, *Doklady Akad Nauk S S R* , 1974, **218**, 1153

45 V N Trembovler, N K Baranetskaya, N.V Fok, G B Zaslavskaya, B M. Yavorskıı, and V N. Setkına, *J Organomet Chem* , 1976, **117**, 339

46. J Nasıelskı and O Denısoff, *J Organomet Chem* , 1975, **102**, 65

47. M S Wrighton and J L Haverty, *Z Naturforsch* , 1975, **30b**, 254

48. A Gılbert, J M Kelly, M. Budzwaıt, and E Koerner Von Gustorf, *Z Naturforsch* , 1976, **31b**, 1091

49. (a) C.H. Bamford, K G Al-Lamee, and C J Konstantınov, *J Chem Soc , Faraday Trans* , 1977, **73**, 1406

(b) C H Bamford and K.G Al-Lamee, *J Chem Soc , Faraday Trans 1*, 1984, **80**, 2175

(c) C.H. Bamford and K G. Al-Lamee, *J Chem Soc , Faraday Trans 1*, 1984, **80**, 2187

50. A.J Rest, J R Sodeau, and D J Taylor, *J Chem Soc , Dalton Trans* , 1978, 651

51. J B Black, M J Boylan, and P S Braterman, *J Chem Soc , Dalton Trans* , 1981, 673

52. W Strohmeıer and H Hellman, *Chem Ber* , 1963, **96**, 2859

53. G Jaouen and R Dabard, *J Organomet Chem*, 1974, **72**, 377.

54. M Cais, M. Kaftory, D H. Kohn, and D Tartarsky, *J Organomet Chem*, 1979, **91**, 1188

55 R.H Hill and M S Wrighton, *Organometallics*, 1987, **6**, 632

56 T.E. Bitterwolf, K.A. Lott, A J Rest, and J. Masetti, *J Organomet Chem*, 1991, **113**, 419.

57. (a) A.S Foust, J K Hoyano, and W A G Graham, *J Organomet Chem*, 1971, **32**, C65.

(b) L.N. Lewis and K G. Caulton, *Inorg Chem*, 1981, **20**, 1139.

58 (a) W Wang, P Jin, Y Liu, Y She, and K Fu, *Chin Phys Lett*, 1991, **8**, 491.

(b) W. Wang, P Jin, Y Liu, Y She, and K Fu, *J Phys Chem*, 1992, **96**, 1278

59 H.B Jonassen, R.I Stearns, J Kentamaa, D W Moore, and A G. Whittaker, *J Am Chem Soc*, 1958, **80**, 2586

60 R. Baker, *Chem Rev*, 1973, **73**, 487

61. E.L Muetterties and J.R Bleeke, *Acc Chem Res*, 1979, **12**, 324.

62. M.L.H. Green and P L I Nagy, *Adv Organomet Chem*, 1964, **2**, 325

63 (a) R F Heck, *Acc Chem Res*, 1979, **12**, 146

(b) B M Trost, *Acc Chem Res*, 1980, **13**, 385

(c) J E Backvall, *Acc Chem Res*, 1983, **16**, 335

(d) H Kurosawa, H Ohnishi, M Emoto, Y Kawasaki, and S Murai, *J Am Chem Soc*, 1988, **110**, 6272

64. W.R Mc Clellan, H H. Hoehn, H.N. Cripps, E.L. Muetterties, and B.W Howk, *J Am Chem Soc*, 1961, **83**, 1601

65 S D. Worley, D.H Gibson, and W L Hsu, *Inorg Chem*, 1981, **20**, 1327.

66. M. Tsutsui and A Courtney, *Adv Organomet Chem*, 1977, **16**, 241.

67. M.L.H. Green and P.L.I Nagy, *J Chem Soc*, 1963, 189

68. M. de los A. Paz-Sandoval, P Powell, M G B Drew, and R.N. Perutz, *Organometallics*, 1984, **3**, 1026.

69 N Zuniga Villarreal, M.A Sandoval, P. Joseph-Nathan, and R.O. Esquive, *Organometallics*, 1991, **10**, 2616

70 G.T Palmer and F Bosolo, *J Am Chem Soc*, 1985, **107**, 3122

71. R.B. Hitam, K.A Mahmoud, and A J Rest, *J Organomet Chem*, 1985, **291**, 321

72 A.J Rest and D J. Taylor, *J Chem Soc, Dalton Trans*, 1983, 1291.

73 T.W Lee and R S. Liu, *J Organomet. Chem*, 1987, **320**, 211.

74. K.M. Young and M.S. Wrighton, *J Am Chem Soc*, 1990, **112**, 157

75 (a) M.S Wrighton and A F Hepp, *J Am Chem Soc*, 1983, **105**, 5934.
(b) I.R. Dunkin, P Harter, and C J Shields, *J Am Chem Soc*, 1984, **106**, 7248.

76 H. Yesaka, T Kobayashi, K Yasufuku, and S Nagakura, *J Am Chem Soc*, 1983, **105**, 6249

77. S. Firth, P M Hodges, M Poliakoff, and J J Turner, *Inorg Chem*, 1986, **25**, 4608

78 T J. Oyer and M S Wrighton, *Inorg Chem*, 1988, **27**, 3691

79 (a) R.J. Sullivan and T L. Brown, *J Am Chem Soc* , 1991, **113**, 9155

(b) R J. Sullivan and T L Brown, *J Am Chem Soc.*, 1991, **113**, 9162.

80. (a) P O Nubel and T.L. Brown, *J Am Chem Soc* , 1982, **104**, 4955.

(b) P O. Nubel and T L Brown, *J Am Chem Soc* , 1984, **106**, 644

81 M.M. Zulu and A.J. Lees, *Organometallics,* 1989, **8**, 955

82. (a) N J Gogan and C K Chu, *J Organomet Chem* , 1975, **93**, 363

(b) N J Gogan and C K Chu, *J Organomet Chem* , 1977, **132**, 103.

(c) N J Gogan and S I De Silva, *Organometallics,* 1990, **9**, 1970

83 S Lotz, M Schindehutte, and P H van Rooyen, *Organometallics,* 1992, **11**, 629.

84 C Woitha and D Rehder, *J Organomet Chem* , 1988, **353**, 315

85 R Borowski, D Rehder, and K. von Deunten, *J Organomet Chem* , 1981, 45, 220

86. R Tsumura and N Nagihara, *Bull Chem Soc Jpn* , 1965, **38**, 1901

87. E O. Fischer, R J J Schneider, and J. Muller, *J Organomet Chem* , 1968, **14**, 4.

88. R.J. Kinney, W D Jones, and R.G Bergmann, *J Am Chem Soc* , 1978, **100**, 7902

89 D G Alway and K.W Barnett, *Inorg Chem* , 1980, **19**, 779

90. E.O Fischer and R.J J. Schneider, *Angew Chem , Int Ed Engl* , 1967, **6**, 569

91 E O Fischer, E Louis, and R J J Schneider, *Angew Chem , Int Ed. Engl* , 1968, **7**, 136

92. D Rehder, L Dahlenburg, and I. Muller, *J Organomet Chem*, 1976, **122**, 53.

93 I. Muller and D Rehder, *J Organomet Chem*, 1977, **139**, 293.

94 E.O Fischer and R J J Schneider, *Chem Ber*, 1970, **103**, 3684.

95. M. Hoch and D Rehder, *J Organomet Chem*, 1985, **288**, C25.

96. C.J. Huffman, L N. Lewis, and K G Caulton, *Inorg Chem*, 1980, **19**, 2755

97 F A. Cotton, L Kruczynsky, and B A. Frenz *J Organomet Chem*, 1978, **93**, 160.

98 S Gamborotta, A Chiese-Villa, and C Guastini, *Inorg Chem*, 1988, **27**, 99.

99 M Hoch and D Rehder, *Inorg Chim Acta*, 1986, **115**, L23.

100. A.N. Nesmeyanov, *Adv Organomet Chem*, 1972, **10**, 56

101. D.F Foust and M D Rausch, *J Organomet Chem*, 1982, **239**, 321.

102 H.G. Alt and H E. Engelhardt, *Z Naturforsch*, 1985, **40b**, 1134.

103 M T Haward, M W George, S M Howdle, and M Poliakoff, *J Chem Soc, Chem Commun*, 1990, 913

104. G C. Faber and R.J Angelici, *Inorg Chem*, 1970, **9**, 1586.

105 L.N. Lewis and K.G Caulton, *Inorg Chem*, 1980, **19**, 1840.

106. R B Hitam and A J Rest, *Organometallics*, 1989, **8**, 1598.

Chapter 2

Laser-Induced Photochemistry of (η^6-arene)$Cr(CO)_3$ Systems

2.1 Introduction

Enormous interest in the photochemistry of $Cr(CO)_6$ both in the gas[1] and condensed phases[2] has been shown in past years Few investigations are reported into the photochemistry of (η^6-benzene)$Cr(CO)_3$ or it's derivatives[3]; of which only three describe the nature of the transient species formed by photolysis in alkane solution Given the dramatic difference between the thermal and photochemical reactions of this compound[4] it is surprising that greater attention has not been focussed on this system Early flash photolysis studies identified (η^6-benzene)$Cr(CO)_2$(S) (S = alkane solvent) as a primary photoproduct, reaction 2.1.1[4(b)] An arene exchange process was also observed following photolysis, reaction 2.1 2 The ability of CO to quench this exchange reaction implicates (η^6-benzene)$Cr(CO)_2$ as an intermediate in this reaction

$$(\eta^6\text{-arene})Cr(CO)_3 \xrightarrow{h\nu} (\eta^6\text{-arene})Cr(CO)_2 + CO \qquad (2.1\ 1)$$

$$(\eta^6\text{-arene})Cr(CO)_3 + \text{arene}' \xrightarrow{h\nu} (\eta^6\text{-arene}')Cr(CO)_3 + \text{arene} \qquad (2\ 1.2)$$

Herein is reported a study of the primary and secondary photochemistry of a range of (η^6-arene)$Cr(CO)_3$ complexes in alkane solution at ambient temperature. This forms part of an investigation into the photochemistry of "half-sandwich" compounds[5] The goals of this study were to characterise the photoproducts and to obtain kinetic data for their reactions with CO and other potential ligands. Both laser flash photolysis and transient infrared spectroscopy (TRIR) were used in these investigations A range of alkyl-substituted η^6-arene compounds was synthesised and

the effect of the substituent on the reactivity of the photoproducts was measured. These results were compared to those obtained for the isoelectronic (η^5-C_5R_5)$Mn(CO)_3$ system (R = H, Me, or Et).

2.2 Primary Photochemical Observations

2.2.1 Photochemistry of (η^6-benzene)$Cr(CO)_3$

2.2.1.1 Electronic Spectrum of (η^6-benzene)$Cr(CO)_3$

The UV/vis spectrum of (η^6-benzene)$Cr(CO)_3$ in cyclohexane solution is presented in Figure 2 2 1 1 1 This absorption spectrum is dominated by metal to ligand charge transfer (MLCT) absorptions[6] The prominant spectral features are two intense bands centred at 220nm and 316nm Both bands have been assigned to charge transfer (CT) transitions, having mainly M --> (η^6-C_6H_6) CT character with some M --> π^*CO CT character Although the low-energy region has not been studied in detail, a shoulder on the 316nm band, at *ca* 370nm, probably involves low-energy LF absorptions A third band centred at 264nm is attributed solely to M --> π^*CO CT transitions Previous investigations of the photochemistry of (η^6-benzene)$Cr(CO)_3$ were monitored solely in the visible region of the spectrum where the transient absorptions are weak

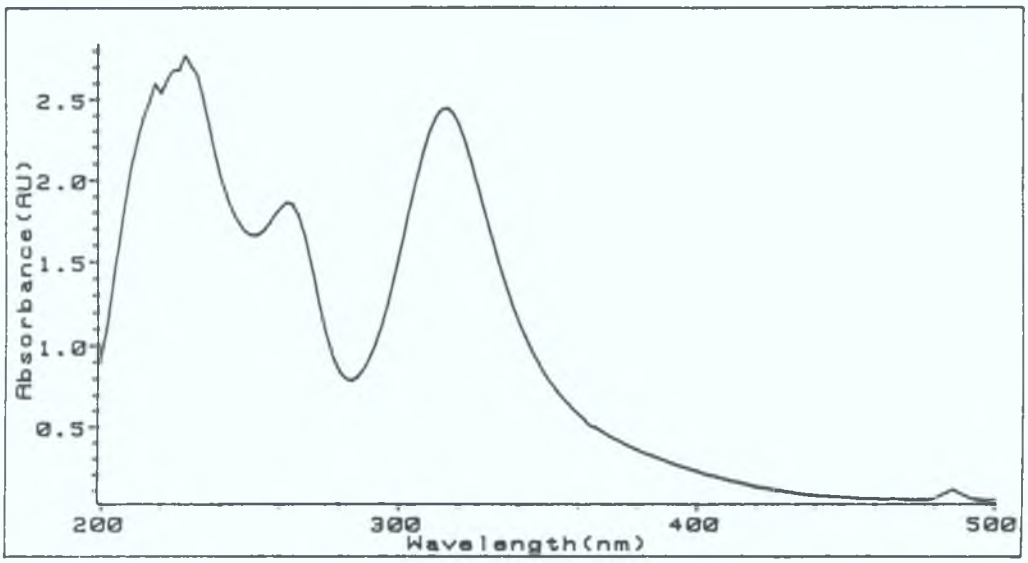

Figure 2.2.1.1.1 UV/vis absorption spectrum of a 2.45 x 10^{-4} mol dm^{-3} solution of (η^6-benzene)$Cr(CO)_3$ in cyclohexane.

2.2.1.2 Preliminary Experimental Results

Two first-order kinetic processes were observed on the microsecond timescale following 355nm laser flash photolysis of (η^6-benzene)$Cr(CO)_3$ in cyclohexane solution (ε_{354nm} = 3060 dm^3 mol^{-1} cm^{-1}) under 1.0 atmosphere of CO. The data yields two observed rate constants, $k_{obs(1)}$ for the short time portion and $k_{obs(2)}$ for the long time portion of the absorption decay. The observed rate constants of the first and second transient species were measured to be 7.9 x 10^4 s^{-1} and 3.0 x 10^3 s^{-1} respectively. Figure 2.2.1.2.1 displays a plot of absorption versus time fitted by a sum of two exponential functions on data obtained after flash photolysis at 280nm. It is clear that the transient signal is intense and high quality kinetic data can be extracted. The absorption attributed to the two observed species does not return to baseline,

Figure 2.2.1.2.2 (a), indicating that the process is not fully reversible over these timescales. This residual absorption is attributed to the presence of a third species which is long lived. In the absence of CO, i.e. when an argon atmosphere was admitted to the reaction cell, the formation of the third transient species predominates and almost completely obscures the absorptions of species 1 and 2 when monitored at 280nm, Figure 2.2.1.2.2 (b). The origin of this third species will be discussed later.

No effect was observed on the rate of decay of either species as the concentration of (η^6-benzene)$Cr(CO)_3$ was altered, Figures 2.2.1.2.3 and 2.2.1.2.4. The lifetime of the first transient species displayed a linear dependence on the concentration of CO; Figure 2.2.1.2.5, while the yield of this species was unaffected. The slope of this line, calculated to be $6.7 \times 10^6 \pm 0.6 \times 10^6$ mol^{-1} dm^3 s^{-1}, gives the second order rate constant for the reaction of this species with CO. No effect was observed on the rate of decay or the yield of the second observed species as the concentration of CO was altered, Figure 2.2.1.2.6. The CO concentration in cyclohexane solution was taken as 1.2×10^{-2} mol dm^{-3} under 1.0 atmosphere of CO at 298K[7].

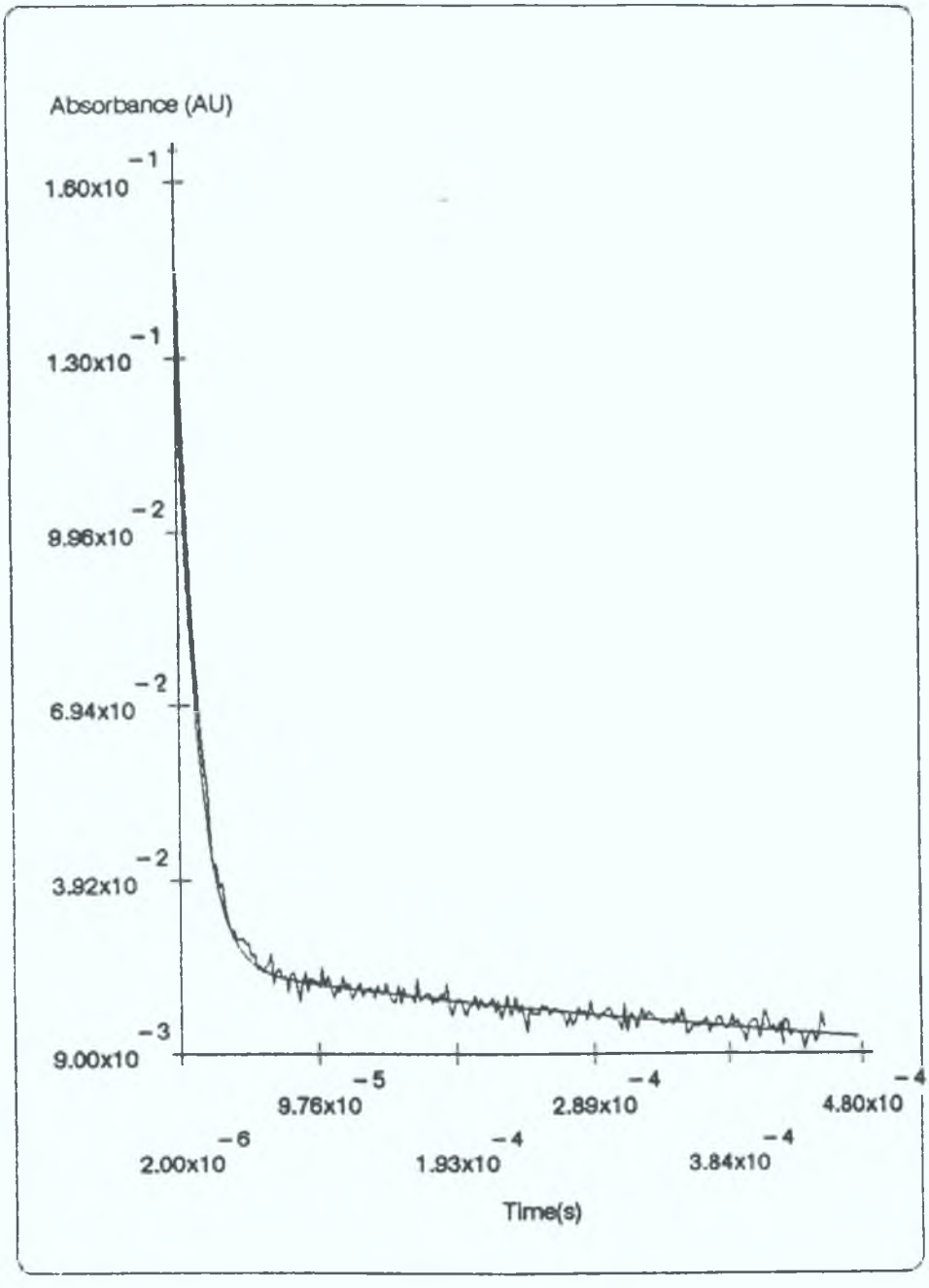

Figure 2.2.1.2.1 Absorbance versus time fitted as a function of two exponential functions on data obtained at 280nm after flash photolysis of a cyclohexane solution of (η^6-benzene)$Cr(CO)_3$ under 1.0 atmosphere of CO at 298K.

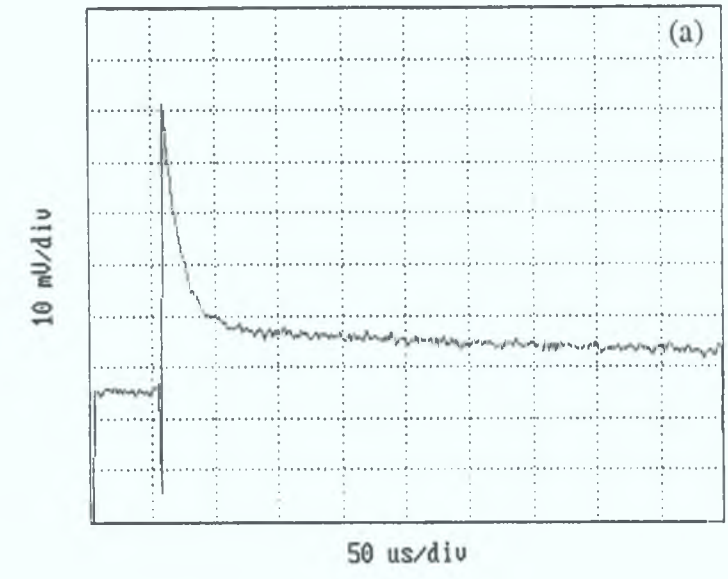

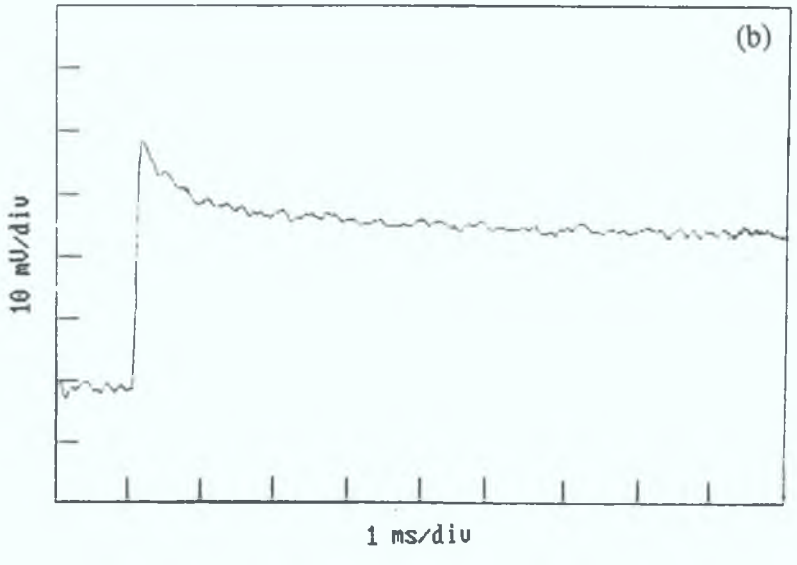

Figure 2.2.1.2.2 Oscilloscope traces of transient absorption species recorded at 280nm under 1.0 atmosphere of CO (a); and under 1.0 atmosphere of argon (b).

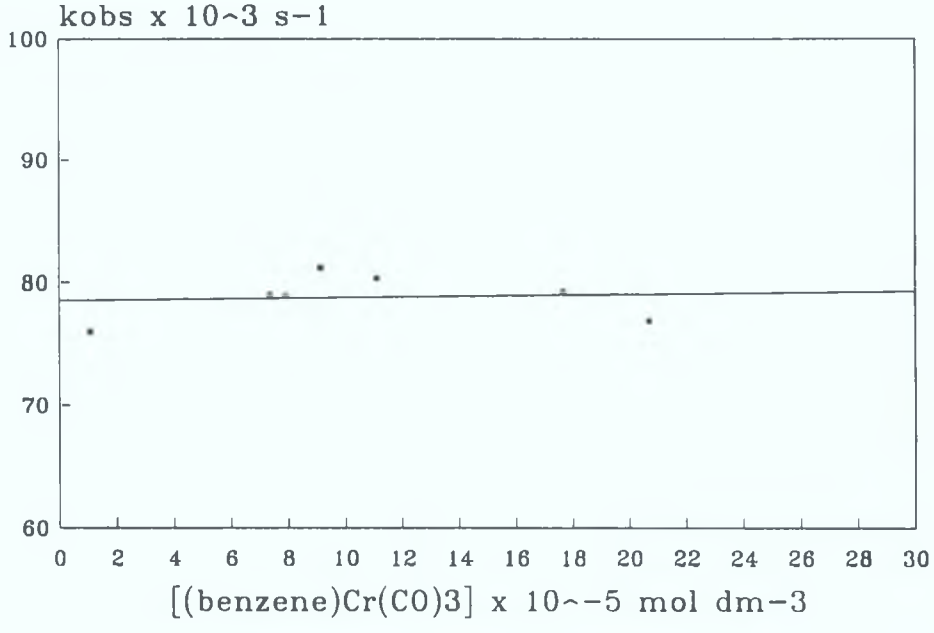

$[(\eta^6\text{-benzene})Cr(CO)_3]$ mol dm^{-3}	k_{obs} s^{-1}
7.36×10^{-5}	78922
7.91×10^{-5}	78921
9.13×10^{-5}	81180
1.07×10^{-4}	75991
1.10×10^{-4}	80322
1.77×10^{-4}	79210
2.07×10^{-4}	76837

Figure 2.2.1.2.3 A plot of $[(\eta^6\text{-benzene})Cr(CO)_3]$ (mol dm^{-3}) against the observed rate constants (s^{-1}) obtained for the decay of the first primary photoproduct at 298K under 1.0 atmosphere of CO.

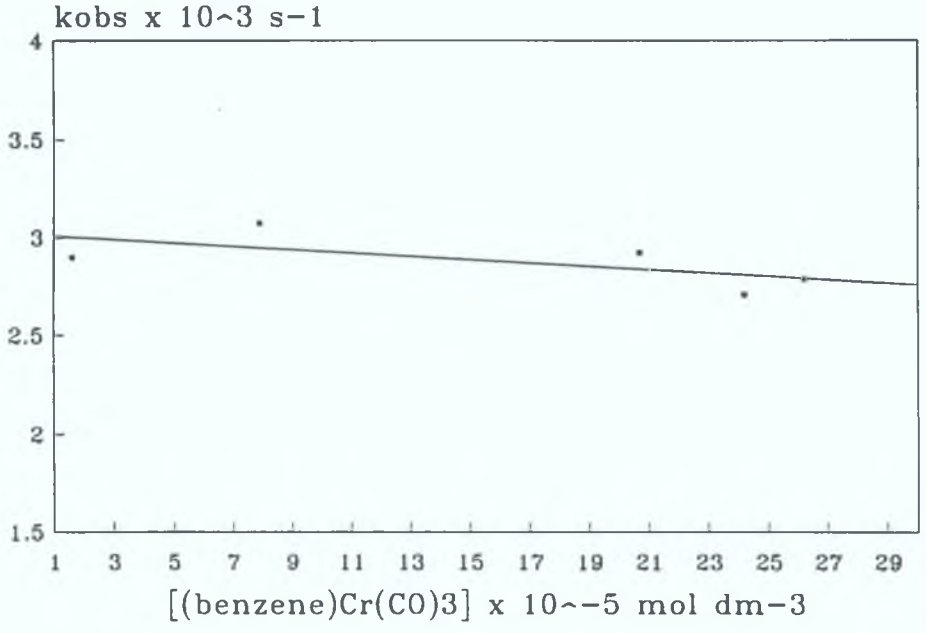

$[(\eta^6\text{-benzene})Cr(CO)_3]$ mol dm^{-3}	k_{obs} s^{-1}
1.62×10^{-5}	2900
7.91×10^{-5}	3075
2.07×10^{-5}	2923
2.42×10^{-4}	2707
2.62×10^{-4}	1789

Figure 2.2.1.2.4 A plot of $[(\eta^6\text{-benzene})Cr(CO)_3]$ (mol dm^{-3}) against the observed rate constants (s^{-1}) obtained for the decay of the second primary photoproduct at 298K under 1.0 atmosphere of CO.

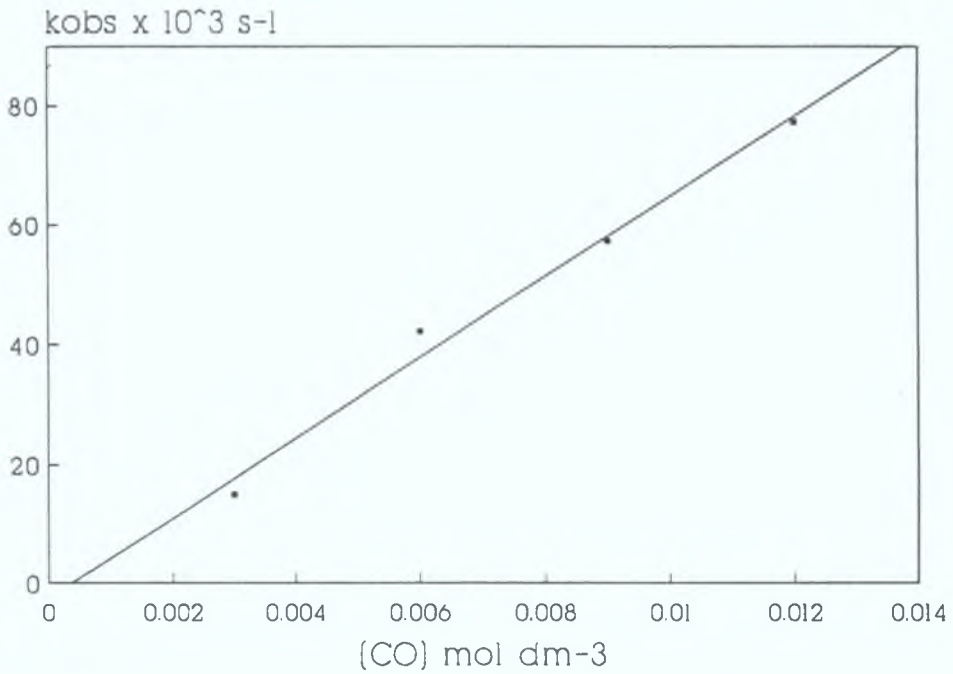

[CO] mol dm^{-3}	k_{obs} s^{-1}
0.003	15048
0.006	42257
0.009	56269
0.012	77323

$k_{[co]} = 6.7 \times 10^6 \pm 0.6 \times 10^6$ dm^3 mol^{-1} s^{-1}

Intercept = -2486 ± 3870 s^{-1}

Corr. Coeff. = 0.993

Figure 2.2.1.2.5 A second order plot of the observed rate constants (s^{-1}) for the decay of the first primary photoproduct with different concentrations of CO (mol dm^{-3}) at 298K.

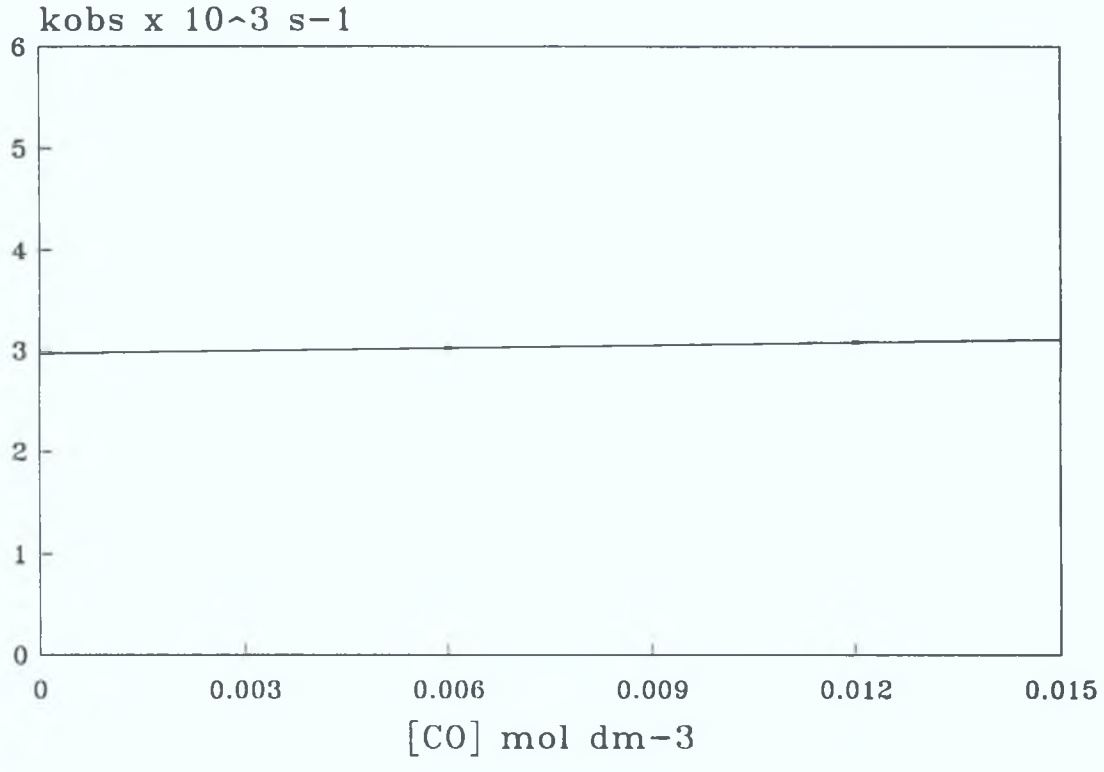

[CO] mol dm^{-3}	k_{obs} s^{-1}
0.006	3023
0.012	3075

Figure 2.2.1.2.6 A plot of the observed rate constants (s^{-1}) for the decay of the second primary photoproduct with different concentrations of CO (mol dm^{-3}) at 298K.

The rate constant for the reaction of species 1 with CO, 6.7 x 10^6 dm^3 mol^{-1} s^{-1}, is similar, if a little faster, to that reported for the reaction of $Cr(CO)_5(S)$ with CO in cyclohexane (3.0 x 10^6 dm^3 mol^{-1})[8]. A study into the primary photochemical reactions of (η^5-C_5H_5)$Mn(CO)_3$[5(f)], structurally analagous to (η^6-benzene)$Cr(CO)_3$, concluded that a molecule of solvent probably occupies the vacant coordination site to give a (η^5-C_5H_5)$Mn(CO)_2(S)$ species; as in the case of $M(CO)_5$ in most reactions[2(b)]. Similar experiments have shown that $M(CO)_5(S)$ is the only detectable species in hydrocarbon solution even on a picosecond time-scale[9]. On the basis of these results, the primary photoproduct, species 1, is assigned to (η^6-benzene)$Cr(CO)_2(S)$, S=cyclohexane, where a molecule of solvent occupies the vacant coordination site of (η^6-benzene)$Cr(CO)_2$ as a "token" ligand. This observation of CO loss as a primary photoreaction is in accordance with matrix isolation studies on (η^6-arene)$Cr(CO)_3$ by several research groups[3(c), 10].

The observed kinetic behaviour implies that two reactive species exist at comparable concentrations in the time domain under study. The question arises as to whether the two species are generated consecutively or simultaneously from the (η^6-benzene)$Cr(CO)_3$ precursor. The results obtained in the presence of various concentrations of CO indicate that species 2 cannot be formed in a reaction involving species 1. If this were the case, then the yield of species 2 would be reduced upon increasing the concentration of CO, assuming that species 1 is the carbonyl loss product (η^6-benzene)$Cr(CO)_2(S)$. It is evident, therefore, that at least two primary photoproducts are produced following the photolysis of (η^6-benzene)$Cr(CO)_3$ in

cyclohexane solution. Previous studies only revealed evidence for the formation of one primary photoproduct as the UV region of the spectrum was not examined.

2.2.1.3 Spectra of Primary Photoproducts

The UV/vis difference spectra obtained from 355nm laser flash photolsis experiments in cyclohexane solution are given in Figure 2.2.1.3.1. The spectrum at 2μs represents the co-addition of the transient absorption spectra of both primary photoproducts. The significant spectral features are the negative band at *ca.* 320nm, arising from depletion of the parent tricarbonyl (λ_{max} = 316nm), and the positive absorption band in the UV region at *ca.* 285nm which occurs in the valley of the absorption profile of the parent compound. In contrast to this strong differential absorption at 285nm, the absorption at higher wavelengths, λ>400nm, is very weak. The transient absorption spectrum at 70μs after the laser pulse is essentially a spectrum of species 2 alone. This spectrum is almost identical to that recorded at 2μs after the laser flash, given the reduced intensity of the transient absorptions. These spectra demonstrate the importance of monitoring these processes in the UV region of the spectrum as neither species absorbs light strongly in the visible region.

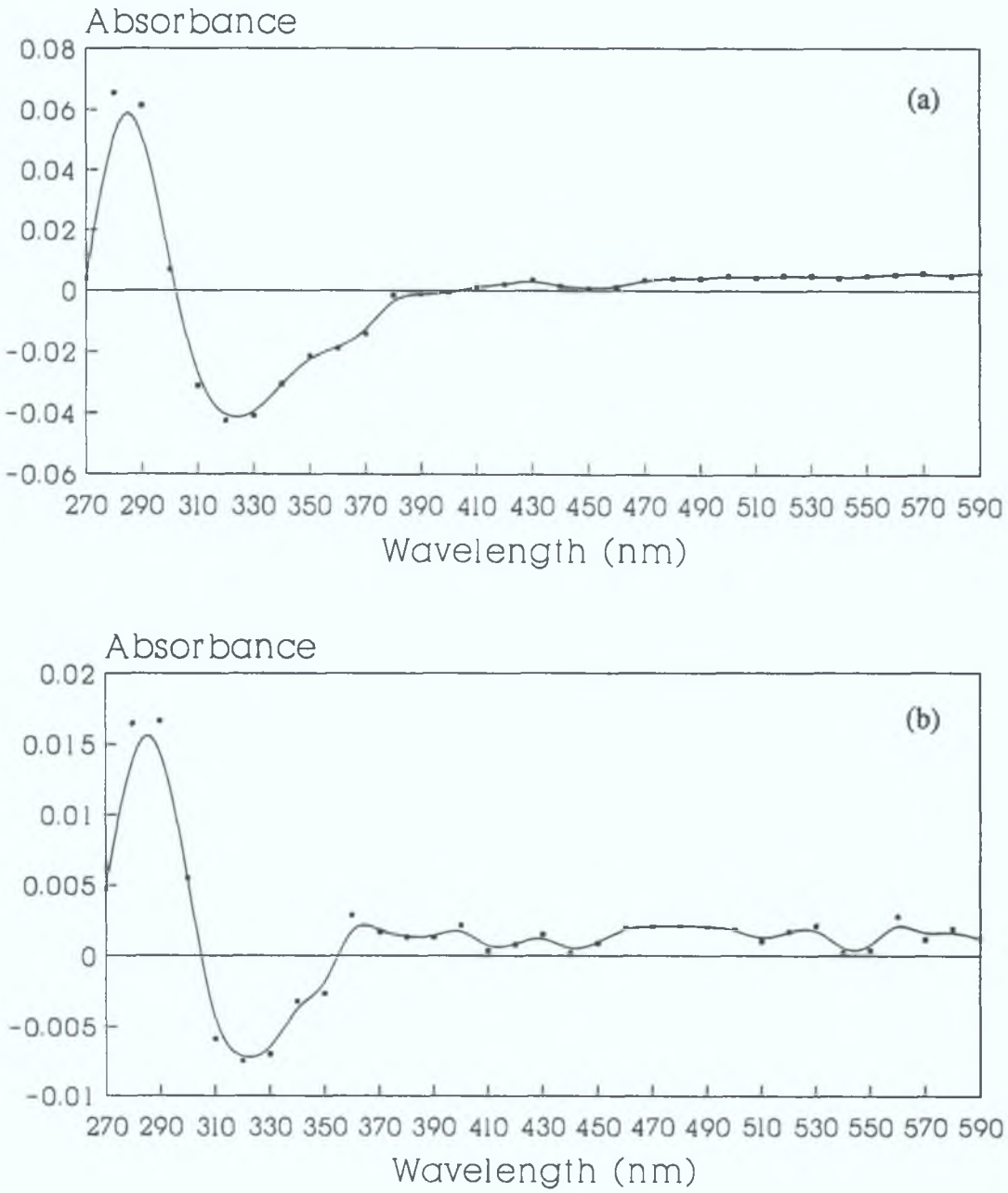

Figure 2.2.1.3.1 UV/vis difference spectra recorded at 2μs (a) and 70μs (b) following 355nm laser flash photolysis of (η^6-benzene)$Cr(CO)_3$ in cyclohexane solution.

2.2.1.4 Effect of Power of Laser on Concentration of Primary Photoproducts

In order to confirm that both transient species were produced as the result of single photon events, an experiment was performed in which the intensity of the laser pulse was varied systematically. The absorbances of the primary photoproducts should vary linearly with the power of the laser. The absorbance was measured at 2μs after the laser flash, at the maximum absorbance of both primary photoproducts, and at 50μs after the laser flash where the decay of species 1 is completed and the absorbance is effectively due to species 2 alone. The results are shown in Figure 2.2.1.4.1, where the relative power of the laser is plotted against the absorbances of the primary photoproducts. There is more error involved in the values recorded at 50μs as the absorbance values plotted were lower. It was concluded that neither of these transient absorptions arose from species produced in multiphoton events.

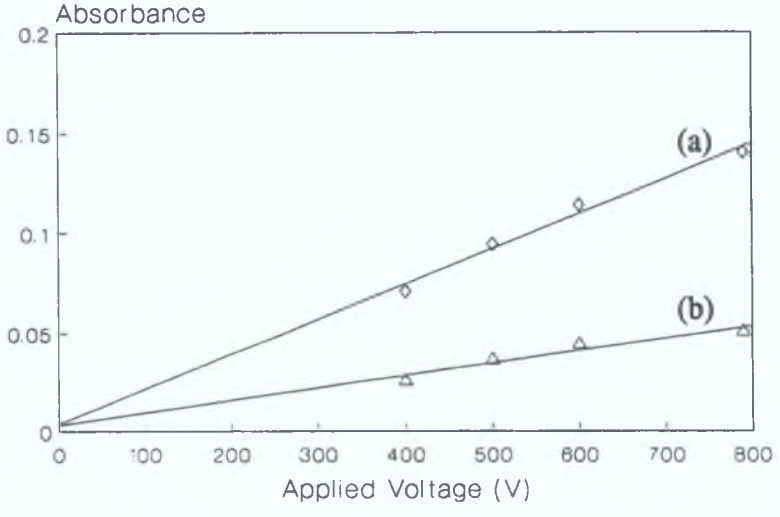

Figure 2.2.1.4.1 Plot showing the variation in the absorbance of the transient species with relative laser power. The absorbances were recorded 2μs(a) and 50μs(b) after the laser pulse.

2.2.1.5 Effect of Laser Irradiation Wavelength on Primary Photoproduct Production

No difference could be observed in the relative yields nor the kinetic behaviour of the primary photoproducts produced following excitation of (η^6-benzene)$Cr(CO)_3$ with 266nm irradiation, as compared to the results obtained on 355nm irradiation. The absorbances were measured at 280nm under at a CO concentration of 1.2×10^{-2} mol dm^{-3}. These results are given in Table 2.2.1.5.1. Therefore, there is no evidence for a wavelength dependancy in the photochemistry of (η^6-benzene)$Cr(CO)_3$. This confirms and extends the observation by Wrighton *et al.* for a lack of wavelength dependance in the photochemistry of (η^6-benzene)$Cr(CO)_3$, for wavelengths > 313nm[6(d)].

	k_{obs} s^{-1}	
	355nm	266nm
(η^6-benzene)$Cr(CO)_2$(S)	77679	82252
Species 2	3800	3049

Table 2.2.1.5.1 A comparison of the observed rate constants of the primary photoproducts produced on laser flash photolysis of (η^6-benzene)$Cr(CO)_3$ with 355nm and 266nm laser irradiation; at a CO concentration of 1.2×10^{-2} mol dm^{-3} at 298K.

2.2.1.6 Effect of Liquid-Pumping on Laser Flash Photolysis Transient Species

It is found that upon three freeze-pump-thaw degassing cycles followed by liquid pumping of the sample solution at room temperature (where cyclohexane solvent is pumped off under vacuum and the solution is effectively concentrated) the yield of the second transient species is greatly reduced and with extensive liquid pumping only species 1 is detectable under these circumstances The rate of decay of species 1 is unaffected by this procedure while the yield is increased slightly The transient signal recorded after liquid pumping of a cyclohexane solution of (η^6-benzene)$Cr(CO)_3$ under 1 0 atmosphere of CO is displayed in Figure 2 2.1 6.1 This signal fits a single first-order kinetic process, k_{obs} = 7 4 x 10^4 s^{-1}, returning almost to the baseline value with little residual absorption.

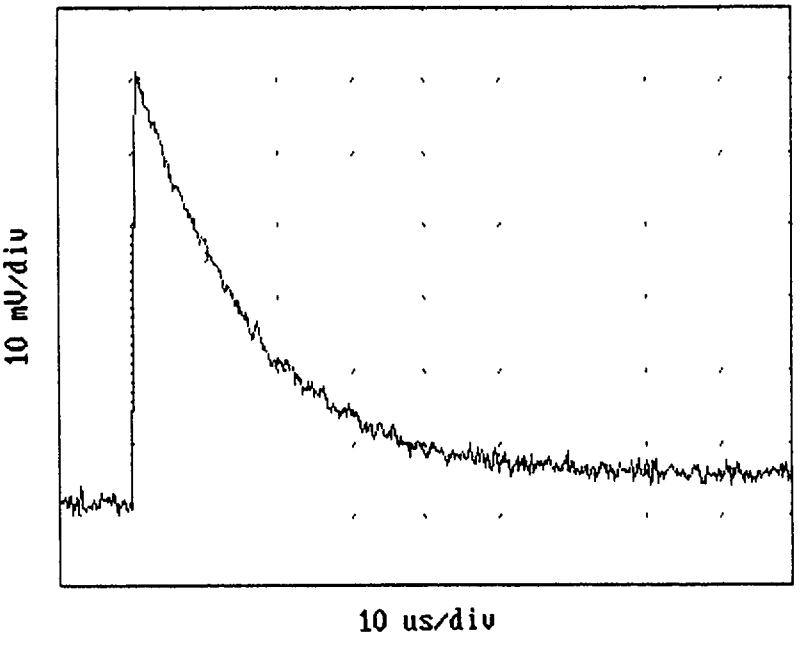

Figure 2.2.1.6.1 Oscilloscope trace of transient absorption species recorded at 280nm under 1 0 atmosphere of CO after liquid pumping of the solution

These experiments conducted with solvents of different dryness suggest that the formation of an impurity complex, possibly involving the binding of water molecules, might be responsible for the second transient absorption signal. No spectral changes are detected in the electronic absorption spectrum of the parent throughout the experiment; indicating that this species eventually regenerates the parent molecule. This transient species could be coordinatively saturated, hence the observation that the second transient species does not react with CO. Impurities in the solvent, some of which may have been introduced during the degassing procedures, have been shown to have a dramatic effect on the photochemistry of $Cr(CO)_6$ as monitored by conventional and ns flash photolysis[11].

2.2.1.7 A Study of the Activation Parameters for the Reaction of (η^6-benzene)$Cr(CO)_2$(S) with CO

Activation parameters for the reaction of (η^6-benzene)$Cr(CO)_2$(S) with CO were measured from Arhenius and Eyring Plots over a temperature range of 283 to 321K. It was assumed that the solubility of CO in cyclohexane remains constant for this range of temperatures[7]. The results are detailed in Table 2.2.1.7.1 and illustrated graphically in Figure 2.2.1.7.1. The calculated activation parameters are similar to those associated with the reaction of $Cr(CO)_5$(S) with CO in cyclohexane: i.e. low activation enthalpy and large negative activation entropy[12]. They are also similar in magnitude to those determined for the reaction of (η^5-C_5H_5)$Mn(CO)_2$(S) and (η^4-C_4H_4)$Fe(CO)_2$(S) with CO[5(b)]. The value of $\Delta S^{\neq}$ is not extremely negative as expected for a purely associative reaction ($\Delta S^{\neq} < -120$ J mol^{-1} K^{-1}); the slightly negative value indicates an interchange mechanism for the transition state.

The activation parameters are therefore consistent with the following reaction scheme, where Ar = η^6-benzene.

$$ArCr(CO)_3 \xrightarrow{h\nu} ArCr(CO)_2 + CO \quad (2.2.1.7.1)$$

$$ArCr(CO)_2 + S \longrightarrow ArCr(CO)_2(S) \quad (2.2.1.7.2)$$

$$ArCr(CO)_2(S) + CO \longrightarrow [ArCr(CO)_2(S)(CO)] \quad (2.2.1.7.3)$$

$$[ArCr(CO)_2(S)(CO)] \longrightarrow ArCr(CO)_3 + S \quad (2.2.1.7.4)$$

Loss of CO and coordination of a cyclohexane molecule by the coordinatively unsaturated fragment occurs in a matter of ps and is not observable over the time-scales used here. Reaction 2.2.1.7.3 is the rate determining step.

Table 2.2.1.7.1 (a) Experimental data for the determination of the energy, entropy and enthalpy of activation for the reaction of (η^6-benzene)$Cr(CO)_2(S)$ with CO; [(η^6-benzene)$Cr(CO)_3$] = 2.1 x 10^{-4} mol dm^{-3} and [CO] = 1.2 x 10^{-2} mol dm^{-3}.

1/T (x 10^3)	Ln(k_{obs}/[CO])	Ln((k_{obs}/[CO])/T)
3.53	15.18	9.53
3.46	15.53	9.86
3.36	15.73	10.03
3.29	16.93	10.21

Arrhenius Plot	Eyring Plot	Activation Parameters
Slope = -2959 ± 404	Slope = -2666 ± 404	E_a = 25 ± 3 kJ mol^{-1}
Int. = 25.68 ± 0.07	Int. = 19.00 ± 0.07	$\Delta H^{\neq}$ = 22 ± 3 kJ mol^{-1}
Corr. Coeff. = 0.982	Corr. Coeff. = 0.978	$\Delta S^{\neq}$ = -40 ± 20 J mol^{-1} K^{-1}

Table 2.2.1.7.1 (b) Experimental data for the determination of the energy, entropy and enthalpy of activation for the reaction of (η^6-benzene)$Cr(CO)_2(S)$ with CO; [(η^6-benzene)$Cr(CO)_3$] = 2.6 x 10^{-4} mol dm^{-3} and [CO] = 1.2 x 10^{-2} mol dm^{-3}.

1/T (x 10^3)	Ln(k_{obs}/[CO])	Ln((k_{obs}/[CO])/T)
3.46	15.44	9.78
3.38	15.60	9.91
3.33	15.72	10.01
3.28	15.96	10.23
3.23	16.06	10.32
3.17	16.20	10.45
3.11	16.52	10.75

Arrhenius Plot	**Eyring Plot**	**Activation Parameters**
Slope = -3050 ± 205	Slope = -2744 ± 203	E_a = 25 ± 2 kJ mol^{-1}
Int. = 25.94 ± 0.06	Int. = 19.21 ± 0.06	$\Delta H^{\neq}$ = 23 ± 2 kJ mol^{-1}
Corr. Coeff. = 0.989	Corr. Coeff. = 0.987	$\Delta S^{\neq}$ = -38 ± 20 J mol^{-1} K^{-1}

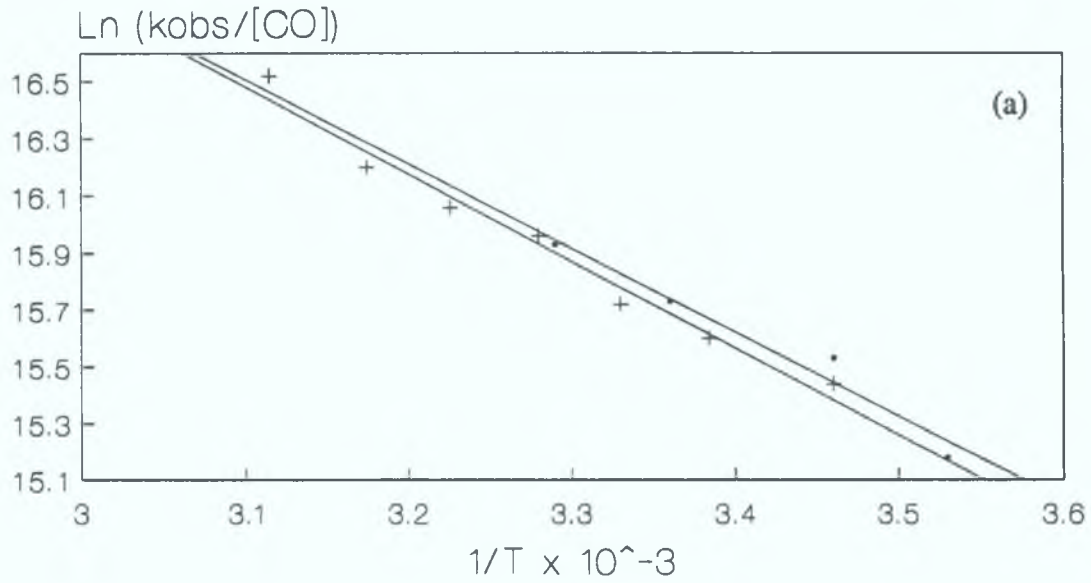

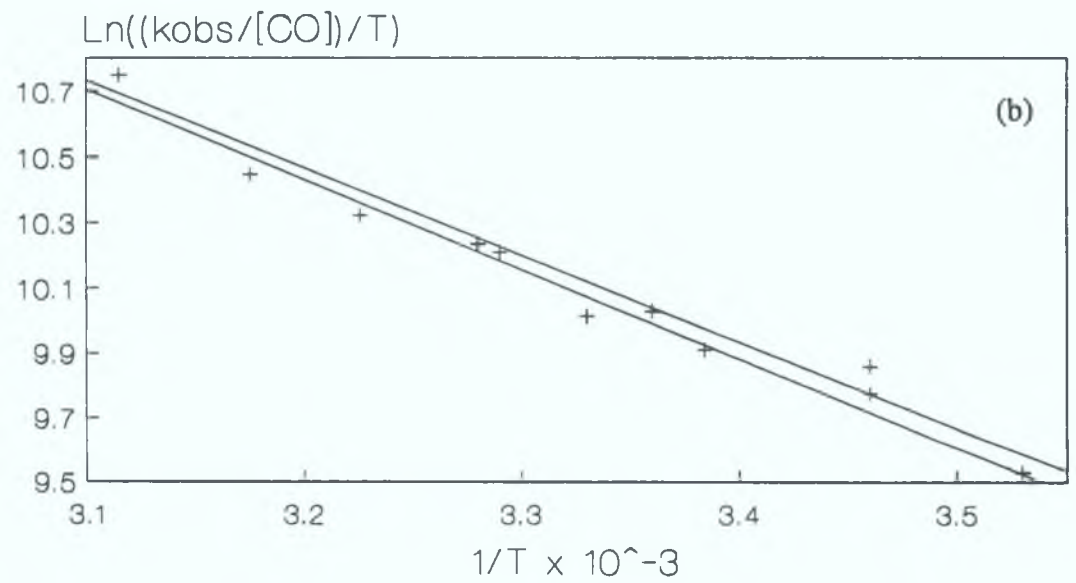

Figure 2.2.1.7.1 Arrhenius (a) and Eyring (b) plots for the reaction of (η^6-benzene)$Cr(CO)_2(S)$ with CO.

2.2.1.8 A Study of the Activation Parameters for Species 2

Species 2 was found not to react with CO or parent. The decay of this species is assumed therefore to be a true first order, and not a psuedo-first order, process. Activation parameters were measured from Arrhenius and Eyring Plots over a temperature range of 284 to 321K. The results are detailed in Table 2.2.1.8.1 and illustrated graphically in Figure 2.2.1.8.1 where T = temperature (K). These values were obtained at a CO concentration of 1.2×10^{-2} mol dm^{-3}.

Table 2.2.1.8.1 (a) Experimental data for the determination of the energy, entropy and enthalpy of activation for the reaction of species 2; $[(\eta^6\text{-benzene})Cr(CO)_3] = 2.1 \times 10^{-4}$ mol dm^{-3}.

$1/T$ ($\times 10^3$)	$Ln(k_{obs})$	$Ln(k_{obs}/T)$
3.52	6.79	1.14
3.46	7.25	1.59
3.36	7.98	2.28
3.29	8.31	2.59

Arrhenius Plot	Eyring Plot	Activation Parameters
Slope = -6711 ± 433	Slope = -6418 ± 432	$E_a = 56 \pm 4$ kJ mol^{-1}
Int. = 30.45 ± 0.08	Int. = 23.77 ± 0.08	$\Delta H^{\neq} = 53 \pm 4$ kJ mol^{-1}
Corr. Coeff. = 0.996	Corr. Coeff. = 0.995	$\Delta S^{\neq} = 0 \pm 20$ J mol^{-1} K^{-1}

Table 2.2.1.8.1 (b) Experimental data for the determination of the energy, entropy and enthalpy of activation for the reaction of species 2; $[(\eta^6\text{-benzene})Cr(CO)_3] = 2.6 \times 10^{-4}$ mol dm^{-3}.

$1/T$ (x 10^3)	$Ln(k_{obs})$	$Ln(k_{obs}/T)$
3.46	7.08	1.42
3.38	7.49	1.80
3.33	8.01	2.31
3.28	8.30	2.58
3.23	8.66	2.93
3.17	9.01	3.25
3.11	9.44	3.66

Arrhenius Plot	Eyring Plot	Activation Parameters
Slope = -6879 ± 190	Slope = -6574 ± 190	$E_a = 57 \pm 2$ kJ mol^{-1}
Int. = 30.86 ± 0.06	Int. = 24.14 ± 0.06	$\Delta H^{\neq} = 55 \pm 2$ kJ mol^{-1}
Corr. Coeff. = 0.998	Corr. Coeff. = 0.998	$\Delta S^{\neq} = 3 \pm 20$ J mol^{-1} K^{-1}

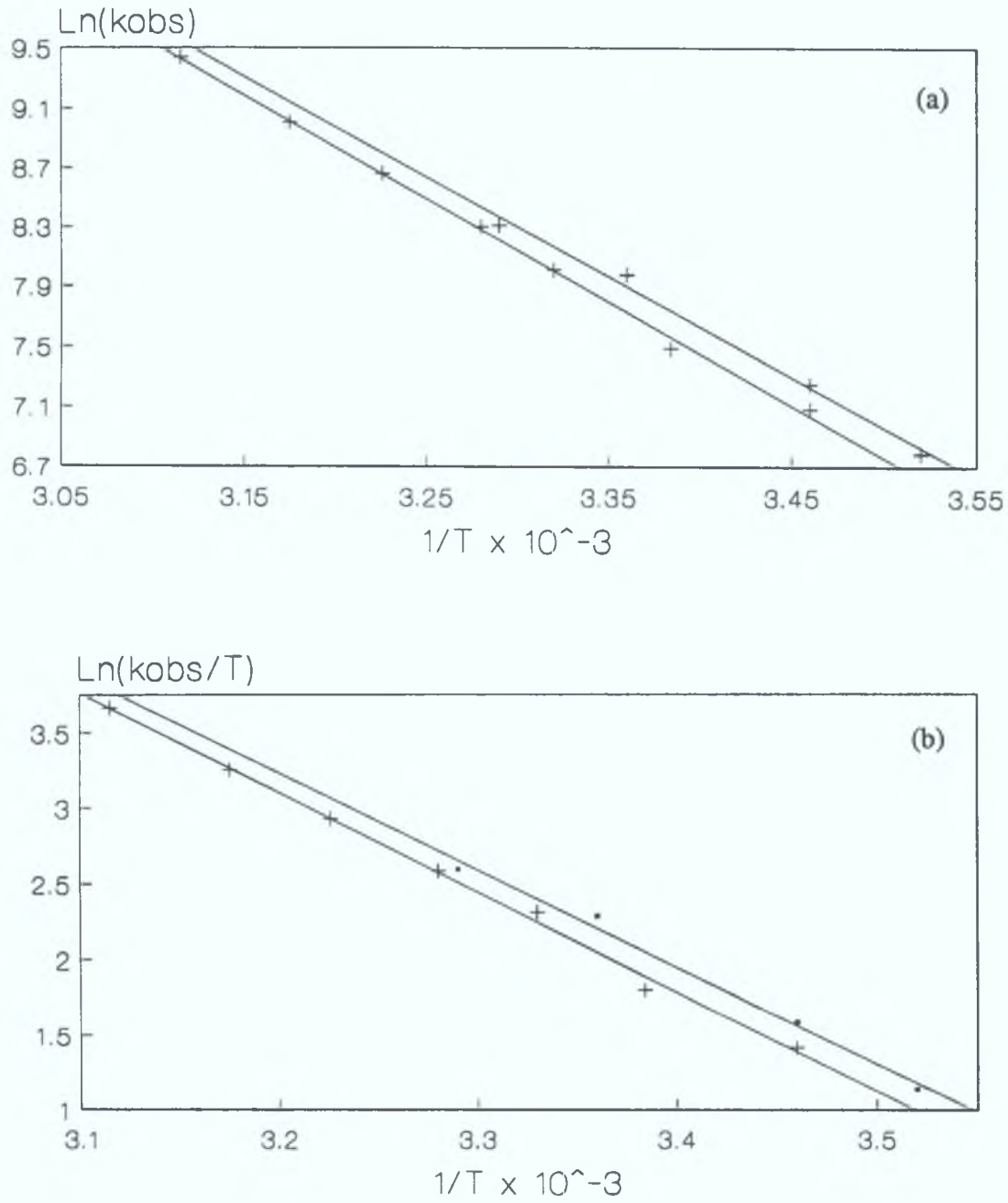

Figure 2.2.1.8.1 Arrhenius (a) and Eyring (b) plots for the reaction of species 2.

From the activation parameters determined it is obvious that two transient species are present which do not react in the same manner. The thermodynamic parameters associated with the reaction of species 2 with CO are clearly different to those expected for the reaction of a formally coordinatively unsaturated carbonyl compound. The enthalpy of activation is significantly larger in this case. It is clear from structural studies on (η^6-benzene)$Cr(CO)_3$ that the three carbonyl ligands in this compound are chemically equivalent[13] and therefore it is impossible to produce more than one single carbonyl loss product from this parent molecule. The only other likely primary photoproduct would seem to be one involving a hapticity change at the arene ligand. A hapticity change of at least two, which would open up a vacant coordination site on the chromium atom, would seem to be the most likely transformation, e.g. a η^6 to a η^4 hapticity change. (η^4-arene)$Cr(CO)_4$ compounds have been reported[14], and a molecular structure of (η^6-C_6Me_6)$Cr(CO)_3$ has been determined by single crystal X-ray diffraction in which the hexamethylbenzene adopts the Dewar benzene conformation[15]. Also, Dewar benzene can be produced by irradiation of benzene under suitable conditions[16]. The observation that species 2 does not react with CO suggests that this species is coordinatively saturated while the results obtained on liquid pumping indicate that this species arises from reaction of a photoproduct with impurity ligand. Consequently, transient species 2 is most plausibly assigned to an (η^4-benzene)$Cr(CO)_3(H_2O)$ species. The production of this complex would not only involve a reaction of the metal centre with the impurity ligand, but also a conformational change at the arene ligand; hence the large enthalpy of activation. It is not possible using UV/vis transient spectroscopy to unambiguously

assign a structure to this proposed η^4-benzene species. The series of reactions occuring may be as follows, where Ar = benzene.

$$(\eta^6\text{-Ar})Cr(CO)_3 \xrightarrow{h\nu} (\eta^4\text{-Ar})Cr(CO)_3 \qquad (2.2.1.8.1)$$

$$(\eta^4\text{-Ar})Cr(CO)_3 + H_2O \longrightarrow (\eta^4\text{-Ar})Cr(CO)_3(H_2O) \qquad (2.2.1.8.1)$$

$$(\eta^4\text{-Ar})Cr(CO)_3(H_2O) \longrightarrow (\eta^6\text{-Ar})Cr(CO)_3 + H_2O \qquad (2.2.1.8.1)$$

On liquid pumping, the removal of solvent impurity could preclude the formation of the $(\eta^4$-benzene$)Cr(CO)_3(H_2O)$ species, leaving the coordinatively unsaturated $(\eta^4$-benzene$)Cr(CO)_3$ species in solution which then regenerates the parent complex; this should occur on much shorter timescales as the coordinatively unsaturated species would be more unstable than the fully coordinatively saturated species.

2.2.1.9 Time Resolved Infrared Spectrum of $(\eta^6$-benzene$)Cr(CO)_2(S)$

The TRIR spectrum obtained within 1μs following the laser flash photolysis of $(\eta^6$-benzene$)Cr(CO)_3$ in n-heptane under 2.0 atmospheres of CO is displayed in Figure 2.2.1.9.1. In this spectrum the negative peaks represent the depletion of the parent absorbances at 1983cm^{-1} and 1915cm^{-1}. The two positive peaks in the ν_{CO} region of the spectrum at 1927cm^{-1} and 1877cm^{-1} correspond to photoproduct production. The number and nature of the bands are consistent with their assignment as the A_1 (1927cm^{-1}) and the B_1 (1877cm^{-1}) terminal carbonyl stretching modes of a $(\eta^6$-benzene$)Cr(CO)_2(S)$ species having local C_{2v} symmetry. The loss of a carbonyl ligand would tend to make the remaining ligands more tightly held to the metal, with an increase in the force constant of the bond and a corresponding decrease in the ν_{CO}

stretching frequencies. The band positions are in agreement with previous studies in methane matrices and nujol mull matrices, Table 2.2.1.9.1.

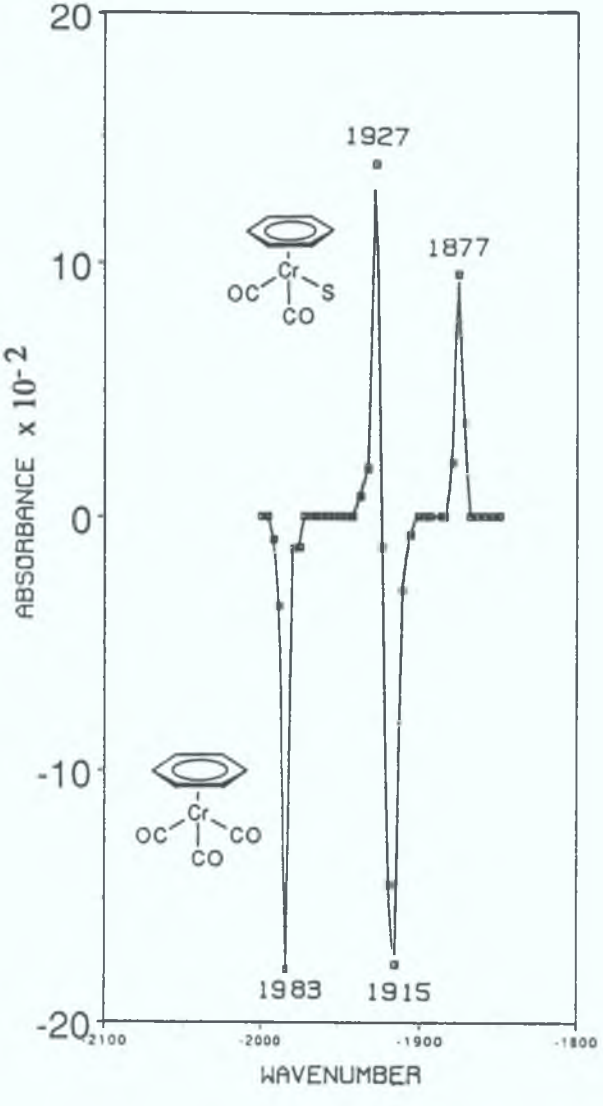

Figure 2.2.1.9.1 Time resolved infrared spectrum of (η^6-benzene)$Cr(CO)_3$ obtained within 1μs after the laser flash in n-heptane solution under 2.0 atmospheres of CO.

Table 2.2.1.9.1 A comparison of the IR stretching frequencies (cm^{-1}) for (η^6-benzene)$Cr(CO)_3$ and (η^6-benzene)$Cr(CO)_2$ detected in various media. [a]Reference 10(b). [b]Reference 10(a). [c]this work.

Medium	Temperature	ν_{CO} (η^6-C_6H_6)$Cr(CO)_3$	ν_{CO} (η^6-C_6H_6)$Cr(CO)_2$
nujol matrix[a]	77K	1980,1909	1921,1868
methane matrix[b]	12K	1983,1913	1925,1870
n-heptane solution[c]	303K	1983,1915	1927,1877

The results of this TRIR experiment confirm, for the first time, that (η^6-benzene)$Cr(CO)_2$(S) is indeed a primary photoproduct in alkane solution at room temperature. As with $M(CO)_5$ species (M = Cr, Mo, or W), it is likely that the vacant coordination site in this intermediate is occupied by a molecule of solvent (S) as a "token" ligand[17]. The second order rate constant for the reaction of this (η^6-benzene)$Cr(CO)_2$(n-heptane) species with CO was calculated to be 3.0×10^7 dm^{-3} mol^{-1} s^{-1}. To allow a direct comparison of the observed rate constants in the TRIR and flash photolysis experiments, the experiments were repeated in identical solvents. The results obtained using the two techniques are in close agreement; Table 2.2.1.9.2, confirming the assignment of the first observed photoproduct in the UV/vis experiments as the solvated (η^6-benzene)$Cr(CO)_2$(S) species.

An interesting point to note is the difference in rate constants between experiments carried out in cyclohexane and n-heptane solution. The rate constants observed in linear alkanes (pentane, n-heptane) are approximately 2-3 times faster than those observed in cyclohexane. This is consistent with the trend for displacement of heptane and cyclohexane from $Cr(CO)_5$(alkane) by strongly bonding ligands. Invariably heptane is displaced faster than cyclohexane[2(a),5,18,19]. Greater rates of displacement for heptane *versus* cyclohexane were also observed for (η^5-C_5H_5)$Mn(CO)_2$(alkane)[5]. This implies that different interaction energies are involved in the coordination of cyclohexane to the metal as chemically these solvents differ only in shape. Gas phase studies with $W(CO)_5$ indicate a binding enthalpy of 44 kJ mol^{-1} for n-pentane and 48 kJ mol^{-1} for cyclohexane[20]. Photoacoustic calorimetric studies have shown that n-heptane and cyclohexane bind to the coordinatively unsaturated $Cr(CO)_5$ fragment with an interaction energy of 40 and 53 kJ mol^{-1} respectively[21]. This observation has been used to explain the differences in reactivity of the photofragments generated in cyclic as opposed to linear alkane solution. The higher activation energies associated with cyclohexane may be attributed to stronger coordination of the cyclohexane molecule to the metal centre. It has been suggested that these complexes have a stereospecific interaction between the metal and alkane that can only be formally described as an intermolecular agostic bond and that these bonds prefer to form with secondary CH rather than primary CH. This may be attributed to the fact that secondary CH bonds are less sterically hindered than primary CH bonds. An electronic factor favouring secondary agostic bonds may

be that secondary CH are more electron rich than primary CH. It is these variations which are thought to result in differences in the reactivity of the photoproducts.

Table 2.2.1.9.2 A comparison of the second order rate constants for the reaction of (η^6-benzene)$Cr(CO)_2(S)$ with CO in various media, as measured by transient UV and TRIR experimental techniques.

Solvent	k_2 dm^3 mol^{-1} s^{-1}	Temp K	Technique
cyclohexane	$6.7 \times 10^6 \pm 0.7 \times 10^6$	303	UV
cyclohexane	$7.5 \times 10^6 \pm 0.8 \times 10^6$	299	TRIR
pentane	$1.8 \times 10^7 \pm 0.2 \times 10^7$	303	UV
n-heptane	$3.0 \times 10^7 \pm 0.3 \times 10^7$	300	TRIR

2.2.1.10 Time Resolved Infrared Spectrum of (η^6-benzene)$Cr(CO)_2(H_2O)$

The TRIR spectrum obtained 20μs following the laser flash photolysis of (η^6-benzene)$Cr(CO)_3$ under 2.0 atmospheres of CO is depicted in Figure 2.2.1.10.1. The cyclohexane solvent used in this experiment was of spectroscopic grade, with no distillation prior to use. The negative band at 1915cm^{-1} arises from depletion of the parent absorption; the edge of the second parent peak is observed as a negative deflection at 1980cm^{-1}. A band attributed to a photoproduct is observed at 1902cm^{-1}; a positive deflection at 1852cm^{-1} indicates the presence of a second photoproduct band. As such, the spectrum is incomplete and should be repeated over a larger

wavenumber range than was monitored in order to fully record the bands of parent and photoproduct. The observed photoproduct is assigned to a (η^6-benzene)$Cr(CO)_2$(impurity) complex. Photoproducts produced on photolysis of metal carbonyl precursors are known to be extremely reactive and can coordinate trace amounts of impurities present in the solvent. Poliakoff *et al.* reported the production of $Cr(CO)_5N_2$ by the UV photolysis of $Cr(CO)_6$ in liquid xenon solution[22]. This species was produced on coordination of trace amounts (<1 p.p.m.) of N_2 present in the noble gas to the photolysis product, reaction 2.2.1.10.1.

$$Cr(CO)_6 + N_2 \xrightarrow{h\nu} Cr(CO)_5(N_2) + CO \qquad (2.2.1.10.1)$$

In the case of this experiment, it is likely that the interference was caused by trace levels of water present in the non-distilled cyclohexane. Church *et al.* observed a complex assigned as the $Cr(CO)_5(H_2O)$ product in a study into the photoreactions of $Cr(CO)_6$[18]. The infrared frequencies of this complex were shifted to lower frequency (i.e. higher energy) of the $Cr(CO)_5$ photoproduct by 14-21cm^{-1}; Table 2.2.1.10.1. In this study the A_1 band of the (η^6-benzene)$Cr(CO)_2$ photoproduct is shifted by 25cm^{-1} to lower frequency as compared to the TRIR spectrum of (η^6-benzene)$Cr(CO)_2$(S) recorded in n-heptane. A similar shift in the B_1 band of the complex allows a predicted frequency of 1850cm^{-1} for the second peak; identical to the position of the positive deflection in the TRIR spectrum observed experimentally. Church *et al.* also noted that the IR bands of $Cr(CO)_5(H_2O)$ were approximately twice as broad as those of $Cr(CO)_5(C_6H_{12})$, a similar feature is noted here on

comparison of the photoproduct bands with those of (η^6-benzene)$Cr(CO)_2$(n-heptane) recorded earlier.

In addition to the bands attributed to parent and (η^6-benzene)$Cr(CO)_2(H_2O)$ photoproduct, there is a very weak band at 1962cm^{-1} evident in this spectrum, and possibly a second band at 1890cm^{-1}. These bands could arise from the absorptions of a (η^4-C_6H_6)$Cr(CO)_3(H_2O)$ species; additional bands of which may be obscured by the more intense absorptions of the other species present. As the (η^4-C_6H_6)$Cr(CO)_3(H_2O)$ complex is not as highly symmetrical as the (η^6-benzene)$Cr(CO)_2$(S) photoproduct any infrared absorptions would be expected to be very weak. Also, the extinction coefficient of the (η^4-C_6H_6)$Cr(CO)_3(H_2O)$ species may be much lower than that of the (η^6-benzene)$Cr(CO)_2$ species, while they may be comparable in the ultraviolet region. However, as this spectrum was recorded 'single-shot' these weak absorption peaks may be attributed to an artifact and these results should ideally be repeated for verification.

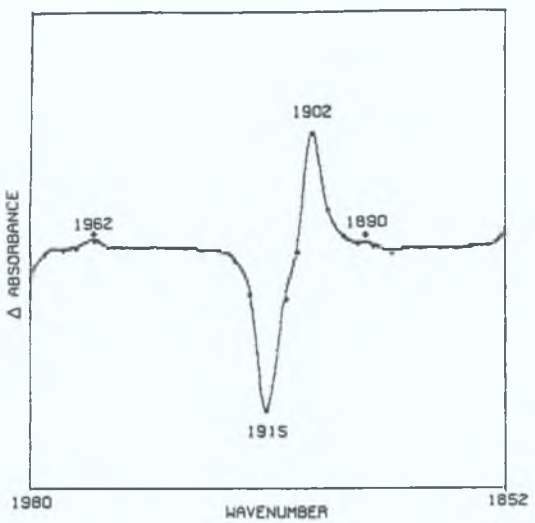

Figure 2.2.1.10.1 Time resolved infrared spectrum of (η^6-benzene)$Cr(CO)_2(H_2O)$ recorded 20μs after the laser pulse in non-distilled cyclohexane solution.

Table 2.2.1.10.1 A comparison of the IR stretching frequencies (cm^{-1}) for $Cr(CO)_5$, $Cr(CO)_5(H_2O)$, (η^6-benzene)$Cr(CO)_2$(n-heptane). and (η^6-benzene)$Cr(CO)_2(H_2O)$. [a]Church *et al.* in cyclohexane solution at 298K[18] [b]this work, n-heptane solution at 303K. [c]this work, cyclohexane solution at 303K.

Complex	ν_{CO}
$Cr(CO)_5$[a]	1960,1937
$Cr(CO)_5(H_2O)$[a]	1946,1916
(η^6-benzene)$Cr(CO)_2$(n-heptane)[b]	1927,1877
(η^6-benzene)$Cr(CO)_2(H_2O)$[c]	1902,1850

2.2.2 Photochemistry of Methyl-Substituted (η^6-arene)$Cr(CO)_3$ Compounds

2.2.2.1 Introduction

In the previous section (η^6-benzene)$Cr(CO)_2(S)$ has been identified as a primary photoproduct on laser flash photolysis of (η^6-benzene)$Cr(CO)_3$ in room temperature solution. A series of substituted (η^6-arene)$Cr(CO)_3$ complexes was synthesised in order to study the effect of methyl-substitution of the arene ring on the observed photoreactions. It was thought that any hapticity change product produced would be increasingly stablised by the presence of the methyl groups, as the electron donating effect of the arene ligand increases throughout the series. The increased bulkiness of the arene ligand also introduces the possibility of steric hindrance as a factor for consideration in the photoreactions.

2.2.2.2 Electronic Spectra of Methyl-Substituted (η^6-arene)$Cr(CO)_3$ Compounds

Absorption spectra of (η^6-benzene)$Cr(CO)_3$ and related complexes that have been studied are dominated by MLCT absorptions[6]. The absorption spectra of the series of (η^6-arene)$Cr(CO)_3$ complexes studied are given in Figure 2.2.2.2.1. The prominent spectral feature is a sharp, intense band centred near 320nm which has been assigned as a M --> arene CT with some M --> π^*CO CT character. The next transition is clearly seen in the spectrum of the benzene complex centred at 264nm. It is assigned solely as a M --> π^*CO CT band. A hypsochromic shift (blue shift) of this band is observed as the number of electron-releasing methyl groups on the arene is increased; consequently this band is less resolved in the other arene complexes. It is

this band alone which reflects the reduction in CO bond order as the degree of methylation increases on going through the series. In the high energy region, a peak centred at *ca.* 220nm also involves a M --> π*CO CT transition. These transitions are summarised in Table 2.2.2.2.1.

All of the compounds detailed exhibit a well defined 'window' in the absorption profile at 280-290nm through which absorptions due to transient species may be observed. Again, the importance of viewing the transient species produced by these compounds in the UV region of the spectrum is emphasised. The extinction coefficients of the arene complexes at the excitation wavelength used in flash photolysis experiments (355nm), and the IR carbonyl stretching frequencies of the parent tricarbonyls in alkane solvent are detailed in Table 2.2.2.2.2. A reduction in the ν_{CO} is observed as the number of methyl groups on the arene ring increases; reflecting the slight decrease in bond order of the CO moiety with increasing electron donation from the arene ligand.

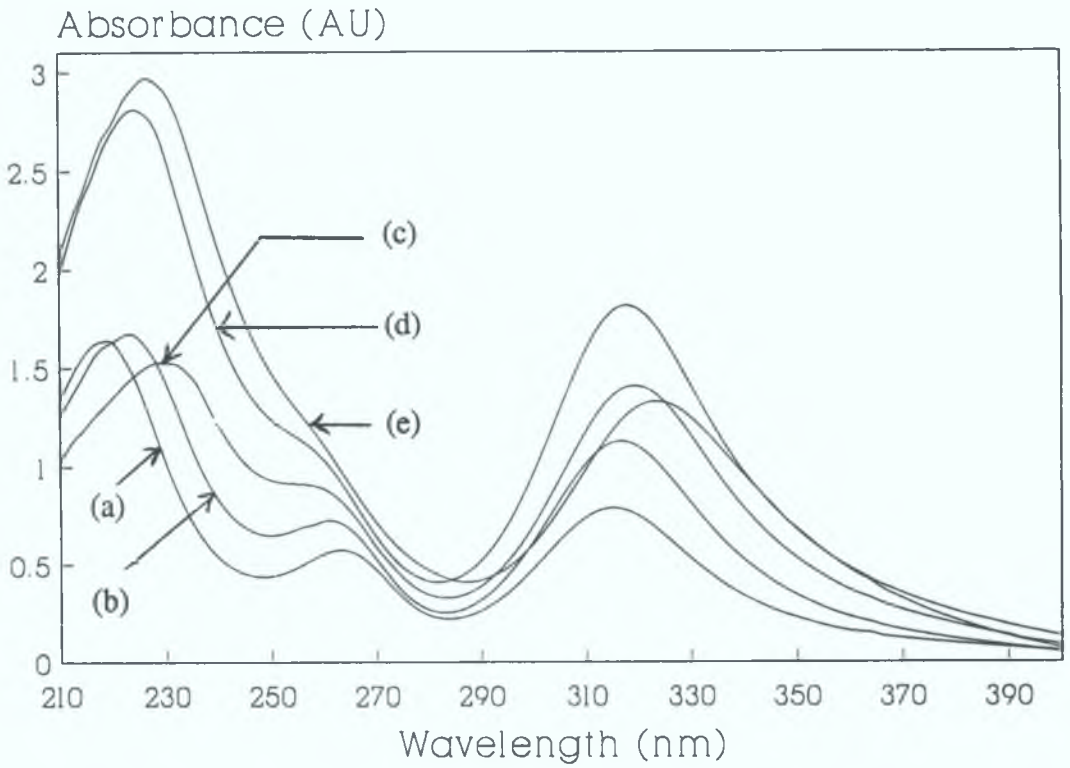

Figure 2.2.2.2.1 UV/vis absorption spectra of (η^6-arene)$Cr(CO)_3$ complexes in cyclohexane solution; (a) (η^6-benzene)$Cr(CO)_3$, 6.43 x 10^{-5} mol dm^{-3}; (b) (η^6-toluene)$Cr(CO)_3$, 7.43 x 10^{-5} mol dm^{-3}; (c) (η^6-p-xylene)$Cr(CO)_3$, 1.35 x 10^{-4} mol dm^{-3}; (d) (η^6-1,3,5-mesitylene)$Cr(CO)_3$, 1.83 x 10^{-4} mol dm^{-3}; and (e) (η^6-C_6H_6)$Cr(CO)_3$, 1.46 x 10^{-4} mol dm^{-3}.

Table 2.2.2.2.1 Spectral data for (η^6-arene)$Cr(CO)_3$ complexes, where (sh) denotes a shoulder on an absorption band

η^6-Arene	Bands, nm	Assignment	Reference
Benzene	376	LF?	[6(a), 6(b)]
	316	M --> arene, π*CO CT	
	264	M --> π*CO CT	
	220	M --> π*CO CT	
Toluene	316	M --> arene, π*CO CT	
	260	M --> π*CO CT	
	224	M --> π*CO CT	
P-Xylene	320	M --> arene, π*CO CT	
	256	M --> π*CO CT	
	230	M --> π*CO CT	
1,3,5-Mesitylene	316	M --> arene, π*CO CT	[6(a)-6(d)]
	254(sh)	M --> π*CO CT	
	216	M --> π*CO CT	
C_6Me_6	324	M --> arene, π*CO CT	[6(d)]
	250(sh)	M --> π*CO CT	
	226	M --> π*CO CT	

Table 2.2.2.2.2 A summary of the UV/vis extinction coefficients at 354nm (in cyclohexane) and the infrared carbonyl stretching frequencies (in n-pentane) for the series of (η^6-arene)$Cr(CO)_3$ compounds.

η^6-Arene	ε_{354nm} dm^3 mol^{-1} cm^{-1}	ν_{CO} cm^{-1}
Benzene	3060	1983,1915
Toluene	3940	1980,1913
P-Xylene	3390	1978,1909
1,3,5-Mesitylene	3220	1972,1904
C_6Me_6	4050	1970,1885

2.2.2.3 Preliminary Experimental Results

Laser flash photolysis of methyl substituted (η^6-arene)$Cr(CO)_3$ complexes (arene = toluene, p-xylene, 1,3,5-mesitylene, C_6Me_6) in non-liquid-pumped cyclohexane solvent under 1.0 atmosphere of CO reveals two first-order kinetics processes on the microsecond time-scale. The data yields two observed rate constants; for the short time portion and for the long time portion of the decay profiles. The observed rate constant of the first observed transient species was found to be directly dependant on the CO concentration present in solution, as previously noted for the (η^6-benzene)$Cr(CO)_2(S)$ complex. Also, the lifetime of this transient absorption monitored at 280-290nm is found to be very similar to that of the (η^6-benzene)$Cr(CO)_2(S)$ species previously assigned from TRIR and laser flash photolysis experiments. By analogy, this first transient species is therefore attributed to the (η^6-arene)$Cr(CO)_2(S)$ species. No evidence was found for a dependance of the

rate of decay of this species on the concentration of (η^6-arene)$Cr(CO)_3$ present in solution; for example in the case of (η^6-1,3,5-mesitylene)$Cr(CO)_3$, Figure 2.2.2.3.1.

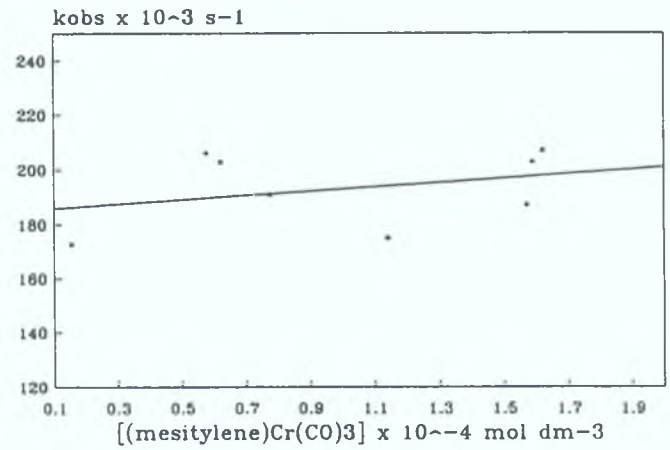

[(η^6-1,3,5-mesitylene)$Cr(CO)_3$] mol dm^{-3}	k_{obs} s^{-1}
1.533×10^{-5}	172720
5.770×10^{-5}	216000
6.211×10^{-5}	202831
7.764×10^{-5}	190846
1.140×10^{-4}	174947
1.571×10^{-4}	187075
1.590×10^{-4}	202831
1.621×10^{-4}	207000

Figure 2.2.2.3.1 A plot of concentration of (η^6-1,3,5-mesitylene)$Cr(CO)_3$ (mol dm^{-3}) against the observed rate constants (s^{-1}) for the decay of (η^6-1,3,5-mesitylene)$Cr(CO)_2(S)$ at 298K under 1.0 atmosphere of CO.

2.2.2.4 Effect of Liquid-Pumping on Laser Flash Photolysis Transient Species

The yield of the second transient species was reduced upon liquid pumping; and on continued liquid pumping this species was no longer observed on microsesond timescales. This was the case with all the substituted arene complexes studied. The oscilloscope traces recorded on laser flash photolysis of (η^6-1,3,5-mesitylene)$Cr(CO)_3$, before and after liquid pumping of the sample solution, are displayed in Figure 2.2.2.4.1. In Figure 2.2.2.4.1(a) the decay process is seen not to be fully reversible under the conditions; as exemplified by the residual absorption, whereas in Figure 2.2.2.4.1(b) the transient signal is almost baseline resolved and a single transient species is observed. Hence, it was possible to record the spectra and analyse the reaction kinetics of the first observed species, the (η^6-arene)$Cr(CO)_2(S)$ species, in the absence of the second species.

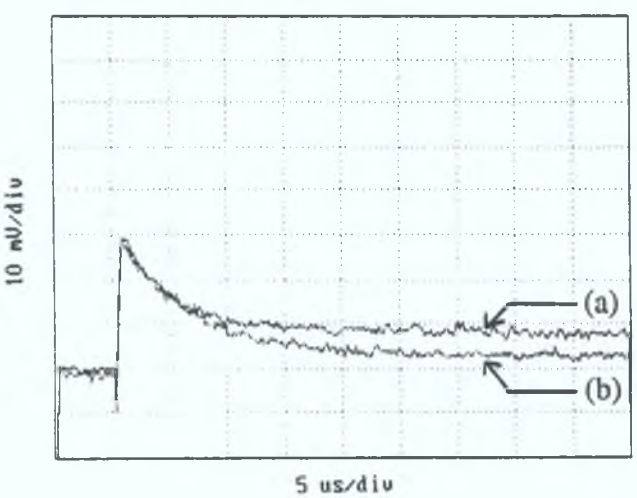

Figure 2.2.2.4.1 Oscilloscope traces recorded at 290nm following the laser flash photolysis of (η^6-1,3,5-mesitylene)$Cr(CO)_3$ in cyclohexane solution; before (a) and after (b) liquid pumping of the solution.

2.2.2.5 Reaction of Methyl-Substituted (η^6-arene)$Cr(CO)_2$(S) Species with CO

The lifetimes of the solvated dicarbonyl complexes depended on the concentration of CO and these data provided the second order rate constants for the reaction of the (η^6-arene)$Cr(CO)_3$ complexes with CO, Tables 2.2.2.5.1 to 2.2.2.5.4. The plots of observed rate constant versus [CO] were typically linear with negligible intercepts, Figure 2.2.2.5.1, indicating that under these conditions no other reactions contributed significantly to the decay of the dicarbonyl species; the sole exception being (η^6-1,3,6-mesitylene)$Cr(CO)_3$ which exhibits a significant intercept of 3.6 x 10^4 s^{-1}, possibly attributed to the effect of solvent impurities on the reaction. The results are summarised in Table 2.2.2.5.5 for a range of arene derivatives.

Table 2.2.2.5.1 The observed rate constants for the reaction of CO with (η^6-toluene)$Cr(CO)_2$(cyclohexane) at differing CO concentrations (mol dm^{-3}) at 298K, [(η^6-toluene)$Cr(CO)_3$] = 3.12 x 10^{-4} mol dm^{-3}.

[CO] mol dm^{-3}	k_{obs} s^{-1}
0.000	2035
0.006	37141
0.012	89501

$k_{[co]}$ = 7.3 x 10^6 ± 0.8 x 10^6 dm^3 mol^{-1} s^{-1}

Intercept = -841 ± 7044 s^{-1}

Table 2.2.2.5.2 The observed rate constants for the reaction of CO with (η^6-p-xylene)$Cr(CO)_2$(cyclohexane) at differing CO concentrations (mol dm^{-3}) at 298K, [(η^6-p-xylene)$Cr(CO)_3$ = 1.56 x 10^{-4} mol dm^{-3}.

[CO] mol dm^{-3}	k_{obs} s^{-1}
0.003	25400
0.006	49700
0.009	65900
0.012	98800

$k_{[co]}$ = 7.9 x 10^6 ± 0.7 x 10^6 dm^3 mol^{-1} s^{-1}

Intercept = -850 ± 4962 s^{-1}

Corr. Coeff. = 0.991

Table 2.2.2.5.3 The observed rate constants for the reaction of CO with (η^6-1,3,5-mesitylene)$Cr(CO)_2$(cyclohexane) at differing CO concentrations (mol dm^{-3}) at 298K, [(η^6-1,3,5-mesitylene)$Cr(CO)_3$] = 7.76 x 10^{-5} mol dm^{-3}.

[CO] mol dm^{-3}	k_{obs} s^{-1}
0.006	113377
0.009	152477
0.012	190846

$k_{[co]}$ = 1.3 x 10^7 ± 0.7 x 10^5 dm^3 mol^{-1} s^{-1}

Intercept = -36030 ± 299 s^{-1}

Table 2.2.2.5.4 The observed rate constants for the reaction of CO with (η^6-C_6Me_6)$Cr(CO)_2$(cyclohexane) at differing CO concentrations (mol dm^{-3}) at 298K, [(η^6-C_6H_6)$Cr(CO)_3$] = 3.95 x 10^{-4} mol dm^{-3}.

[CO] mol dm^{-3}	k_{obs} s^{-1}
0.003	29300
0.006	65000
0.009	92400
0.012	140000

$k_{[co]}$ = 1.2 x 10^7 ± 0.9 x 10^6 dm^3 mol^{-1} s^{-1}

Intercept = -8200 ± 6165 s^{-1}

Corr. Coeff. = 0.994

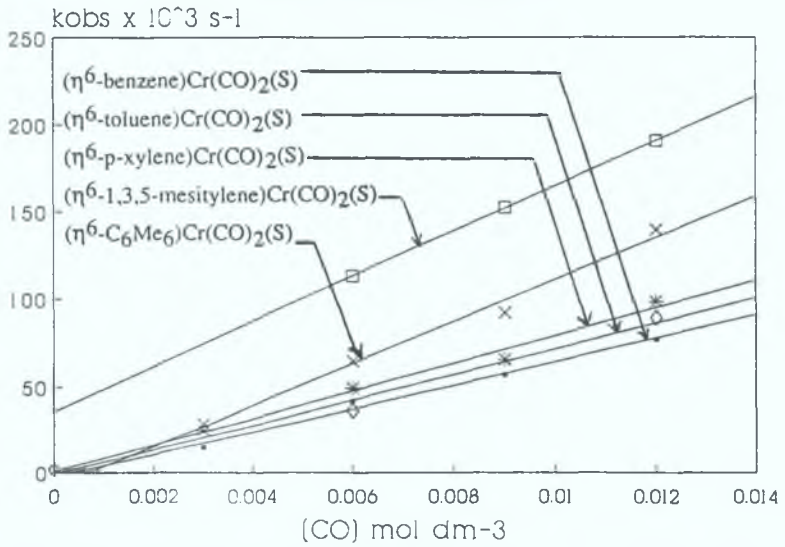

Figure 2.2.2.5.1 Second order plots of the observed rate constants for the decay of (η^6-arene)$Cr(CO)_2$(cyclohexane) complexes at differing concentrations of CO (mol dm^{-3}) at 298K.

Table 2.2.2.5.5 A summary of the second order rate constants for the reaction of CO with (η^6-arene)$Cr(CO)_2$(cyclohexane) complexes at 298K. [a]Reference 23.

η^6-Arene	k_2 dm^3 mol^{-1} s^{-1}
P-Fluorobenzene[a]	$2.4 \times 10^6 \pm 0.3 \times 10^6$
Chlorobenzene[a]	$4.3 \times 10^6 \pm 0.5 \times 10^6$
Benzene	$6.7 \times 10^6 \pm 0.6 \times 10^6$
Toluene	$7.3 \times 10^6 \pm 0.8 \times 10^6$
P-Xylene	$7.9 \times 10^6 \pm 0.7 \times 10^6$
1,3,5-Mesitylene	$1.3 \times 10^7 \pm 0.7 \times 10^5$
C_6Me_6	$1.2 \times 10^7 \pm 0.9 \times 10^6$
C_6Et_6[a]	$4.4 \times 10^7 \pm 5.0 \times 10^6$

It is seen that the second order rate constant for the reaction

(η^6-C_6R_6)$Cr(CO)_2$(S) + CO ----------> (η^6-C_6R_6)$Cr(CO)_3$ (2.2.2.5.1)

exhibits a general increase with increasing number of alkyl substituents. The results show that substitution on the arene ring increases the reactivity of the (η^6-arene)$Cr(CO)_2$(S) intermediate towards CO. The origin of this effect would appear to be the result of steric, rather than electronic, factors, as increasing the number of methyl substituents on the arene ring should reduce the electron deficient nature of the metal atom and stabilise the (η^6-arene)$Cr(CO)_2$(S) intermediate, rather than destabilise it as observed here. Included for comparison are the second order rate

constants for the reaction of a selection of halogenated and ethyl-substituted (η^6-arene)$Cr(CO)_2(S)$ complexes with CO[23]. The observed trend is maintained for these complexes; the strongly electron withdrawing effect of the halogen group increases the lifetime of the (η^6-arene)$Cr(CO)_2(S)$ species, while the (η^6-C_6Et_6)$Cr(CO)_2(S)$ species is much shorter-lived and therefore more reactive towards CO.

The rate constant for the reaction of (η^6-C_6Me_6)$Cr(CO)_3$ with CO is nearly twice that of the benzene complex. This is consistent with previous observations by M. Poliakoff *et. al.* for the analogous (η^5-C_5H_5)$Mn(CO)_2(S)$ and (η^5-C_5Me_5)$Mn(CO)_2(S)$ systems[24]. In both cases the rate constants of the fully methyl substituted complex are approximately twice that of the non-substituted complex in their respective solvent; Table 2.2.2.5.6. The second order rate constants are faster in the case of (η^6-arene)$Cr(CO)_3$ than those of the analagous (η^5-C_5R_5)$Mn(CO)_3$ system, indicating that the (η^6-C_6H_6)$Cr(CO)_2(S)$ intermediates are less stable, and therefore more reactive, than their manganese analogues. A more exact comparison between the two systems would require the acquisition of all rate data in identical solvents, as it has already been shown that rate constants are dependant on the nature of the solvent used.

Table 2.2.2.5.6 A comparison of the second order rate constants for the reaction of $(\eta^5\text{-}C_5R_5)Mn(CO)_2(S)$ and $(\eta^6\text{-}C_6H_6)Cr(CO)_2(S)$ with CO at 298K. [a]Reference 24.

complex	R	k_2 (x 10^6) $dm^3\ mol^{-1}\ s^{-1}$	Solvent
$(\eta^5\text{-}C_5R_5)Mn(CO)_2(S)$	H	0.81	n-heptane
	Me	1.60	
$(\eta^6\text{-}C_6H_6)Cr(CO)_2(S)$[a]	H	6.70	cyclohexane
	Me	12.00	

2.2.2.6 UV/vis Difference Spectra of Methyl Substituted $(\eta^6$-arene$)Cr(CO)_2(S)$ Photoproducts

UV/vis difference spectra of the $(\eta^6$-arene$)Cr(CO)_2(S)$ transient species were recorded for all the methyl substituted complexes. The difference spectra, given in Figures 2.2.2.6.1 and 2.2.2.6.2, are very similar for all complexes. In all cases the negative band at 320-330nm corresponds to depletion of the parent $(\eta^6$-arene$)Cr(CO)_3$ absorption at 315-325nm and an absorption maximum is observed in the 'window' of the parent spectrum at 280-290nm. The absorption in the visible region of all spectra is very weak and featureless, again emphasising the importance of monitoring these systems in the UV region rather than the visible region. The photochemical reactions were completely reversible as exemplified by the return of the transient absorptions to the baseline level. In all cases the spectra were recorded at low parent $(\eta^6$-arene$)Cr(CO)_3$ concentration to reduce the possibility of secondary photochemical reactions occuring.

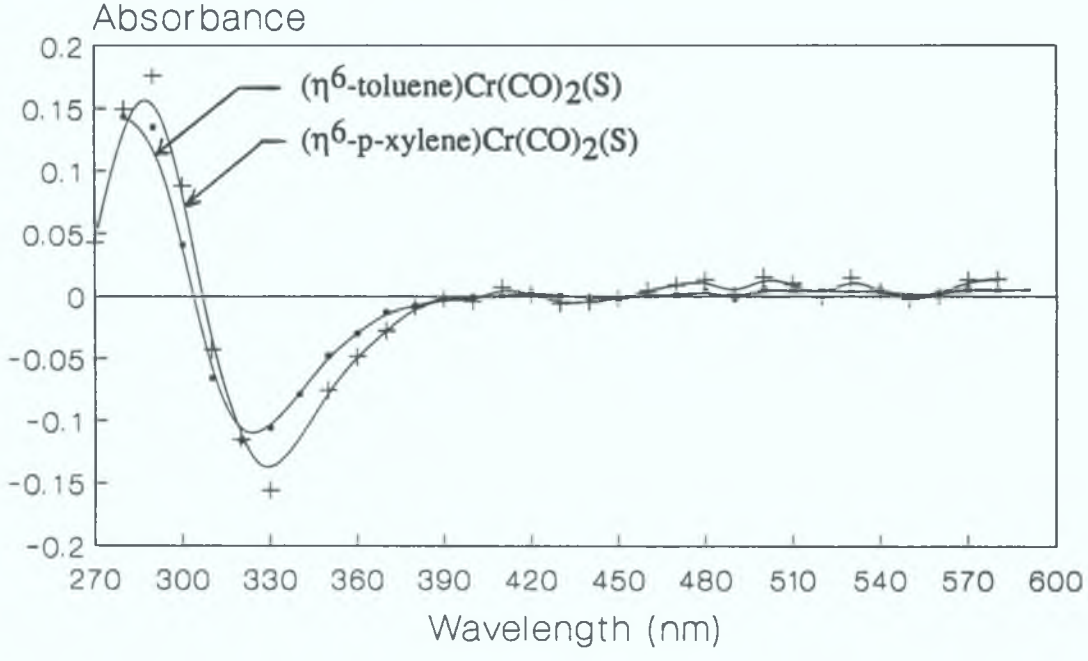

Figure 2.2.2.6.1 UV/vis difference spectra of (η^6-toluene)$Cr(CO)_2$(S) and (η^6-p-xylene)$Cr(CO)_2$(S) obtained at 1μs after the laser pulse in cyclohexane solution under 1.0 atmosphere of CO.

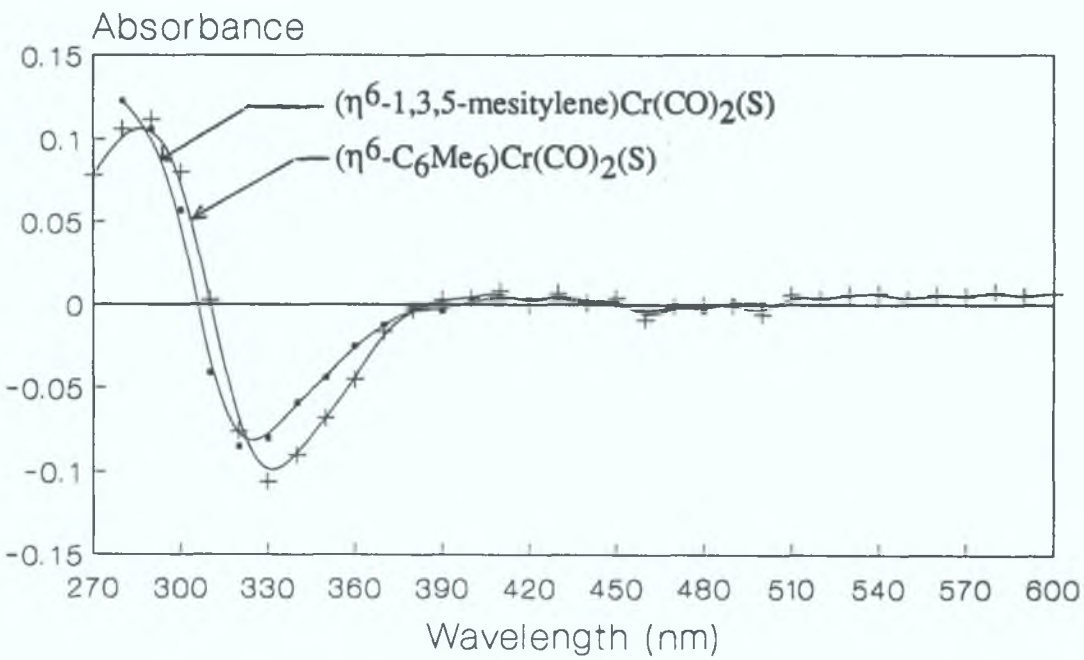

Figure 2.2.2.6.2 UV/vis difference spectra of $(\eta^6$-1,3,5-mesitylene)$Cr(CO)_2(S)$ and $(\eta^6$-$C_6Me_6)Cr(CO)_2(S)$ obtained at 1μs after the laser pulse in cyclohexane solution under 1.0 atmosphere of CO.

These spectra highlight the limitations of flash photolysis in regions of the spectrum where both the parent and the photoproduct absorb strongly. Differences are evident in the spectra of the parent (η^6-arene)$Cr(CO)_3$ complexes in the 230-260nm region, attributed to the M -->π*CO transition. However, these occur outside the current wavelength range of analysis; 270-600nm. It is readily apparent that the spectra of the (η^6-arene)$Cr(CO)_2$(S) species recorded are almost 'mirror images' of the spectra of the parent complex as the apparent absorption maximum for a transient species occurs in the 'valley' of the absorption profile of the parent complex. Given these similarities, it would be impossible to distinguish or identify an unknown (η^6-arene)$Cr(CO)_2$(S) complex based on its absorption characteristics alone; a comparison of the reaction kinetics at its absorption maximum would be necessary. This contrasts with the vibrational spectra of these complexes, which exhibit slight, but characteristic, shifts in the absorption peaks of the parent tricarbonyl complexes. TRIR spectra would be expected to give unique absorption bands for each (η^6-arene)$Cr(CO)_2$(S) complex well resolved from the relevant parent bands. Identification of the reactive intermediate can easily be achieved in this case from its spectral characteristics alone, with use of the complementary kinetic analysis for verification.

2.2.2.7 Effect of Power of Laser on Concentration of (η^6-arene)$Cr(CO)_2(S)$ Species

In order to eliminate the possibility that the production of the (η^6-arene)$Cr(CO)_2(S)$ species were the result of multiple photon excitation of the parent tricarbonyls, experiments were conducted in which the energy of the laser pulse was varied. The absorbance of the primary photoproducts were found to vary linearly with laser power; indicating that the production of these species occured by means of a single photon event. A linear dependance was observed in the case of all (η^6-arene)$Cr(CO)_2(S)$ species, Figure 2.2.2.7.1.

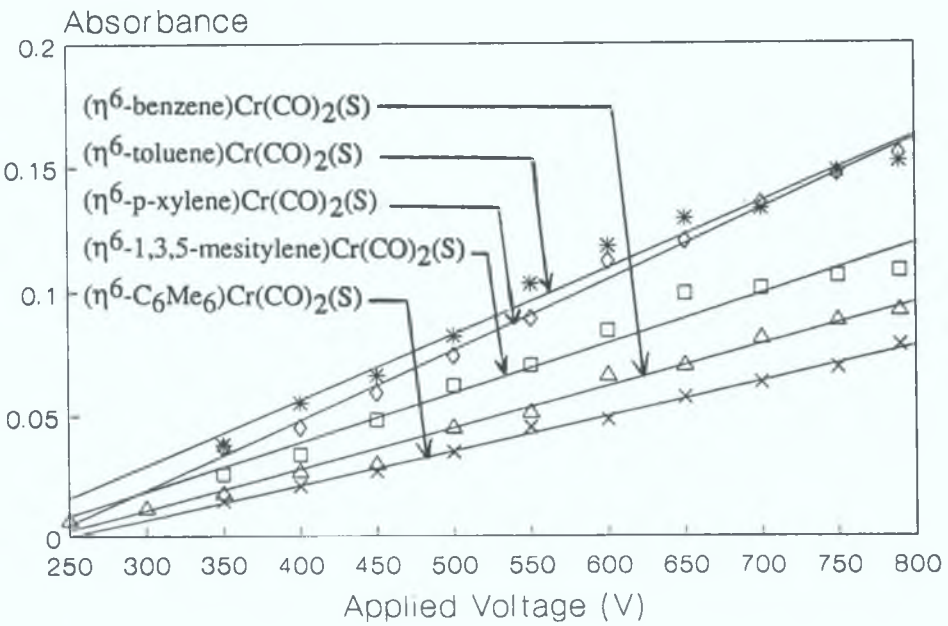

Figure 2.2.2.7.1 Plot showing the variation in absorbance of the (η^6-arene)$Cr(CO)_2(S)$ species with relative laser power. The absorbances are recorded 1μs after the laser flash.

2.2.2.8 A Study of the Activation Parameters for the Reaction of Methyl Substituted (η^6-arene)$Cr(CO)_2(S)$ Species with CO

Activation parameters for the reaction of (η^6-arene)$Cr(CO)_2(S)$ with CO were determined from Arrhenius and Eyring plots giving the temperature dependance of the reaction between 280 and 313K. The results are detailed in Tables 2.2.2.8.1 to 2.2.2.8.4 and illustrated graphically in Figures 2.2.2.8.1 to 2.2.2.8.4.

Table 2.2.2.8.1 (a) Experimental data for the determination of the energy, entropy, and enthalpy of activation for the reaction of (η^6-toluene)$Cr(CO)_2(S)$ with CO; [(η^6-toluene)$Cr(CO)_3$] = 1.0×10^{-4} mol dm^{-3} and [CO]= 1.2×10^{-2} mol dm^{-3}.

$1/T (\times 10^3)$	$Ln(k_{obs}/[CO])$	$Ln((k_{obs}/[CO])/T)$
3.56	15.32	9.68
3.47	15.45	9.79
3.41	15.66	9.98
3.36	15.88	10.18
3.33	15.97	10.27
3.29	16.06	10.35
3.25	16.19	10.46
3.21	16.31	10.56

Arrhenius Plot	Eyring Plot	Activation Parameters
Slope = -2978 ± 137	Slope = -2686 ±140	Ea = 25 ± 1 kJ mol^{-1}
Int. = 25.86 ± 0.04	Int. = 19.18 ± 0.04	$\Delta H^{\neq}$ = 22 ± 1 kJ mol^{-1}
Corr. Coeff. = 0.994	Corr. Coeff. = 0.992	$\Delta S^{\neq}$ = -38 ± 20 J mol^{-1} K^{-1}

Table 2.2.2.8.1 (b) Experimental data for the determination of the energy, entropy, and enthalpy of activation for the reaction of (η^6-toluene)$Cr(CO)_2$(S) with CO; [(η^6-toluene)$Cr(CO)_3$] = 1.6 x 10^{-4} mol dm^{-3} and [CO]= 1.2 x 10^{-2} mol dm^{-3}.

1/T (x 10^3)	Ln(k_{obs}/[CO])	Ln((k_{obs}/[CO])/T)
3.56	15.23	9.59
3.50	15.42	9.76
3.44	15.55	9.88
3.39	15.72	10.04
3.34	15.85	10.15
3.32	15.98	10.28
3.27	16.11	10.38
3.22	16.26	10.52

Arrhenius Plot	Eyring Plot	Activation Parameters
Slope = -3086 ± 83	Slope = -2791 ± 81	Ea = 26 ± 1 kJ mol^{-1}
Int. = 26.19 ± 0.02	Int. = 19.51 ± 0.02	$\Delta H^{\neq}$ = 23 ± 1 kJ mol^{-1}
Corr. Coeff. = 0.998	Corr. Coeff. = 0.997	$\Delta S^{\neq}$ = -35 ± 20 J mol^{-1} K^{-1}

Table 2.2.2.8.2 (a) Experimental data for the determination of the energy, entropy and enthalpy of activation for the reaction of (η^6-p-xylene)$Cr(CO)_2(S)$ with CO; [(η^6-p-xylene)$Cr(CO)_3$] = 4.4 x 10^{-5} mol dm^{-3} and [CO]= 1.2 x 10^{-2} mol dm^{-3}.

1/T (x 10^3)	Ln(k_{obs}/[CO])	Ln((k_{obs}/[CO])/T)
3.46	15.59	9.68
3.44	15.70	9.79
3.39	15.82	9.98
3.32	15.93	10.18
3.24	16.26	10.27
3.19	16.47	10.35

Arrhenius Plot	Eyring Plot	Activation Parameters
Slope = -3075 ± 206	Slope = -2772 ± 204	Ea = 26 ± 2 kJ mol^{-1}
Int. = 26.23 ± 0.05	Int. = 19.52 ± 0.05	$\Delta H^{\neq}$ = 23 ± 2 kJ mol^{-1}
Corr. Coeff. = 0.991	Corr. Coeff. = 0.989	$\Delta S^{\neq}$ = -35 ± 20 J mol^{-1} K^{-1}

Table 2.2.2.8.2 (b) Experimental data for the determination of the energy, entropy and enthalpy of activation for the reaction of (η^6-p-xylene)$Cr(CO)_2(S)$ with CO; [(η^6-p-xylene)$Cr(CO)_3$] = 1.6 x 10^{-4} mol dm^{-3} and [CO]= 1.2 x 10^{-2} mol dm^{-3}.

1/T (x 10^3)	Ln(k_{obs}/[CO])	Ln((k_{obs}/[CO])/T)
3.47	15.48	9.82
3.38	15.86	10.17
3.32	15.94	10.23
3.27	16.17	10.54
3.22	16.38	10.64

Arrhenius Plot	Eyring Plot	Activation Parameters
Slope = -3030 ± 236	Slope = -2732 ± 235	Ea = 25 ± 2 kJ mol^{-1}
Int. = 26.08 ± 0.05	Int. = 19.38 ± 0.05	$\Delta H^{\neq}$ = 23 ± 2 kJ mol^{-1}
Corr. Coeff. = 0.991	Corr. Coeff. = 0.989	$\Delta S^{\neq}$ = -36 ± 20 J mol^{-1} K^{-1}

Table 2.2.2.8.3 (a) Experimental data for the determination of the energy, entropy and enthalpy of activation for the reaction of (η^6-1,3,5-mesitylene)$Cr(CO)_2(S)$ with CO; [(η^6-1,3,5-mesitylene)$Cr(CO)_3$] = 5.6 x 10^{-4} mol dm^{-3} and [CO] = 1.2 x 10^{-2} mol dm^{-3}.

1/T (x 10^3)	Ln(k_{obs}/[CO])	Ln((k_{obs}/[CO])/T)
3.55	15.87	10.23
3.48	16.04	10.38
3.41	16.19	10.51
3.36	16.29	10.59
3.31	16.49	10.78
3.28	16.73	11.01
3.23	16.83	11.10
3.21	16.92	11.17

Arrhenius Plot	Eyring Plot	Activation Parameters
Slope = -3164 ± 211	Slope = -2868 ± 210	Ea= 26 ± 2 kJ mol^{-1}
Int. = 27.03 ± 0.07	Int. = 20.34 ± 0.07	$\Delta H^{\neq}$ = 24 ± 2 kJ mol^{-1}
Corr. Coeff. = 0.987	Corr. Coeff. = 0.984	$\Delta S^{\neq}$ = -29 ± 20 J mol^{-1} K^{-1}

Table 2.2.2.8.3 (b) Experimental data for the determination of the energy, entropy and enthalpy of activation for the reaction of (η^6-1,3,5-mesitylene)$Cr(CO)_2(S)$ with CO; [(η^6-1,3,5-mesitylene)$Cr(CO)_3$] = 1.5 x 10^{-4} mol dm^{-3} and [CO] = 1.2 x 10^{-2} mol dm^{-3}.

1/T (x 10^3)	Ln(k_{obs}/[CO])	Ln((k_{obs}/[CO])/T)
3.56	16.13	10.49
3.51	16.25	10.60
3.46	16.36	10.71
3.41	16.54	10.86
3.38	16.60	10.91
3.32	16.77	11.07
3.28	16.94	11.22

Arrhenius Plot	Eyring Plot	Activation Parameters
Slope = -2872 ± 93	Slope = -2578 ± 91	Ea = 24 ± 1 kJ mol^{-1}
Int. = 26.33 ± 0.02	Int. = 19.65 ± 0.02	$\Delta H^{\neq}$=21 ± 1 kJ mol^{-1}
Corr. Coeff. = 0.998	Corr. Coeff. = 0.997	$\Delta S^{\neq}$ = -34 ± 20 J mol^{-1} K^{-1}

Table 2.2.2.8.4 (a) Experimental data for the determination of the energy, entropy and enthalpy of activation for the reaction of $(\eta^6\text{-}C_6Me_6)Cr(CO)_2(S)$ with CO; $[(\eta^6\text{-}C_6Me_6)Cr(CO)_3] = 1.1 \times 10^{-4}$ mol dm^{-3} and $[CO] = 1.2 \times 10^{-2}$ mol dm^{-3}.

$1/T$ (x 10^3)	$Ln(k_{obs}/[CO])$	$Ln((k_{obs}/[CO])/T)$
3.57	15.47	9.83
3.50	15.66	10.01
3.46	15.81	10.14
3.42	15.98	10.30
3.37	16.09	10.40
3.34	16.20	10.50
3.30	16.34	10.62

Arrhenius Plot	Eyring Plot	Activation Parameters
Slope = -3258 ± 81	Slope = -2966 ± 81	Ea = 27 ± 2 kJ mol^{-1}
Int. = 27.08 ± 0.02	Int. = 20.41 ± 0.02	$\Delta H^{\neq}$ = 25 ± 2 kJ mol^{-1}
Corr. Coeff. = 0.998	Corr. Coeff. = 0.998	$\Delta S^{\neq}$ = -28 ± 20 J mol^{-1} K^{-1}

Table 2.2.2.8.4 (b) Experimental data for the determination of the energy, entropy and enthalpy of activation for the reaction of $(\eta^6\text{-}C_6Me_6)Cr(CO)_2(S)$ with CO; $[(\eta^6\text{-}C_6Me_6)Cr(CO)_3] = 8.2 \times 10^{-5}$ mol dm^{-3} and $[CO] = 1.2 \times 10^{-2}$ mol dm^{-3}.

$1/T$ (x 10^3)	$Ln(k_{obs}/[CO])$	$Ln((k_{obs}/[CO])/T)$
3.53	15.61	9.97
3.46	15.71	10.05
3.41	15.94	10.26
3.35	16.16	10.42
3.32	15.32	10.61
3.29	16.40	10.68
3.25	16.45	10.72
3.19	16.63	10.88

Arrhenius Plot	Eyring Plot	Activation Parameters
Slope = -3190 ± 189	Slope = -2892 ± 190	$E_a = 27 \pm 2$ kJ mol^{-1}
Int. = 26.83 ± 0.06	Int. = 20.13 ± 0.06	$\Delta H^{\neq} = 24 \pm 2$ kJ mol^{-1}
Corr. Coeff. = 0.990	Corr. Coeff. = 0.988	$\Delta S^{\neq} = -30 \pm 20$ J mol^{-1} K^{-1}

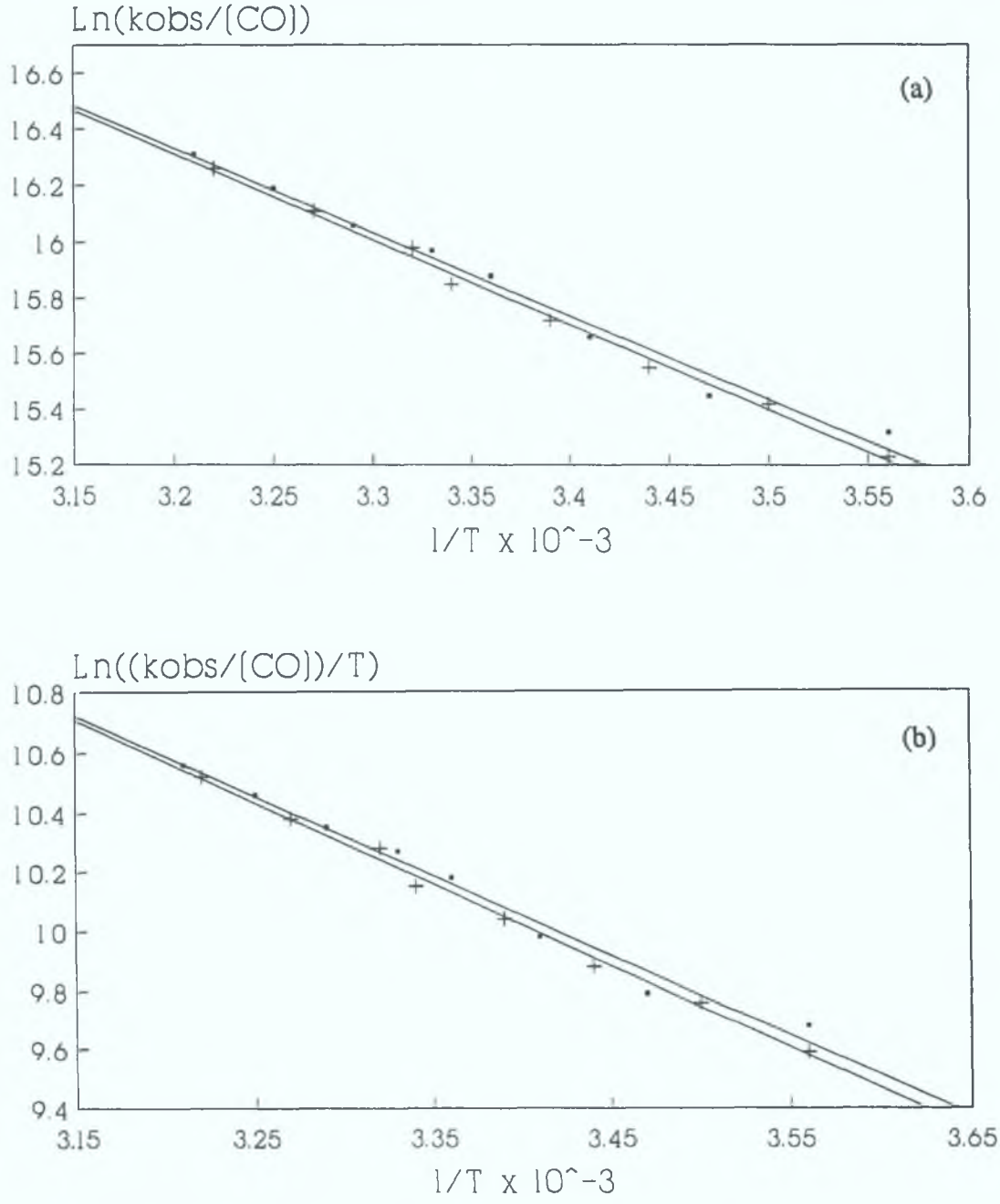

Figure 2.2.2.8.1 Arrhenius (a) and Eyring (b) plots for the reaction of (η^6-toluene)$Cr(CO)_2(S)$ with CO.

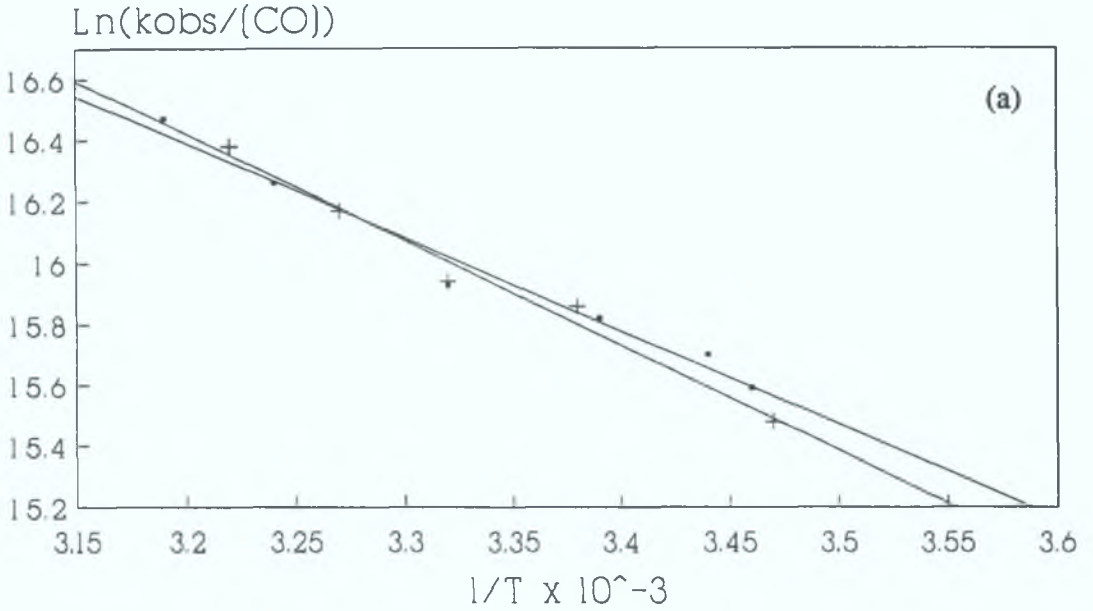

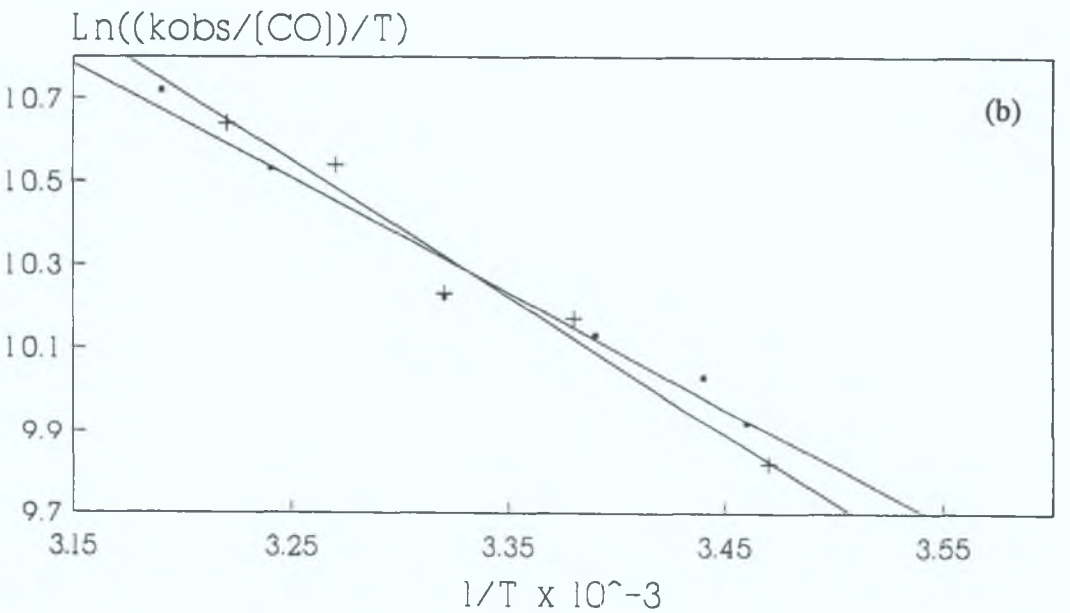

Figure 2.2.2.8.2 Arrhenius (a) and Eyring (b) plots for the reaction of (η^6-p-xylene)$Cr(CO)_2(S)$ with CO.

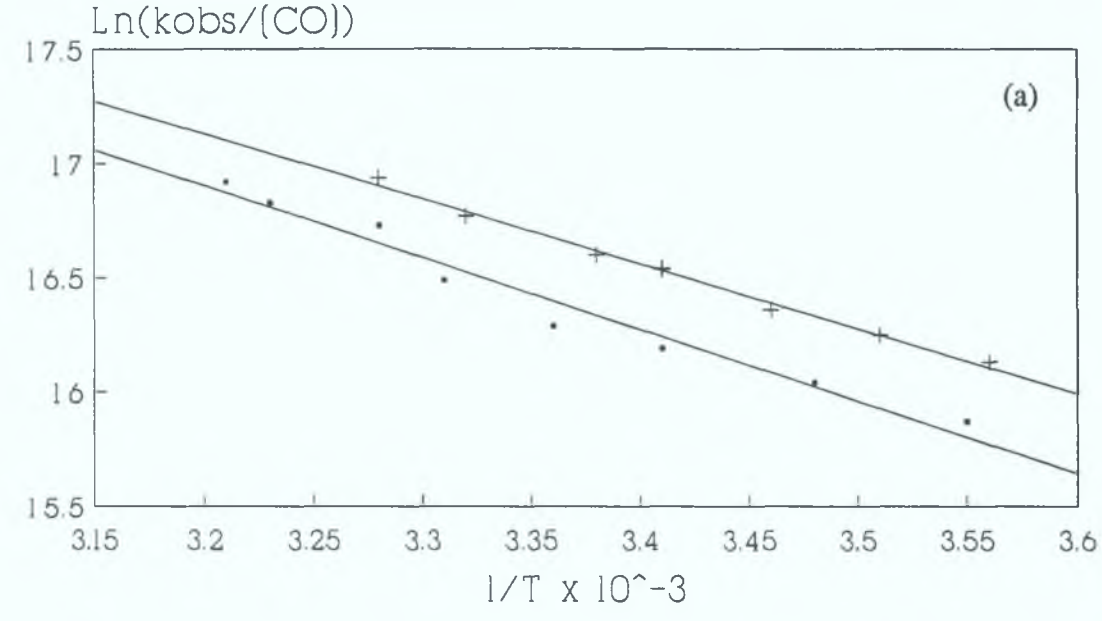

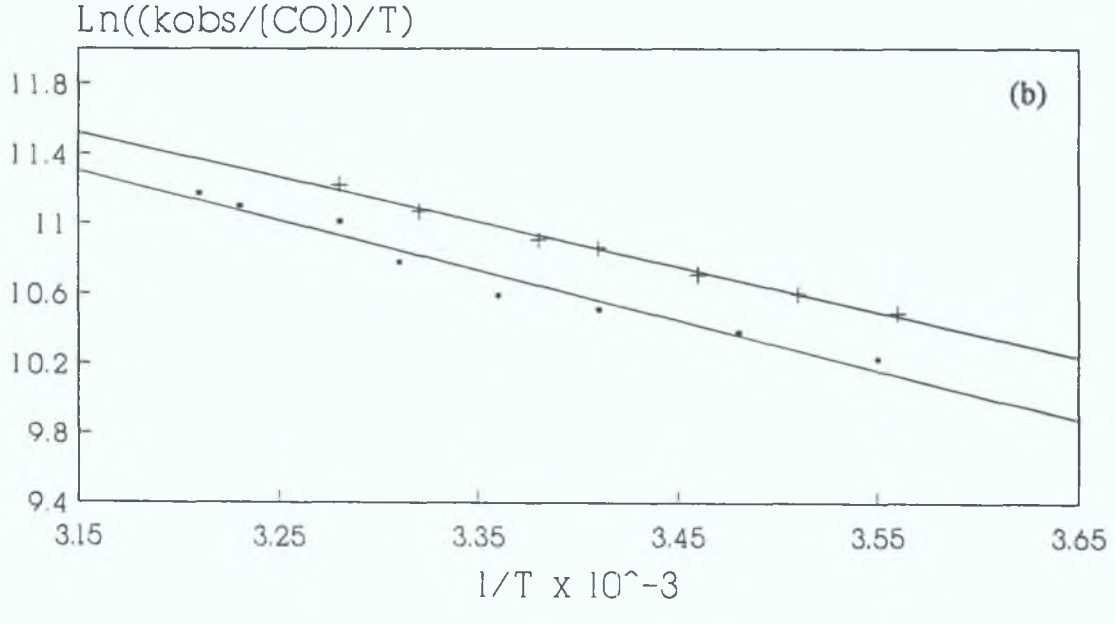

Figure 2.2.2.8.3 Arrhenius (a) and Eyring (b) plots for the reaction of (η^6-1,3,5-mesitylene)$Cr(CO)_2(S)$ with CO.

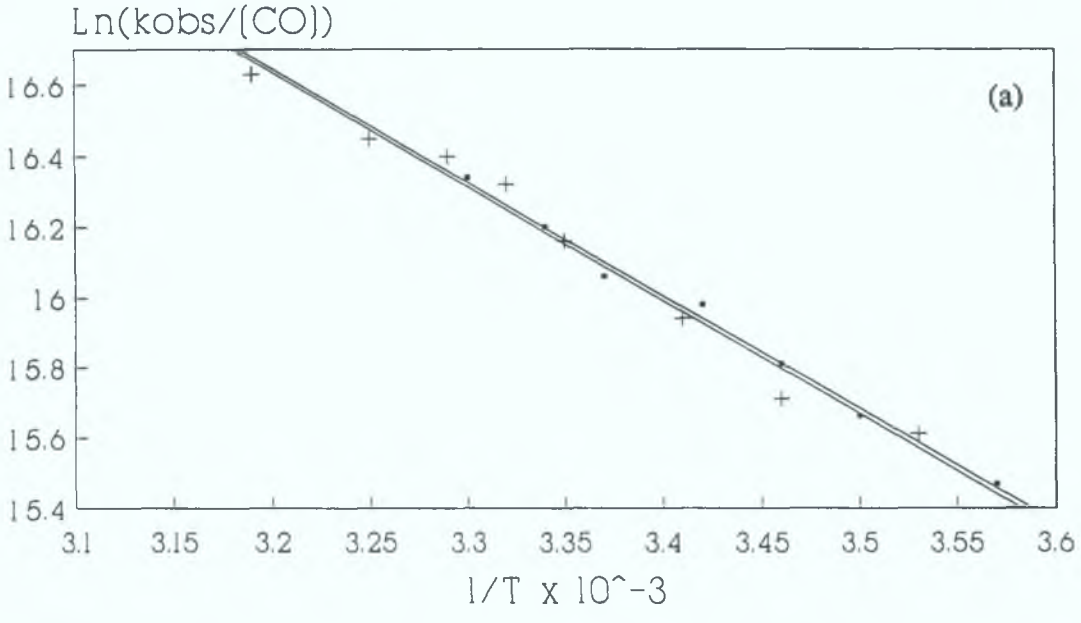

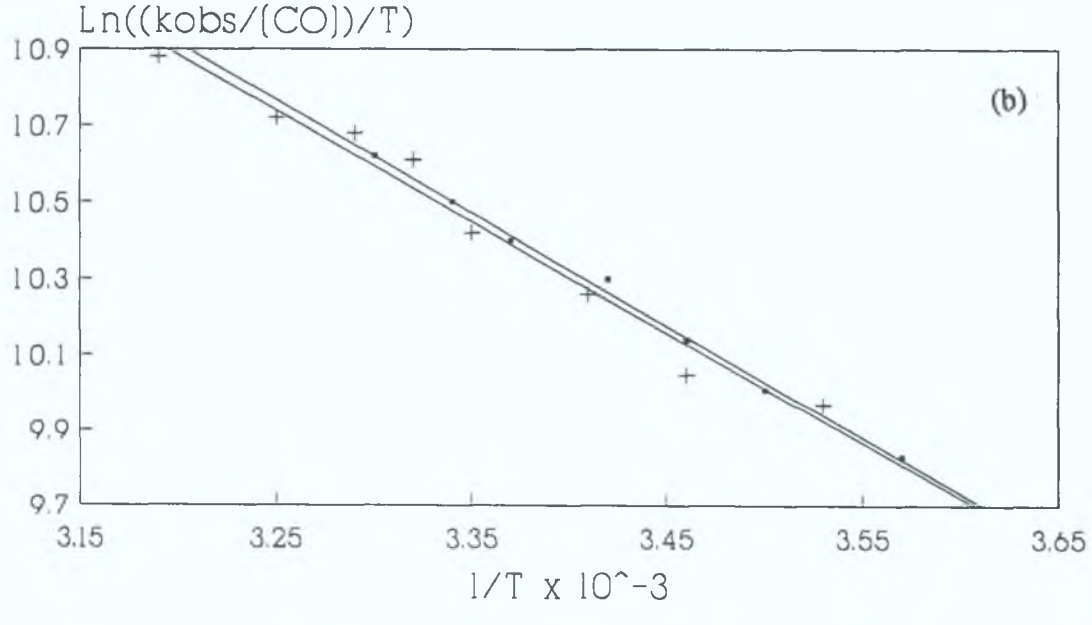

Figure 2.2.2.8.4 Arrhenius (a) and Eyring (b) plots for the reaction of (η^6-C_6Me_6)$Cr(CO)_2$(S) with CO.

Table 2.2.2.8.5 A summary of the activation parameters for the reaction of (η^6-arene)$Cr(CO)_2$(S) complexes with CO in cyclohexane solution. [a] Reference 23.

η^6-Arene	E_a kJ mol^{-1}	$\Delta H^{\neq}$ kJ mol^{-1}	$\Delta S^{\neq}$ J mol^{-1} K^{-1}	$\Delta G^{\neq}$ kJ
Chlorobenzene[a]	25	23	-40	35
Benzene	25	23	-39	35
Toluene	26	23	-37	34
P-Xylene	26	23	-36	33
1,3,5-Mesitylene	25	23	-32	33
C_6Me_6	27	25	-29	34
C_6Et_6[a]	24	22	-24	29

Summarised in Table 2.2.2.8.5 are the activation parameters for the reaction of a series of (η^6-arene)$Cr(CO)_2$(S) species with CO, giving the temperature dependance of the reaction between 280 and 313K in cyclohexane. Included for comparison are the values for (η^6-chlorobenzene)$Cr(CO)_2$(S) and (η^6-C_6Et_6)$Cr(CO)_2$(S)[23]. It is note-worthy that the enthalpy of activation for the reaction of CO with all complexes is constant at 25 ± 2 kJ mol^{-1}. This may be compared to the reported binding energies of cyclohexane to $Cr(CO)_5$ of 52 kJ mol^{-1} from time-resolved photoacoustic measurements[21]. Assuming the interaction energy between $Cr(CO)_5$ and cyclohexane is similar to that of (η^6-arene)$Cr(CO)_2$ and cyclohexane, it is unlikely that the dissociative loss of solvent from (η^6-

arene)$Cr(CO)_2(S)$ is implicated in the rate determining step for this reaction. The constant $\Delta H^{\neq}$ among the species studied may reflect a common level of bond breaking in the transition state[25].

The second order rate constants for reaction of (η^6-arene)$Cr(CO)_2(S)$ complexes with CO have shown that the values for C_6Me_6 are just over twice that of the benzene complex. This variation in reaction rate is attributed mainly to variation in activation entropy $\Delta S^{\neq}$, since the $\Delta H^{\neq}$ values remain unchanged within experimental error. The $\Delta S^{\neq}$ value for the CO recombination reaction of each compound is not extremely negative as expected for a purely associative reaction. Again, these observations are consistent with an interchange mechanism for CO binding, rather than a prior dissociation of the solvent molecule in the rate determining step. The activation entropy becomes progressively less negative as the number of methyl substituents on the arene increases. The presence of methyl substituents on the arene ligand increases the electron density on the metal atom, as confirmed by the regular decrease in ν_{CO} in the parent complexes. Although this would presumably have the effect of destabilising the chromium-alkane interaction in the dicarbonyl species, the effect on CO binding would be less significant. This may be the explanation for the lack of significant change in $\Delta H^{\neq}$ on methyl substitution.

A number of arguments may be proposed to explain the increase in $\Delta S^{\neq}$ in this series. One approach lies in the consideration that in the more highly exothermic steps it will be expected that the transition state will resemble reactants closely; while in endothermic steps the products will provide the best models for the transition state[26]. Therefore, the increasing electron density at the chromium atom in the

series C_6H_6, C_6H_5Me, $C_6H_4Me_2$, $C_6H_3Me_3$, C_6Me_6 may cause the transition state to become progressively later, that is more product-like. The transition state for the reaction of CO with (η^6-benzene)$Cr(CO)_2$(S) therefore presumably consists of solvated (η^6-benzene)$Cr(CO)_2$ with little association of the CO; this is reflected in the less negative value for $\Delta S^{\neq}$. As the transition state becomes later, it consists of a greater degree of association of the CO with the chromium centre; this is reflected in a decreasing of $\Delta S^{\neq}$. Thus, with the (η^6-benzene)$Cr(CO)_2$ reaction the larger negative $\Delta S^{\neq}$ indicates a larger degree of coordination of the CO to the chromium in the transition state. In an extension of this argument, the increase in $\Delta S^{\neq}$ in this series may imply an increase in the degrees of freedom for the molecule in the transition state, consistent with greater steric constraints in the (η^6-arene)$Cr(CO)_2$(S) complex. This can be taken to indicate a considerable increase in degrees of freedom as the alkane-metal distance increases. These degrees of freedom could be associated with an increased movement of the alkane fragment, which is inhibited in the (η^6-arene)$Cr(CO)_2$(S) complex, or a reduction in the rotational freedom of the alkyl substituents on the arene ligand.

2.2.2.9 The Effect of Arene Substitution on the Second Observed Species

The second observed species on laser flash photolysis of (η^6-arene)$Cr(CO)_3$ in cyclohexane, which has been tentatively assigned to a (η^4-Ar)$Cr(CO)_3(H_2O)$ species, was observed in the case of all substituted arene complexes. In all cases the species was observed not to react with parent (η^6-arene)$Cr(CO)_3$ complex or CO, for example in the case of (η^6-1,3,5-mesitylene)$Cr(CO)_3$, Figures 2.2.2.9.1 and

2.2.2.9.2. The rate constants for the decay of this transient species under one atmosphere of CO are detailed in Table 2.2.2.9.1 for all the complexes studied. As the degree of substitution of the arene ring increases, the rate of decay of this species decreases slightly, indicating that the species is becoming slightly more stable as the number of methyl groups on the arene ring increases; in direct contrast to the behaviour of the (η^6-arene)$Cr(CO)_2$(S) species on substitution.

A summary of the activation parameters for the complexes studied is given in Table 2.2.2.9.2. Activation parameters were determined for the decay of this species in the case of (η^6-p-xylene)$Cr(CO)_3$ and (η^6-1,3,5-mesitylene)$Cr(CO)_3$; these values are detailed in Table 2.2.2.9.3 and illustrated in Figure 2.2.2.9.3. $\Delta H^{\neq}$ and E_a are similar for all compounds studied. The slightly positive values of $\Delta S^{\neq}$ indicate a more associative transition state for the production of this species than for the production of the (η^6-arene)$Cr(CO)_2$(S) species. As with the (η^6-arene)$Cr(CO)_2$(S) series studied, the values of $\Delta S^{\neq}$ get increasingly more positive as the degree of substitution increases. This increase in $\Delta S^{\neq}$ is more significant in the case of the impurity complex. If this transient species arises from a hapticity change at the arene ligand, where the arene ligand adopts the Dewar benzene conformation, it would be expected that (η^4-C_6Me_6)$Cr(CO)_4$ would be formed upon flash photolysis of (η^6-C_6Me_6)$Cr(CO)_3$. (η^4-C_6Me_6)$Cr(CO)_4$ is thermally stable; hence, the overall system would not be reversible in this case. The experimental results showed this system to be completely photochemically reversible. This observation precludes the possibility that a complex of conformation (η^4-Dewar benzene)$Cr(CO)_4$ is being formed although the formation of another hapticity change product is not eliminated. The

other likely consideration was that the second species is attributed to the formation of $(\eta^6\text{-arene})Cr(CO)_2(H_2O)$. In this case the experimental findings may represent the characterisation of the following reaction; in which a complex formed by the binding of trace impurity levels of water regenerates the parent complex by reaction with CO.

$(\eta^6\text{-arene})Cr(CO)_2(H_2O) + CO \text{ --------> } (\eta^6\text{-arene})Cr(CO)_3 + H_2O$ (2.2.2.9.1)

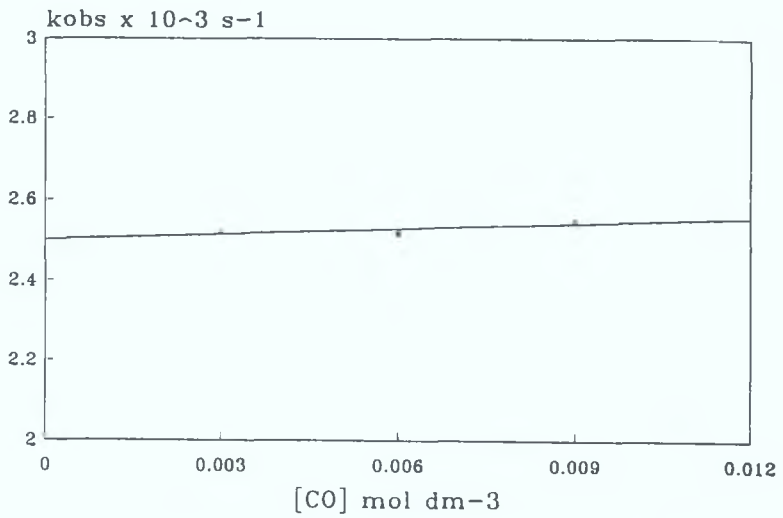

[CO] mol dm^{-3}	k_{obs} s^{-1}
0.003	2520
0.006	2516
0.009	2548

Figure 2.2.2.9.1 A plot of concentration of CO (mol dm^{-3}) against the observed rate constants (s^{-1}) for the decay of the second observed photoproduct on laser flash photolysis of $(\eta^6\text{-1,3,5-mesitylene})Cr(CO)_3$ at 298K.

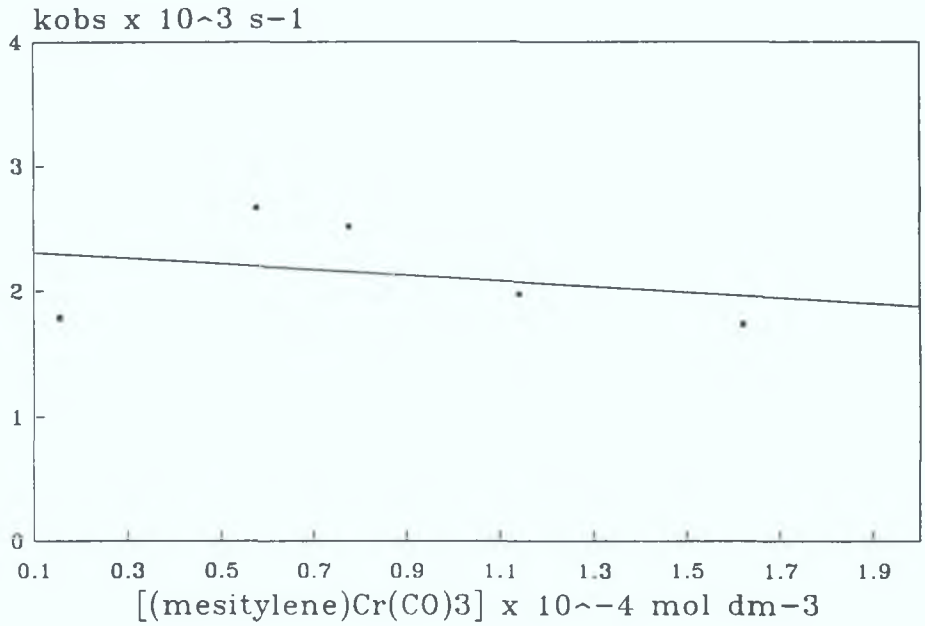

[(η^6-1,3,5-mesitylene)Cr(CO)$_3$] mol dm^{-3}	k_{obs} s^{-1}
1.55 x 10^{-5}	1889
5.77 x 10^{-5}	2670
7.76 x 10^{-5}	2256
1.14 x 10^{-4}	1977
1.62 x 10^{-4}	1770

Figure 2.2.2.9.2 A plot of concentration of (η^6-1,3,5-mesitylene)Cr(CO)$_3$ (mol dm^{-3}) against the observed rate constants (s^{-1}) for the decay of the second primary photoproduct at 298K under 1.0 atmosphere of CO.

Table 2.2.2.9.1 A summary of the observed rate constants (s^{-1}) for the decay of the second transient species in cyclohexane at 298K under 1.0 atmosphere of CO for a series of (η^6-arene)$Cr(CO)_3$ complexes.

η^6-Arene	k_{obs} s^{-1}
Benzene	3.0×10^3
Toluene	2.2×10^3
P-Xylene	2.3×10^3
1,3,5-Mesitylene	2.0×10^3
C_6Me_6	1.7×10^3

Table 2.2.2.9.2 A summary of the activation parameters for the reaction of the second transient species in cyclohexane for selected (η^6-arene)$Cr(CO)_3$ complexes.

η^6-Arene	E_a kJ mol^{-1}	$\Delta H^{\neq}$ kJ mol^{-1}	$\Delta S^{\neq}$ J mol^{-1} K^{-1}	$\Delta G^{\neq}$ kJ
Benzene	57	54	+2	52
P-Xylene	54	51	+29	43
1,3,5-Mesitylene	59	57	+43	44

Table 2.2.2.9.3 (a) Experimental data for the determination of the energy, entropy and enthalpy of activation for species 2; $[(\eta^6\text{-p-xylene})Cr(CO)_3] = 4.4 \times 10^{-5}$ mol dm^{-3}.

$1/T (\times 10^3)$	$Ln(k_{obs})$	$Ln(k_{obs}/T)$
3.44	7.20	1.52
3.39	7.82	2.14
3.24	8.52	2.78
3.19	8.99	3.24

Arrhenius Plot	Eyring Plot	Activation Parameters
Slope = -7473 ± 863	Slope = -6172 ± 863	$E_a = 54 \pm 8$ kJ mol^{-1}
Int. = 29.58 ± 0.18	Int. = 22.87 ± 0.18	$\Delta H^{\neq} = 51 \pm 8$ kJ mol^{-1}
Corr. Coeff. = 0.983	Corr. Coeff. = 0.981	$\Delta S^{\neq} = 29 \pm 20$ J mol^{-1} K^{-1}

Table 2.2.2.9.3 (b) Experimental data for the determination of the energy, entropy and enthalpy of activation for species 2; [(η^6-1,3,5-mesitylene)$Cr(CO)_3$] = 1.1 x 10^{-4} mol dm^{-3}.

$1/T$ (x 10^3)	$Ln(k_{obs})$	$Ln(k_{obs}/T)$
3.53	6.03	0.38
3.39	6.98	1.30
3.22	8.29	2.55

Arrhenius Plot	Eyring Plot	Activation Parameters
Slope = -7109 ± 220	Slope = -6809 ± 218	E_a = 59 ± 2 kJ mol^{-1}
Int. = 31.12 ± 0.05	Int. = 24.42 ± 0.05	$\Delta H^{\neq}$ = 57 ± 2 kJ mol^{-1}
Corr. Coeff. = 0.999	Corr. Coeff. = 0.999	$\Delta S^{\neq}$ = 43 ± 20 J mol^{-1} K^{-1}

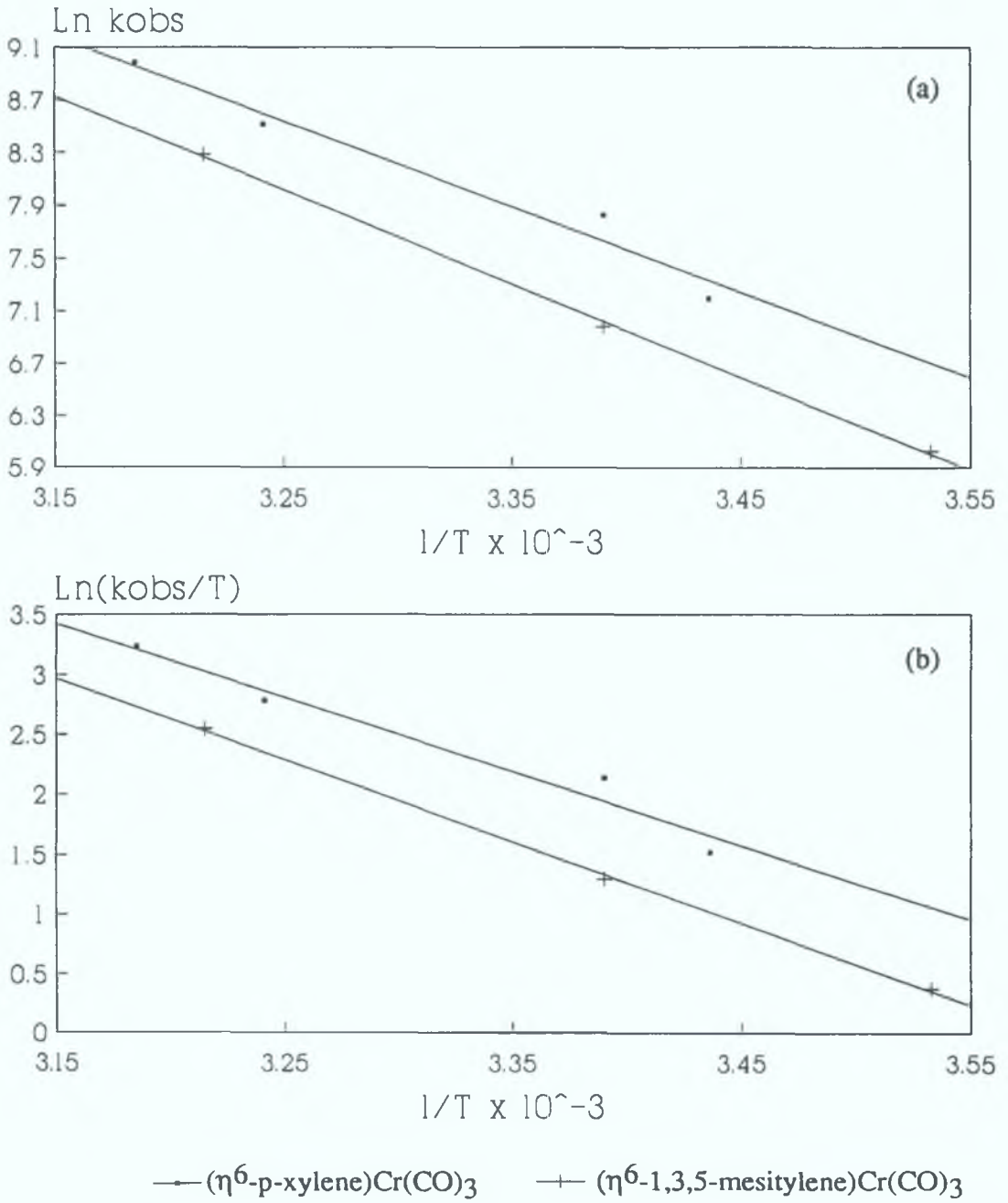

Figure 2.2.2.9.3 Arrhenius (a) and Eyring (b) plots for the reaction of species 2 for (η^6-p-xylene)$Cr(CO)_3$ and (η^6-1,3,5-mesitylene)$Cr(CO)_3$.

2.3 Secondary Photochemical Observations

2.3.1 Photochemistry of (η^6-benzene)$Cr(CO)_3$

In conditions of low CO concentration (i.e. experiment conducted under an argon atmosphere) and high parent concentration laser flash photolysis of (η^6-benzene)$Cr(CO)_3$ in cyclohexane solution revealed the presence of further absorbing transient species in addition to the primary photoproducts described earlier. Once again, the photochemical reactions observed were greatly influenced by liquid-pumping of the sample solution. The experimental results obtained in both cases are presented.

2.3.1.1 Photochemistry in Non-Liquid Pumped Solution

Laser flash photolysis of a 4.80 x 10^{-4} mol dm^{-3} solution of (η^6-benzene)$Cr(CO)_3$ in cyclohexane solution revealed the presence of a third absorbing transient species. The rate of grow-in of this species was directly dependant on the concentration of CO present in solution. The second order rate constant for this reaction was calculated to be 7.6 x 10^6 dm^3 mol^{-1} s^{-1}, Figure 2.3.1.1.1. This value is very similar to that calculated in previous experiments for the reaction of (η^6-benzene)$Cr(CO)_2(S)$ with CO, indicating that this species may be formed by reaction of the solvated CO-loss product. The yield of this species (as measured by means it's absorption at full formation) was reduced as the CO concentration in solution increased Table 2.3.1.1.1. The species is concluded to be a secondary photoproduct in the system. The rate of decay of this species is independant of CO concentration; k_{obs} was calculated to be 20.6 s^{-1}. The UV/vis difference spectrum of this species obtained within 3200μs of the laser pulse is given in Figure 2.3.1.1.2. A slightly

negative band at *ca.* 325nm occurs in the region of the M --> arene CT band of the parent tricarbonyl compound. The transient species has a weak absorption band in the UV region of the spectrum at 280nm and a stronger band in the visible region of the spectrum at *ca.* 425nm.

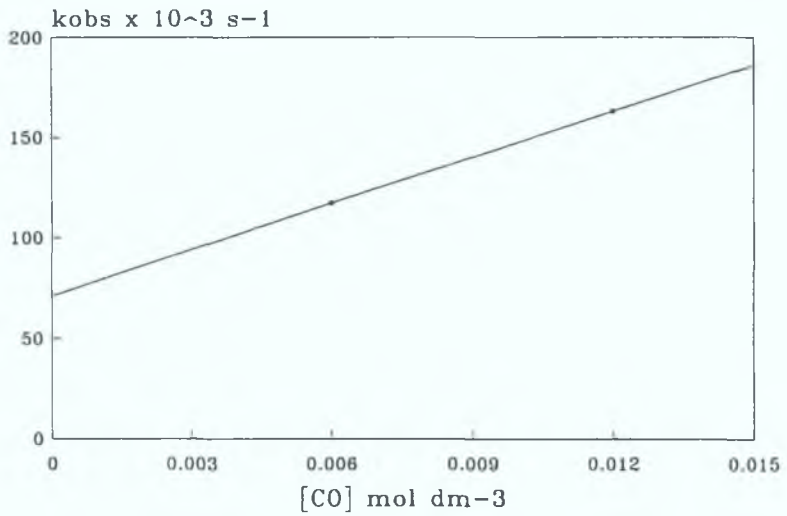

[CO] mol dm^{-3}	k_{obs} s^{-1}
0.006	117000
0.012	163000

$k_{[co]} = 7.6 \times 10^6 \pm 0.8 \times 10^6$ dm^3 mol^{-1} s^{-1}

Intercept = 7098 ± 8000 s^{-1}

Figure 2.3.1.1.1 A second order plot of the observed rate of formation (s^{-1}) of the secondary photoproduct at differing CO concentrations (mol dm^{-3}) at 298K.

Table 2.3.1.1.1 The yield of the secondary photoproduct observed on laser flash photolysis of (η^6-benzene)$Cr(CO)_3$ at differing CO concentrations at 298K.

[CO] mol dm^{-3}	Absorption
0.006	8.84×10^{-2}
0.012	4.46×10^{-2}

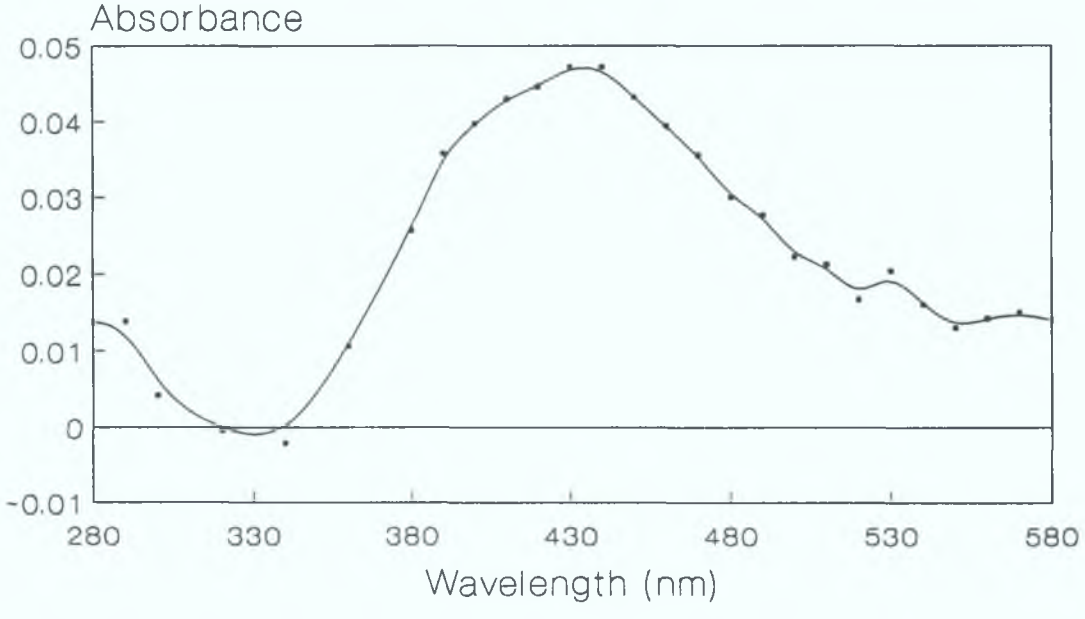

Figure 2.3.1.1.2 UV/vis difference spectrum of secondary photoproduct recorded 3200μs after the flash on photolysis of (η^6-benzene)$Cr(CO)_3$ in non-liquid pumped cyclohexane solution at 298K under 0.5 atmosphere of CO.

2.3.1.2 Photochemistry in Liquid-Pumped Solution

2.3.1.2.1 Preliminary Experimental Results

Laser flash photolysis of a (η^6-benzene)$Cr(CO)_3$ sample solution degassed and liquid pumped to a final concentration of 4.57 x 10^{-4} mol dm^{-3} again revealed the presence of a third absorbing transient species. The rate of formation of this species was measured to be 1.6 x 10^4 s^{-1} under argon atmosphere. The formation of this species was strongly suppressed on addition of CO to the solution. Hence the absorption characteristics were examinable optimally under inert (argon) atmosphere. This species was long-lived; no decay was observed over timebases of less than 200,000μs (200ms). At longer timebases any decay observed can be attributed to diffusion of the photoproduct away from the detection zone; where the species diffuses into the surrounding solution thereby reducing the concentration of the sample in the monitoring area and an apparent 'decay' is observed. The photochemical system appeared to be reversible, as UV/vis spectra monitored throughout the experiment showed no significant changes, indicating that the parent tricarbonyl was eventually regenerated.

The UV/vis difference spectrum of this transient species obtained within 60μs of the laser pulse in liquid pumped cyclohexane solution under argon is given in Figure 2.3.1.2.1.1. Two absorption maxima are evident; a weak absorption centred at *ca.* 520nm and a stronger band centred at 280nm. A slight depletion at 340nm indicates that there is spectral overlap of the band centred at 280nm with the parent spectrum in this region. The wavelength of maximum depletion does not coincide exactly with the true absorption maximum of 325nm for (η^6-benzene)$Cr(CO)_3$. This

transient spectrum differs significantly from that obtained utilising a non-liquid pumped sample.

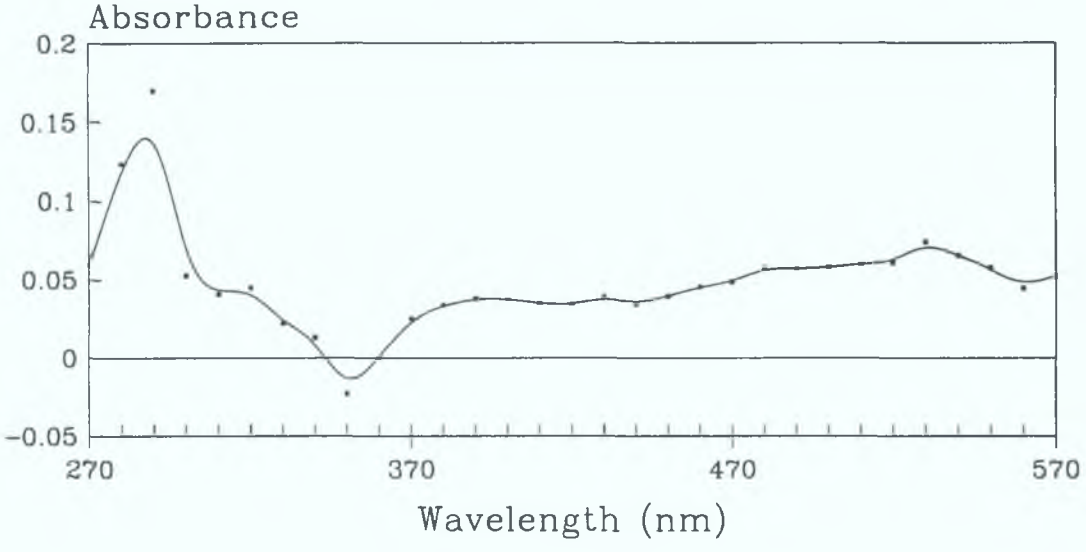

Figure 2.3.1.2.1.1 UV/vis difference spectrum recorded 60μs following flash photolysis of a liquid pumped cyclohexane solution of (η^6-benzene)$Cr(CO)_3$ under 1.0 atmosphere of argon.

The secondary photoproduct observed in liquid pumped solution appears to correspond to that observed by Gilbert *et al.* on laser flash photolysis of (η^6-benzene)$Cr(CO)_3$[3(b)]. A species was observed to form which absorbed throughout the visible spectrum with λ_{max} of *ca.* 500nm. As with the experiments performed here, the species was strongly quenched if the solution was saturated under 1.0 atmosphere of CO.

The transient absorption spectrum recorded in non-liquid-pumped cyclohexane solution is identical to that observed by Creaven [5(b)] in previous flash photolysis

experiments on (η^6-benzene)$Cr(CO)_3$ and assigned as a dinuclear η^6-benzene)$_2Cr_2(CO)_5$ species. The reduction in the level of this species in solution subjected to a liquid-pumping procedure points to its identity as an impurity complex and may indicate that the liquid pumping stage was inadequate in these previous experiments. The assignment of this species as the (η^6-benzene)$_2Cr_2(CO)_5$ species in these earlier experiments is then put in doubt. The photochemical behaviour recorded by Creaven indicated that an additional species was perhaps present. An absorption centred around 510nm was noted in the UV/vis spectrum of (η^6-benzene)$Cr(CO)_3$ following flash photolysis, and this is co-incident with the absorption maximum of the species recorded in liquid-pumped solution.

A possible explanation for the observation of different transient species in solutions of differing dryness is that different conformational isomers of a dinuclear species are formed depending on the levels of solvent impurities present to influence the reaction. A *trans* arrangement for the arene rings in an (η^6-benzene)$_2Cr_2(CO)_5$ complex is the less sterically crowded and would be expected to be the preferred conformation for this species based on analagous isolable complexes, e.g. $(C_5H_5)_2Re_2(CO)_5$[27]. It is possible that a *cis*-isomer is produced in the case of a non-liquid pumped sample as the presence of the water molecule coordinated to the dicarbonyl species may sterically hinder the formation of a *trans*-isomer. This unstable complex may then reform the parent molecule.

The secondary photoproduct observed in liquid-pumped sample solution is most plausibly assigned to the dinuclear species (η^6-benzene)$Cr(CO)_2(\mu$-$CO)Cr(CO)_2(\eta^6$-benzene) formed by reaction of the solvated dicarbonyl photoproduct with parent

tricarbonyl, reaction 2.3.1.2.1.1. Similarly, $(\eta^5\text{-}C_5H_5)Mn(CO)_3$ is known to form $(\eta^5\text{-}C_5H_5)_2Mn_2(CO)_5$ following photolysis in hydrocarbon solution at ambient temperatures[5(a)], reactions 2.3.1.2.1.2 to 2.3.1.2.1.4.

$ArCr(CO)_2(S) + ArCr(CO)_3$ ----------> $Ar_2Cr_2(CO)_5$ (2.3.1.2.1.1)

$CpMn(CO)_3$ ----------> $CpMn(CO)_2 + CO$ (2.3.1.2.1.2)

$CpMn(CO)_2 + S$ ----------> $CpMn(CO)_2(S)$ (2.3.1.2.1.3)

$CpMn(CO)_2(S) + CpMn(CO)_3$ ----------> $Cp_2Mn_2(CO)_5$ (2.3.1.2.1.4)

(where Ar = η^6-arene and Cp = $\eta^5\text{-}C_5H_5$)

A similar dimerisation reaction was observed upon flash photolysis of $Cr(CO)_6$ in perfluoro solvents, where the $Cr(CO)_5$ photoproduct reacted with parent, presumably to form $Cr_2(CO)_{11}$[2(b)]. The formation of dinuclear species is not uncommon and has also been reported in the $(\eta^5\text{-}C_5H_5)Co(CO)_2$[28] and $CpV(CO)_4$[29] systems. Rest *et al.* observed $(\eta^6\text{-benzene})_2Cr_2(CO)_5$ following photolysis of $(\eta^6\text{-benzene})Cr(CO)_3$ in nujol matrices at 77K[10(b)]. The proposed dinuclear species may contribute significantly to the long-lived absorption at 280nm, as it appears from the difference UV/vis spectrum that it's extinction coefficient is much higher at this wavelength than in the visible region of the spectrum. In conditions of high parent concentration and low CO concentration the formation of this species would be favoured.

2.3.1.2.2 Effect of Variations in Parent (η^6-benzene)$Cr(CO)_3$ Concentration

The rate of grow-in of the secondary photoproduct in liquid-pumped cyclohexane solution was measured as a function of parent concentration. A linear dependance was apparent, Table 2.3.1.2.2.1. A plot of k_{obs} versus parent concentration is shown in Figure 2.3.1.2.2.1. The slope of the line, which passes through the origin, gives a second order rate constant of 4.9×10^7 mol^{-1} dm^3 s^{-1} for the reaction of (η^6-benzene)$Cr(CO)_2(S)$ with (η^6-benzene)$Cr(CO)_3$ at 298K. It is note-worthy that the rate constant for the reaction of (η^6-benzene)$Cr(CO)_2(S)$ with CO is smaller than that for the formation of (η^6-benzene)$_2Cr_2(CO)_5$. Similar behaviour was observed for the (η^5-C_5H_5)$Mn(CO)_3$ system[5(a)].

A study of the dependance of the formation of the dinuclear species on the concentration of (η^6-benzene)$Cr(CO)_3$ was conducted in earlier experiments by Creaven[5(b)]. This study was rather subjective as the kinetic traces deviated from first-order over longer timescales, consequently a degree of error was incurred in the positioning of the baseline. In the study reported here the kinetic traces followed psuedo-first order kinetics involving no subjectivity in the positioning of the baseline. This difference is perhaps reflected in the intercept of both studies; a significant non-zero intercept was calculated in the previous study, whereas the line plotted in Figure 2.3.1.2.2.1 effectively passes through the origin.

It was observed during the course of this experiment that the rate of grow-in of the dinuclear species was directly affected by liquid-pumping of the sample solution. A sample was prepared for analysis in which the liquid-pumping stage was omitted. The rate of grow-in of the dinuclear species was faster than predicted in the case of

this non-liquid-pumped sample. This point is shown on Figure 2.3.1.2.2.1 for comparison; it is seen to lie at a distance from the best-fit line calculated by linear regression for the remaining points. This experiment demonstrates the reactivity of the primary photoproduct, (η^6-benzene)$Cr(CO)_2(S)$, towards impurities (H_2O) present in solution thereby illustrating that a number of reaction pathways are present for consumption of this primary photoproduct. Impurity species may compete with the parent complex for reaction with the (η^6-benzene)$Cr(CO)_2(S)$, with a consequent acceleration in the rate of disappearance of the (η^6-benzene)$Cr(CO)_2(S)$ intermediate.

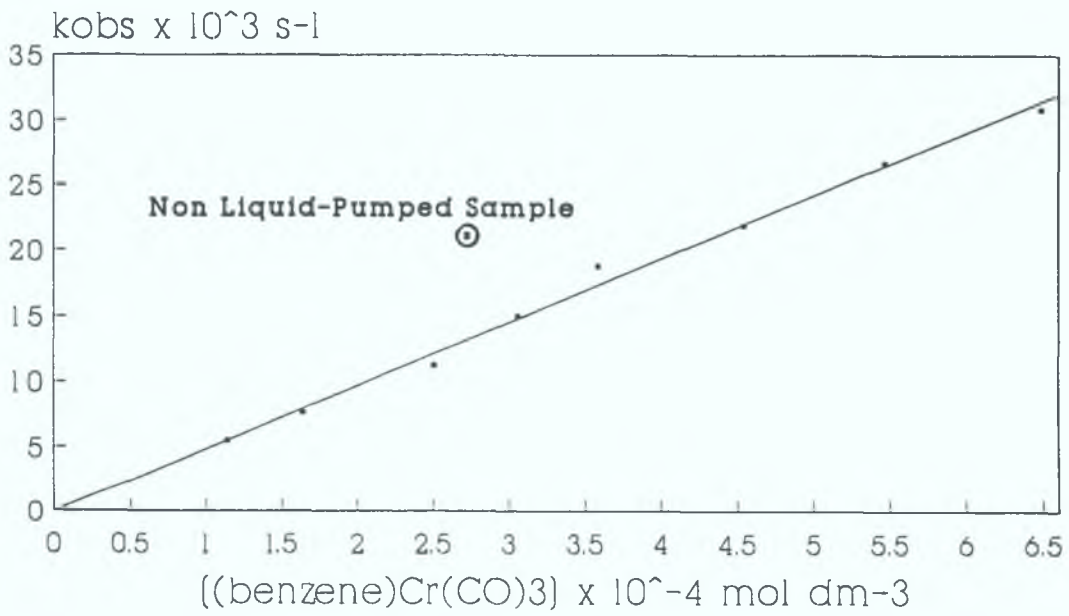

Figure 2.3.1.2.2.1 A plot of the the observed rate constants (s^{-1}) for the formation of the secondary photoproduct at differing concentrations of (η^6-benzene)$Cr(CO)_3$ (mol dm^{-3}) at 298K.

Table 2.3.1.2.2.1 The observed rate constants (s^{-1}) for the formation of the secondary photoproduct at differing concentrations of (η^6-benzene)$Cr(CO)_3$ (mol dm^{-3}) at 298K. [a]non liquid-pumped sample.

[(η^6-benzene)$Cr(CO)_3$], mol dm^{-3}	k_{obs}, s^{-1}
1.14×10^{-4}	5506
1.64×10^{-4}	7650
2.51×10^{-4}	11259
2.71×10^{-4}	20943[a]
3.05×10^{-4}	15006
3.58×10^{-4}	18802
4.54×10^{-4}	21897
5.47×10^{-4}	26705
6.49×10^{-4}	30839

$k[(\eta^6\text{-benzene})Cr(CO)_3]$ = slope = $4.9 \times 10^7 \pm 1.5 \times 10^6$ dm^3 mol^{-1} s^{-1}

Intercept = -7.46 ± 754.81 s^{-1}

Corr. Coeff. = 0.997

2.3.1.2.3 Preliminary TRIR Studies on Dinuclear Species Formation

The TRIR spectrum from 1730 to 1997cm^{-1} obtained within 10μs following the laser flash photolysis of a 4.1 x 10^{-4} mol dm^{-3} solution of (η^6-benzene)Cr(CO)$_3$ in n-heptane under 2.0 atmospheres of argon is displayed in Figure 2.3.1.2.3.1. The two negative peaks at 1984cm^{-1} and 1916cm^{-1} represent the depletion of the parent absorption bands. The two positive peaks at 1929cm^{-1} and 1877cm^{-1} correspond to the production of the primary photoproduct (η^6-benzene)Cr(CO)$_2$(S). The parent absorptions are only partially regenerated, Figure 2.3.1.2.3.2, the rate of which corresponds to the rate of (η^6-benzene)Cr(CO)$_2$(S) decay; k_{obs} = 3.13 x 10^4 s^{-1}.

The TRIR spectrum from 1730 to 1997cm^{-1} obtained 500μs following the laser flash photolysis of (η^6-benzene)Cr(CO)$_3$ in n-heptane under 2.0 atmospheres of argon is displayed in Figure 2.3.1.2.3.3. The two negative peaks at 1986 and 1919cm^{-1}, attributed to depletion of the parent absorptions, are still apparent. Numerous positive peaks arising from the production of photoproducts are observable in this spectrum; the assignment of which are complicated by the number of bands and spectral overlap of peaks. The parent and photoproduct absorbances in this spectrum are 'off-scale'; if properly scaled many weak 'photoproduct' absorptions would be reduced to background noise and baseline variations. The species exhibiting positive bands centred at 1946cm^{-1}(s) and 1903cm^{-1}(s) and 1795cm^{-1}(w) is seen to grow-in from the carbonyl-loss product, (η^6-benzene)Cr(CO)$_2$(S). The rate of formation was measured as 3.6 x 10^4 s^{-1}. This species is long-lived; no decay was observed over a timescale of 2ms. A second transient species observable at 1895cm^{-1} (denoted by '*' in Figure 2.3.1.2.3.3) is formed at a faster rate than the decay of the carbonyl-loss

carbonyl-loss product and is only relatively long-lived in comparison to the lifetime of the first species. The assignment of further bands to this species is complicated by spectral overlap of bands

It is readily apparent from this spectrum that the number of carbonyl bands are too numerous to be attributed to a single species. It would appear that there are several bands in the bridging carbonyl region of the spectrum, suggesting that more than one species with bridging carbonyl groups is present. The carbonyl stretching frequencies assigned to (η^6-benzene)$_2$Cr$_2$(CO)$_5$ by Rest *et al* in nujol matrices at 77K were detected at 1989, 1937, 1885 and 1778cm^{-1}, with a fifth band in the region 1920-1935cm^{-1} obscured by other spectral bands[10(b)] It is possible that the 1946, 1903 and 1795cm^{-1} bands detected in this experiment correspond to the 1937, 1885 and 1778cm^{-1} absorptions of this species; representing a shift of 10-17cm^{-1} to higher wavenumber (i e. lower energy) on the band positions observed in matrix experiments. The intermediate peaks at 1946, 1903 and 1795cm^{-1} are then tentatively assigned to the formation of a (η^6-benzene)$_2$Cr$_2$(CO)$_5$ species. The remaining intense intermediate peak at 1827cm^{-1} cannot possibly result from this species, as a shift of *ca* 50cm^{-1} on the 1778cm^{-1} peak observed in matrix results is not plausible. Furthermore, this peak cannot then be conclusively attributed to the absorptions of a bridging carbonyl group as it is just within the acceptable wavenumber range

This experiment has since been repeated; the TRIR spectrum obtained within 20μs after the laser pulse under 2 0 atmospheres of argon is given in Figure 2 3 1 2.3 4[30] The essential features of this spectrum are identical to that in Figure 2.3.1 2 3 3 , given that the previous spectrum is incorrectly scaled, i e depletion of

the parent absorptions is evident at 1986 and 1920cm^{-1} and three intense photoproduct bands are observed at 1945, 1895 and 1828cm^{-1}

These experiments would seem to corroborate the observation of more than one dinuclear species in laser flash photolysis experiments on (η^6-benzene)Cr(CO)$_3$. It is possible that one species remained unobserved by Rest *et al* in the single reported matrix isolation experiment in which the formation of (η^6-benzene)$_2$Cr$_2$(CO)$_5$ was noted[10(b)]. It is also possible that the same species is not observed on photolysis in room temperature solution as is observed in low-temperature matrices. In matrix isolation experiments the photochemical products are trapped in the rigid matrix and effectively prevented from undergoing further reaction, while in room temperature solution subsequent reactions may occur to produce the species detected in these laser flash photolysis and TRIR experiments

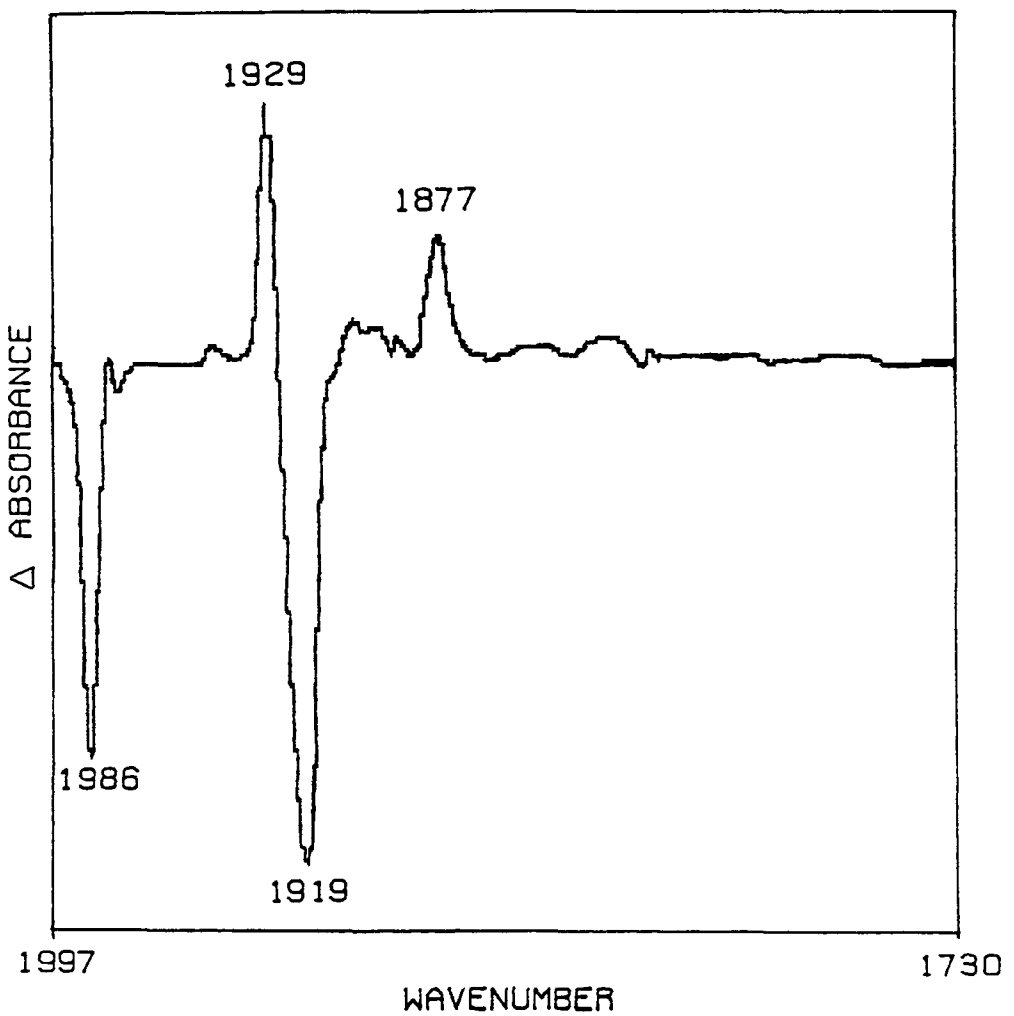

Figure 2.3.1.2.3.1 Time resolved infrared spectrum obtained 10μs after laser photolysis of (η^6-benzene)$Cr(CO)_3$ in n-heptane solution under 2 0 atmospheres of argon at 303K.

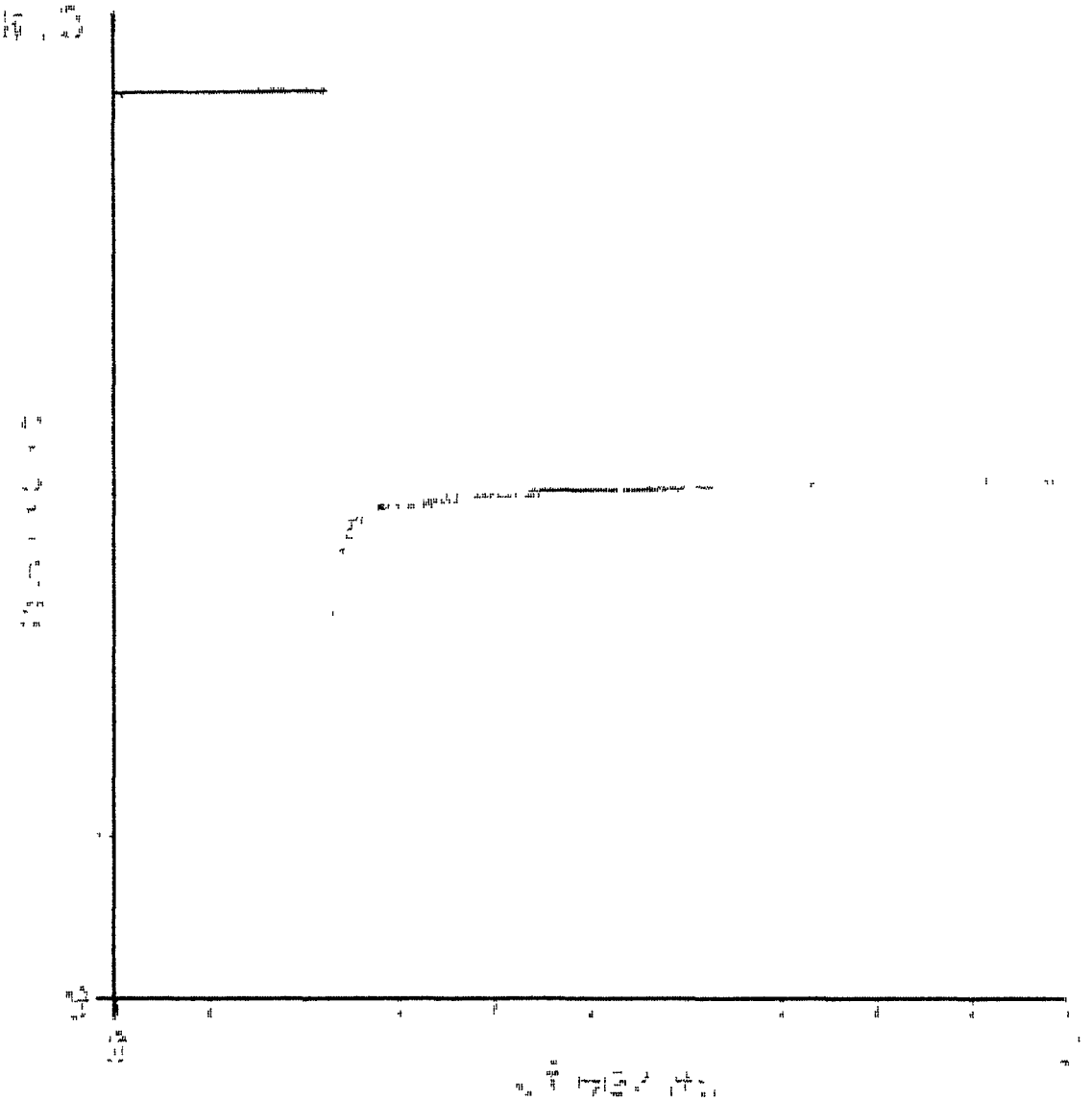

Figure 2.3.1.2.3.2 Time resolved infrared transient signal recorded at 1984cm^{-1} following laser flash photolysis of (η^6-benzene)Cr(CO)$_3$ in n-heptane solution under 2 0 atmospheres of argon showing partial regeneration of the parent absorption

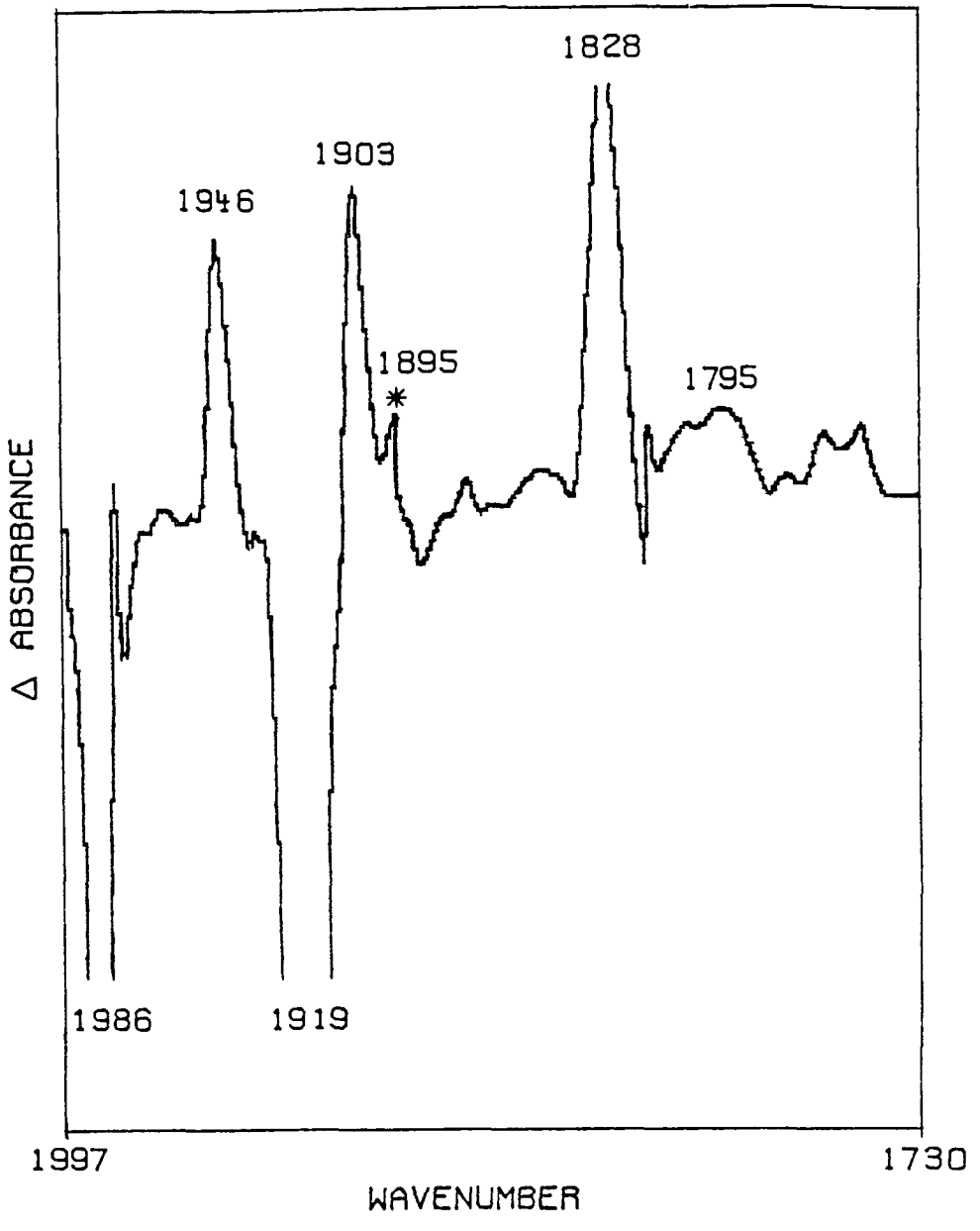

Figure 2.3.1.2.3.3 Time resolved infrared spectrum obtained 500μs after laser photolysis of (η^6-benzene)$Cr(CO)_3$ in n-heptane solution under 2.0 atmospheres of argon at 303K.

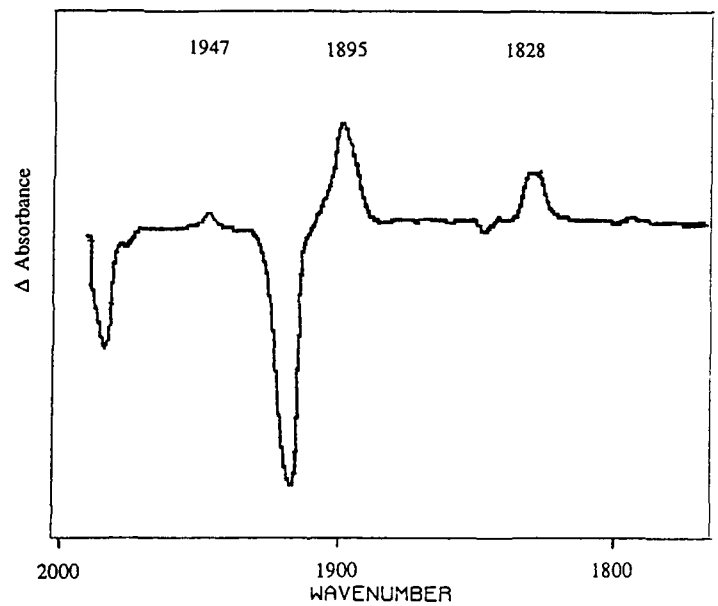

Figure 2.3.1.2.3.4 Time resolved infrared spectrum obtained within 20μs of laser flash photolysis of (η^6-benzene)$Cr(CO)_3$ in n-heptane solution under 2.0 atmospheres of argon[30]

2.3.2 Photochemistry of Methyl Substituted (η^6-arene)$Cr(CO)_3$ Compounds

Experiments were conducted to determine if the series of methyl substituted (η^6-arene)$Cr(CO)_3$ complexes underwent reactions resulting in the formation of dinuclear species. Steric constraints may influence the formation of dinuclear species in this case as the arene ligand is increasing in size with increased methylation The availability of metal orbitals, both in sufficient number and of the correct orientation for the formation of bridging carbonyl ligands is not expected to differ markedly in any of these complexes and is not a major factor for consideration in these reactions. These investigations were carried out for the most part at high concentration of parent, when the propensity for formation of a dinuclear complex is high These

experiments were typically conducted under argon atmosphere to eliminate the possibility of competing reactions of the primary photoproducts with the CO ligand to regenerate the parent complex

2.3.2.1 Photochemistry in Non-Liquid Pumped Solution

Experimental results obtained on the photochemistry of substituted (η^6-arene)$Cr(CO)_3$ complexes in non liquid-pumped cyclohexane revealed similar behaviour to that of the unsubstitued case The UV/vis spectra generated following laser flash photolysis of a 1 8 x 10^{-4} mol dm^{-3} solution of (η^6-p-xylene)$Cr(CO)_3$ in non liquid-pumped cyclohexane under 0 5atm CO are given in Figure 2 3 2 1.1. The initial spectrum at 1μs is identical to that of the (η^6-p-xylene)$Cr(CO)_2$(S) species (λ_{max} 280nm, λ_{min} 330nm), indicating that any further species are generated from this precursor The spectrum at 16μs has absorption maxima at 425nm and <280nm and an absorption minimum at 330nm This spectral evidence indicates that this species is formed directly from the (η^6-p-xylene)$Cr(CO)_2$(S) species. This conclusion is supported by the direct dependance of the rate of formation of this third absorbing transient species on CO concentration, Figure 2 3.2.1 2. The second order rate constant for this reaction is approximately the same as that for the reaction of (η^6-p-xylene)$Cr(CO)_2$(S) with CO, both sets of values are plotted in Figure 2.3 2.1.2 for comparison The rate of decay of this species is also dependant on the concentration of CO in solution, suggesting that the decay of this species involves a reaction with CO

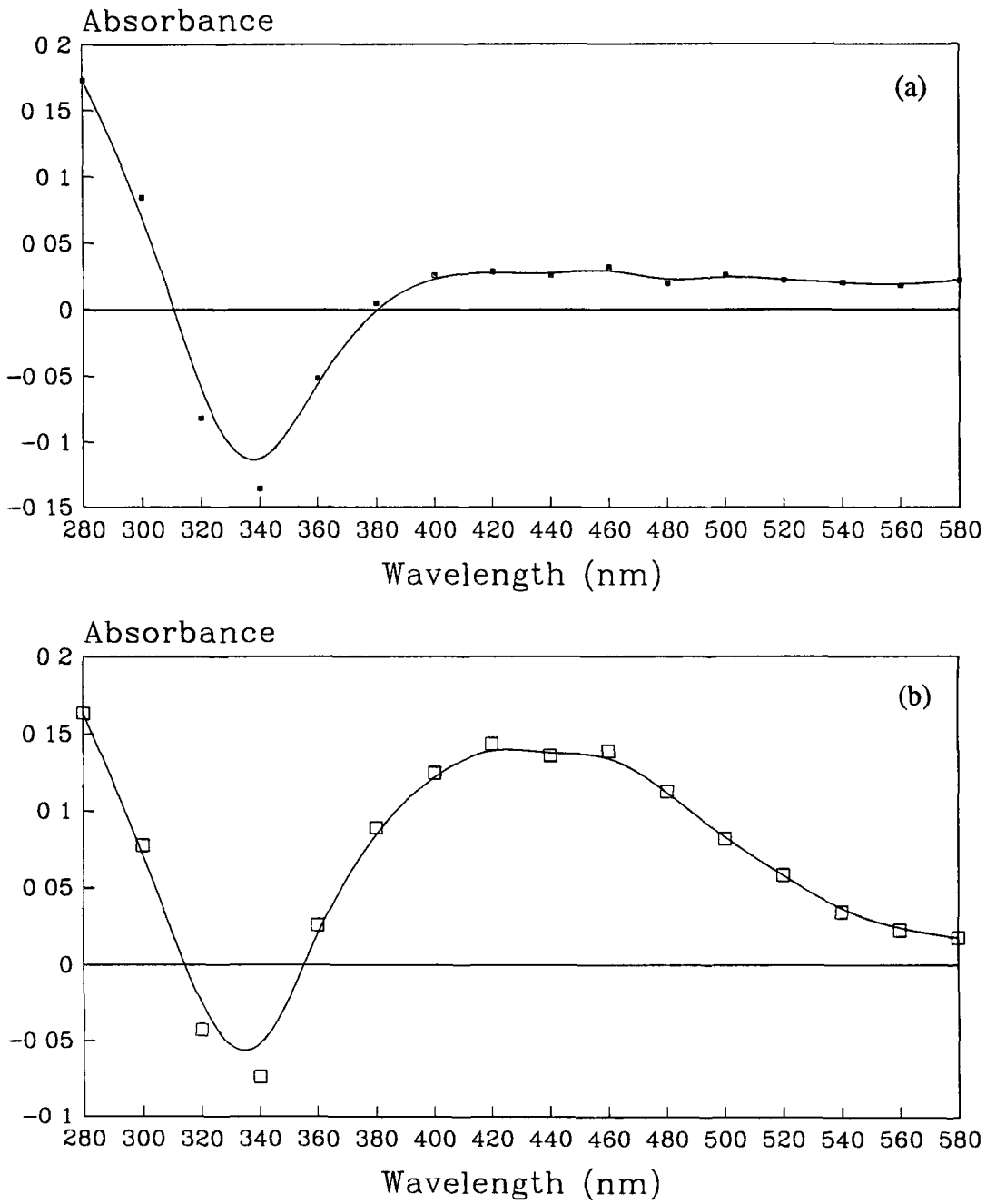

Figure 2.3.2.1.1 UV/vis difference spectra generated 1μs (a) and 16μs (b) after the laser flash photolysis of (η^6-p-xylene)$Cr(CO)_3$ under 0 5 atmosphere of CO

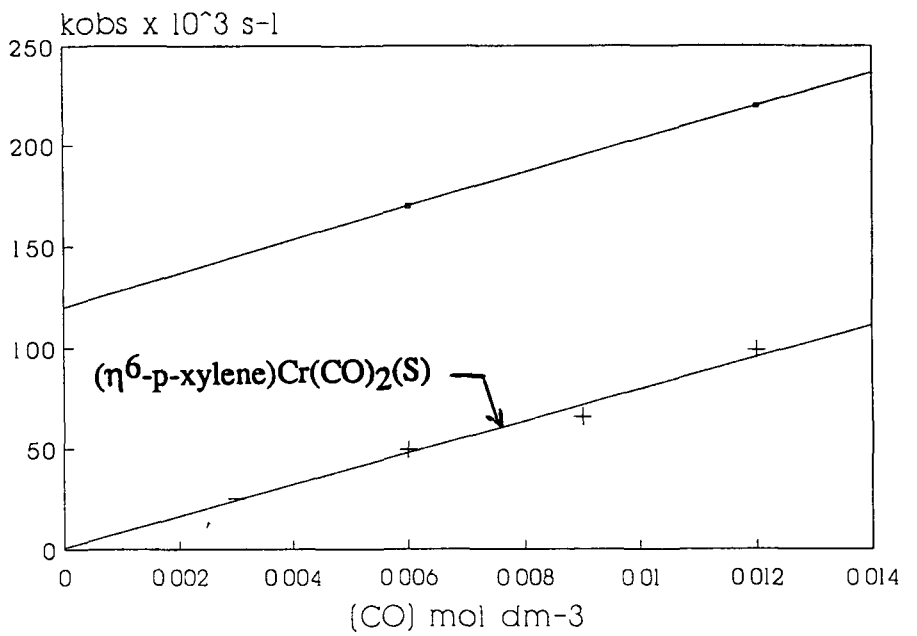

[CO] mol dm^{-3}	k_{obs} (grow-in) s^{-1}	k_{obs} (decay) s^{-1}
0 006	1 7 x 10^5	1.8
0 012	2.2 x 10^5	3 5

$k_{[CO]}$ (grow-in) = 7 92 x 10^6 ± 0 8 x 10^6 dm^3 mol^{-1}

Intercept = 1 27 x 10^5 s^{-1}

Figure 2.3.2.1.2 The observed rates of formation and decay (s^{-1}) of the secondary photoproduct produced on laser flash photolysis of (η^6-p-xylene)$Cr(CO)_3$ at differing CO concentrations (mol dm^{-3}) The values for the reaction of (η^6-p-xylene)$Cr(CO)_2$(S) with CO are plotted for comparison purposes

2.3.2.2 Photochemistry in Liquid-Pumped Solution

2.3.2.2.1 Preliminary Experimental Results

Laser flash photolysis of liquid-pumped solutions of substituted (η^6-arene)$Cr(CO)_3$ complexes in cyclohexane revealed different behaviour from that occuring in the case of non-liquid pumped solutions; as in the case of (η^6-benzene)$Cr(CO)_3$ The most extensively studied was the (η^6-C_6Me_6)$Cr(CO)_3$ complex, the results of which are outlined below.

Laser flash photolysis of a liquid-pumped sample of a 3 8 x 10^{-4} mol dm^{-3} solution of (η^6-C_6Me_6)$Cr(CO)_3$ in cyclohexane under 1.0 atmosphere of argon reveals the formation of two transient species, hereafter referred to as the third and fourth transient species respectively, in addition to the primary photoproducts described earlier UV/vis difference spectra obtained at 36μs and 170μs are given in Figures 2.3 2 2 1 1 and 2.3 2.2.1 2 A spectrum of the third transient species obtained at 36μs after the laser flash has absorption maxima at 280nm and ~410nm in the visible region; depletion of the parent absorption at 320nm is evident at 340nm. The absorption at longer wavelengths is weak This species appears to be an intermediate as it is fully formed within 40μs, Figure 2 3 2 2 1 3, and subsequently decays by means of a double exponential process, Figure 2.3 2 2.1 4. This process is not fully reversible on this timescale, under these conditions, as exemplified by the residual absorption. The fourth species has an absorption maximum at 280nm and a rather broad band centred at ~580nm in the visible region, Figure 2 3 2 2 1.5 This species is long-lived and stable over a timebase of <200,000μs

It is apparent from the difference UV/vis spectra that both species have strong

absorptions at 290nm, in the 'valley' of the absorption profile of the parent complex. The $(\eta^6\text{-}C_6Me_6)Cr(CO)_2(S)$ species was also shown to have an 'apparent' λ_{max} at this wavelength. It is therefore very difficult to extract meaningful kinetic data at this wavelength Analysis of the rate constants at the absorption maxima in the visible region, at which there is less spectral overlap, is much more effective

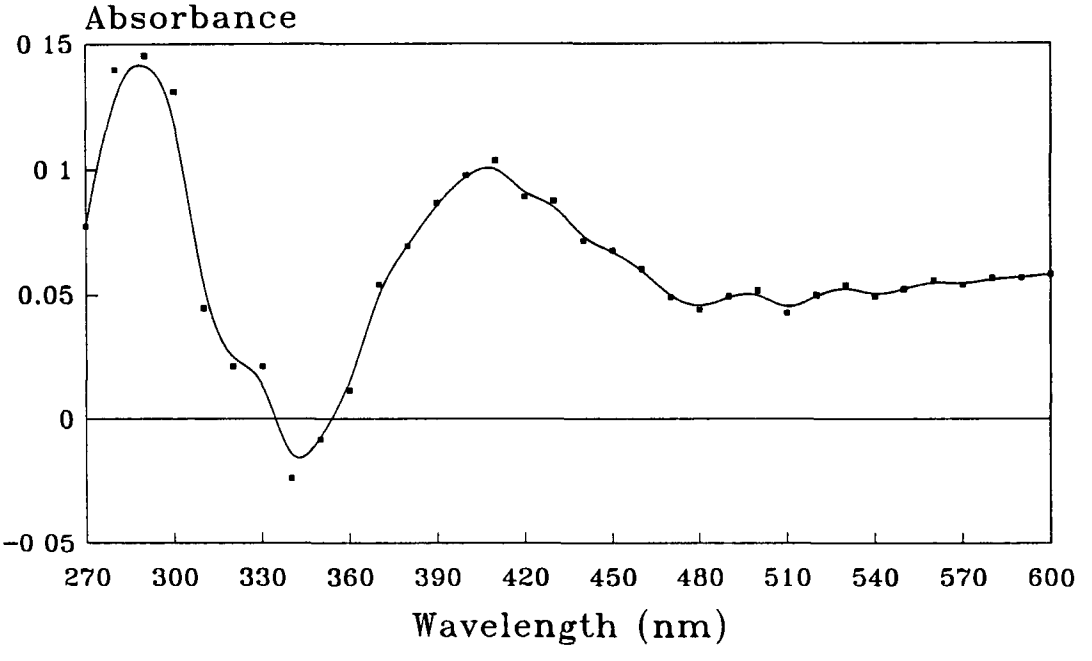

Figure 2.3.2.2.1.1 UV/vis difference spectrum of the third transient species recorded at 36μs following flash photolysis of a liquid pumped cyclohexane solution, of $(\eta^6\text{-}C_6Me_6)Cr(CO)_3$ concentration 3 8 x 10^{-4} mol dm^{-3}, under 1.0 atmosphere of argon.

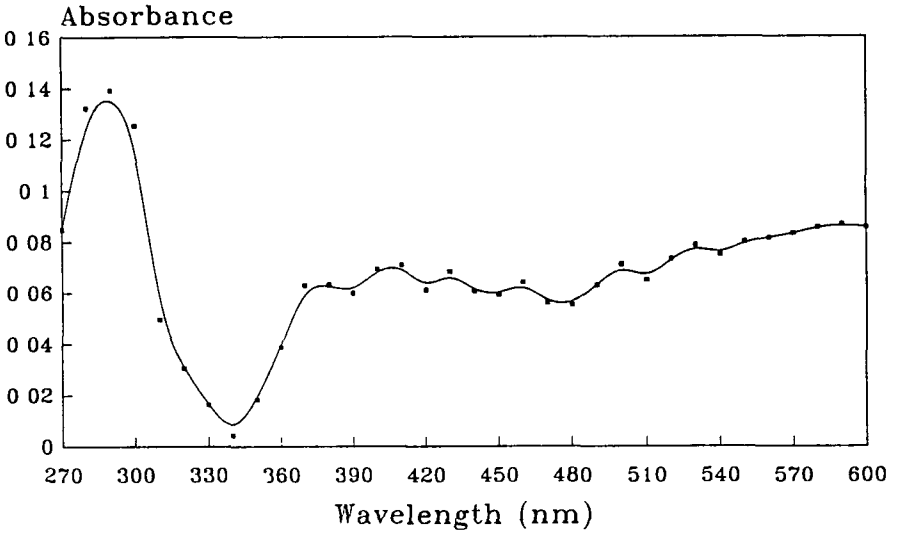

Figure 2.3.2.2.1.2 UV/vis difference spectrum of the fourth transient species recorded at 170μs following flash photolysis of a liquid pumped cyclohexane solution, of $(\eta^6\text{-}C_6Me_6)Cr(CO)_3$ concentration 3 8 x 10^{-4} mol dm^{-3}, under 1.0 atmosphere of argon

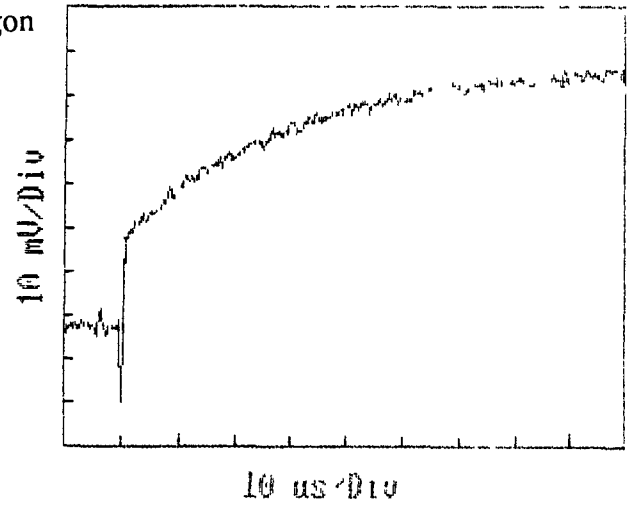

Figure 2.3.2.2.1.3 A transient signal obtained for the formation of the third absorbing transient species monitored at 410nm under 1 0 atmosphere of argon, at a $(\eta^6\text{-}C_6Me_6)Cr(CO)_3$ concentration of 3 8 x 10^{-4} mol dm^{-3}

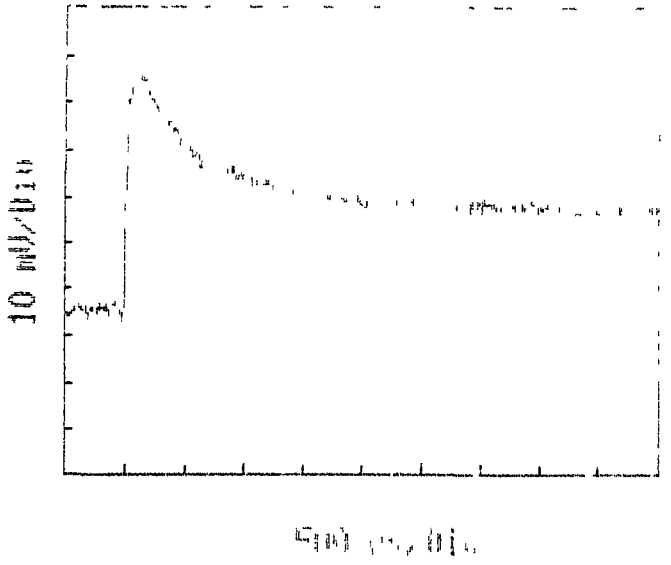

Figure 2.3.2.2.1.4 A transient signal obtained for the decay of the third absorbing transient species monitored at 410nm under 1 0 atmosphere of argon at a (η^6-C_6Me_6)$Cr(CO)_3$ concentration of 3 8 x 10^{-4} mol dm^{-3}

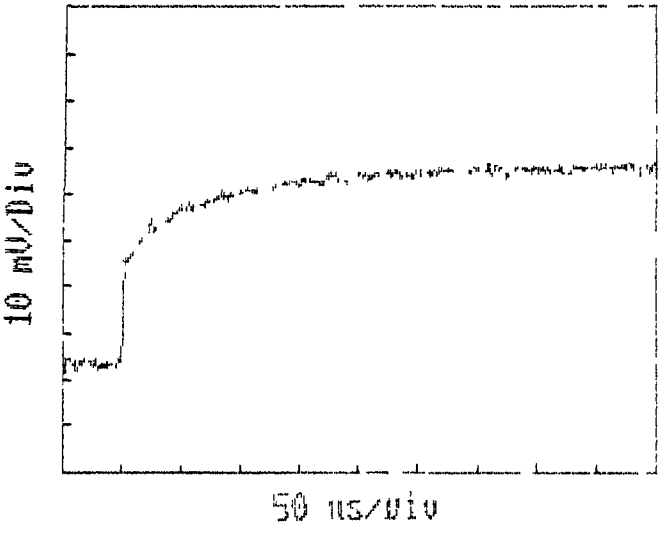

Figure 2.3.2.2.1.5 A transient signal obtained for the fourth absorbing transient species monitored at 580nm under 1 0 atmosphere of argon at a (η^6-C_6Me_6)$Cr(CO)_3$ concentration 3 8 x 10^{-4} mol dm^{-3}

2.3.2.2.2 Effect of Variations in CO Concentration

The observed rate of formation of the third transient species, monitored at 410nm, was determined to be directly dependant on the concentration of CO present in solution; yielding a second order rate constant of 1 1 x 10^7 dm^3 mol^{-1} s^{-1}; Figure 2.3 2.2 2 1. This value is almost identical to that obtained for the reaction of (η^6-C_6Me_6)$Cr(CO)_2$(S) with CO, both series of values are plotted in Figure 2 3.2.2.2.1 for comparison purposes. The yield of this species decreased with increasing CO concentration These results indicate that this species is a secondary photoproduct formed by reaction of the primary photoproduct (η^6-C_6Me_6)$Cr(CO)_2$(S) Although the rate of decay of this species did not always fit a single exponential function, an analysis of the initial portion of the decay signal revealed that it was also linearly dependant on CO concentration, yielding a second order rate constant from the slope of the line of 2 1 x 10^6 dm^3 mol^{-1} s^{-1}, Figure 2 3 2 2 2 2 The formation of the fourth transient species, with λ_{max} 580nm was strongly suppressed in the presence of CO, even under 0 25atm CO the only absorption detected at this wavelength was that attributed to the decay of the primary photoproduct (η^6-C_6Me_6)$Cr(CO)_2$(S) which absorbs weakly in the visible region The rate of formation was measured as 7 7 x 10^3 s^{-1} under argon atmosphere The rate of formation of this species also did not always fit a single exponential function, possibly on account of spectral overlap of absorptions of the third and fourth species in this region

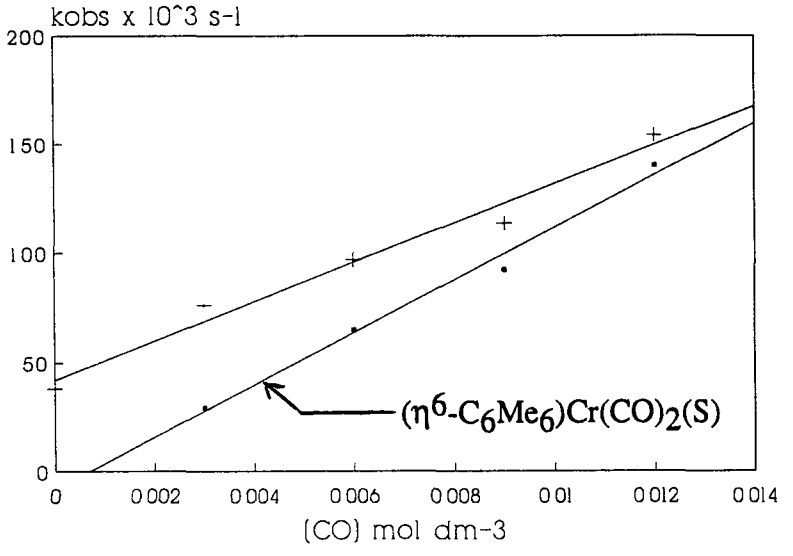

[CO] mol dm^{-3}	k_{obs} s^{-1}
0 000	38187
0 003	76227
0 006	96878
0 009	113550
0 012	153690

$k_{[CO]} = 1\ 12 \times 10^7 \pm 0\ 82 \times 10^6\ dm^3\ mol^{-1}\ s^{-1}$

Intercept = -26100 ± 12256 s^{-1}

Corr Coeff. = 0.997

Figure 2.3.2.2.2.1 The observed rate constants (s^{-1}) for the production of the third photoproduct, monitored at 410nm, on laser flash photolysis of $(\eta^6\text{-}C_6Me_6)Cr(CO)_3$ at differing CO concentrations (mol dm^{-3}) at 298K The rate constants for the reaction of $(C_6Me_6)Cr(CO)_2(S)$ with CO are plotted for comparison purposes.

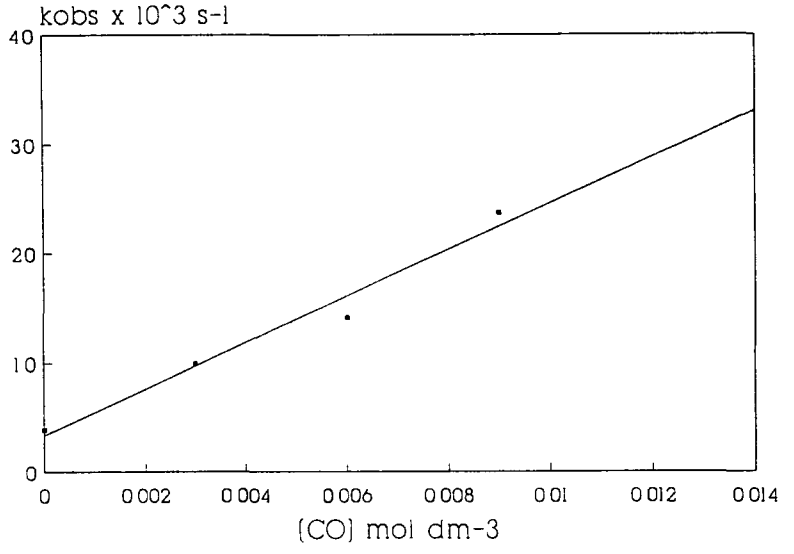

[CO] mol dm^{-3}	k_{obs} s^{-1}
0 000	3880
0 003	9910
0 006	14100
0 009	23700

$k_{[co]} = 2.13 \times 10^6 \pm 2\ 5 \times 10^5$ dm^3 mol^{-1} s^{-1}

Intercept = 3294 ± 1693 s^{-1}

Corr Coeff. = 0 986

Figure 2.3.2.2.2.2 The observed rate constants (s^{-1}) for the decay of the third photoproduct, monitored at 410nm, on laser flash photolysis of $(\eta^6\text{-}C_6Me_6)Cr(CO)_3$ at differing CO concentrations (mol dm^{-3}) at 298K

2.3.2.2.3 Effect of Variations in Parent (η^6-C_6Me_6)$Cr(CO)_3$ Concentration

The effect of changes in parent (η^6-C_6Me_6)$Cr(CO)_3$ concentration upon the observed rate of formation of both species was investigated experimentally The rate of formation of the third species displayed a linear dependance upon (η^6-C_6Me_6)$Cr(CO)_3$ concentration, Table 2 3.2.2 3 1, although the correlation coefficient of 0 962 is very poor given the large number of points (12) used in the calculation A plot of k_{obs} versus parent concentration is shown in Figure 2.3 2 2.3 1 The slope of the line gives a second order rate constant of 5 3 x 10^7 dm^3 mol^{-1} s^{-1} By analogy with the (η^6-benzene)$Cr(CO)_3$ system this value may represent the rate of reaction of (η^6-C_6Me_6)$Cr(CO)_2$(S) with parent If this result is taken as valid, despite the poor linear regression fit, it is not dissimilar to the value of 4 9 x 10^7 dm^3 mol^{-1} s^{-1} determined for the reaction of (η^6-benzene)$Cr(CO)_3$ with its primary photoproduct (η^6-benzene)$Cr(CO)_2$(S) Whereas the analogous plot of k_{obs} versus parent concentration for (η^6-benzene)$Cr(CO)_3$ passes through the origin, the plot in the η^6-C_6Me_6 case exhibits a significant and positive intercept of 1 7 x 10^4 s^{-1}

Only the first exponential decay was analysed at 410nm No dependance of the rate of decay of this species on parent concentration was found; Figure 2.3 2.2.3 2. A study of the dependance of the rate of formation of the fourth species was performed. At higher concentrations the transient signal resolved into the individual components of a double exponential function, both of which were not found to be dependant on parent (η^6-C_6Me_6)$Cr(CO)_3$ concentration, Figures 2.3 2.2 3 3 to 2.3 2 2 3 4 and Table 2 3 2 2 3 2 At lower concentrations the faster component of the exponential function is not readily resolved

Table 2.3.2.2.3.1 The observed rate constants (s^{-1}) for the production of the third transient species, monitored at 410nm, at varying concentrations of (η^6-C_6Me_6)$Cr(CO)_3$ (mol dm^{-3})

[(η^6-C_6Me_6)$Cr(CO)_3$] mol dm^{-3}	k_{obs} s^{-1}
1 27 x 10^{-4}	23072
1 46 x 10^{-4}	24206
1 56 x 10^{-4}	21870
1 76 x 10^{-4}	27137
2.72 x 10^{-4}	28502
3 10 x 10^{-4}	37512
3 66 x 10^{-4}	34477
3 97 x 10^{-4}	41092
4 61 x 10^{-4}	39435
4 77 x 10^{-4}	42532
5 63 x 10^{-4}	42609
6 05 x 10^{-4}	49814

k_2 = slope = 5 29 x 10^7 ± 4.8 x 10^6 dm^3 mol^{-1} s^{-1}

Intercept = 16492 ± 2645 s^{-1}

Corr Coeff. = 0 962

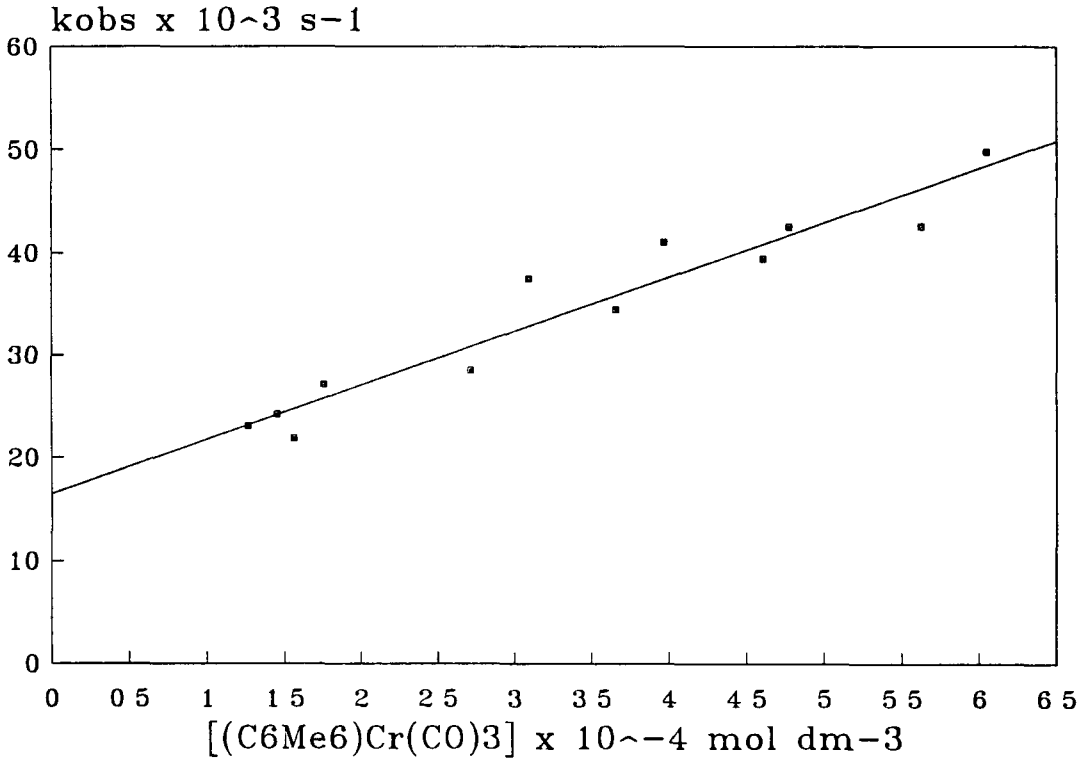

Figure 2.3.2.2.3.1 A plot of the observed rate of formation of the third transient species, monitored at 410nm, against concentration of $(\eta^6\text{-}C_6Me_6)Cr(CO)_3$

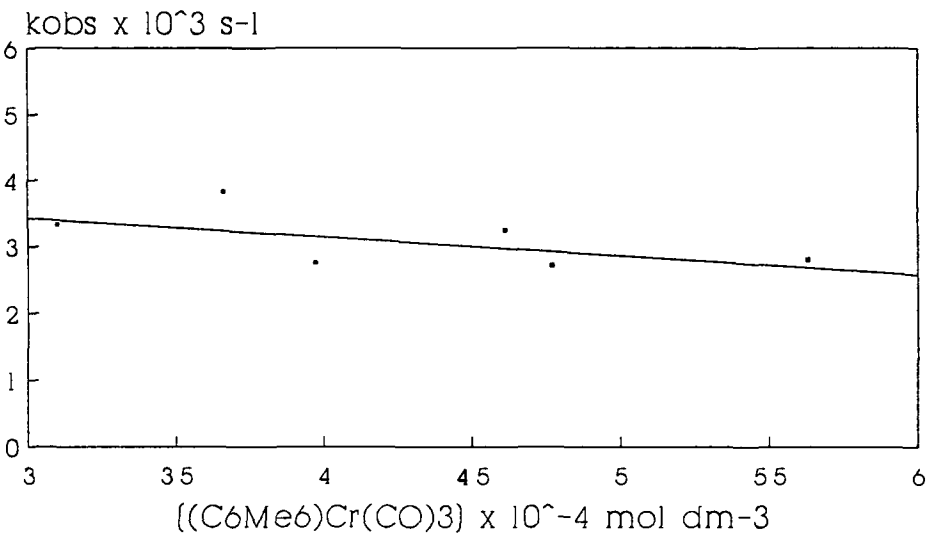

$[(\eta^6\text{-}C_6Me_6)Cr(CO)_3]$ mol dm^{-3}	k_{obs} s^{-1}
3 10 x 10^{-4}	3329
3 66 x 10^{-4}	3829
3 97 x 10^{-4}	2758
4 26 x 10^{-4}	2748
4 61 x 10^{-4}	3246
4 77 x 10^{-4}	2721
5 63 x 10^{-4}	2807

Figure 2.3.2.2.3.2 The observed rate constants (s^{-1}) for the decay of the third transient species, monitored at 410nm, at varying concentrations of (η^6-$C_6Me_6)Cr(CO)_3$ (mol dm^{-3})

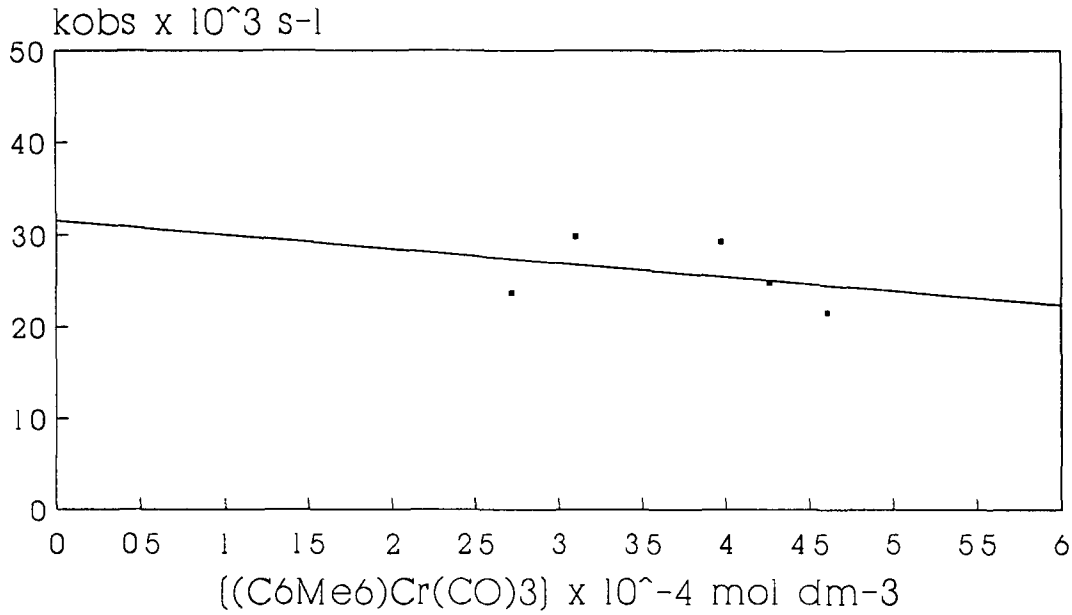

$[(\eta^6\text{-}C_6Me_6)Cr(CO)_3]$ mol dm^{-3}	k_{obs} s^{-1}
2.72 x 10^{-4}	23710
3 10 x 10^{-4}	29840
3 97 x 10^{-4}	29254
4 26 x 10^{-4}	24801
4 61 x 10^{-4}	21535

Figure 2.3.2.2.3.3 The observed rate constants (s^{-1}) for the first exponential function on analysis of the 'grow-in' of the fourth transient species, monitored at 580nm, at varying concentrations of $(\eta^6\text{-}C_6Me_6)Cr(CO)_3$ (mol dm^{-3})

Table 2.3.2.2.3.2 The observed rate constants (s^{-1}) for the second exponential function on analysis of the 'grow-in' of the fourth transient species at 580nm at varying concentrations of $(\eta^6\text{-}C_6Me_6)Cr(CO)_3$ (mol dm^{-3}).

$[(\eta^6\text{-}C_6Me_6)Cr(CO)_3]$ mol dm^{-3}	k_{obs} s^{-1}
5 34 x 10^{-5}	6119
6 55 x 10^{-5}	4465
9 09 x 10^{-5}	4532
1 46 x 10^{-4}	5892
1 56 x 10^{-4}	6887
1 71 x 10^{-4}	4296
1.76 x 10^{-4}	5261
2 08 x 10^{-4}	5166
2 72 x 10^{-4}	5335
3 10 x 10^{-4}	6600
3 97 x 10^{-4}	5850
4 26 x 10^{-4}	5137
4 61 x 10^{-4}	6775

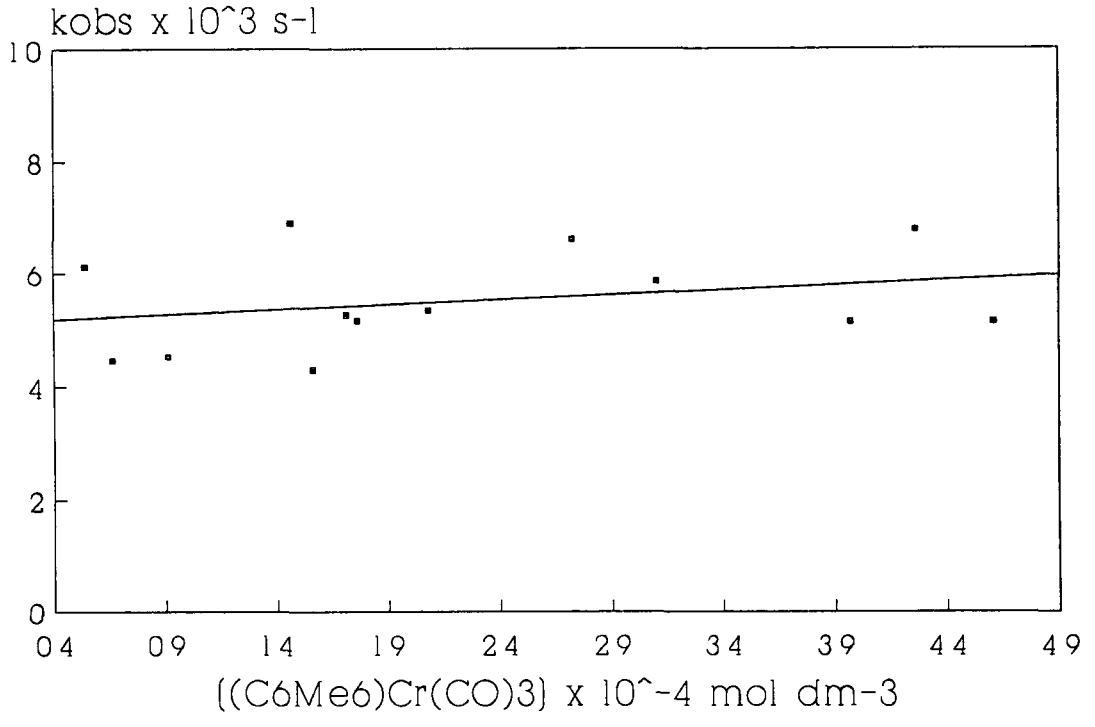

Figure 2.3.2.2.3.4 The observed rate constants (s^{-1}) for the second exponential function on analysis of the 'grow-in' of the fourth transient species, monitored at 580nm, at varying concentrations of $(\eta^6\text{-}C_6Me_6)Cr(CO)_3$ (mol dm^{-3}).

Once again, the question arises as to whether these species were generated consecutively or simultaneously Similarities are apparent in the rates of reaction of both species. The rate of formation of the third species at 410nm is similar to the first 'grow-in' of the fourth species at 580nm Similarly, the rate of decay of the third species at 410nm is not very dissimilar to that of the second 'grow-in' of the fourth transient species Since, in a sequential mechanism involving the reaction of species A to form species B, the rate of consumption of species A must equal the rate of formation of species B, these results indicate that a consecutive reaction leads to the formation of the fourth species from the third The third species has also been shown to react with CO, $k_2 = 2\ 13 \times 10^6$ $dm^3\ mol^{-1}\ s^{-1}$ It is not surprising then that the formation of the fourth species is suppressed in the presence of CO because of this competitive reaction Both species absorb at 580nm, albeit weakly, hence hindering any analysis of individual rates at this wavelength As there is no region of the spectrum where one species absorbs exclusively, the region at 410nm is most amenable to the study of these reaction rates by virtue of the large difference in the absorption of both species in this region

In the analysis of (η^6-benzene)$Cr(CO)_3$ the secondary photoproduct observed to absorb at 425nm in non-liquid-pumped solution was attributed to an impurity complex, possibly formed by the binding of trace amounts of water present in the solvent. In the case of (η^6-C_6Me_6)$Cr(CO)_3$ this species is observed in solutions in which the liquid-pumping stage has been both included and omitted This could imply that the (η^6-C_6Me_6)$Cr(CO)_3$ system is more readily influenced by trace impurities present in the solvent and that the reduced levels present on liquid-pumping are

sufficient to greatlly influence the photochemical reactions. The results could also indicate that the degassing procedure is ineffective in the removal of solvent impurities, and may even introduce impurities into the solution.

2.3.2.2.4 A Study of the Activation Parameters for Dinuclear Species Formation

Activation parameters for the reaction of the third and fourth observed species were determined to aid their identification. All determinations were conducted under an atmosphere of argon, as the formation of fourth species (absorbing at 580nm) has been shown to be strongly suppressed by the presence of CO in solution. Hence, although all species have been previously shown to react with CO, it is not necessary to include this factor in the calculations. Also, as it is not certain that these species react with parent, the concentration of parent was not considered in these determinations. Activation parameters for the reaction of the unidentified species were measured from Arrhenius and Eyring Plots over a temperature range of 283 to 321K The results are detailed in Tables 2 3 2 2.4 1 to 2.3.2 2.4.3 and illustrated graphically in Figures 2 3 2.2 4 1 to 2 3 2 2.4 3.

The correlation coefficient for the analysis of the production of the third species is excellent, at 0 997, while the accuracies of the remaining determinations are poor. All kinetic traces, except those for the production of the third species, were analysed for double exponential functions, but no improvement in the linear regression fit to the analysis points was achieved. If it is taken that the reactions occur sequentially, then the values in Tables 2.3.2 2.4 2 and 2 3 2 2 4.3 should relate to the same reaction, while it is clear that there is a large variation in these values

The activation entropy values, $\Delta S^{\neq}$, for all reactions are large and negative indicating an associative rate determining step, although not extremely so as expected for a purely associative reaction This indicates that interchange mechanisms may predominate in these reactions The $\Delta S^{\neq}$ values are more negative than those determined for the reaction of (η^6-arene)$Cr(CO)_2(S)$ species with CO, indicating a higher level of association in these secondary reactions The activation enthalpies for all reactions are also much higher than those of the (η^6-arene)$Cr(CO)_2(S)$ system The activation enthalpy values are not unlike those measured for the formation of a bridging species in the flash photolysis of (η^5-C_5H_5)$Mn(CO)_3$ in which study a value of 30 kJ mol^{-1} was recorded[5(b)]. The values are also similar to that found for the low-temperature oxidative addition of R_3SiH compounds to (η^5-C_5H_5)$Mn(CO)_2$[3(d)] Regrettably, the activation parameter data does not assist greatly in the differentiation of the secondary photochemical species from one another as the values determined are quite similar for all.

Table 2.3.2.2.4.1 (a) Experimental data for the determination of the energy, entropy and enthalpy of activation for the formation of the third species, monitored at 410nm; $[(\eta^6\text{-}C_6Me_6)Cr(CO)_3] = 4.7 \times 10^{-4}$ mol dm^{-3}

$1/T$ (x 10^3)	$Ln(k_{obs})$	$Ln(k_{obs}/T)$
3 57	10 00	4 37
3.52	10 10	4 45
3 48	10 26	4 60
3 43	10 43	4.76
3 40	10 58	4 89
3 36	10 72	5 02
3 32	10 90	5 19

Arrhenius Plot	Eyring Plot	Activation Parameters
Slope = -3645 ± 124	Slope = -3354 ± 123	$E_a = 30 \pm 1$ kJ mol^{-1}
Int. = 22 96 ± 0.03	Int = 16.28 ± 0 03	$\Delta H^{\neq} = 28 \pm 1$ kJ mol^{-1}
Corr Coeff = 0 997	Corr Coeff = 0 997	$\Delta S^{\neq} = -62 \pm 20$ J mol^{-1} K^{-1}

Table 2.3.2.2.4.1 (b) Experimental data for the determination of the energy, entropy and enthalpy of activation for the formation of the third species, monitored at 410nm; $[(\eta^6\text{-}C_6Me_6)Cr(CO)_3] = 3\ 1 \times 10^{-4}$ mol dm^{-3}.

$1/T\ (\times 10^3)$	$Ln(k_{obs})$	$Ln(k_{obs}/T)$
3 54	10 05	4 41
3 48	10 39	4 72
3 43	10 51	4 83
3 38	10 73	5 04
3 33	10 91	5.20
3 28	11 03	5.31
3 24	11 28	5 54

Arrhenius Plot	Eyring Plot	Activation Parameters
Slope = -3808 ± 178	Slope = -3513 ± 178	$E_a = 32 \pm 2$ kJ mol^{-1}
Int. = 23 58 ± 0 05	Int. = 16 89 ± 0 05	$\Delta H^{\neq} = 29 \pm 2$ kJ mol^{-1}
Corr Coeff = 0 995	Corr Coeff = 0.994	$\Delta S^{\neq} = -57 \pm 20$ J mol^{-1} K^{-1}

Table 2.3.2.2.4.2 (a) Experimental data for the determination of the energy, entropy and enthalpy of activation for the decay of the third species, monitored at 410nm; $[(\eta^6\text{-}C_6Me_6)Cr(CO)_3] = 4\ 7 \times 10^{-4}$ mol dm^{-3}

$1/T\ (\times 10^3)$	$Ln(k_{obs})$	$Ln(k_{obs}/T)$
3 57	7 02	1 38
3 52	7 13	1 48
3 48	7 45	1 79
3 43	7 71	2 04
3 40	7 79	2 10
3 36	7 93	2.23
3 32	8 15	2.44

Arrhenius Plot	Eyring Plot	Activation Parameters
Slope = -4658 ± 316	Slope = -4368 ± 316	$E_a = 39 \pm 2$ kJ mol^{-1}
Int. = 23 60 ± 0 07	Int. = 16 93 ± 0.07	$\Delta H^{\neq} = 36 \pm 2$ kJ mol^{-1}
Corr Coeff = 0 989	Corr Coeff = 0.987	$\Delta S^{\neq} = -57 \pm 20$ J mol^{-1} K^{-1}

Table 2.3.2.2.4.2 (b) Experimental data for the determination of the energy, entropy and enthalpy of activation for the decay of the third species, monitored at 410nm; $[(\eta^6\text{-}C_6Me_6)Cr(CO)_3] = 3.1 \times 10^{-4}$ mol dm^{-3}

$1/T$ (x 10^3)	$Ln(k_{obs})$	$Ln(k_{obs}/T)$
3 53	7 64	2 00
3 48	8.05	2 39
3 43	8 34	2 67
3 38	8 35	2 66
3 33	8 73	3 03
3 28	8 88	3 16
3 24	9 09	3 36

Arrhenius Plot	**Eyring Plot**	**Activation Parameters**
Slope = -4611 ± 347	Slope = -4316 ± 348	$E_a = 38 \pm 3$ kJ mol^{-1}
Int. = 24 04 ± 0 09	Int = 17 35 ± 0.09	$\Delta H^{\neq} = 36 \pm 3$ kJ mol^{-1}
Corr Coeff = 0 986	Corr. Coeff = 0 984	$\Delta S^{\neq} = -53 \pm 20$ J mol^{-1} K^{-1}

Table 2.3.2.2.4.3 (a) Experimental data for the determination of the energy, entropy and enthalpy of activation for the formation of the fourth species, monitored at 580nm; $[(\eta^6\text{-}C_6Me_6)Cr(CO)_3] = 4\ 7 \times 10^{-4}$ mol dm^{-3}

$1/T\ (\times 10^3)$	$Ln(k_{obs})$	$Ln(k_{obs}/T)$
3 56	8 31	2.67
3 52	8 45	2 80
3 47	8 53	2 86
3 43	8 63	2 95
3 40	8 84	3.15
3 36	9 10	3 40
3 32	9 31	3 60

Arrhenius Plot	Eyring Plot	Activation Parameters
Slope = -4036 ± 433	Slope = -3745 ± 432	$E_a = 34 \pm 3$ kJ mol^{-1}
Int = 22 60 ± 0 09	Int. = 15 93 ± 0 09	$\Delta H^{\neq} = 31 \pm 3$ kJ mol^{-1}
Corr Coeff = 0 973	Corr. Coeff = 0.968	$\Delta S^{\neq} = -65 \pm 20$ J mol^{-1} K^{-1}

Table 2.3.2.2.4.3 (b) Experimental data for the determination of the energy, entropy and enthalpy of activation for the formation of the fourth species, monitored at 580nm, $[(\eta^6\text{-}C_6Me_6)Cr(CO)_3] = 2\ 8 \times 10^{-4}$ mol dm^{-3}

$1/T\ (\times 10^3)$	$Ln(k_{obs})$	$Ln(k_{obs}/T)$
3 53	8 62	2 98
3 48	9 00	3 33
3 43	9 16	3 49
3 39	9 22	3 54
3 33	9 35	3 65
3 28	9 68	3 96
3 24	9 79	4 06

Arrhenius Plot	Eyring Plot	Activation Parameters
Slope = -3669 ± 299	Slope = -3365 ± 299	$E_a = 31 \pm 3$ kJ mol^{-1}
Int. = 21 67 ± 0 08	Int. = 14 966 ± 0 08	$\Delta H^{\neq} = 28 \pm 3$ kJ mol^{-1}
Corr Coeff = 0 984	Corr Coeff = 0 981	$\Delta S^{\neq} = -73 \pm 20$ J mol^{-1} K^{-1}

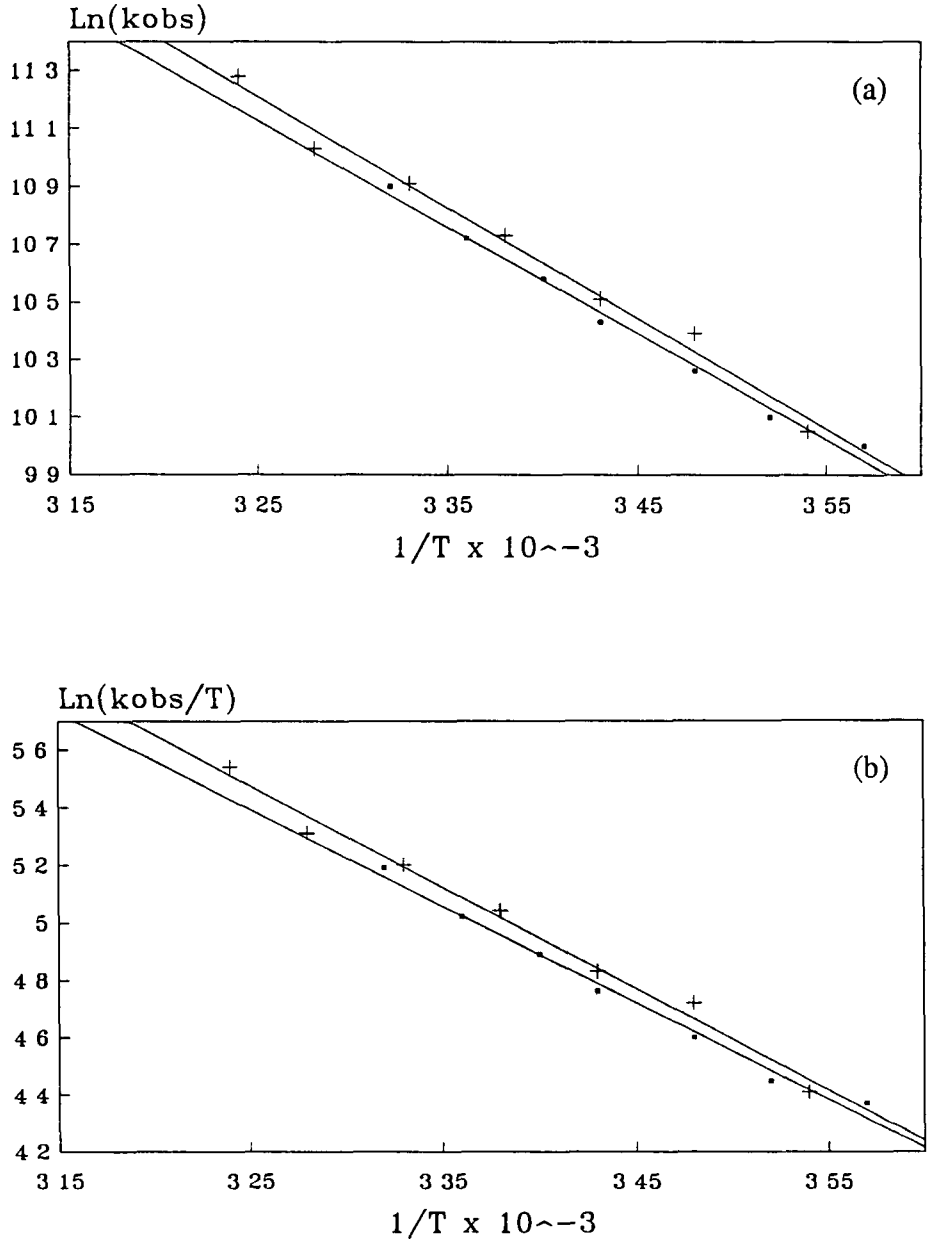

Figure 2.3.2.2.4.1 Arrhenius (a) and Eyring (b) plots for the formation of the third species, monitored at 410nm

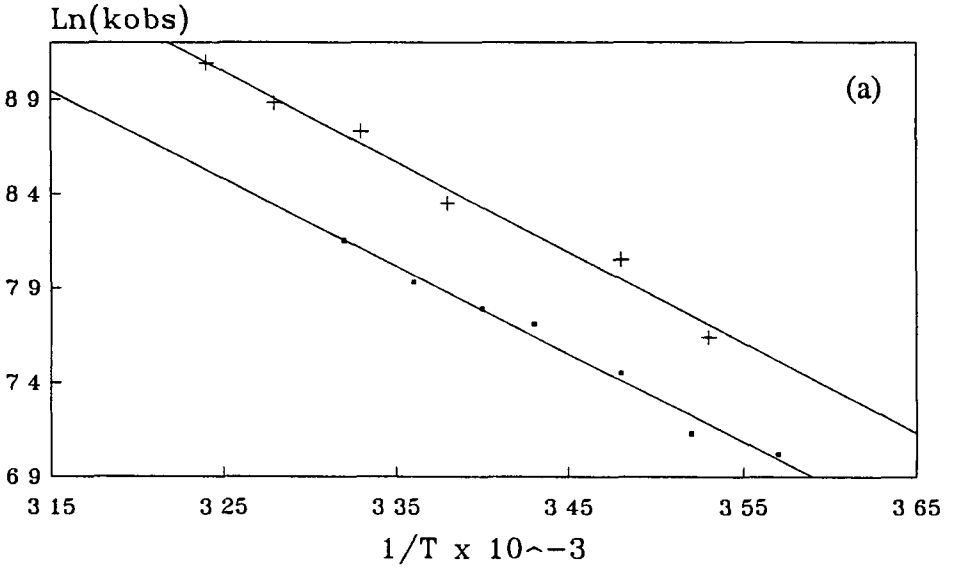

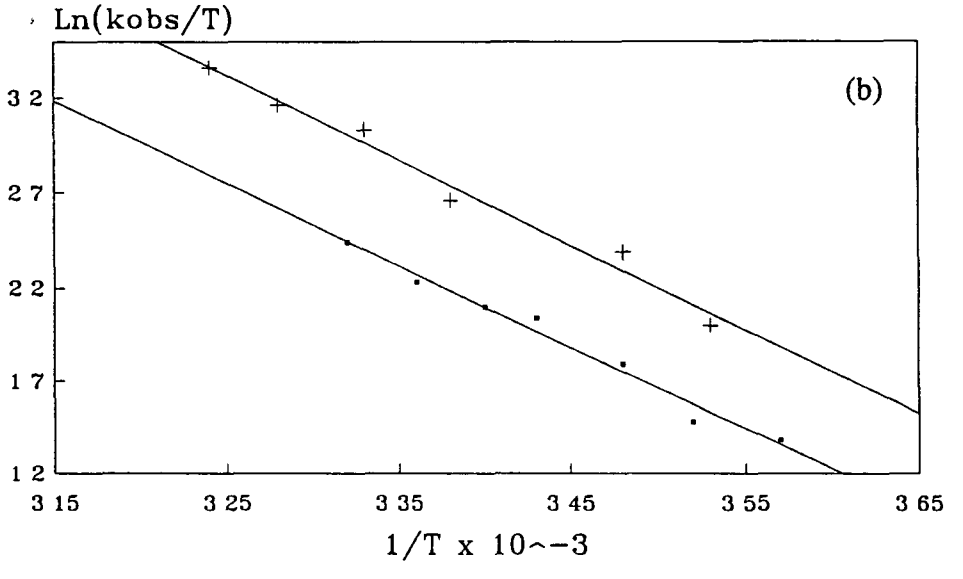

Figure 2.3.2.2.4.2. Arrhenius (a) and Eyring (b) plots for the decay of the species, monitored at 410nm

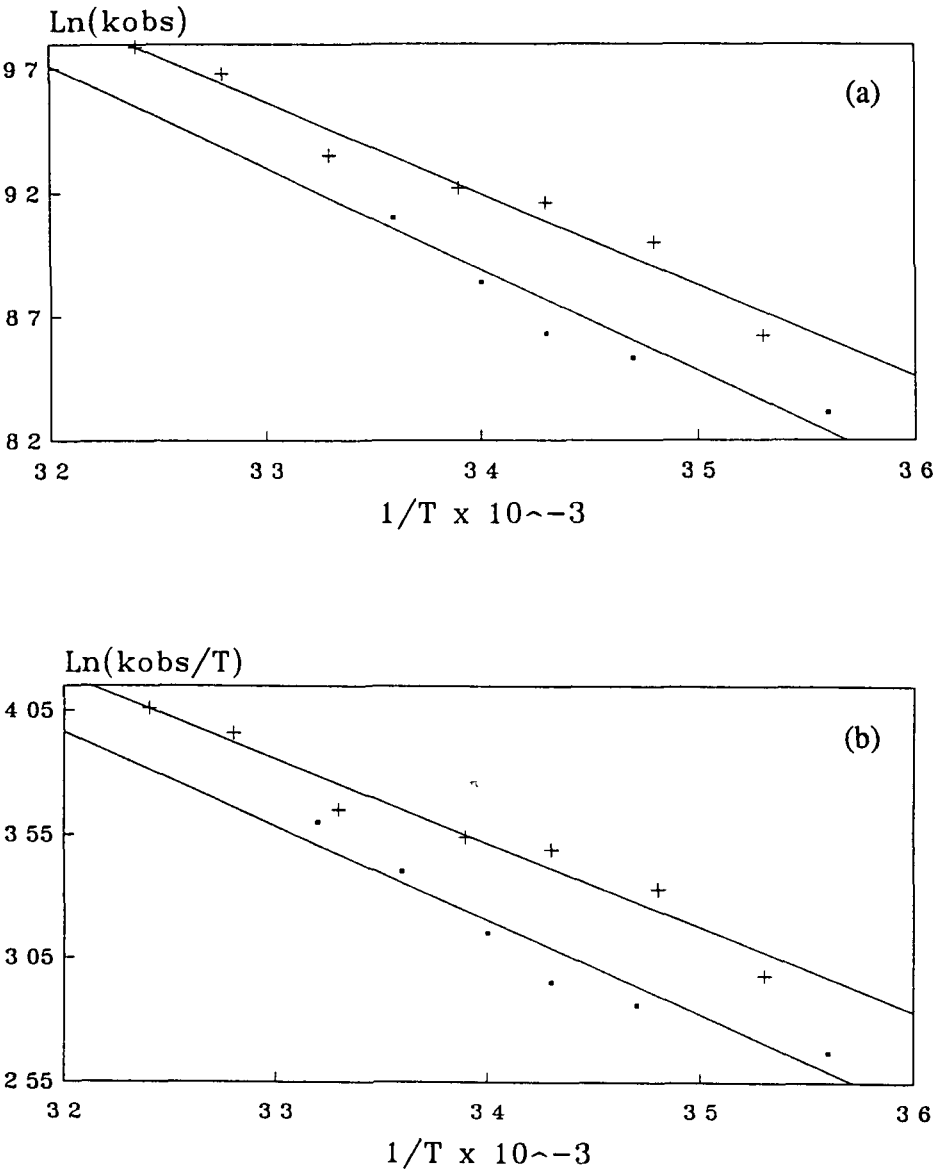

Figure 2.3.2.2.4.3 Arrhenius (a) and Eyring (b) plots for the formation of the fourth species, monitored at 580nm

2.4 Summary

These experiments have demonstrated conclusively that the (η^6-arene)$Cr(CO)_2(S)$ species is a primary photoproduct in the photochemistry of (η^6-arene)$Cr(CO)_3$ TRIR studies were used for confirmation, as assignments of photoproducts based on their spectroscopic and kinetic properties in the UV/vis region are rather ambiguous The nature of the recombination reaction of the (η^6-arene)$Cr(CO)_2(S)$ species with CO has been fully characterised. The second order rate constant for this reaction increases as the number of methyl substituents on the arene ring increases, from 6 7 x 10^6 dm^3 mol^{-1} s^{-1} for (η^6-benzene)$Cr(CO)_2(S)$ to 1.2 x 10^7 dm^3 mol^{-1} s^{-1} for (η^6-C_6H_6)$Cr(CO)_2(S)$ The enthalpy of activation for all the complexes is constant at 25 ± 2 kJ mol^{-1}, while the activation entropy becomes gradually less negative as the degree of methylation of the arene group increases. The difference UV/vis absorption spectra of all (η^6-arene)$Cr(CO)_2(S)$ species are almost identical, owing to the similarity of the parent spectra in the region of study.

In these investigations a second primary photoproduct was observed, in addition to the (η^6-arene)$Cr(CO)_2(S)$ species, following the irradiation of (η^6-arene)$Cr(CO)_3$ complexes. Previous flash photolysis studies were largely confined to the visible region of the spectrum and this photoproduct went unobserved[3(b), 5(b)] This species does not react with CO suggesting that it is coordinatively saturated, while the results obtained on liquid pumping indicate that it is generated by reaction with an impurity ligand Consequently, this species may be assigned to a hapticity-change product, possibly of the form (η^4-arene)$Cr(CO)_3(H_2O)$ The production of this complex involves both a reaction of the metal centre with the impurity ligand and a

conformational change at the arene group; reflected in the large enthalpy of activation determined for this reaction It has been proposed that η^6 to η^4 hapticity shifts may play a key role in substitution reactions of arene complexes[31], and may be of particular importance in the transition-metal-catalysed hydrogenation of arenes[32], but well established examples of η^4-arene complexes remain unusual[33] The possible observation of a $(\eta^4\text{-Ar})Cr(CO)_3$ species opens up the possibility of the hydrogenation of benzene by use of this photochemically generated intermediate To date, most of the studies on the hydrogenation of dienes in the presence of group 6 transition metal carbonyls have centred on the hydrogenation of norbornadiene[34]. $(\eta^4\text{-Ar})Cr(CO)_3$ compounds should resemble the $(\eta^4\text{-norbornadiene})M(CO)_3$ species, which is known to be the catalytically active species in the hydrogenation of norbornadiene. The assignments would explain the observations of other workers in the field that $(\eta^6\text{-arene})Cr(CO)_3$ undergoes both carbonyl loss and arene exchange reactions on irradiation It is possible to suggest a facile route to arene exchange which maintains the integrity of the chromium tricarbonyl unit *via* a η^4-arene intermediate complex, Scheme 2 4 1

SCHEME 2 4 1

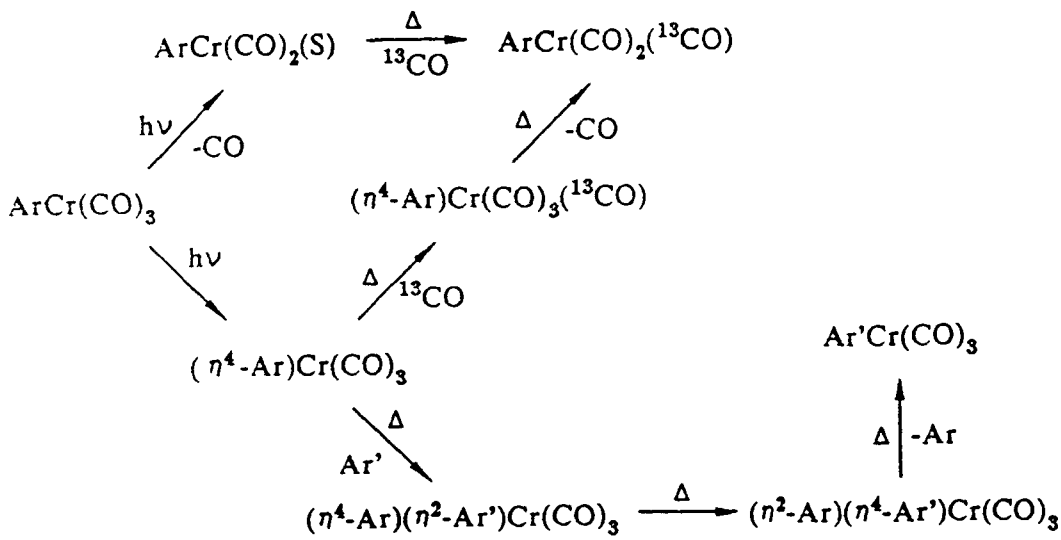

Experiments conducted using solvents of different dryness indicate that this second species is formed by a reaction with traces of water impurities present in the solvent. Alternatively, this second species may be assigned simply as a (η^6-arene)$Cr(CO)_2(H_2O)$ complex A transient spectrum of a species assigned as an impurity complex was recorded in the TRIR spectrum of (η^6-benzene)$Cr(CO)_3$ in non-distilled cyclohexane solution The water molecule is an excellent ligand and may react with the 'naked' CO-loss product, (η^6-arene)$Cr(CO)_2$, in order to stabilise it. This reaction should occur on the picosecond timescale and would then appear as a primary reaction given the resolution of the instrumentation used In the case of sample solutions subjected to a liquid-pumping procedure, designed to remove traces of dissolved impurities, the levels of the impurity complex would be reduced dramatically, as observed

The secondary photochemical reactions of (η^6-arene)$Cr(CO)_3$ complexes were also studied in this series of experiments The compounds were photolysed in argon saturated cyclohexane solution to eliminate the recombination reaction of the dicarbonyl photoproduct with CO On photolysis of (η^6-benzene)$Cr(CO)_3$ in cyclohexane solution subjected to a liquid-pumping procedure a long-lived transient species was observed, the rate of formation of which was directly dependant on the concentration of parent tricarbonyl, $k_2 = 4\,9 \times 10^7$ dm^3 mol^{-1} s^{-1} This species was attributed to a dinuclear complex of the form (η^6-benzene)$Cr(CO)_2(\mu$-CO)$Cr(CO)_2(\eta^6$-benzene), formed by reaction of the (η^6-benzene)$Cr(CO)_2$(S) species with parent tricarbonyl The formation of a dinuclear complex from photolysis of (η^6-benzene)$Cr(CO)_3$ has been noted in Nujol matrices at 77K[10(b)]

The formation of dinuclear species in such a manner is not unusual and has also been reported in the $Cr(CO)_6$[2(b)], (η^5-C_5H_5)$Co(CO)_2$[28], (η^5-C_5H_5)$Mn(CO)_3$[5(a)] and (η^5-C_5H_5)$V(CO)_4$[29] systems As with the (η^5-C_5H_5)$Mn(CO)_3$ system, the rate of formation of this species, k_{obs} $4\,9 \times 10^7$ mol^{-1} dm^3 s^{-1}, was faster than that of the recombination reaction of the dicarbonyl photoproduct with CO The photoreactions again differed significantly if carried out in solutions of varying dryness. Care must then be exercised in the interpretation of these results as reactions of the (η^6-arene)$Cr(CO)_2$(S) species with traces of impurities can dominate the chemistry in the absence of quenching ligands such as CO The formation of such dinuclear species limits the scope of these species in catalytic applications, as the catalytically active carbonyl-loss product is essentially 'poisoned' and prevented from further reaction by the formation of a dinuclear complex

Secondary reaction photochemistry was observed in the case of the substituted (η^6-arene)$Cr(CO)_3$ complexes Of the substituted benzene complexes, the most interesting photochemically was the (η^6-C_6Me_6)$Cr(CO)_3$ compound In the photochemistry of (η^6-benzene)$Cr(CO)_3$ the secondary photoproduct observed to absorb at 425nm in non-liquid-pumped solution was attributed to an impurity complex, possibly formed by the binding of trace amounts of water present in the alkane solvent In the case of (η^6-C_6Me_6)$Cr(CO)_3$ this species is observed in solutions in which the liquid-pumping stage has been both included and omitted. Therefore, two secondary reaction products are apparent in the (η^6-C_6Me_6)$Cr(CO)_3$ in all experimental studies, the former of which appears to be an intermediate in the formation of the latter The experimental observations may imply that the (η^6-C_6Me_6)$Cr(CO)_3$ system is more readily influenced by trace levels of solvent impurities and that the reduced levels present following the liquid-pumping procedure are sufficient to influence the photochemical reactions The results could also indicate that the degassing procedure is ineffective in the removal of solvent impurities, and may even introduce impurities into the solution

In the (η^6-C_6Me_6)$Cr(CO)_3$ system, some evidence was found for the formation of a dinuclear species of the form (η^6-arene)$Cr(CO)_2(\mu$-CO)$Cr(CO)_2(\eta^6$-arene), as proposed in the benzene case The increased methylation of the arene group may sterically hinder the formation of such a species A long-lived transient species was observed, the rate of formation of which was directly dependant on the concentration of parent tricarbonyl, k_2 = 5 3 x 10^7 dm^3 mol^{-1} s^{-1} Although the degree of error incurred in this analysis was large, by analogy with the (η^6-benzene)$Cr(CO)_3$ case

this species may be attributed to a dinuclear complex of the form (η^6-C_6Me_6)$Cr(CO)_2(\mu$-CO)$Cr(CO)_2(\eta^6$-C_6Me_6), formed by reaction of the (η^6-C_6Me_6)$Cr(CO)_2$(S) species with parent tricarbonyl A possible explanation for the presence of both secondary photochemical species is the formation of a dinuclear complex which subsequently undergoes a decarbonylation reaction of a similar nature to that reported in the (η^4-$C_4H_4)_2Fe_2(CO)_3$[35] and (η^5-C_5H_5)$V(CO)_4$[29(a)] systems, reaction 2.4 1

(η^5-$C_5H_5)_2V_2(CO)_5$ ----------> CO + (η^5-$C_5H_5)_2V_2(CO)_4$ (2.4.1)

2.5 Conclusions

The (η^6-arene)$Cr(CO)_2$(alkane) species has been identified as a primary photoproduct in the photochemistry of (η^6-arene)$Cr(CO)_3$ systems (*vide* UV/vis and IR), where arene = benzene, toluene, p-xylene, 1,3,5-mesitylene and C_6Me_6 The rate of reaction of this species with CO is dependant on the nature of the alkane, and on the nature and degree of substitution of the arene The enthalpies of activation are constant at 25 ± 2 kJ mol^{-1} while the entropy of activation increases upon methyl substitution of the arene The photochemistry is greatly influenced by solvent impurities, and complexes attributed to the binding of these impurities are ascribed to some of the primary and secondary photoproducts observed The production of a dinuclear complex of the form (η^6-arene)$Cr(CO)_2(\mu CO)Cr(CO)_2(\eta^6$-arene) is noted in the case of arene = benzene and C_6Me_6. The formation of such a complex in the case of the remaining methyl substituted arenes is not a certainty

2.6 References

1. (a) W H. Breckenridge and D M Stewart, *J Am Chem Soc* , 1986, **108**, 364

   (b) T A Seder, S P Church, A J Ouderkirk, and E. Weitz, *J Am Chem Soc* , 1985, **107**, 1432

2 (a) J D Simon and K S Peters, *Chem Phys Lett* , 1983, **98**, 53

   (b) J M Kelly, C Long, and R Bonneau, *J Chem Phys* , 1983, **87**, 3344.

   (c) R K. Upmacis, G E Gadd, M. Poliakoff, M.B Simpson, J J Turner, R. Whyman, and A F Simpson, *J Chem Soc , Chem Commun* , 1985, 27.

   (d) J D Simon and X. Xie, *J Phys Chem* , 1989, **93**, 291

   (e) X Xie and J D Simon, *J Am Chem Soc* , 1990, **112**, 1130

   (f) J.R. Sprague, S M Arrivo, and K G Spears, *J Phys Chem* , 1991, **95**, 10528

3 (a) W Strohmeier and D von Hobe, *Z Naturforsch* , 1963, **18b**, 770

   (b) A Gilbert, J M Kelly, M Budzwait, and E Koerner von Gustorf, *Z Naturforsch* , 1976, **31b**, 1091

   (c) J D Black, M J Boylan, and P S Braterman, *J Chem Soc , Dalton Trans* , 1981, 673

   (d) R H Hill and M S Wrighton, *Organometallics*, 1987, **6**, 632

   (e) W Wang, P Jin, Y She, and K. Fu., *Chinese Phys Lett* , 1991, **8**, 491.

   (f) W Wang, Y Lin, Y S Liu, and K Fu , *J Phys Chem* , 1992, **96**, 1278.

4 (a) T G Traylor, K J Stewart, and M J Goldberg , *J Am Chem Soc* , 1984, 106, 4445

(b) J.A.S. Howell, N F. Ashford, D.T. Dixon, J.C. Kola, and T.A. Albright, *Organometallics*, 1991, **10**, 1852.

5. (a) B.S Creaven, A J. Dixon, J M. Kelly, C. Long., and M. Poliakoff, *Organometallics*, 1987, **6**, 2600

(b) B S. Creaven, *"Photochemical, Thermal and Spectroscopic Studies of Metal Carbonyl Compounds"*, Ph. D Thesis, Dublin City University, 1989

6. (a) G L Geoffroy and M S. Wrighton, *"Organometallic Photochemistry"*, Academic Press, New York, 1979

(b) D G. Carroll and S P McGlynn, *Inorg Chem* , 1968, **7**, 1285.

(c) R.T Lindquist and M Cais, *J Org Chem* , 1962, **27**, 1167

(d) M.S Wrighton and J L Haverty, *Z Naturforsch* , 1976, **31b**, 1091.

7. See experimental chapter for discussion of CO solubility in cyclohexane.

8 J.M. Kelly, H. Herrman, and E Koerner von Gustorf, *J Chem Soc , Chem Commun* , 1973, 105

9 J.D Simon, X Xie, *J Phys Chem* , 1986, **90**, 6751.

10 (a) A`J Rest, J.R Sodeau, and D J Taylor, *J Chem Soc , Dalton Trans* , 1978, 651

(b) T.E Bitterwolf, K A Lott, A.J Rest, and J Mascetti, *J Organomet Chem* , 1991, **113**, 419

11 J.M Kelly, D V Bent, H. Hermann, D Schulte-Frohlinde, and E. Koerner von Gustorf, *J Organomet Chem* , 1974, **69**, 259

12 J Dineen, *"The Chemistry of $Cr(CO)_6$ in Some Common Hydrocarbon Solvents"*, M Sc Thesis, University of Dublin, 1990

13 M F Bailey and L F Dahl, *Inorg Chem.*, 1965, **4**, 1314.

14 E.O Fischer, C G Kreiter, and W Berngruber, *Angew Chem , Int Ed Engl ,* 1967, **6**, 634.

15. G Huttner and O S Mills , *J Organomet Chem* , 1971, **29**, 275

16. H R. Ward and J S Wishnok , *J Am Chem Soc* , 1968, **90**, 1085

17 S Zhang and G R Dobson, *Organometallics,* 1992, **11**, 2447, and references therein

18 S P Church, F W Grevels, H Hermann, and K Schaffner, *Inorg Chem* , 1985, **24**, 418

19 G K Yang, V Vaida, and K G Peters, *Polyhedron,* 1988, **7**, 1619

20 S. Zhang and G R Dobson, *Inorg Chim Acta,* 1989, **165**, L11

21 J M Morse, G H Parker, and T J Burley, *Organometallics,* 1989, **8**, 2471

22 M B Simpson, M Poliakoff, J J Turner, W B Maier, and J G McLaughlin, *J Chem Soc , Chem Commun* , 1983, 1355.

23 B S Creaven, M W George, A G. Ginsburg, C Hughes, J M. Kelly, C. Long, I M Mc Grath, and M T Pryce, accepted for publication in *Organometallics,* 1993

24 F P A Johnson, M W George, V N Bagratashvili, L N Vereshchagina, and M Poliakoff, *J Chem Soc , Mendeleev Commun* , 1991, 26

25 K.M Young and M S Wrighton, *Organometallics,* 1989, **8**, 1063.

26 G S Hammond, *J Am Chem Soc* , 1955, **77**, 334

27 (a) A S Foust, J K Hoyano, and W A G Graham, *J Organomet Chem* , 1971, **32**, C65

(b) L N Lewis and K G Caulton, *Inorg Chem* , 1981, **20**, 1139.

28. E P Wasserman, R.G. Bergman, and C.B. Moore, *J Am Chem Soc* , 1988, **110**, 6076

29 (a) L.N Lewis and K G Caulton, *Inorg Chem* , 1980, **19**, 1840.

(b) M W George, Ph D Thesis, University of Nottingham, 1990.

30 C. Hughes and M W George, personal communication.

31 (a) V S Leong and N Cooper, *Organometallics*, 1988, **7**, 2058.

(b) I.S. Butler and A A Ismail, *Inorg Chem* , 1986, **25**, 3910.

(c) A. Barbati, F Calderazzo, R Poli, and P F Zanussi, *J Chem Soc* , *Dalton Trans* , 1986, 2569

32 (a) E.L Muetterties and J R Bleeke, *Acc Chem Res* , 1979, **12**, 324.

(b) C.R Landis and J Halpern, *Organometallics*, 1983, **2**, 840

(c) W A. Fondyce, R Wilczynski, and J Halpern, *J Organomet Chem* , 1985, **296**, 115

33. (a) For a review of arene-metal complexes see· E L. Muetterties, J.R. Bleeke, and E J Wucherer, *Chem Rev* , 1982, **82**,499

(b) G Huttner, S Lange, and E O. Fischer, *Angew Chem , Int Ed Engl* , 1971, **10**, 556

(c) F H. Herbstein and M G Reisner, *J Chem Soc , Chem Commun.*, 1972, 1077

(d) W J Bowger, J W Meikert, W E Geiger, and A.L. Rheingold, *Organometallics*, 1989, **8**, 191

(e) J Merkert, R M Nielson, M J Weaver, and W E. Geiger, *J Am Chem Soc*, 1989, **111**, 7094

(f) J O Albright, S Datta, B Dezube, J K. Kouba, D S. Marynick, S S Wreford, and B M Foxman, *J Am Chem Soc*, 1979, **101**, 611.

(g) J W Hull, Jnr, and W L. Gladfelter, *Organometallics*, 1984, **3**, 605

(h) H Schaufele, D Hu, H. Pritzkow, and U Zenneck, *Organometallics*, 1989, **8**, 396

34. (a) J Nasielski, P Kirsch, and L Wilputte-Steinert, *J Organomet Chem*, 1971, **27**, C13

(b) G Platbrood and L Wilputte-Steinert, *Bull Soc Chim Belg*, 1973, **82**, 733

(c) M S Wrighton and M A Schroeder, *J Am Chem Soc*, 1973, **95**, 5764

(d) G Platbrood and L Wilputte-Steinert, *J Organomet Chem*, 1974, **70**, 393

(e) I Fischer, M Budzwait, and E Koerner von Gustorf, *J Organomet. Chem*, 1976, **105**, 325

(f) S A. Jackson, M. Hodges, M Poliakoff, J J Turner, and F.W Grevels, *J Am Chem Soc*, 1990, **112**, 1221

(g) P M Hodges, S A Jackson, J Jacke, M Poliakoff, J J Turner, and F W Grevels, *J Am Chem Soc*, 1990, **112**, 1224

(h) F.W Grevels, J Jacke, W E Klotzbucher, and K Schaffner, *J Organomet Chem*, 1990, **382**, 201

35 O. Jaenicke, R.C Kerber, B Kirsch, E. Koerner von Gustorf, and R. Rumin, *J Organomet Chem*, 1980, **187**, 361.

Chapter 3

Laser-Induced Photochemistry of $Mn(CO)_4$-η^3-C_3H_4-C_6H_5

3.1 Introduction

η^3-Allyl organometallic complexes have attracted much interest since it was first demonstrated in the late 1950's that $(C_4H_7)Co(CO)_3$ has a η^3-bonding configuration[1]. The allyl ligand is of particular interest because it can engage in either η^1 or η^3 bonding to a transition metal, that is it can be either σ-bonded (η^1) or σ- and π-bonded (η^3). Reversible equilibria of the type η^3-allyl to σ-allyl are crucial to the importance of metal allyl complexes in organic synthesis[2] and catalysis[2,3]. Such polyene hapticity changes could avoid the inhibiting need for seven co-ordination number species in S_N2 reactions of small first-row transition metal elements[4]

Our interest in these η^3-allyl organometallic species stems from the study of a related dinuclear complex $Mn(CO)_4$-η^3-C_3H_4-η^6-C_6H_5-$Cr(CO)_3$. Preliminary laser flash photolysis experiments revealed that the photochemical reactions of this system were complex This prompted a thorough investigation into the photochemistry of the individual components of this system as an aid to understanding the overall photochemistry observed For this reason the photochemistry of the π-allyl manganese complex $Mn(CO)_4$-η^3-C_3H_4-C_6H_5, in which the chromium centre is absent, was examined The photochemistry of the $(\eta^6$-arene$)Cr(CO)_3$ species was also reexamined in a separate series of experiments It was hoped that an understanding of the photochemical reactions occuring in these systems would enable the photochemistry of the dinuclear species to be simplified as it could be visualised in terms of the individual reactions of its component parts A study of the photochemistry of $Mn(CO)_4$-η^3-C_3H_4-C_6H_5 in alkane solution at ambient

temperature is hereby presented The observed photoproducts are characterised and kinetic data is presented for the reaction of these species with CO and other potential ligands Only laser pulse photolysis was available for this investigation.

3.2 Electronic Spectrum of $Mn(CO)_4$-η^3-C_3H_4-C_6H_5

The UV/vis absorption spectrum of $Mn(CO)_4$-η^3-C_3H_4-C_6H_5 in cyclohexane solution is presented in Figure 3 2 1 This spectrum is dominated by an absorption centred at 242nm with a low energy shoulder on this band centred at 292nm. The study of the electronic structure of low symmetry Mn derivatives (beyond C_{4v}) is not well developed[5] By analogy with the spectrum of $Mn(CO)_5(\eta^1$-$C_3H_5)$[6] these absorption bands may be assigned as metal to ligand charge transfer bands, i e. from e_π molecular orbitals of the metal to π^* CO levels which do not interact with the manganese orbitals The spectrum does not exhibit bands attributed to ligand field absorptions, presumably any bands are obscured by the more intense Mn to π^* CO charge transfer bands Photochemical results presented on $Mn(CO)_5(\eta^1$-$C_5Cl_5)$ and $Mn(CO)_5(\eta^1$-$C_6H_5CH_2)$ complexes were consistent with lowest excited states that involved population of the σ^*_z and σ^*_{xy} orbitals from the overlap of the Mn $3d_z2$ and $3d_{x2-y2}$ orbitals with the ligand centred σ orbitals[7]

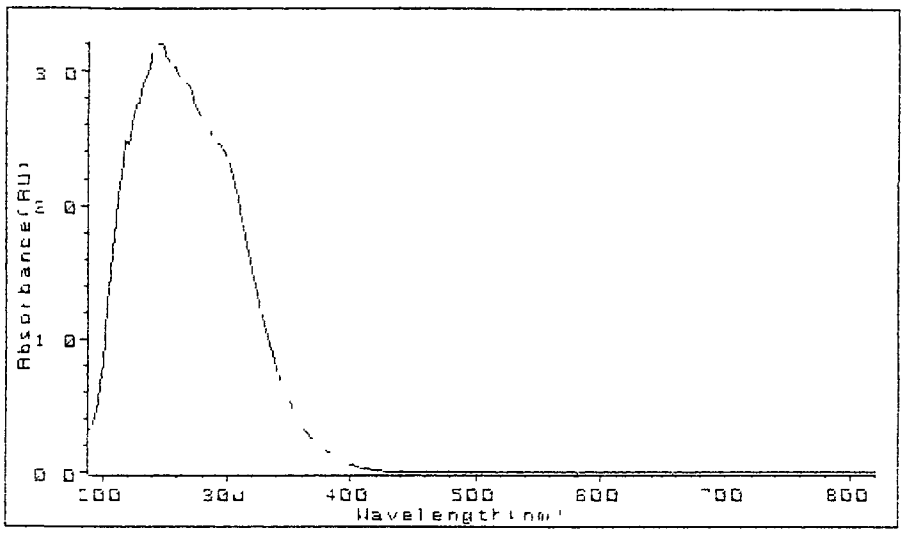

Figure 3.2.1 UV/vis absorption spectrum of a 2 20 x 10^{-4} mol dm^{-3} solution of $Mn(CO)_4$-η^3-C_3H_4-C_6H_5 in cyclohexane.

3.3 Preliminary Experimental Results

Under 1 0 atmosphere of argon a single transient species was typically observed following the flash photolysis of a solution of $Mn(CO)_4$-η^3-C_3H_4-C_6H_5 (ε_{354nm}= 2050 dm^3 mol^{-1} cm^{-1}) in cyclohexane The decay of this species follows a first order decay process, Figure 3 3 1 Under 0 25 atmosphere of CO the transients were weak, Figure 3 3 2, and shock waves were typically observed on the traces, presumably due to local heating effects, while under 1 0 atmosphere of CO no transient species were detected From these observations it was apparent that the formation of the observed transient species was suppressed by CO This indicated that it was not a primary photoproduct as the addition of CO greatly affected its yield This suggested that perhaps two transient species of varying reactivity were formed; an extremely reactive one, with a lifetime shorter than that observed, and that

detected, a secondary photoproduct This theory gained credibility as a later study recorded a grow-in of the transient species on a timescale of 0 2μs, the rate of which was measured as 2 9 x 10^6 s^{-1} under argon atmosphere, Figure 3 3 3 The lifetime of this species is just within the limit of detection of the present instrumentation (>200ns). This primary transient species is hereafter referred to as species 1, while the secondary photoproduct typically observed is referred to as species 2

Similar type behaviour has been noted in the flash photolysis of $CH_3Mn(CO)_5$[8] TRIR and UV/vis detection were used to demonstrate that the primary photoproduct was $CH_3Mn(CO)_4$ formed by photoejection of a CO ligand. This species was identified as the solvated *cis*-$CH_3Mn(CO)_4(S)$ complex under argon and CO atmosphere The yield of this solvatocomplex was reduced by a factor of 5 in experiments conducted under a CO atmosphere. To account for these observations, it was proposed that $CH_3Mn(CO)_4$ can react competitively with either C_6H_{12} to form *cis*-$CH_3Mn(CO)_4(S)$ or with CO to regenerate $CH_3Mn(CO)_5$ The formation of a $CH_3Mn(CO)_4$ intermediate of trigonal-bipyramidal C_{3v} geometry or of square-pyramidal geometry was proposed to account for these observations Either geometric or electronic constraints might give such a species sufficient lifetime to demonstrate selectivity in coordinating a sixth ligand Similar behaviour was also noted in the laser flash photolysis of (η^5-$C_5H_5CH_3$)$Mn(CO)_2PPh_3$[9] In this case, the first transient species was identified from reaction kinetics as the non-solvated (η^5-$C_5H_5CH_3$)$Mn(CO)PPh_3$ complex It was proposed that the bulky triphenylphosphine ligand sterically prevented the cyclohexane molecule from coordinating to the unsaturated metal centre It was also postulated that the coordinatively unsaturated

complex was stabilised by an intramolecular reaction, the nature of which was unknown but which was believed to involve an orthometallation reaction

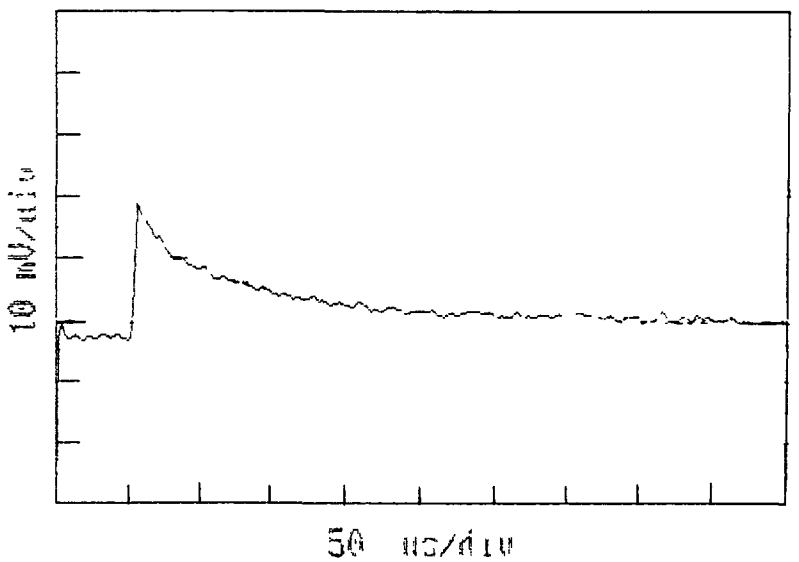

Figure 3.3.1 The decay of the secondary photoproduct under 1.0 atmosphere of argon at 405nm, $[Mn(CO)_4\text{-}\eta^3\text{-}C_3H_4\text{-}C_6H_5] = 6\ 55 \times 10^{-4}$ mol dm^{-3}

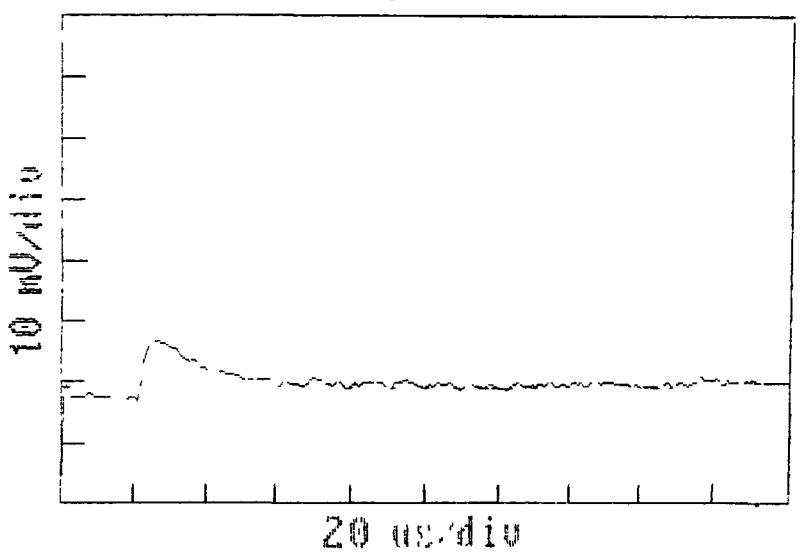

Figure 3.3.2 The decay of the secondary photoproduct under 0 25 atmosphere of CO at 410nm, $[Mn(CO)_4\text{-}\eta^3\text{-}C_3H_4\text{-}C_6H_5] = 8\ 29 \times 10^{-4}$ mol dm^{-3}

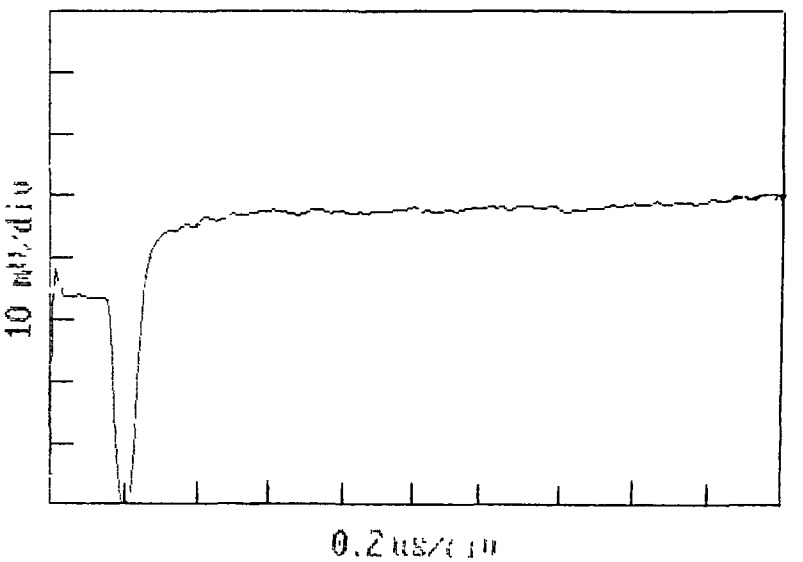

Figure 3.3.3 The 'grow-in' of the secondary photoproduct under 1 0 atmosphere of argon at 410nm, $[Mn(CO)_4\text{-}\eta^3\text{-}C_3H_4\text{-}C_6H_5] = 6\ 20 \times 10^{-4}$ mol dm^{-3}.

3.4 UV/vis Difference Spectra of Transient Species

The difference absorption spectrum from 280nm to 590nm obtained under argon atmosphere within 10μs of the laser pulse at a $Mn(CO)_4\text{-}\eta^3\text{-}C_3H_4\text{-}C_6H_5$ concentration of $3\ 9 \times 10^{-4}$ mol dm^{-3} is given in Figure 3.4 1 The most significant feature in this transient absorption spectrum of the species 2 is the band in the visible region of the spectrum centred at 410nm This species exhibits a weak absorption in the long wavelength region of the spectrum up to 600nm The spectrum obtained under argon atmosphere within 250μs of the laser pulse is given in Figure 3 4.2. This spectrum is very similar to that recorded at 10μs, however the absorption peak centred at 415nm is broader and there is a pronounced shoulder on the long

wavelength side of the absorption peak at *ca* 460nm. This may indicate the formation of a further species from the species 2, albeit in quite low yield.

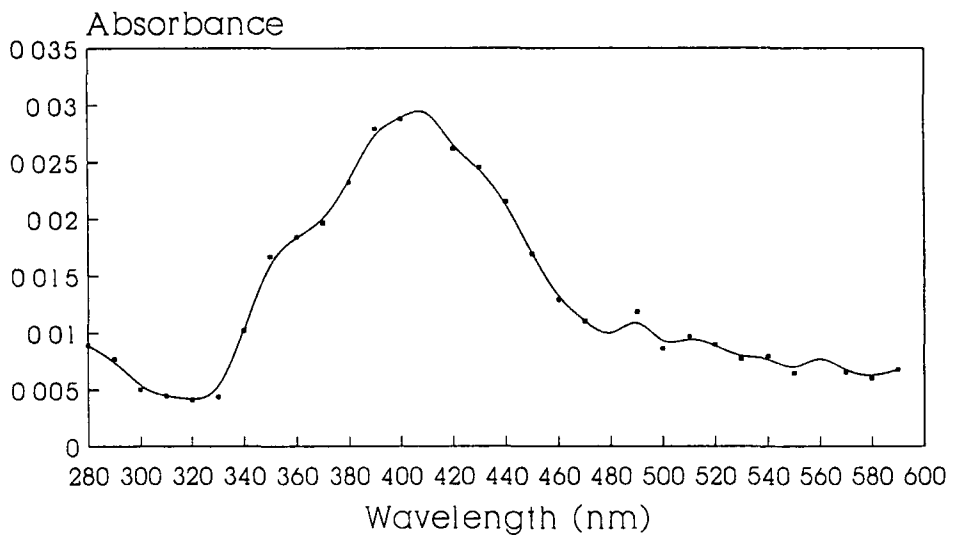

Figure 3.4.1 UV/vis difference spectrum of species 2 recorded at 20μs following the laser flash photolysis of $Mn(CO)_4$-η^3-C_3H_4-C_6H_5 in cyclohexane solution at 298K

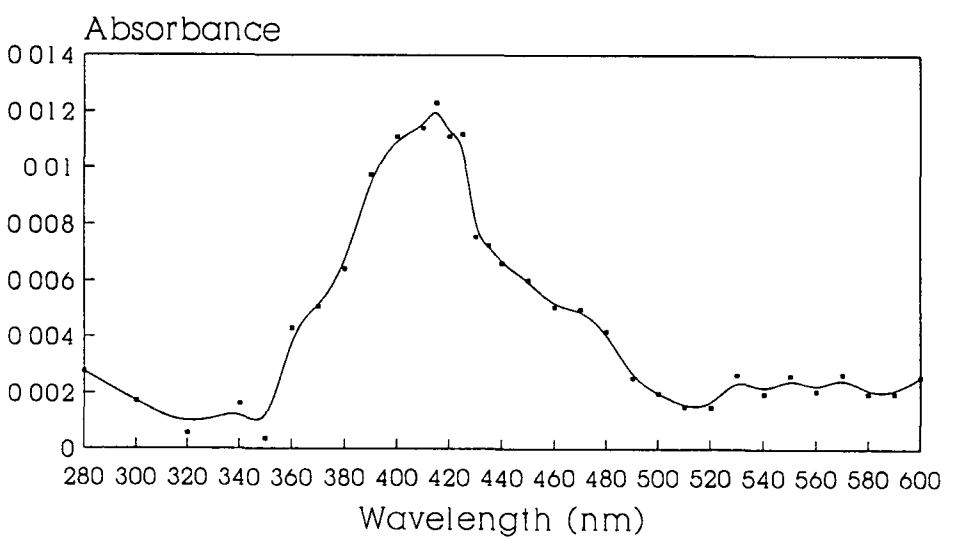

Figure 3.4.2 UV/vis difference spectrum recorded at 250μs following the laser flash photolysis of $Mn(CO)_4$-η^3-C_3H_4-C_6H_5 in cyclohexane solution at 298K

3.5 Effect of Variations in CO Concentration

The rate of decay of species 2 was directly dependant on CO concentration. The CO concentration was increased incrementally up to a maximum value of 3 0 x 10^{-3} mol dm^{-3}, beyond which value the low transient yield served to make the decay rate immeasurable To minimise shock waves on the transient signals the laser energy was reduced from the normal operating setting of 790V to 600V However, the presence of even such small concentrations of CO served to dramatically decrease the observed yield The second order rate constant for the reaction of the transient species with CO was calculated to be 3 6 x 10^{7} dm^{3} mol^{-1} s^{-1}, Figure 3 5 1. The corresponding second order rate constant for the reaction of $CH_3Mn(CO)_4$ with CO is reported as 2.2 x 10^{6} dm^{3} mol^{-1} s^{-1}[8] Although the calculated value is not as fast as that reported for the reaction of $(\eta^5\text{-}C_5H_4CH_3)Mn(CO)_2(PPh_3)$ with CO, 1.05 x 10^{8} dm^{3} mol^{-1} s^{-1}[9], the rate constant has increased by over an order of magnitude.

3.6 Effect of Variations in Parent $Mn(CO)_4\text{-}\eta^3\text{-}C_3H_4\text{-}C_6H_5$ Concentration

The observed rate constants for the decay of the species 2 at 410nm display a linear dependance on the parent tetracarbonyl concentration under argon atmosphere, Figure 3 6 1 This trend presents evidence for the formation of a dinuclear species in a reaction involving this species and the parent complex The spectrum recorded at 250μs after the laser pulse most likely pertains to this species The second order rate constant was determined to be 1 7 x 10^{7} dm^{3} mol^{-1} s^{-1} from the slope of the psuedo-first order plot, the intercept of which is practically zero given the experimental error

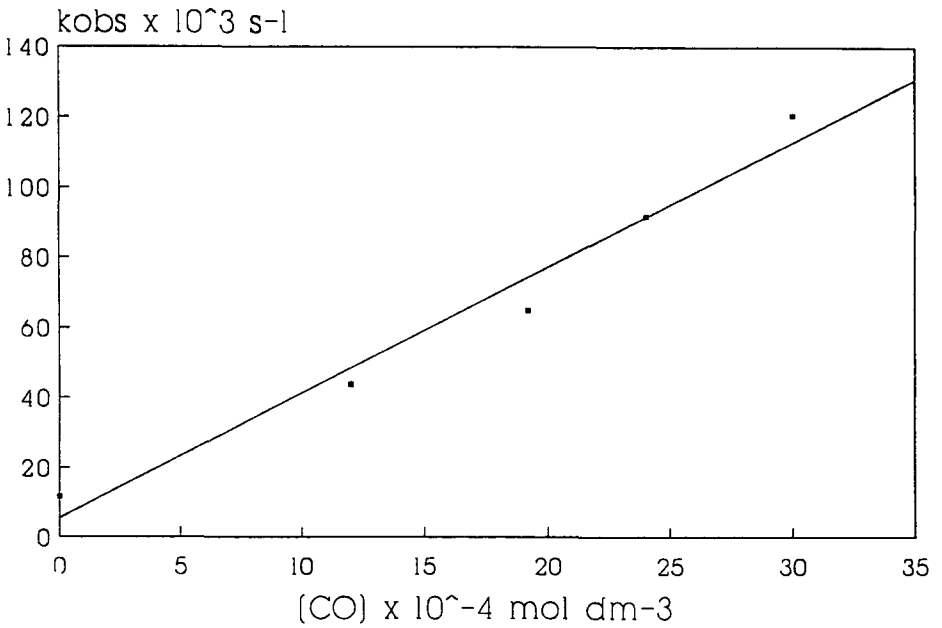

[CO] mol dm^{-3}	k_{obs} s^{-1}
0 00	11613
1 30 x 10^{-3}	43728
1 92 x 10^{-3}	64671
2 40 x 10^{-3}	91568
3 00 x 10^{-3}	120502

$k_{[co]}$ = 3 6 x 10^{7} ± 4 0 x 10^{6} dm^{3} mol^{-1} s^{-1}

Intercept = 4400 ± 9172 s^{-1} Corr Coeff = 0 982

Figure 3.5.1 The observed rate constants (s^{-1}) for the reaction of CO with species 2, monitored at 410nm at differing CO concentrations (mol dm^{-3}) at 298K. The $[Mn(CO)_4\text{-}\eta^3\text{-}C_3H_4\text{-}C_6H_5]$ in cyclohexane solution was 8 37 x 10^{-4} mol dm^{-3} for this experiment

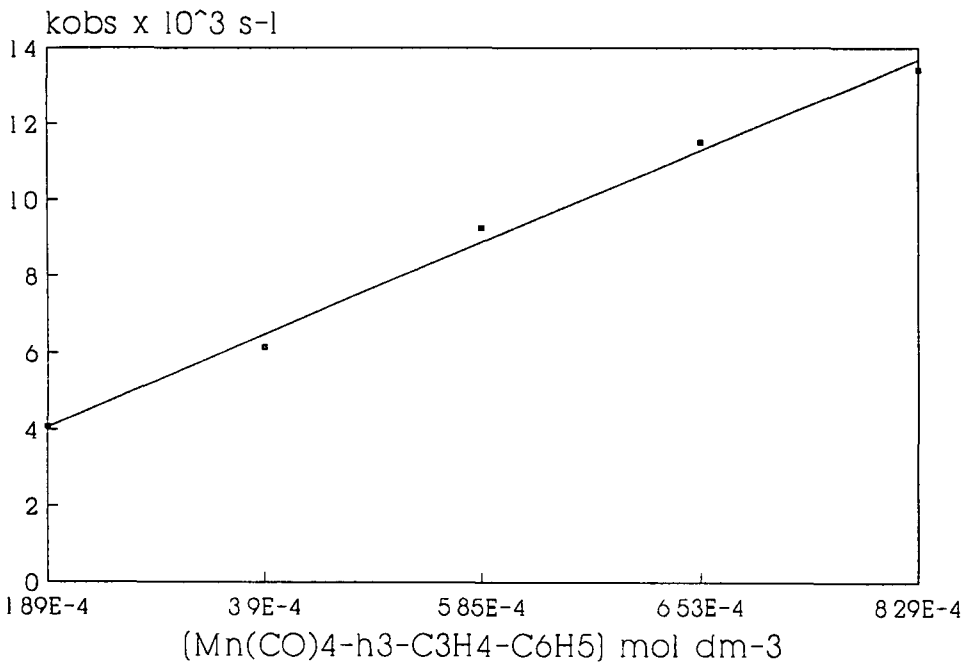

$[Mn(CO)_4\text{-}\eta^3\text{-}C_3H_4\text{-}C_6H_5]$ mol dm^{-3}	k_{obs} s^{-1}
8 29 x 10^{-4}	13435
6 53 x 10^{-4}	11502
5 85 x 10^{-4}	9251
3 90 x 10^{-4}	6131
1 89 x 10^{-4}	4079

$k_{[Mn(CO)_4\text{-}\eta^3\text{-}C_3H_4\text{-}C_6H_5]} = 1\ 34 \times 10^7 \pm 1\ 53 \times 10^6\ dm^3\ mol^{-1}\ s^{-1}$

Intercept = 1503 ± 855 s^{-1} Corr Coeff. = 0.981

Figure 3.6.1 Plot showing the variation in k_{obs} (s^{-1}) for the decay of species 2 with concentration of $Mn(CO)_4\text{-}\eta^3\text{-}C_3H_4\text{-}C_6H_5$ (mol dm^{-3})

3.7 Discussion

Species 1 has been shown to be an extremely short-lived photoproduct capable of reacting with CO CO substitution has been observed on decarbonylation of $(\eta^3\text{-}C_3H_5)Mn(CO)_4$ in the presence of PPh_3 and PMe_2Ph ligands[10]. $(\eta^3\text{-}C_3H_5)Mn(CO)_3$ has also been formed reversibly from photolysis of $(\eta^3\text{-}C_3H_5)Mn(CO)_4$ in inert CH_4 and Ar matrices at *ca* 12K[5] Species 1 is therefore assigned as a primary carbonyl-loss photoproduct, $Mn(CO)_3\text{-}\eta^3\text{-}C_3H_4\text{-}C_6H_5$, which can react with CO to regenerate the parent tetracarbonyl. Under CO atmosphere the efficiency of this recombination reaction is such that no transient species are detected. The bulky allyl-phenyl group may inhibit the interaction of this coordinatively unsaturated 16-electron species with solvent, but allow CO to interact due to it's small size Thus, the results indicate that perhaps a molecule of solvent does not occupy the vacant coordination site in this photoproduct As free rotation is possible about the C-C single bond, the allyl group of this carbonyl loss product may undergo a rapid η^3 to η^5 rearrangement to stabilise the coordinatively unsaturated fragment with concomitant dearomatisation of the phenyl group, thereby forming species 2, $Mn(CO)_3\text{-}\eta^5\text{-}C_3H_4\text{-}C_6H_5$ Young and Wrighton observed a similar reaction in their investigations into the photochemistry of $\eta^1\text{-}C_6H_5\text{-}CH_2\text{-}Mn(CO)_5$[7] Species 2 is therefore assigned to the acyclic pentadienyl complex $Mn(CO)_3\text{-}\eta^3\text{-}C_3H_4\text{-}C_6H_5$ formed by a conformational change at the allyl ligand of species 1

The experimental observations demonstrate that the pentadienyl complex may react with CO, presumably to regenerate the parent complex, or with the parent carbonyl to form a long-lived dinuclear complex, species 3 The rate of reaction of

this species with CO (3.6×10^7 dm^3 mol^{-1} s^{-1}) again indicates that it is not solvated over the timescale of the experiment The dinuclear species is formed in quite low yield and is stable over relatively long time-scales, eventually reverting back to the parent complex, as evidenced by the UV/vis spectrum of the sample solution which showed minimal variations throughout the experiments; indicating satisfactory thermal reversibility of the photochemical processes The exact structure of such a dinuclear species is unknown The rate of its formation is slower than that calculated for the (η^6-benzene)$_2$Cr$_2$(CO)$_5$ species, possibly due to the extra bulkiness of the allyl-phenyl ligand which could hinder dinuclear species formation It is noteworthy that, in this system, the order of reactivity of the observed secondary photoproduct with CO and parent is the reverse of that observed in the (η^6-benzene)Cr(CO)$_3$ case. The rate constant for the reaction of (η^6-benzene)Cr(CO)$_2$(S) with CO was determined to be significantly smaller than that for the formation of (η^6-benzene)$_2$Cr$_2$(CO)$_5$, as with the (η^5-C_5H_5)Mn(CO)$_3$[11] and (η^5-C_5H_5)V(CO)$_4$ systems[12] Here, this order is reversed as the second order rate constant for the reaction of species 2 with CO is just over twice that for the formation of the dinuclear species

It is extremely unlikely that an Mn(CO)$_5$(η^1-C_3H_5) species is formed in these photochemical reactions Such a species would require the presence of CO to form the pentacarbonyl species, by which to stabilise the coordinatively unsaturated complex, whereas the transient species observed in these experiments were typically suppressed by the presence of CO The electronic spectrum of the Mn(CO)$_5$(η^1-C_3H_5) species exhibits bands at 215nm and 270nm[5]. This does not correspond to

any of the difference UV/vis spectra recorded in these experiments, although it may correspond to that of species 1, the difference UV/vis spectrum of which was not attained.

The proposed reactions occuring on photochemistry of $Mn(CO)_4$-η^3-C_3H_4-C_6H_5 in cyclohexane solvent are illustrated in Scheme 3 7 1.

SCHEME 3 7.1

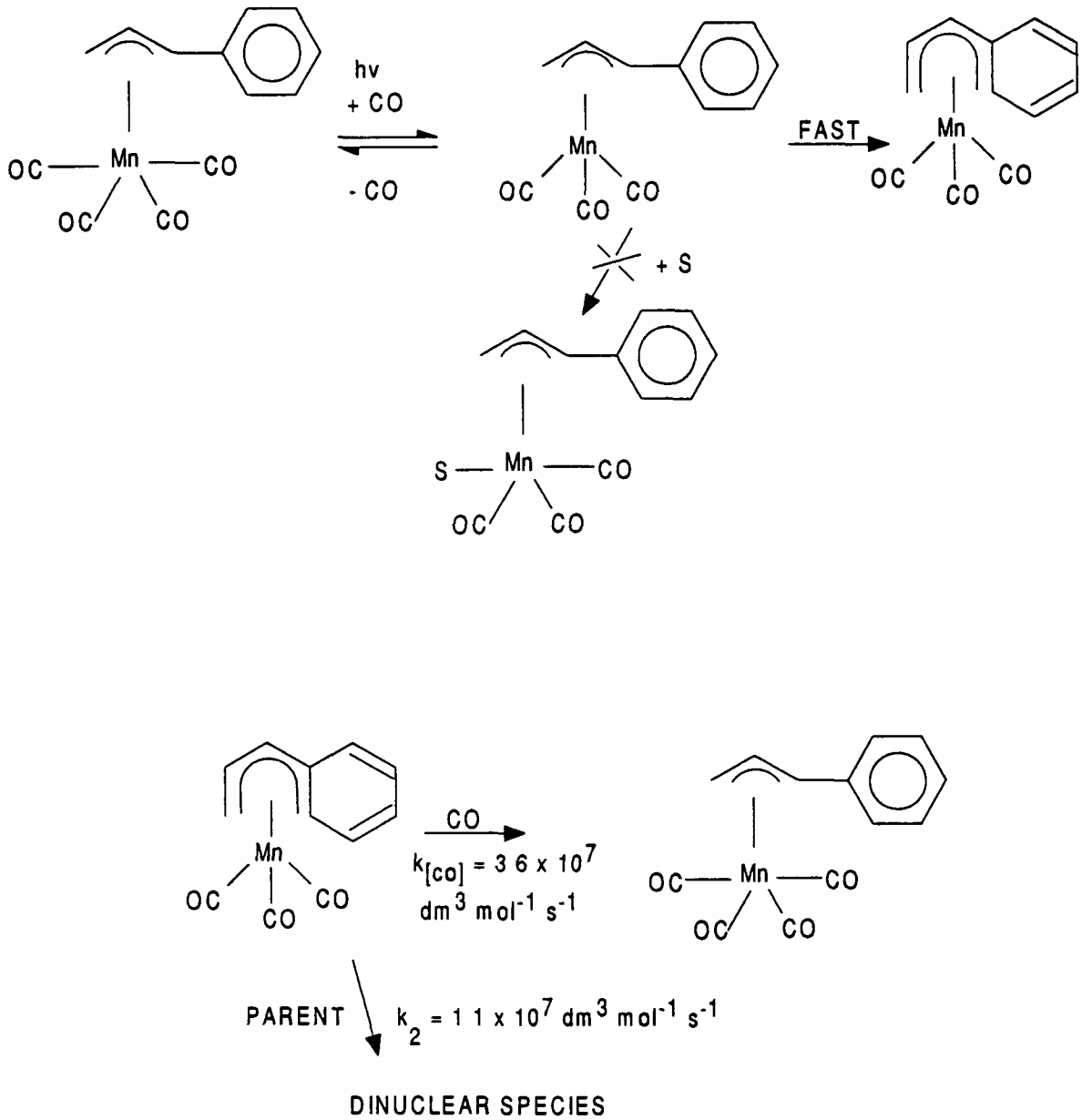
hv
+ CO
- CO
FAST
+ S
CO
k[co] = 3 6 x 10^7
dm^3 mol^-1 s^-1
PARENT
k2 = 1 1 x 10^7 dm^3 mol^-1 s^-1
DINUCLEAR SPECIES

3.8 Conclusions

Laser flash photolysis of $Mn(CO)_4$-η^1-C_3H_4-C_6H_5 in cyclohexane solution produced evidence for the formation of three transient species. The first transient was assigned as a primary carbonyl-loss photoproduct, $Mn(CO)_3$-η^3-C_3H_4-C_6H_5 No transient species were detected under CO atmosphere because of the efficiency of the recombination reaction of this species with CO The second transient was identified from reaction kinetics as an acyclic pentadienyl $Mn(CO)_3$-η^5-C_3H_4-C_6H_5 complex. This complex appeared non-solvated as the bulky allyl-phenyl group sterically prevented the cyclohexane molecule from coordinating to the metal centre. The fast second order rate constant for the reaction of this species with CO indicated that the CO molecule was able to coordinate to the metal centre, while the larger cyclohexane solvent molecule was not. The formation of a dinuclear species in low yield from this photoproduct was also noted.

3.9 References

1 H.B. Jonassen, R I Stearns, J Kentamaa, D W Moore, and A.G Whittaker, *J. Am Chem. Soc* , 1958, **80**, 2586

2. R. Baker, *Chem Rev* , 1973, **73**, 487.

3. H. Bonnemann, *Angew Chem , Int Ed Engl* , 1973, **12**, 964

4. D.A. Brown, N J Fitzpatrick, and N J Mathews, *J Organomet Chem* , 1975, **88**, C28

5. R.B. Hitam, K A. Mahmoud, and A.J Rest, *J Organomet Chem* , 1985, **291**, 321

6. G L Geoffroy and M S Wrighton, *"Organometallic Photochemistry"*, Academic Press, New York, 1979

7. K.M. Young and M S. Wrighton, *J Am Chem Soc* , 1990, **112**, 157.

8. S.T. Belt, D W Ryba, and P C Ford, *Inorg Chem* , 1990, **29**, 3633.

9 B Crocock, *"The Photochemistry of Monosubstituted Triphenylphosphine Derivatives of Some Metal Carbonyl Complexes"*, Ph D. Thesis, Dublin City University, 1992.

10. G.T Palmer and F Bosolo, *J Am Chem Soc* , 1985, **107**, 3122.

11. (a) B S Creaven, A J Dixon, J M. Kelly, C. Long., and M Poliakoff, *Organometallics,* 1987, **6**, 2600

(b) B S Creaven, *"Photochemical, Thermal and Spectroscopic Studies of Metal Carbonyl Compounds"*, Ph D Thesis, Dublin City University, 1989

12 (a) L.N Lewis and K G Caulton, *Inorg Chem* , 1980, **19**, 1840

(b) M W George, Ph D Thesis, University of Nottingham, 1990

Chapter 4

Laser Induced Photochemistry of $Mn(CO)_4$-η^3–C_3H_4-η^6-C_6H_5-$Cr(CO)_3$

4.1 Introduction

The synthesis of heterobimetallic compounds constitutes a research area that is currently very active[1] Because of the wide application of π-arene complexes of chromium in stereoselective[2] and regiocontrolled[3] syntheses, the additional activation of π-bonded arene rings by their attachment to a second organometallic fragment has gained interest. There are no reported photochemical studies on these complexes to date, although the photochemical behaviour of dinuclear CO loss intermediates is potentially very varied. In dinuclear compounds the coordinatively unsaturated molecule resulting from CO loss can engage in a form of "self-repair", e g. through the formation of bridging[4] or semi-bridging[5] CO linkages. Alternatively, or in addition to these rearrangements, the dinuclear CO-loss intermediate may subsequently react with other substrates Complexes containing two or more π-donor sites and no direct M-M bond have been studied to determine the extent of electron delocalisation through an extended π-system and, in particular, to study the effect of metal complexation on electron delocalisation[6] The hetero-bimetallic complex $Mn(CO)_4$-η^3-C_3H_4-η^6-C_6H_5-$Cr(CO)_3$ is an example of such a complex with an extended bridging ligand, and may be used to study through-ligand metal-metal interaction

In this chapter the photochemistry of the heterodinuclear complex $Mn(CO)_4$-η^3-C_3H_4-η^6-C_6H_5-$Cr(CO)_3$ is investigated by means of laser flash photolysis and TRIR studies. This represents the first reported photochemical study on a heterodinuclear complex to date An attempt is made to rationalise the photochemical results in terms of previous photochemical studies on the uncomplexed η^3-C_3H_4-

$Mn(CO)_4$ and (η^6-benzene)$Cr(CO)_3$ moities. The effect of complexation upon the UV/vis absorption spectra of the individual component complexes is also studied.

4.2 Electronic Spectrum of $Mn(CO)_4$-η^3-C_3H_4-η^6-C_6H_5-$Cr(CO)_3$

The UV/vis spectrum of $Mn(CO)_4$-η^3-C_3H_4-η^6-C_6H_5-$Cr(CO)_3$ in cyclohexane solution is presented in Figure 4.2 1 The assignment of bands in relatively large organometallic compounds as is described here is difficult. The most intense band in the spectrum of this complex is at 218nm. This band is assigned as a Cr to π^*CO charge transfer band by analogy with the spectrum of (η^6-benzene)$Cr(CO)_3$ Spectroscopic studies performed by Gogan and Chu[6] into the effect of complexation on $Cr(CO)_3$-(benzoylcyclopentadienyl)-$Mn(CO)_3$ derivatives have concluded that π-complexing of the $Cr(CO)_3$ group onto the arene ring causes a hypsochromic shift in the Mn-C band, e g. a shift from 344 to 330nm was reported for a benzoyl compound This may indicate that the 242nm band of the (η^3-allyl)$Mn(CO)_4$ species is shifted to higher energy such as it is superimposed on the absorption of the $Cr(CO)_3$ group in this region. A shoulder on the low energy side of this absorption maximum, at 254nm, may be assigned to a hypsochromic shift of either the 264nm absorption of (η^6-benzene)$Cr(CO)_3$ or the 292nm absorption of the (η^3-allyl)$Mn(CO)_4$ species The band centred at 328nm is most logically assigned to the Cr to π^*CO charge transfer band with some Cr to arene character by analogy with the spectrum of (η^6-benzene)$Cr(CO)_3$ All the bands except the weak band centred at 406nm are observed in the non-complexed compounds This band is similar to that reported in the UV/vis spectra of $Cr(CO)_3$-(benzoylcyclopentadienyl)-$Mn(CO)_3$

derivatives[6] It was assigned as a charge transfer band from Cr to C. Gray and Beach[7] observed a band at 440nm in the spectrum of $Cr(CO)_6$ which they proposed to be of the same nature.

The positions of the band maxima in the uncomplexed (η^6-benzene)$Cr(CO)_3$ and (η^3-allyl)$Mn(CO)_4$ species and in the dinuclear complex $Mn(CO)_4$-η^3-C_3H_4-η^6-C_6H_5-$Cr(CO)_3$ are given in Table 4 2 1.

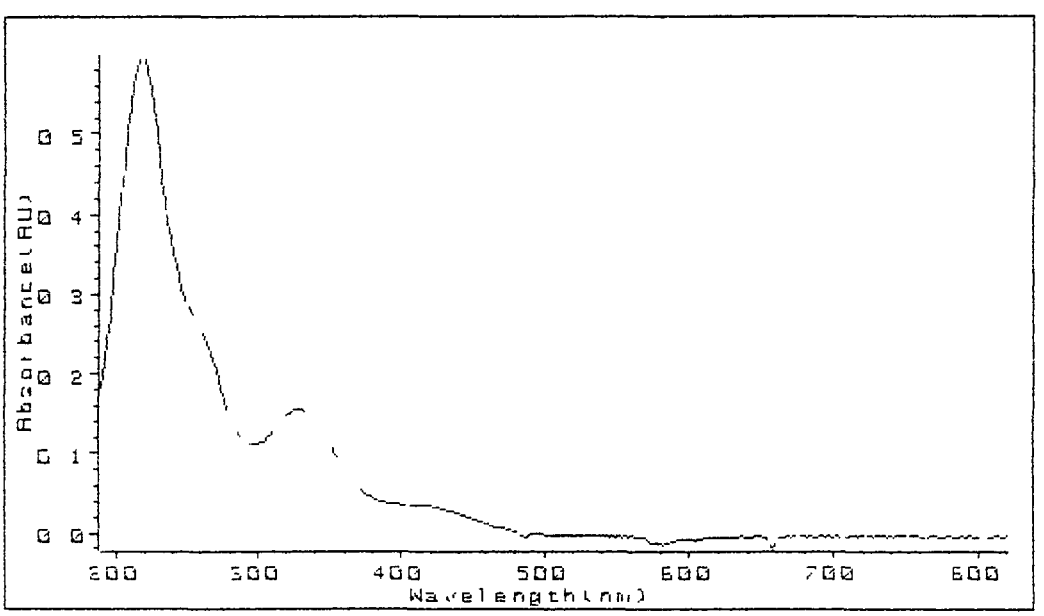

Figure 4.2.1 UV/vis absorption spectrum of a 1.55 x 10^{-4} mol dm^{-3} solution of $Mn(CO)_4$-η^3-C_3H_4-η^6-C_6H_5-$Cr(CO)_3$ in cyclohexane

Table 4.2.1 Spectral data for (η^6-benzene)$Cr(CO)_3$, (η^3-allyl)$Mn(CO)_4$ and $Mn(CO)_4$-η^3-C_3H_4-η^6-C_6H_5-$Cr(CO)_3$ complexes

Complex	Bands nm	Assignment	Reference
(η^6-benzene)$Cr(CO)_3$	376	LF?	[8]
	316	Cr---> arene, π*CO CT	
	264	Cr---> π* CO CT	
	220	Cr---> π* CO CT	
(η^3-allyl)$Mn(CO)_4$	292(sh)	Mn---> π* CO CT	[9]
	242	Mn---> π* CO CT	
$Mn(CO)_4$-η^3-C_3H_4-η^6 -C_6H_5-$Cr(CO)_3$	406	Cr---> C CT	
	328	Cr---> arene, π*CO CT	
	254(sh)	Mn/Cr---> π* CO CT?	
	218	Mn/Cr---> π* CO CT	

4.3 Preliminary Experimental Results

Under 1.0 atmosphere of CO and utilising the third harmonic of the Nd^{3+} YAG fundamental at 355nm, at least three transient species were observed to absorb at 300nm following the irradiation of $Mn(CO)_4$-η^3-C_3H_4-η^6-C_6H_5-$Cr(CO)_3$ (ε_{354nm}= 8090 dm^3 mol^{-1} cm^{-1}) in cyclohexane at ambient temperatures. The first species was formed within the laser flash and was quite short-lived, the rate constant for the decay of this species was measured as 4 7 x 10^5 s^{-1}, Figure 4.3 1

Experiments conducted at varying concentrations of CO revealed that the yield and lifetime of the this first observed species were independent of CO concentration to within experimental error; these results are tabulated in Tables 4 3 1 and plotted in Figures 4 3 2 and 4 3 3 This indicates that the transient species is not susceptible to reaction with CO Further experiments conducted at varying concentrations of parent complex revealed that the lifetime of this species was also unaffected by parent concentration, Figure 4 3 4 It is concluded from these observations that this species does not react with either CO or parent complex, suggesting that an intramolecular reaction occurs These results may then represent an example of an intraligand photoreaction, most probably by means of the facile η^3 to η^1 or η^5 hapticity changes of the allyl portion of the dinuclear complex This reaction is essentially a unimolecular process, the rate of which is independant of the concentration of other potential ligands (such as CO or parent) Intraligand reactions involving *cis-trans* isomerisation[8], cyclisation[9], 1,3-hydrogen shifts[10], dimerisation[11], and hydrogenation[12] represent some of the reported examples where the groups attached to a transition metal undergo a chemical transformation as a consequence of photochemical excitation of the metal complex

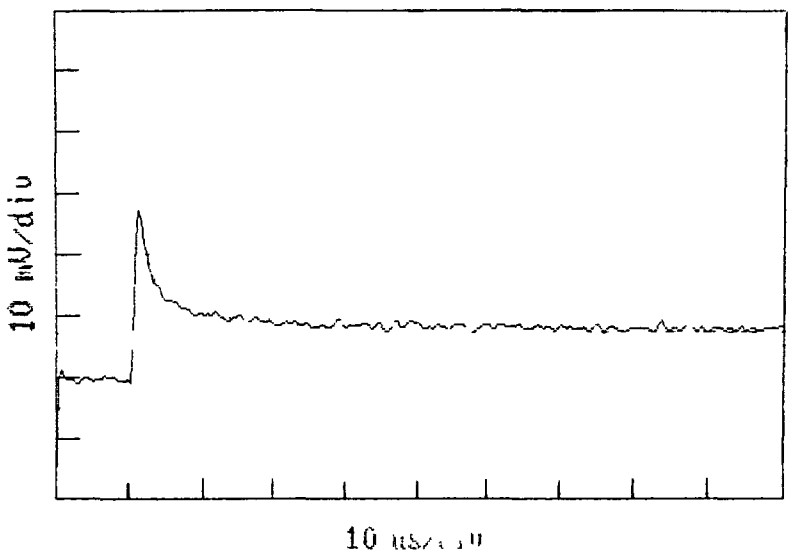

Figure 4.3.1 Transient signal displaying the decay of the first and second species observed at 300nm after flash photolysis of a 1 16 x 10^{-4} mol dm^{-3} solution of $Mn(CO)_4$-η^3-C_3H_4-η^6-C_6H_5-$Cr(CO)_3$ in cyclohexane under 1 0 atmosphere of CO at 298K

Table 4.3.1 The observed rate constants for the decay of the first transient species at 300nm at 298K at varying CO concentrations (mol dm^{-3}); [$Mn(CO)_4$-η^3-C_3H_4-η^6-C_6H_5-$Cr(CO)_3$] = 9 49 x 10^{-5} mol dm^{-3} The yield of this species (as measured by the absorbance at 0μs after the laser flash) is also tabulated.

[CO] mol dm^{-3}	k_{obs} s^{-1}	Absorbance
0 000	497044	2 687 x 10^{-2}
0 003	476135	2 279 x 10^{-2}
0 006	469513	2 619 x 10^{-2}
0 009	452918	3 066 x 10^{-2}
0 012	496373	3 030 x 10^{-2}

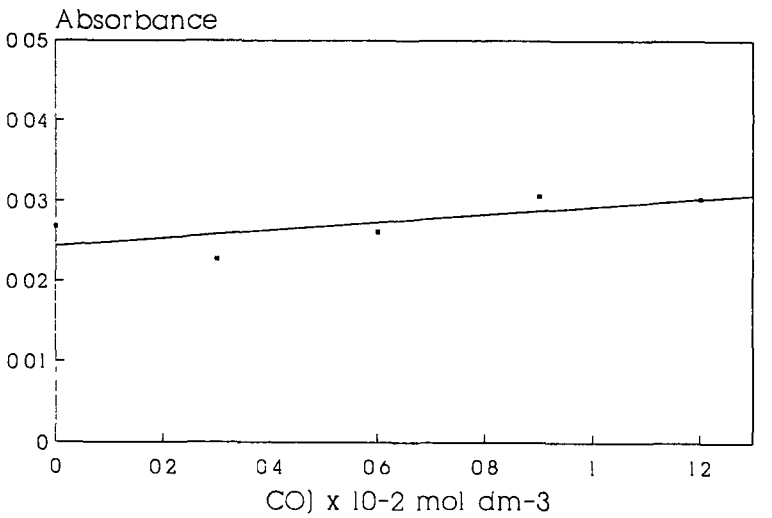

Figure 4.3.2 A plot of the observed yield at 0μs after the laser flash (in absorbance units) of the first transient species at differing CO concentrations (mol dm^{-3}) at 298K.

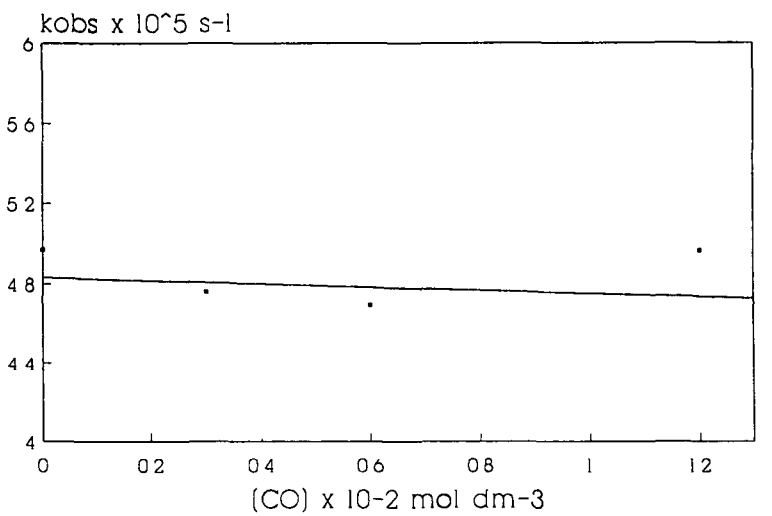

Figure 4.3.3 A plot of the observed rate constants (s^{-1}) for the decay of the first transient species with differing concentrations of CO (mol dm^{-3}) at 298K.

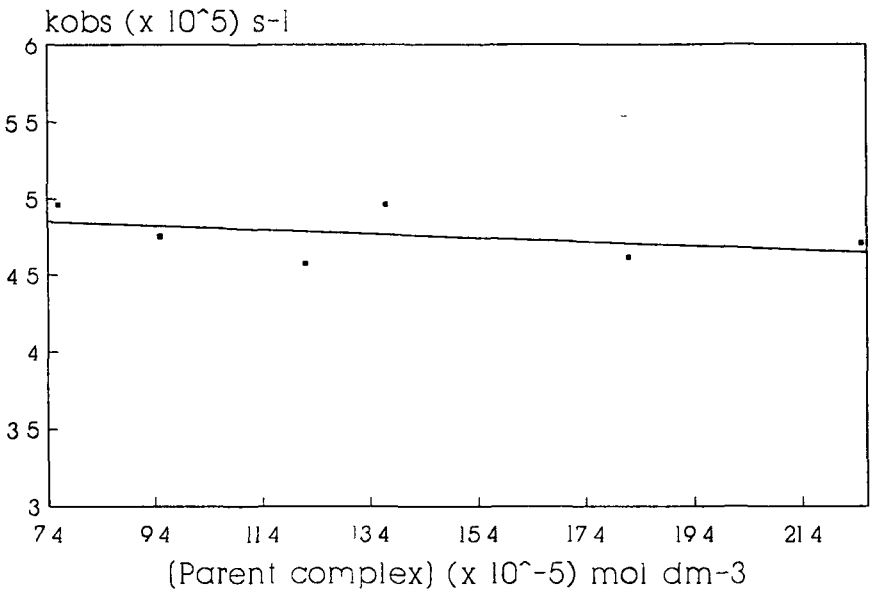

$[Mn(CO)_4\text{-}\eta^3\text{-}C_3H_4\text{-}\eta^6\text{-}C_6H_5\text{-}Cr(CO)_3]$ mol dm^{-3}	k_{obs} s^{-1}
7 573 x 10^{-5}	496373
9 492 x 10^{-5}	475404
1 224 x 10^{-4}	457225
1 369 x 10^{-4}	496358
1.816 x 10^{-4}	461455
2 254 x 10^{-4}	470643

Figure 4.3.4 A plot of $[(Mn(CO)_4\text{-}\eta^3\text{-}C_3H_4\text{-}\eta^6\text{-}C_6H_5\text{-}Cr(CO)_3]$ (mol dm^{-3}) against the observed rate constants (s^{-1}) for the decay of the first transient species at 298K under 1 0 atmosphere of CO at 300nm

The rate of decay of the second observed species was calculated to be 7.9 x 10^4 s^{-1} This transient species is assigned to the product of the intramolecular reaction of the first observed species This transient species was typically observed as a second decay super-imposed on that of the first species producing a 'bi-phasic' decay analysing for a double-exponential function, Figure 4 3 1 It is difficult to ascertain if the rate of decay of species 2 is dependant on CO concentration, as under reduced levels of CO and under argon atmosphere the formation of a third species 'masks' this decay profile Experiments conducted with solvents of different dryness under argon atmospheres have suggested that the photochemical observations are complicated by the reaction of a primary photoproduct with traces of water present in the solvent to form an impurity complex This was indicated as the level of liquid-pumping influenced the degree to which these transient absorptions retured to the baseline value This observation is consistent with the impurity complexes observed on photochemical excitation of (η^6-arene)$Cr(CO)_3$ complexes in cyclohexane solution reported earlier

A third transient species was observed in these experiments. Under argon atmosphere the formation of this species is super-imposed on the decays of species 1 and 2, Figure 4 3 5, and it is therefore impossible to accurately measure the rate of its formation The rate of decay of species 3 was measured as 6 3 x 10^2 s^{-1} under these conditions, Figure 4 3 6 This species is not produced when the experiments are carried out under CO atmosphere This suppression of the yield of this species by the presence of CO in solution strongly indicates that it is a secondary photoproduct formed by the reaction of a species which can also react competitively with CO.

Given that species 1 has been determined not to react with CO, this would seem to eliminate the possibility that species 1 is a precursor in the formation of this species. These results may indicate that this species is a photochemical product of another section of the dinuclear complex

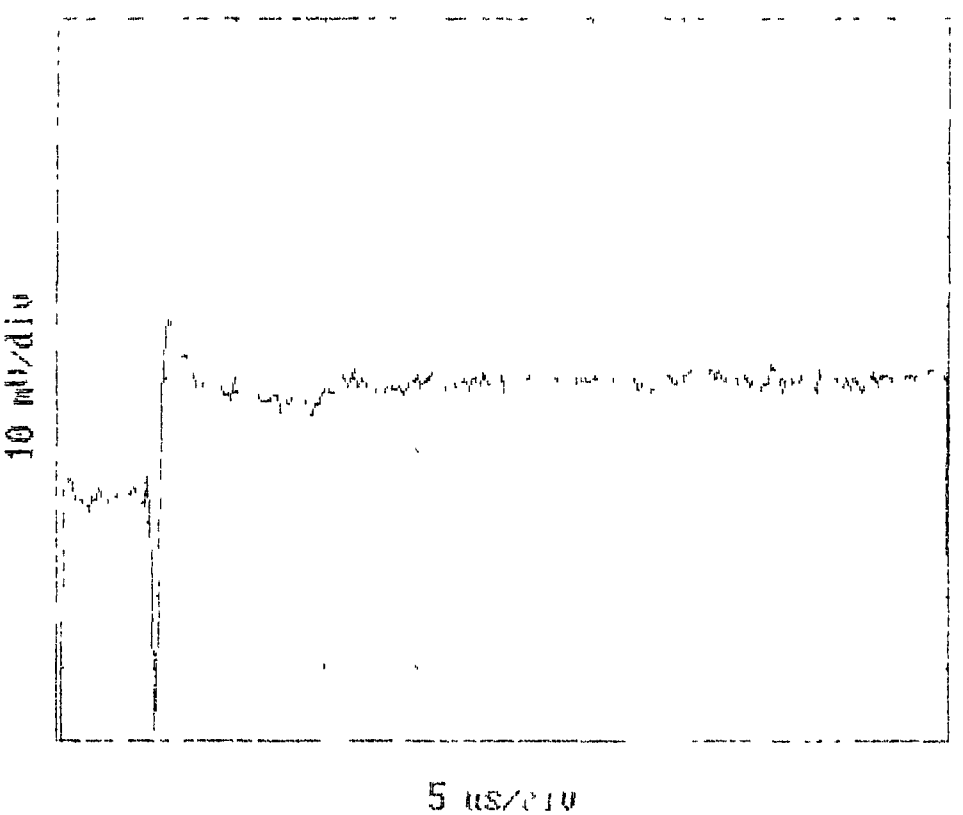

Figure 4.3.5 Transient signal of the formation of the third transient species observed at 300nm after flash photolysis of a cyclohexane solution of $Mn(CO)_4$-η^3-C_3H_4-η^6-C_6H_5-$Cr(CO)_3$ under 1.0 atmosphere of argon at 298K

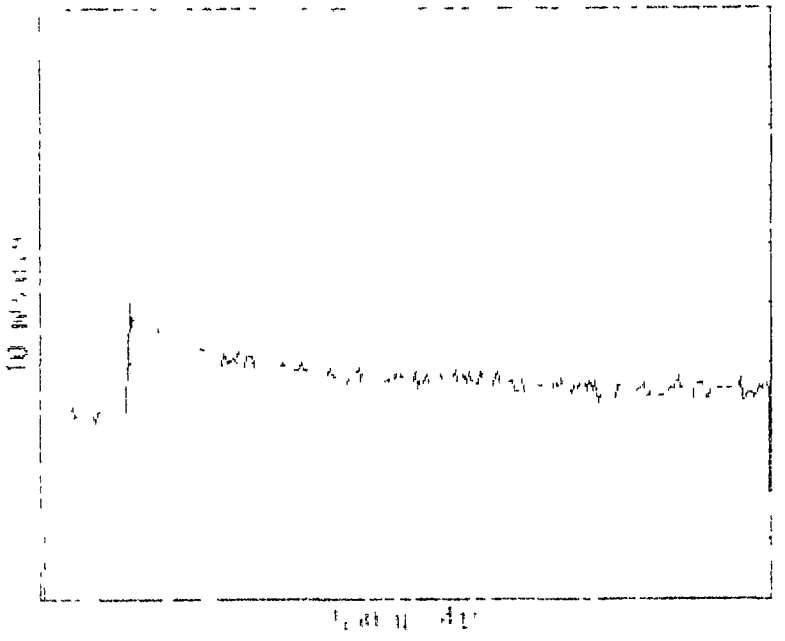

Figure 4.3.6 Transient signal of the decay of the third transient species observed at 300nm after flash photolysis of a cyclohexane solution of $Mn(CO)_4$-η^3-C_3H_4-η^6-C_6H_5-$Cr(CO)_3$ under 1 0 atmosphere of argon at 298K.

4.4 UV/vis Difference Spectrum of the First Observed Species

The UV/vis difference spectra obtained within 1μs of the laser pulse under 1.0 atmosphere of CO and 1 0 atmosphere of argon are given in Figures 4 4 1(a) and (b). The spectra are practically identical, supporting the conclusion that this species is the first observed species both in the presence and absence of CO This transient spectrum shows negative bands at 345nm and 430nm, attributed to depletion of the 328nm and 406nm absorptions of the parent molecule, Figure 4.2.1 The transient intermediate exhibits an apparent absorption maximum in the UV region of the spectrum at 300nm, in the region of the valley in the absorption profile of the parent complex

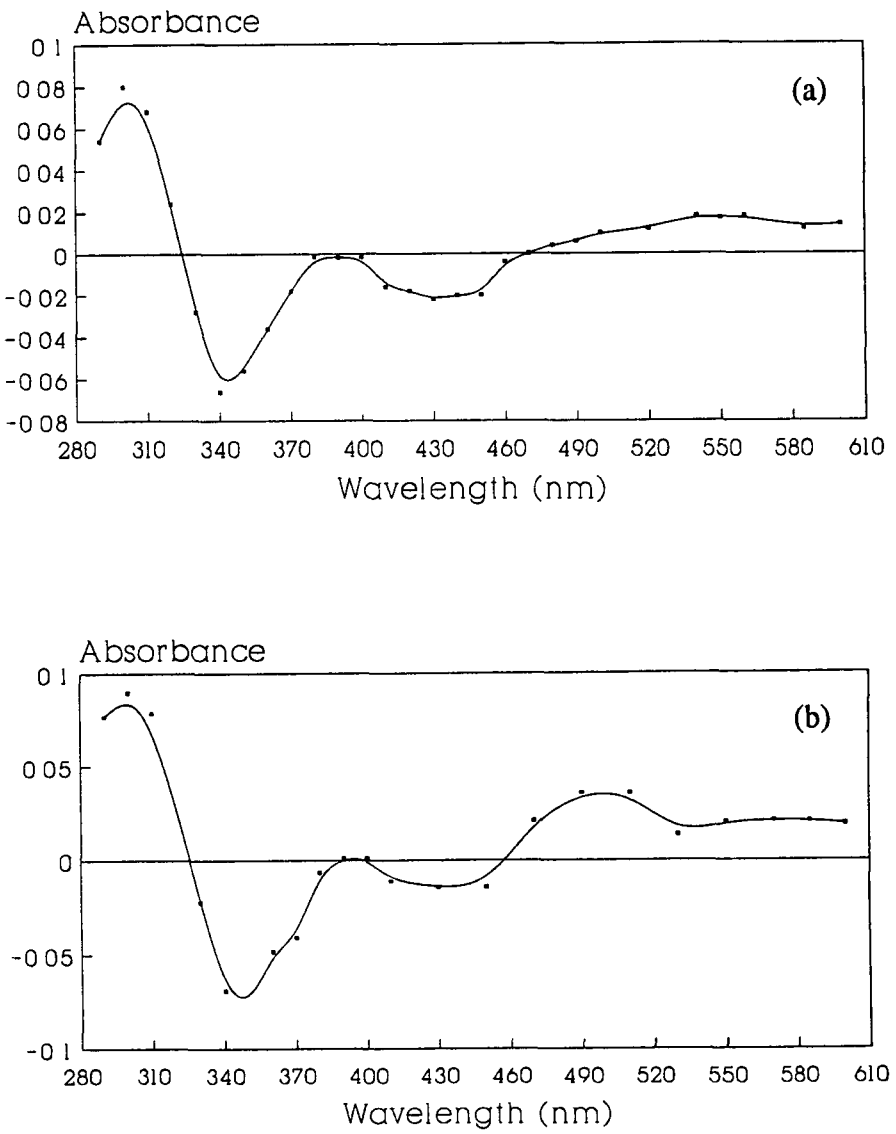

Figure 4.4.1 UV/vis difference spectra recorded 1μs following the laser flash photolysis of $Mn(CO)_4$-η^3-C_3H_4-η^6-C_6H_5-$Cr(CO)_3$ in cyclohexane solution (a) under argon atmosphere and (b) under CO atmosphere; [$Mn(CO)_4$-η^3-C_3H_4-η^6-C_6H_5-$Cr(CO)_3$] = 1 27 x 10^{-4} mol dm^{-3} for both spectra

4.5 UV/vis Difference Spectrum of the Third Observed Species

The UV/vis difference spectrum of the third observed species obtained 12μs after the laser flash under argon atmosphere is given in Figure 4.5 1. This spectrum exhibits absorption peaks at 300nm and 400nm and a depletion band at 350nm.

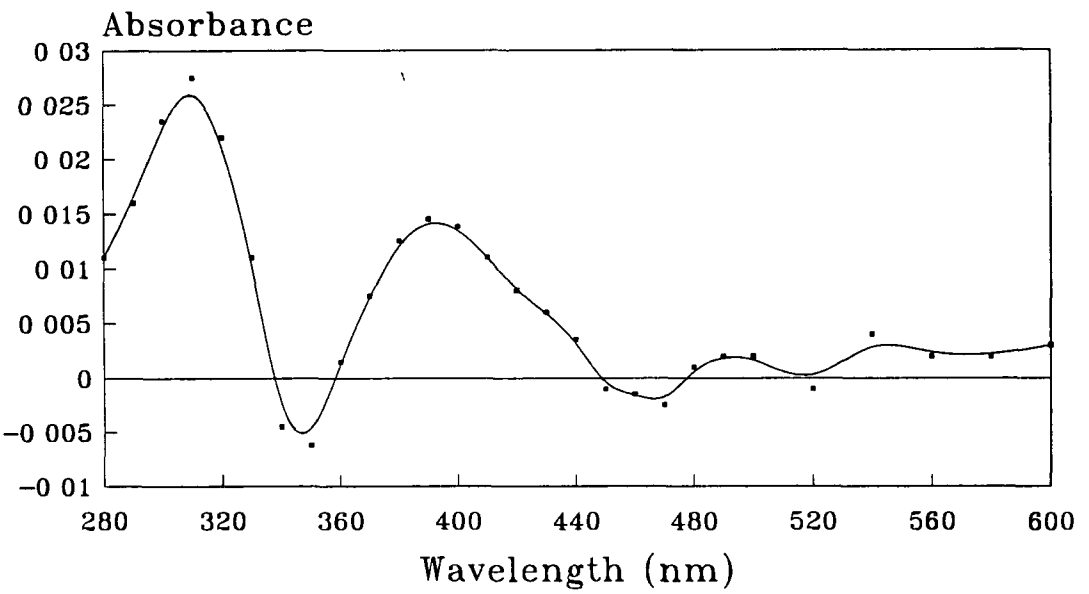

Figure 4.5.1 UV/vis difference spectrum of the third observed species recorded 12μs after laser flash photolysis of $Mn(CO)_4$-η^3-C_3H_4-η^6-C_6H_5-$Cr(CO)_3$ in cyclohexane solution under argon atmosphere

4.6 A Study of the Activation Parameters for the Intramolecular Reaction of the First Observed Species

The first species has been found not to react with CO or parent The decay of this species is assumed therefore to be a true first order, and not a psuedo-first order, process. Activation parameters were determined for the intramolecular reaction of this species from Arrhenius and Eyring Plots over a temperature range of 284 to 314K.

The results are detailed in Table 4 6 1 and illustrated graphically in Figure 4 6.1. These values were obtained at a CO concentration of 1.2 x 10^{-2} mol dm^{-3}.

Table 4.6.1 (a) Experimental data for the determination of the energy, entropy and enthalpy of activation for the intramolecular reaction involving species 1; $[Mn(CO)_4\text{-}\eta^3\text{-}C_3H_4\text{-}\eta^6\text{-}C_6H_5\text{-}Cr(CO)_3]$ = 1 1 x 10^{-4} mol dm^{-3}

1/T (x 10^3)	Ln(k_{obs})	Ln(k_{obs}/T)
3 52	12 67	7 02
3 45	12 82	7 15
3 39	12 91	7 22
3 33	13 11	7 41
3 26	13 26	7 54
3 19	13 37	7 63

Arrhenius Plot	Eyring Plot	Activation Parameters
Slope = -2149 ± 112	Slope = -1887 ± 119	Ea = 18 ± 1 kJ mol^{-1}
Int = 20 24 ± 0 03	Int = 13 67 ± 0 03	$\Delta H^{\neq}$ = 16 ± 1 kJ mol^{-1}
Corr Coeff = 0 995	Corr Coeff = 0 992	$\Delta S^{\neq}$ = -84 ± 20 J mol^{-1} K^{-1}

Table 4.6.1 (b) Experimental data for the determination of the energy, entropy and enthalpy of activation for the intramolecular reaction involving species 1; $[Mn(CO)_4\text{-}\eta^3\text{-}C_3H_4\text{-}\eta^6\text{-}C_6H_5\text{-}Cr(CO)_3] = 1.2 \times 10^{-4}$ mol dm^{-3}

$1/T (\times 10^3)$	$Ln(k_{obs})$	$Ln(k_{obs}/T)$
3.51	12.71	7.06
3.38	13.05	7.36
3.25	13.25	7.52
3.17	13.43	7.68

Arrhenius Plot	Eyring Plot	Activation Parameters
Slope = -2055 ± 157	Slope = -1758 ± 156	$E_a = 17 \pm 1$ kJ mol^{-1}
Int = 19.95 ± 0.04	Int = 13.25 ± 0.04	$\Delta H^{\neq} = 15 \pm 1$ kJ mol^{-1}
Corr. Coeff. = 0.994	Corr. Coeff. = 0.992	$\Delta S^{\neq} = -87 \pm 20$ J mol^{-1} K^{-1}

The thermodynamic parameters associated with the decay of the first observed species are consistent with the occurance of an intramolecular process. The enthalpy and energy of activation are quite low at 16 and 18 kJ mol^{-1} respectively. These values are significantly lower (by approximately 7 kJ mol^{-1}) than those determined for the reaction of $(\eta^6$-benzene$)Cr(CO)_3$ with CO indicating that a unimolecular process requires less energy than is required for reaction with CO. The $\Delta S^{\neq}$ value for this reaction is large and negative indicating that the reaction is almost associative in nature, although the transition state is probably best described by an interchange

mechanism. An intramolecular reaction would require a more ordered transition state, and this is probably reflected in the large negative value of $\Delta S^{\neq}$

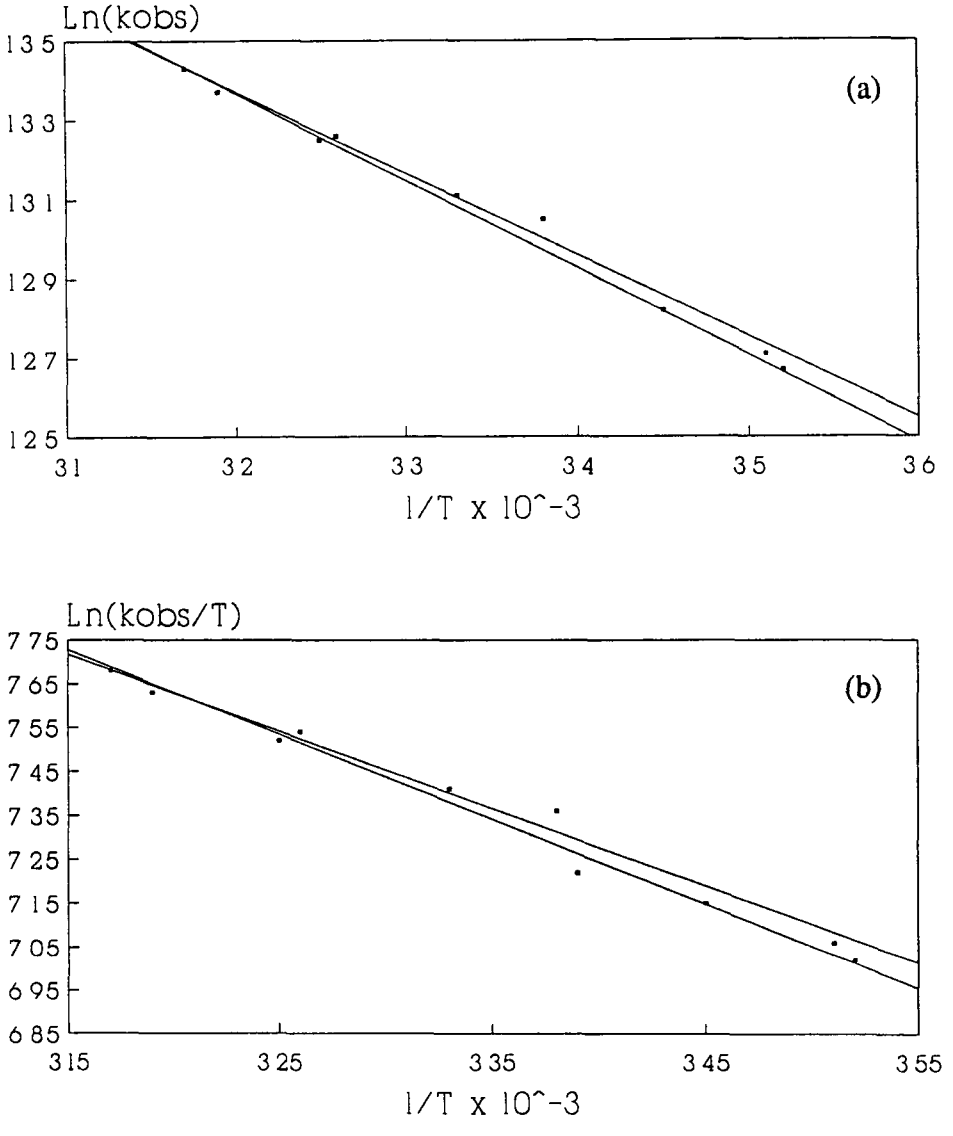

Figure 4.6.1 Arrhenius (a) and Eyring (b) plots for the intramolecular reaction of the first transient species

4.7 A Study of the Activation Parameters for the Reaction of the Second Transient Species

No conclusive evidence was found for the reaction of species 2 with CO or parent Therefore these factors are not considered in the calculations. Activation parameters were measured from Arrhenius and Eyring Plots over a temperature range of 284 to 314K The results are detailed in Table 4 7 1 and illustrated graphically in Figure 4 7 1, where T = temperature (K)

Table 4.7.1 (a) Experimental data for the determination of the energy, entropy and enthalpy of activation for the reaction of species 2, $[Mn(CO)_4\text{-}\eta^3\text{-}C_3H_4\text{-}\eta^6\text{-}C_6H_5\text{-}Cr(CO)_3] = 1\ 2 \times 10^{-4}$ mol dm^{-3}

$1/T\ (\times 10^3)$	$Ln(k_{obs})$	$Ln(k_{obs}/T)$
3 51	11 06	5 40
3 42	11 19	5 51
3 38	11 33	5 64
3 33	11 44	5 73
3 25	11 61	5 88

Arrhenius Plot	Eyring Plot	Activation Parameters
Slope = -2207 ± 148	Slope = -1912 ± 148	$E_a = 18 \pm 1$ kJ mol^{-1}
Int. = 18 78 ± 0 03	Int. = 12 09 ± 0 03	$\Delta H^{\neq} = 16 \pm 1$ kJ mol^{-1}
Corr Coeff = 0 993	Corr Coeff = 0 991	$\Delta S^{\neq} = -97 \pm 20$ J mol^{-1} K^{-1}

Table 4.7.1 (b) Experimental data for the determination of the energy, entropy and enthalpy of activation for the reaction of species 2; $[Mn(CO)_4\text{-}\eta^3\text{-}C_3H_4\text{-}\eta^6\text{-}C_6H_5\text{-}Cr(CO)_3] = 1.1 \times 10^{-4}$ mol dm^{-3}

$1/T (\times 10^3)$	$Ln(k_{obs}/[CO])$	$Ln((k_{obs}/[CO])/T)$
3 52	10 36	4 83
3 45	10 70	5 04
3 39	10 90	5 21
3 33	11 00	5 29
3 19	11 58	5 71

Arrhenius Plot	Eyring Plot	Activation Parameters
Slope = -3506 ± 247	Slope = -3211 ± 249	$E_a = 29 \pm 2$ kJ mol^{-1}
Int. = 22 74 ± 0 06	Int = 16 05 ± 0 06	$\Delta H^{\neq} = 27 \pm 2$ kJ mol^{-1}
Corr Coeff = 0 993	Corr Coeff = 0 991	$\Delta S^{\neq} = -64 \pm 20$ J mol^{-1} K^{-1}

The slope of an Arrhenius or Eyring plot does not alter on inclusion or omission of CO in the calculations, however the intercept is affected Therefore, if species 2 reacts with CO, the only parameter which will differ is the $\Delta S^{\neq}$ value; since the intercept of the Eyring plot is utilised in its calculation It has been calculated that the values of $\Delta S^{\neq}$ becomes less negative by ~37 J mol^{-1} K^{-1} on inclusion of the concentration of CO in this determination

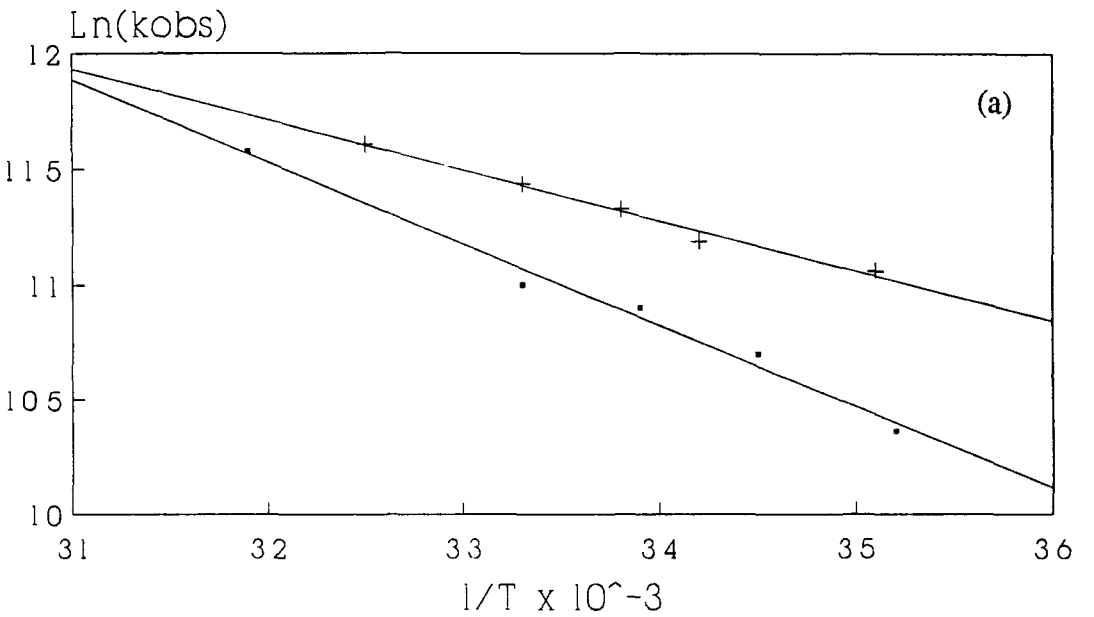

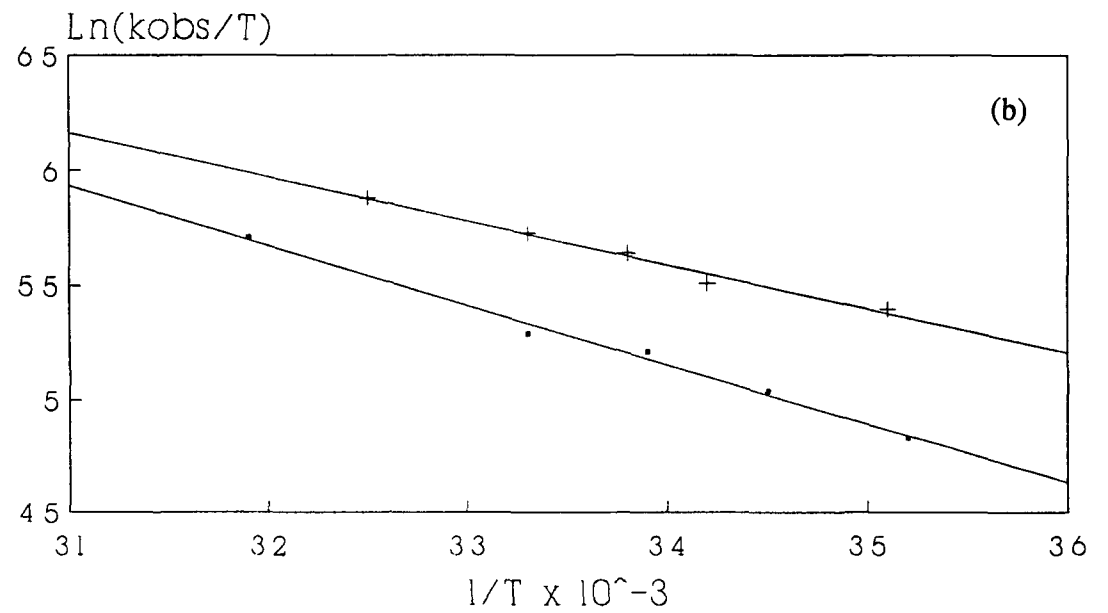

Figure 4.7.1 Arrhenius (a) and Eyring (b) plots for the reaction of the second transient species

4.8 Preliminary Time Resolved Infrared Study

A FTIR of a 4.77 x 10^{-5} mol dm^{-3} solution of $Mn(CO)_4$-η^3-C_3H_4-η^6-C_6H_5-$Cr(CO)_3$ in n-heptane is given in Figure 4 8 1 Five peaks are observable in the carbonyl stretching region, at 2072, 2001 5, 1978, 1970 and 1915 cm^{-1}. Although this molecule has overall C_s symmetry, an approximate C_{3v} and C_s local symmetry can be assumed for the solution spectra of the $Cr(CO)_3$ and $Mn(CO)_4$ portions The IR stretching frequencies of the uncomplexed metal centres and the dinuclear species are given in Table 4 8 1 Two carbonyl bands were recorded for (η^6-benzene)$Cr(CO)_3$ in n-heptane, at 1983 and 1915 cm^{-1} Four bands are reported for the η^3-$C_3H_5Mn(CO)_4$ species of C_s symmetry, at 2081, 2001, 1983, and 1965cm^{-1}[13]. Thus, in the dinuclear species, the band at 1915cm^{-1} is attributed solely to the (η^6-benzene)$Cr(CO)_3$ moiety, as the bands at 2072, 2001 and 1970cm^{-1} are attributed solely to the $Mn(CO)_4$-η^3-allyl moiety The remaining band at 1978cm^{-1} is ascribed to both the (η^6-benzene)$Cr(CO)_3$ and $Mn(CO)_4$-η^3-allyl species Both species exhibit a band at *ca* 1983cm^{-1} in their uncomplexed state, it is likely that these bands overlap in the spectrum of the dinuclear complex and give rise to a single band at 1978cm^{-1} A shoulder on this peak in the FTIR spectrum confirms that this band is asymmetrical

Table 4.8.1 A comparison of the IR stretching frequencies (cm^{-1}) for (η^6-benzene)$Cr(CO)_3$, $Mn(CO)_4$-η^3-allyl and $Mn(CO)_4$-η^3-C_3H_4-η^6-C_6H_5-$Cr(CO)_3$. [a] this work in n-heptane [b] Reference 13

Complex	ν_{CO} cm^{-1}
(η^6-benzene)$Cr(CO)_3$	1983,1915[a]
$Mn(CO)_4$-η^3-allyl	2081,2001,1983,1965[b]
$Mn(CO)_4$-η^3-C_3H_4-η^6-C_6H_5-$Cr(CO)_3$	2072,2002,1978,1970,1915[a]

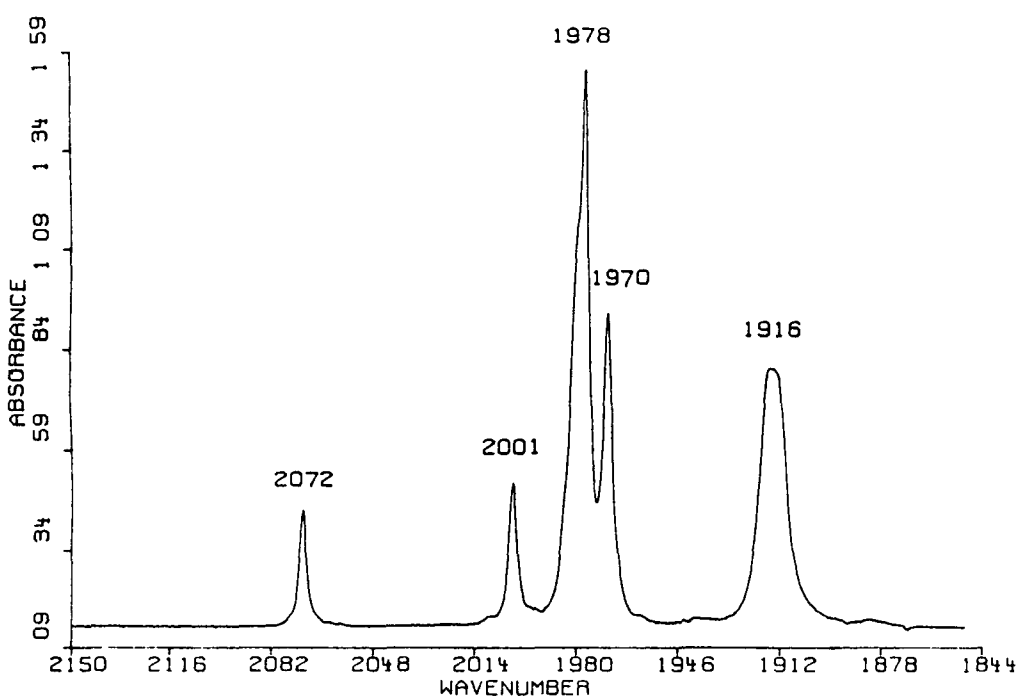

Figure 4.8.1 FTIR spectrum of a 4 77 x 10^{-5} mol dm^{-3} solution of $Mn(CO)_4$-η^3-C_3H_4-η^6-C_6H_5-$Cr(CO)_3$ in n-heptane

The TRIR spectrum from 1997 to 1844cm^{-1} obtained 10μs following laser flash photolysis of a 4 77 x 10^{-5} mol dm^{-3} solution of $Mn(CO)_4$-C_3H_4-η^6-C_6H_5-$Cr(CO)_3$ in n-heptane solution under 2 0 atmospheres of argon is given in Figure 4 8.2 Three of the absorption bands of the parent complex lie in this region of analysis and are therefore amenable to study All three bands are depleted, these are detected as the negative absorptions with peak positions at 1984, 1971 and 1920cm^{-1}. These parent absorptions are not fully regenerated, indicating that long-lived transient species are produced from the parent complex Three absorptions attributed to transient photoproducts are observed at 1976, 1932 and 1907cm^{-1}. The identity of the intermediate(s) species giving rise to these absorptions is still uncertain, although a simple carbonyl loss product from one of the metal moities does not seem likely If an (η^6-arene)$Cr(CO)_2$(S) species was produced, for example, depletion of the 1915 and 1978 cm^{-1} absorptions, arising from the (η^6-arene)$Cr(CO)_3$ species only, would be expected, with the production of bands at *ca* 1929 and 1877cm^{-1} by comparison with previous TRIR experiments on this section of the dinuclear complex

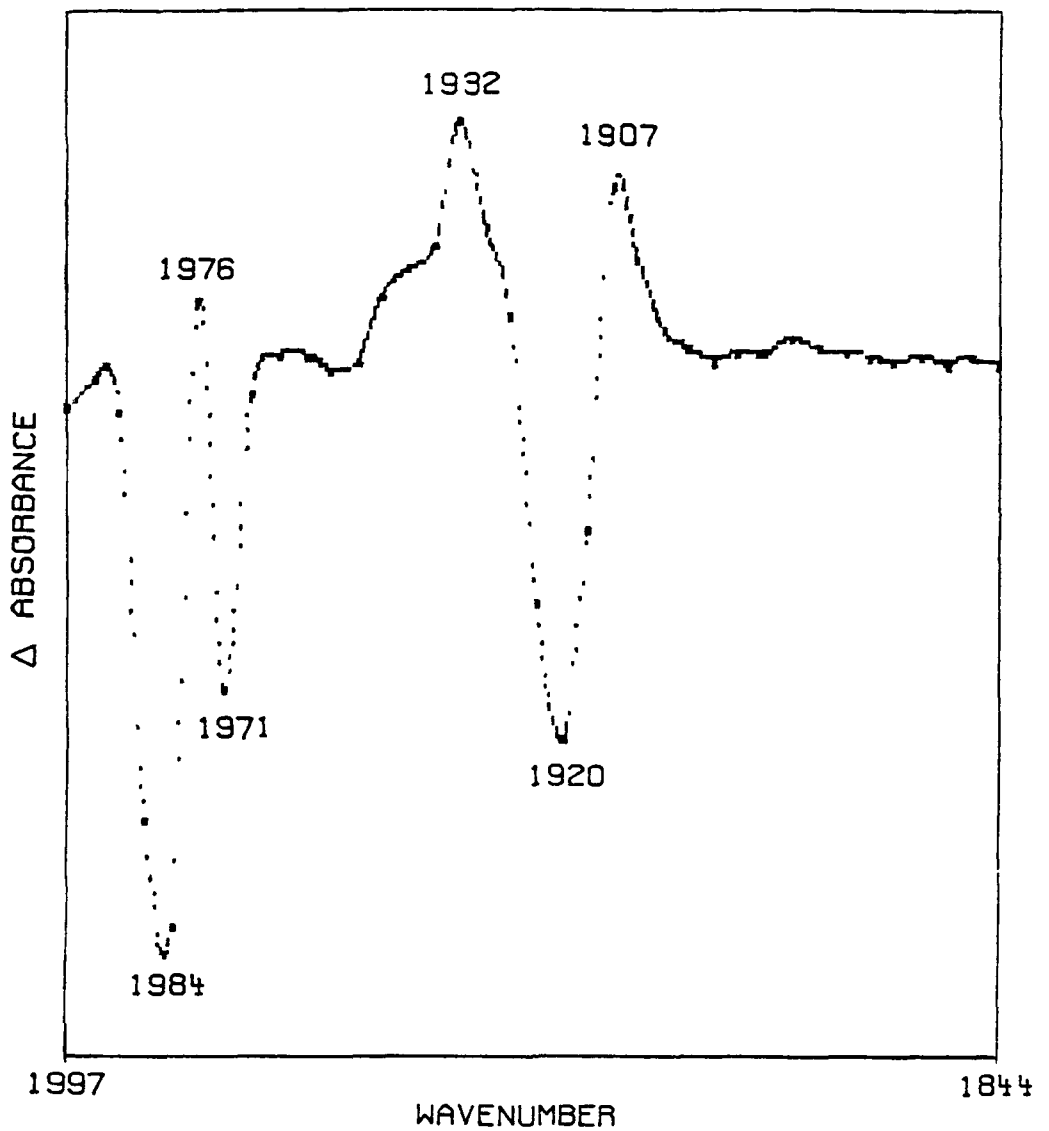

Figure 4.8.2 TRIR spectrum obtained 10μs following laser flash photolysis of $Mn(CO)_4$-η^6-C_3H_4-η^6-C_6H_5-$Cr(CO)_3$ in n-heptane under 2.0 atmospheres of argon.

4.9 Discussion

It is proposed that the photochemistry is centred on the chromium system. This would corroborate the results obtained in a photochemical study by A. Wright *et al* [14] where $Mn(CO)_4$-η^3-C_3H_4-η^6-C_6H_5-$Cr(CO)_3$ was photolysed in the presence of the PPh_3 ligand; yielding exclusively the chromium substituted species $Mn(CO)_4$-η^3-C_3H_4-η^6-C_6H_5-$Cr(CO)_2(PPh_3)$, reaction 4 9 1 This study indicates that chromium is the more photochemically labile centre in this dinuclear complex; as net photosubstitution generally occurs at the site from which CO was extruded in the primary photoprocess[15]

Reaction 4 9 1

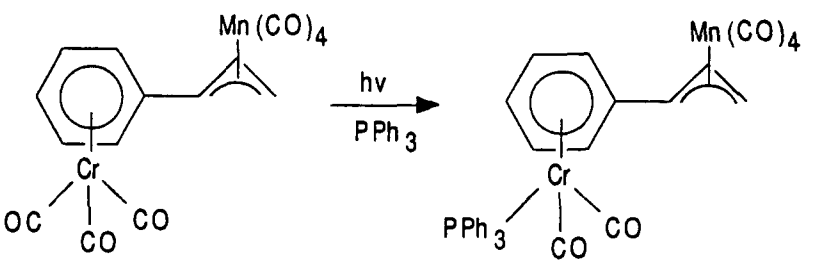

As with photolysis of (η^6-arene)$Cr(CO)_3$ the first observed species is attributed to a carbonyl loss product of the Cr centre This species may undergo an intramolecular rearrangement by rotation of the C-C single bond, thereby allowing the chromium centre to interact with the manganese and abstract a CO ligand to return to coordinative saturation The manganese centre may concomitantly undergo a η^3 to η^5 rearrangement to stabilise the new coordinatively unsaturated fragment produced. The rate of such a intramolecular transformation would be independent of parent or CO concentration; as observed in the experimental work conducted. The

thermodynamic parameters determined for the decay of the primary photoproduct are consistent with this unimolecular process The energy and enthalpy of activtion are lower, by approximately 7 kJ mol^{-1}, than those determined for the reaction of (η^6-benzene)$Cr(CO)_2(S)$ with CO, indicating that less energy is necessary for the unimolecular process than is required for a recombination reaction with CO. The negative values of $\Delta S^{\neq}$ are consistent with a more ordered transition state for this reaction. These reactions are illustrated in Scheme 4 9 1.

SCHEME 4 9.1

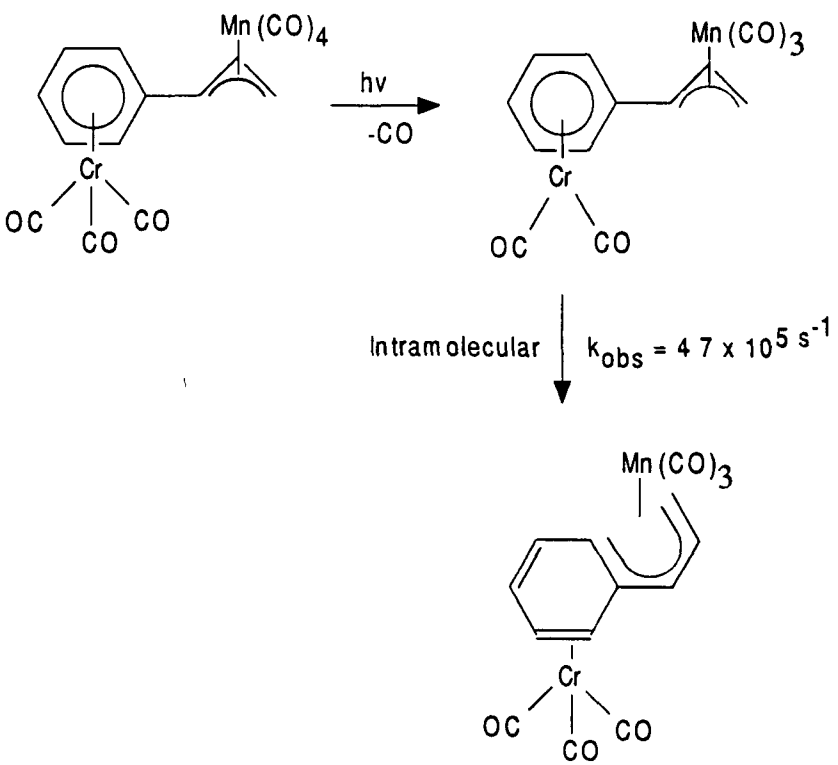

The TRIR spectrum recorded in n-heptane solution at 10μs after the laser flash exhibits depletion of all parent absorptions in the region of analysis. The proposed

reaction scheme is consistent with these results The initial labilisation of a CO ligand at the Cr centre, with a rearrangement and the loss of a CO at the Mn centre would result in the depletion of the ν_{CO} at both sites The formation of an intramolecular product therefore ultimately requires the abstraction of CO from both metal centres. The TRIR results indicated that the photochemical reactions occuring were complex, and further experiments are necessary to assign the exact nature of the ν_{CO} bands

The third observed species is difficult to assign The fact that it is not observed under CO atmosphere suggests that it is a secondary photoproduct formed in a competitive reaction in which its precursor may react with CO or form this product. This behaviour reflects that observed on flash photolysis of $Mn(CO)_4$-η^3-C_3H_4-C_6H_5 and may indicate that photolysis products of both metal centres are produced on photoexcitation The formation of impurity complexes cannot be eliminated as a possibility in these reactions A transient species observed in solutions in which the liquid-pumping procedure was deemed to be inadequate, is assigned to such an impurity product It was observed that the decay of the first species was more nearly baseline resolved as the degree of liquid-pumping was increased The presence of a solvent impurity, e g water, may not influence the intramolecular reaction, as the rate of this reaction has been shown to be independent of any ligand concentration present It is unlikely that a dinuclear species, of the form observed in the photoreactions of (η^6-arene)$Cr(CO)_3$ complexes, is formed in these reactions; as the extreme bulk of the dinuclear complex should sterically inhibit such a reaction It is also unlikely that scission of the dinuclear complex into separate portions occurs, as

this is only observed in dinuclear complexes containing a M-M bond to produce radical species.

4.10 Conclusions

Photolysis of $Mn(CO)_4$-η^6-C_3H_4-η^6-C_6H_5-$Cr(CO)_3$ in cyclohexane solution produced evidence for the formation of at least three transient species The first transient species was attributed to a CO-loss product of the chromium centre The formation of the second observed species occured by means of an intramolecular reaction of species 1, the rate of which was independent of both CO and parent ligand concentration The nature of this reaction involved rotation about the C-C bond of the allyl group with abstraction of CO from the Mn centre and concomitant η^3 to η^5 rearrangement to stabilise the coordinatively unsaturated fragment produced. A third transient species of unknown origin was also observed in these studies.

4.11 References

1. D W. Stephan, *Coord Chem Rev* , 1989, **95**, 41.
2. (a) J. Besançon, J Tıroflet, A Card, and Y Desausoy, *J Organomet Chem* , 1973, **59**, 267

   (b) B Caro and G Joauen, *J Organomet Chem.*, 1982, **228**, 87.

   (c) F Rose-Munch, O Bellot, M Laurent, A. Semra, F Robert, and Y Jeannın, *J Organomet Chem* , 1991, **402**, 1
3. (a) M F Semmelhack, J. Bısaha, and M. Czarney, *J Am Chem Soc* , 1979, **101**, 768

   (b) M. Ghavshou and D A Widdowson, *J Chem Soc , Perkın Trans* , 1983, **1**, 3065
4. (a) T L. Meyer and J V Caspar, *Chem Rev* , 1985, **85**, 187

   (b) J V Caspar and T J Meyer, *J Am Chem Soc* , 1980, **102**, 7795

   (c) A.F Hepp, J P Blaha, C. Lewıs, and M S Wrighton, *Organometallıcs,* 1984, **3**, 174

   (d) B O. Moore, M B Sımpson, M Polıakoff, and J J Turner, *J Chem Soc , Chem Commum* , 1984, 972

   (e) A J. Dıxon, M.A. Healy, M Polıakoff, and J J Turner, *J Chem Soc , Chem Commum* , 1986, 944
5. (a) A Fox and A Poe, *J Am Chem Soc* , 1980, **102**, 2479

   (b) A F Hepp and M S Wrighton, *J Am Chem Soc* , 1983, **105**, 5934

   (c) I A Dunkın, P Harter, and C.J Shıelds, *J Am Chem Soc* , 1984, **106**, 7248

(d) S P Church, H Hermann, F -G Grevels, and K. Schaffner, *J Chem Soc , Chem Commum* , 1984, 785.

(e) T A Seder, S P Church, and E. Weitz, *J Am Chem Soc* , 1986, **108**, 7518

6. (a) N J. Gogan and C.K Chu, *J Organomet Chem* , 1975, **93**, 363.

(b) N J Gogan and C K Chu, *J Organomet Chem* , 1977, **132**, 103.

6. (c) N J. Gogan and S I De Sılva, *Organometallıcs,* 1990, **9**, 1970

7. H B. Gray and N A Beach, *J Am Chem Soc* , 1963, **85**, 2922.

8 (a) M S Wrighton, D L Morse, and L Pdungsap, *J Am Chem Soc* , 1975, **93**, 2073

(b) R R. Zarnegar, C.R Bock, and D G Whıtten, *J Am Chem Soc* , 1973, **95**, 4367

(c) P Zarnegar and D G Whıtten, *J Am Chem Soc* , 1971, **93**, 3776.

(d) M Wrighton, G.S. Hammond, and H B Gray, *J. Am Chem Soc* , 1970, **92**, 6068

(e) M Wrighton, G S. Hammond, and H B Gray, *J Am Chem Soc* , 1971, **93**, 3285.

9 (a) Y Yamada, D Mılıjkovıc, P Wehrlı, B Goldıng, P Loliger, R. Keese, K. Muller, and A. Eschenmoser, *Angew Chem , Int Ed* , 1969, **8**, 343.

(b) A Eschenmoser, *Quart Rev* , 24, 366, 1970

(c) E Gotschı and A. Eschenmoser, *Angew Chem , Int Ed* , 1973, **12**, 912

10 M. Wrighton, G S Hammond, and H B Gray, *J Organomet Chem* , 1974, **70**, 283

11. M S. Wrighton and M A Schroeder, *J Am Chem Soc* , 1974, **96**, 6235

12. (a) Wrighton and M A. Schroeder, *J Am Chem Soc* , 1973, **95**, 5674.

(b) J Nasielski, P. Kirsch, and L. Wilputte-Steinert, *J Organomet Chem* , 1971, **27**, C13

(c) G. Platbrood and L. Wilputte-Steinert, *J Organomet Chem* , 1974, **70**, 393

(d) G. Platbrood and L Wilputte-Steinert, *J Organomet Chem.*, 1974, **70**, 407

13. (a) G Davidson and D C Andrews, *J Chem Soc , Dalton Trans* , 1972, 126.

(b) A. Ouderman and T S. Sorensen, *J Organomet Chem* , 1978, **156**, 259

14 A. Wright, personal communication.

15 T J Oyer and M S Wrighton, *Inorg Chem* , 1988, **27**, 3689

Chapter 5

Laser Induced Photochemistry of $(\eta^5\text{-}C_5H_5)V(CO)_4$

5.1 Introduction

The monocyclopentadienyl carbonyl complexes of transition metals have received much attention as versatile compounds in coordination chemistry, oxidative-addition reactions and metal promoted organic synthesis[1] Attractive results have been obtained also in the field of dinitrogen fixation by using the manganese derivative $(\eta^5\text{-}C_5H_5)Mn(CO)_3$[2] The lability of the vanadium analogue $(\eta^5\text{-}C_5H_5)V(CO)_4$ towards photosubstitution is well documented[3-10] A recent study in frozen gas matrices at *ca* 12K has provided infrared spectroscopic evidence that irradiation of $(\eta^5\text{-}C_5H_5)V(CO)_4$ results in two types of reversible processes[11]. One process, in Ar and CH_4 matrices, was photoejection of CO to yield the species $(\eta^5\text{-}C_5H_5)V(CO)_n$ (n=1-3) The second process, in Ar, CH_4, N_2 and CO matrices, was proposed to involve a change in the ring hapticity with the formation of $(\eta^3\text{-}Cp)V(CO)_4$ and probably $(\eta^3\text{-}Cp)V(CO)_5$ in CO matrices The relative proportions of each photoproduct was found to exhibit a wavelength dependancy Such a possibility that a C_5H_5 ring could change its hapticity, e g reversible η^5 to η^3 (ring slippage or partial dechelation), has been suggested for $(\eta^5\text{-}C_5H_5)Co(CO)_2$ in a CO matrix[12] Although the photochemistry of $(\eta^5\text{-}C_5H_5)V(CO)_4$ has been investigated in the presence of coordinating species, for example H_2[13], there are no published accounts, to date, of investigations into the photochemistry of $(\eta^5\text{-}C_5H_5)V(CO)_4$ in room temperature solution in the absence of excess ligand or coordinating solvents Previous known studies[14,15] have been hampered by difficulties of experimental irreproducibility This chapter presents the results obtained in a series of experiments designed to study the photochemistry of $(\eta^5\text{-}C_5H_5)V(CO)_4$ in cyclohexane solution

at room temperature. Different laser excitation wavelengths were utilised to investigate the reported wavelength dependancy

5.2 Electronic Spectrum of $(\eta^5\text{-}C_5H_5)V(CO)_4$

The UV/vis absorption spectrum of $(\eta^5\text{-}C_5H_5)V(CO)_4$ in cyclohexane solution is given in Figure 5 2 1 The spectrum of $(\eta^5\text{-}C_5H_5)V(CO)_4$ is dominated by absorption bands in the UV region centred at 280nm and 366nm with a weak absorption in the blue region of the spectrum at *ca* 410nm. The long wavelength band could possibly be a d-->d transition while those bands at higher energy are likely to be V --> π*CO CT transitions[11,16]

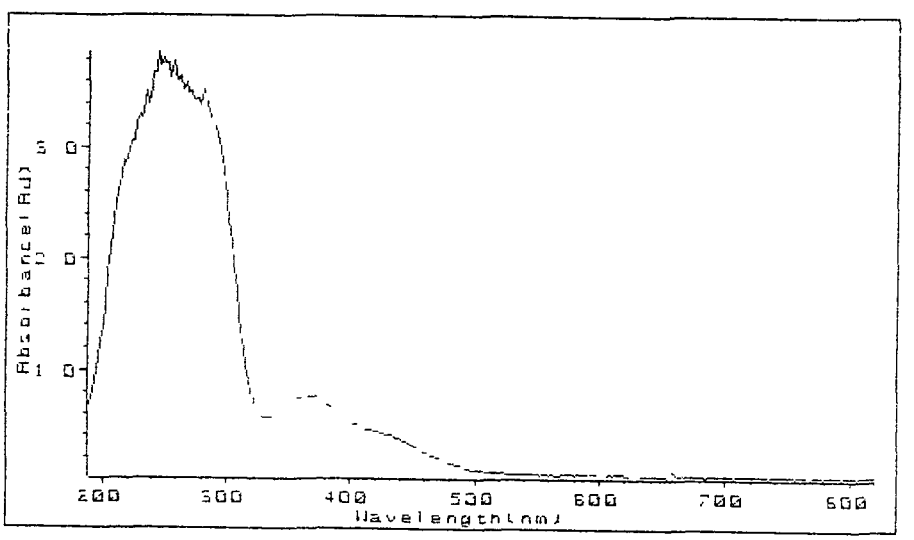

Figure 5.2.1 UV/vis absorption spectrum of a 2 0 x 10^{-4} mol dm^{-3} solution of $(\eta^5\text{-}C_5H_5)V(CO)_4$ in cyclohexane

5.3 Experimental Modifications

Additional sample preparation stages were introduced to limit the number of possible experimental parameters leading to irreproducibility Cyclohexane solvent was distilled from $LiAlH_2$ and stored in an air-tight bottle over 4A molecular sieve. $(\eta^5\text{-}C_5H_5)V(CO)_4$ was sublimed using a microsublimation apparatus with a liquid nitrogen 'cold-finger' prior to use The cell was surrounded by aluminium foil at all times to shield the sample from all stray light which could cause photodecomposition prior to laser flash photolysis A sample of dry cyclohexane was admitted to the reaction cell and flushed with CO for at least 10 minutes, providing a CO saturated solution over which there was a positive pressure of CO This was carried out in order to minimise photodegradation by decarbonylation of the starting material. A microgram quantity of sample was added, on dissolution the cell was attached to the vacuum line and degassed by four cycles of a 'freeze-thaw' degassing procedure followed by a liquid pumping stage at room temperature All experiments were performed under CO atmosphere to minimise sample decomposition

5.4 Preliminary Experimental Observations

The laser flash photolysis of $(\eta^5\text{-}C_5H_5)V(CO)_4$ in cyclohexane provided evidence for the formation of at least three transient species In some experiments only one primary photoproduct was observed, whereas in other experiments the formation of both a primary and secondary photoproduct was noted. The rates of the primary photoproduct produced in both cases differed markedly such that it was concluded that both primary photoproducts could not be attributed to the same

species The experimental results are therefore divided into two distinct series of results and are presented and summarised accordingly

5.5 Observation of a Possible $(\eta^3\text{-}C_5H_5)V(CO)_4$ Species

5.5.1 355nm Laser Flash Photolysis of $(\eta^5\text{-}C_5H_5)V(CO)_4$ with UV/vis Monitoring

On 355nm photolysis of a 7 15 x 10^{-4} mol dm^{-3} solution of $(\eta^5\text{-}C_5H_5)V(CO)_4$ in cyclohexane (ε_{354nm} = 2270 dm^3 mol^{-1} cm^{-1}) a single photoproduct was observed to form within the laser flash The lifetime of this species decreased on increasing the concentration of CO present in solution while the yield of this species was relatively unaltered, Figure 5 5 1 1 This indicates that the photoproduct is a primary photoproduct capable of reacting with CO The second order rate constant for the reaction of this species with CO was calculated to be 5 6 x 10^3 dm^3 mol^{-1} s^{-1} A typical primary photoproduct transient signal monitored at 270nm is shown in Figure 5 5 1 2

The rate of reaction of this primary photoproduct with CO is very much different to that expected for a coordinatively unsaturated carbonyl loss product, the rate of the recombination reaction of the analagous complex $(\eta^6\text{-benzene})Cr(CO)_3$ with CO has been measured as 6 7 x 10^6 dm^3 mol^{-1} s^{-1} Rest *et al* assigned the species formed on long wavelength photolysis of $(\eta^5\text{-}C_5H_5)V(CO)_4$ in all matrices as the $(\eta^3\text{-}C_5H_5)V(CO)_4$ species [11] This species coordinated CO present in the matrix to fill the vacant coordination site on the complex, reaction 5 5 1.1

$$(\eta^5Cp)V(CO)_4 \xrightarrow{h\nu} (\eta^3Cp)V(CO)_4 \xrightarrow{+CO} (\eta^3Cp)V(CO)_5 \qquad (5\ 5\ 1\ 1)$$

Therefore, the primary photoproduct observed in this case may be attributed most plausibly to such a hapticity change product

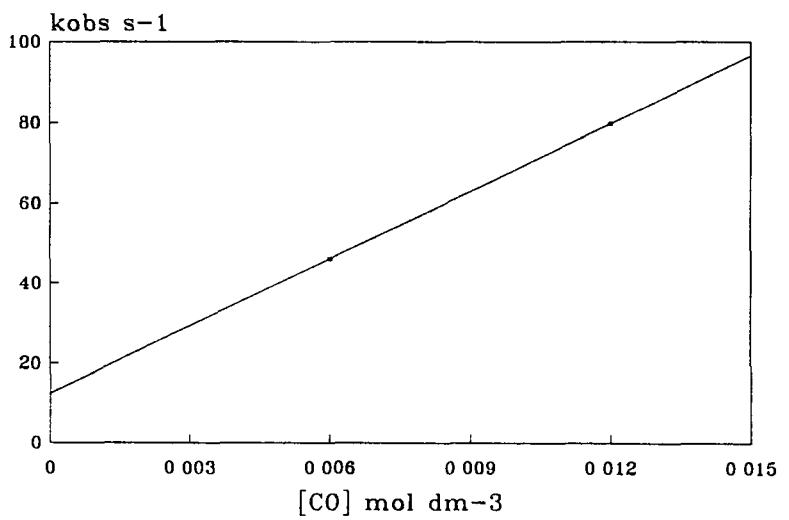

[CO] mol dm^{-3}	k_{obs} s^{-1}	Absorbance[a]
0 006	46 1	0 165
0 012	79 8	0 184

$k_{[co]} = 5\ 6 \times 10^3\ dm^3\ mol^{-1}\ s^{-1}$

Intercept = 15 94 s^{-1}

Figure 5.5.1.1 The observed rate constants (cm^{-1}) for the decay of the primary photoproduct at 298K at varying CO concentration (mol dm^{-3}) [a]0μs after the laser flash.

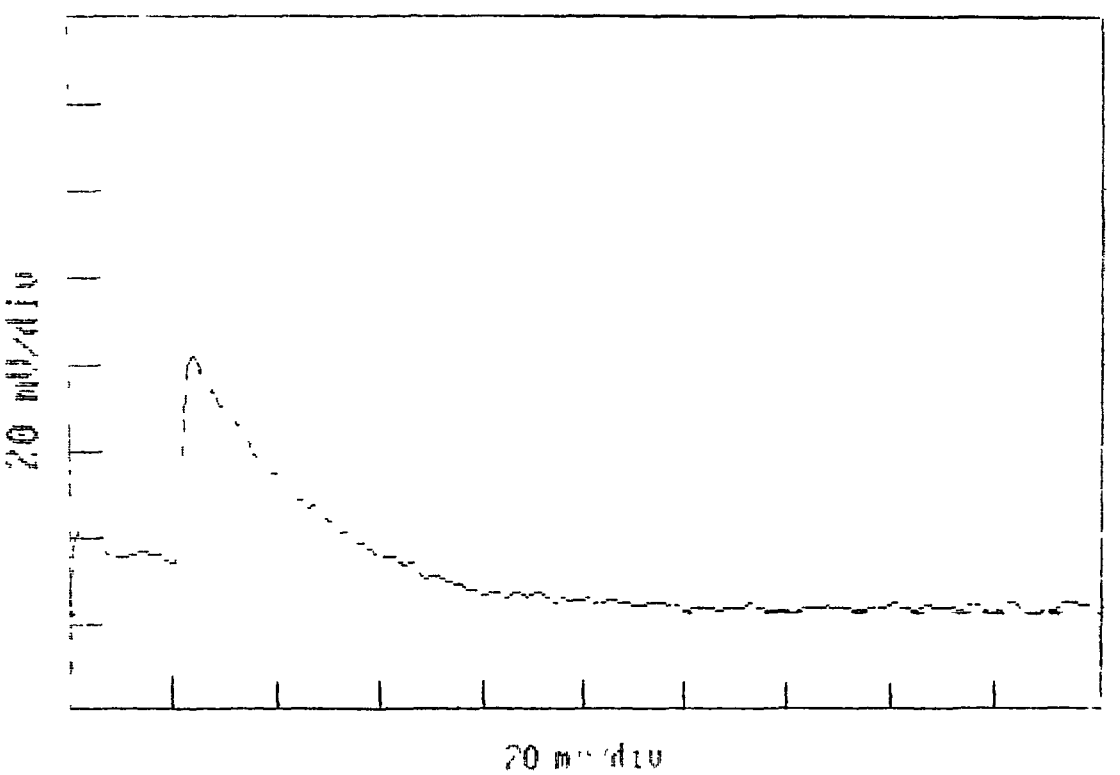

Figure 5.5.1.2 Transient for the decay of the primary photoproduct observed at 270nm

5.5.1.1 UV/vis Difference Spectrum of Primary Photoproduct

The UV/vis difference spectrum of the primary photoproduct recorded under 0 5atm CO from 270 to 620nm at 320μs after the laser flash has maxima at 290nm and 415nm, Figure 5 5 1 1 1 The valley in the UV/vis absorption spectrum of (η^5-C_5H_5)V(CO)$_4$ (Figure 5 2 1) corresponds to the maximum at 290nm for the primary photoproduct, also the band maximum at 366nm in the UV/vis absorption spectrum of (η^5-C_5H_5)V(CO)$_4$ corresponds to a valley in the difference absorption profile of the photoproduct The spectrum recorded following the decay of this species at 1200μs after the laser pulse is also given It exhibits a single peak at 300nm and a depletion in the region 340nm to 530nm This depletion indicates that the primary photoproduct is reacting with parent thereby further depleting the parent absorption in this region.

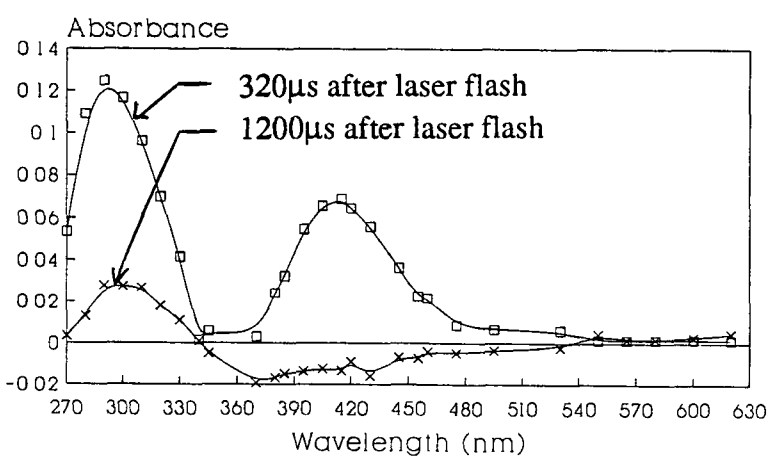

Figure 5.5.1.1.1 UV/vis difference spectra recorded of the primary photoproduct recorded at 320μs and 1200μs after the laser pulse under 0 5atm CO

5.5.1.2 Effect of Laser Power on Concentration of Primary Photoproduct

In order to confirm that the formation of the first observed species was as a result of a single photon event, an experiment was performed where the intensity of the laser pulse was varied The absorbance of the photoproduct should vary linearly with the power of the laser This was found to be the case, as is shown in Figure 5.5.1.2.1, where the relative power of the laser is plotted against the absorbance of the primary photoproduct present at 400μs after the laser flash

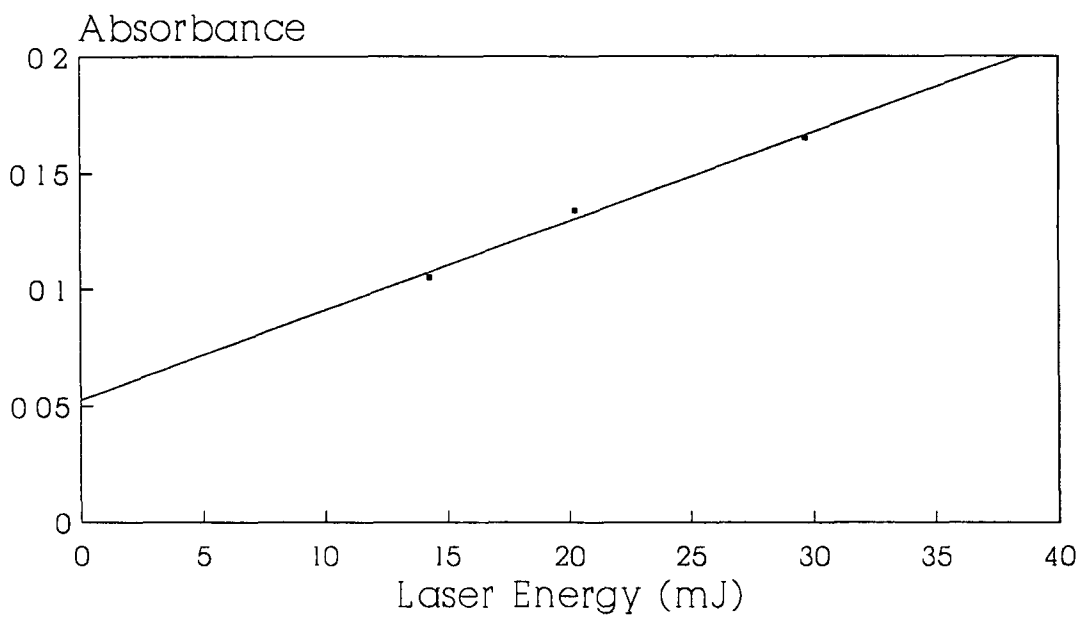

Figure 5.5.1.2.1 Plot showing the variation in absorbance of the primary photoproduct species with relative laser power.

5.5.1.3 Experimental Irreproducibility

The observed rate of decay of the primary photoproduct at various concentrations of parent $(\eta^5\text{-}C_5H_5)V(CO)_4$ is given in Table 5 5 1.3 1. There is no apparent trend in these results However the rate constant varies greatly from sample to sample The 'scatter' of these points about a constant value is well outside acceptable limits (±10%) These results highlight the irreproducibility encountered with this system despite all efforts taken to reduce experimental variations and sample decomposition These results also have important implications for the rate data presented earlier Care must then be taken in the interpretation of experimental data as any rate constant data acquired cannot be taken as absolute

Table 5.5.1.3.1 Summary of the observed rate constants for the decay of the primary photoproduct, [a][CO] = 1 2 x 10^{-2} mol dm^{-3} (average k_{obs} = 189 8 ± 215.6 s^{-1}), [b][CO] = 0 6 x 10^{-2} mol dm^{-3} (average k_{obs} = 96 4 ± 112 1 s^{-1})

$[(\eta^5\text{-}C_5H_5)V(CO)_4]$ mol dm^{-3}	k_{obs} s^{-1} *a*	k_{obs} s^{-1} *b*
2 07 x 10^{-4}	501 0	258 4
3 13 x 10^{-4}	17 5	4 1
4 32 x 10^{-4}	160 7	77 1
7 15 x 10^{-4}	79 8	46 1

5.5.2 266nm Laser Flash Photolysis with UV/vis Monitoring

Preliminary studies performed utilising 266nm irradiation revealed a possible wavelength dependancy in the photochemistry of $(\eta^5\text{-}C_5H_5)V(CO)_4$ On 355nm laser flash photolysis of a 2 1 x 10^{-4} mol dm^{-3} sample of $(\eta^5\text{-}C_5H_5)V(CO)_4$ in cyclohexane a primary photoproduct was observed at the monitoring wavelength of 270nm. The second order rate constant of this species with CO was calculated to be 4.04 x 10^4 dm^3 mol^{-1} s^{-1} This solution was then studied using 266nm irradiation (ε_{266nm}= 11520 x 10^4 dm^3 mol^{-1} cm^{-1}) and the second order rate constant of the primary photoproduct with CO was calculated to be 2 5 x 10^4 dm^3 mol^{-1} s^{-1} A slight difference in the second order rate constants for the reaction of the primary photoproduct species with CO was therefore observed on altering the irradiation wavelength, Table 5 5 2 1

In a subsequent study a primary photoproduct with a second order rate constant for reaction with CO of 7 42 x 10^3 dm^3 mol^{-1} s^{-1} was observed on 266nm laser flash photolysis of a 1 5 x 10^{-4} mol dm^{-3} solution of $(\eta^5\text{-}C_5H_5)V(CO)_4$ in cyclohexane The UV/vis difference spectrum of this species was recorded from 270nm to 540nm under 1 0 atmosphere of CO, Figure 5 5.2.1 An absorption maximum is observed at 320nm with a shoulder on the low energy side of this absorption centred at *ca* 390nm The resolution of the shoulder absorption band is increased in spectra recorded at longer time intervals after the laser flash, e.g. 51200μs This spectrum is markedly different from that recorded for the primary photoproduct utilising 355nm laser irradiation

Table 5.5.2.1 The observed rate constant for the reaction of the primary photoproduct complex at 298K at varying CO concentration (mol dm^{-3}) and laser irradiation wavelength

[CO] mol dm^{-3}	k_{obs} s^{-1}	
	355nm irradiation	266nm irradiation
0 006	258 4	143 8
0 012	501 0	293 7

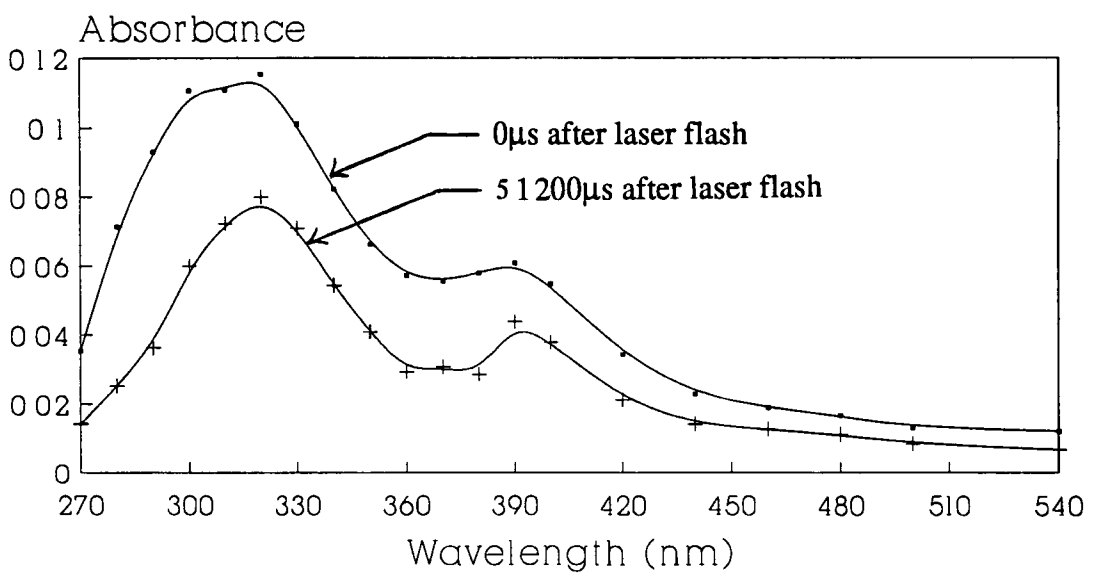

Figure 5.5.2.1 UV/vis difference spectra of the primary photoproduct recorded at 0μs and 51200μs after the laser pulse under 1 0 atm CO utilising 266nm laser irradiation.

5.6 Observation of a Possible $(\eta^5\text{-}C_5H_5)V(CO)_3(S)$ Species

On 355nm photolysis of a 5 34 x 10^{-4} mol dm^{-3} solution of $(\eta^5\text{-}C_5H_5)V(CO)_4$ in cyclohexane at least two photoproducts were observed. An initial grow-in was observed over very short timebases, the rate of which was accelerated on increasing the concentration of CO present in solution This indicates that this species was a primary photoproduct capable of reacting with CO The second order rate constant for this reaction was calculated to be 9 2 x 10^7 dm^3 mol^{-1} s^{-1}, Figure 5.6.1. A second species was formed from this initial photoproduct, the yield of which decreased on increasing the concentration of CO present in solution while the rate of decay of this species was relatively unaltered This indicated that it was a secondary photoproduct in the system, Figure 5 6 2 Typical transients for the primary and secondary photoproduct transient species are shown in Figures 5 6.3 and 5.6.4 respectively

The rate constant for the reaction of this transient species with CO is very much different from that attributed to the $(\eta^3\text{-}C_5H_5)V(CO)_4$ species The second order rate constant with CO, of 9 2 x 10^7 dm^3 mol^{-1} s^{-1}, is significantly larger in this case and resembles more closely the reaction of a carbonyl loss product with CO; for example the rate of reaction of $(\eta^6\text{-}C_6Et_6)Cr(CO)_2(S)$ with CO is reported as 4 4 x 10^7 dm^3 mol^{-1} s^{-1}[17] Photolysis of $(\eta^5\text{-}C_5H_5)V(CO)_4$ in frozen gas matrices at *ca* 12K produced IR spectroscopic evidence for the loss of CO as a primary photochemical pathway[11] Photolysis of $(\eta^5\text{-}C_5H_5)V(CO)_4$ and H_2 in solution at both cryogenic and room temperatures gave rise to IR bands attributed to a single complex $(\eta^5\text{-}C_5H_5)V(CO_3)(H_2)$[13] This species was produced by loss of a CO

ligand to produce the coordinatively unsaturated $16e^-$ complex $(\eta^5\text{-}C_5H_5)V(CO)_3$ with subsequent coordination of H_2 The $16e^-$ coordinatively unsaturated species of $M(CO)_5$ (M=Cr, Mo, or W) complexes are recognised as coordinating to solvent molecules in solution photolysis[18] The rate of this coordination has been measured, using picosecond spectroscopy, to occur within 1ps of the flash in alkane solvent[19]. This primary photoproduct is therefore most plausibly assigned to the complex $(\eta^5\text{-}C_5H_5)V(CO)_3$(cyclohexane) formed by loss of a single CO ligand. This species is probably formed within the duration of the flash (10ns) as in the case of the Group VIB pentacarbonyl solvated species The reaction is summarised in reaction 5 6 1

$$CpV(CO)_4 \xrightarrow{h\nu} CpV(CO)_3 + CO \xrightarrow{S} CpV(CO)_3(S) \qquad (5\ 6\ 1)$$

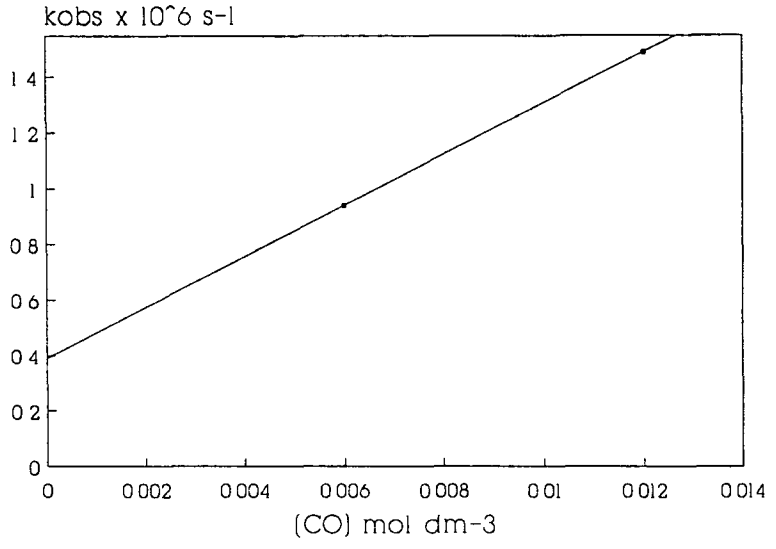

[CO] mol dm^{-3}	k_{obs} s^{-1}
0 006	9 40 x 10^5
0 012	1 49 x 10^6

$k_{[co]}$ = 9 2 x 10^7 dm^3 mol^{-1} s^{-1}

Intercept = 3 9 x 10^5 s^{-1}

Figure 5.6.1 The observed rate constants (s^{-1}) for the reaction of the primary photoproduct at 298K at varying CO concentration (mol dm^{-3})

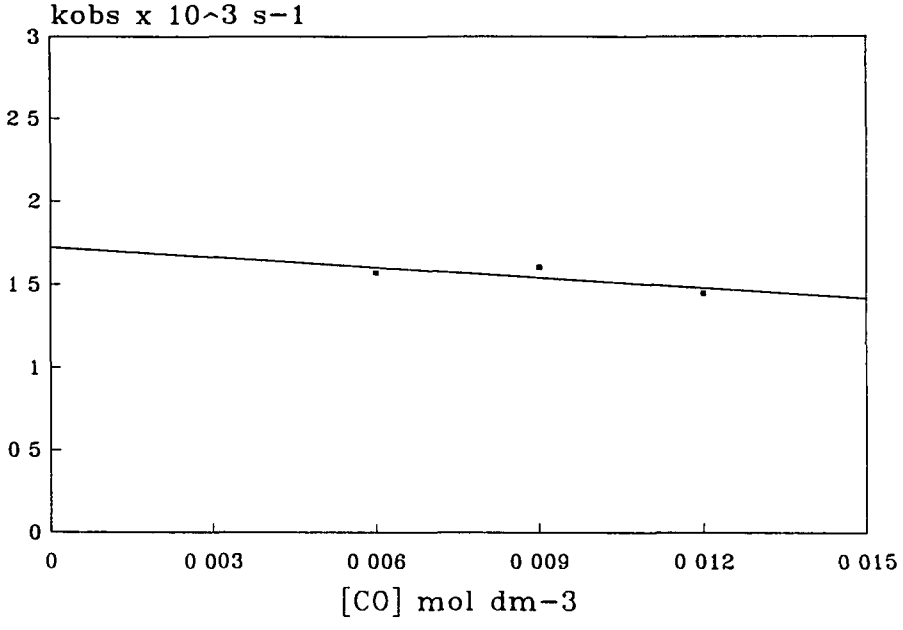

[CO] mol dm^{-3}	k_{obs} s^{-1}	Absorbance[a]
0 006	1568	12 05 x 10^{-2}
0 009	1602	8 93 x 10^{-2}
0 012	1444	7 99 x 10^{-2}

Figure 5.6.2 The observed rate constants (s^{-1}) for the decay of the secondary photoproduct at varying concentrations of CO (mol dm^{-3}) at 298K. [a] Yield 0μs after the laser flash

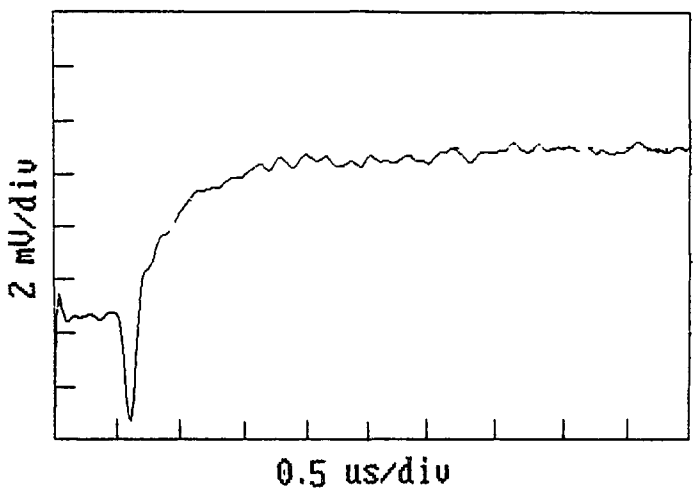

Figure 5.6.3 Transient signal for the reaction of the primary photoproduct observed at 420nm to generate a secondary photoproduct, $[(\eta^5\text{-}C_5H_5)V(CO)_4] = 5.34 \times 10^{-4}$ mol dm^{-3}

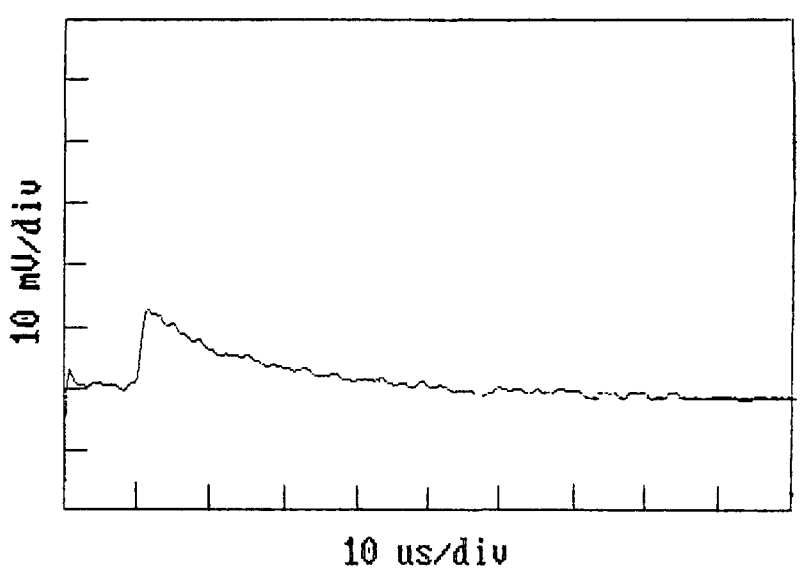

Figure 5.6.4 Transient signal for the decay of the secondary photoproduct monitored at 440nm, $[(\eta^5\text{-}C_5H_5)V(CO)_4] = 5\ 34 \times 10^{-4}$ mol dm^{-3}

5.6.1 UV/vis Difference Spectra of Primary and Secondary Photoproducts

The UV/vis difference spectra recorded from 410nm to 650nm at 0μs and 10μs after the laser pulse under 0 5atm CO are given in Figure 5 6 1.1 The spectrum recorded at 0μs after the laser flash exhibits an absorption maximum at 420nm in the visible region The spectrum recorded on formation of the secondary photoproduct, at 10μs after the laser flash, displays an absorption maximum centred at 440nm The absorption at longer wavelengths is very weak Sample decomposition occured during the course of this experiment

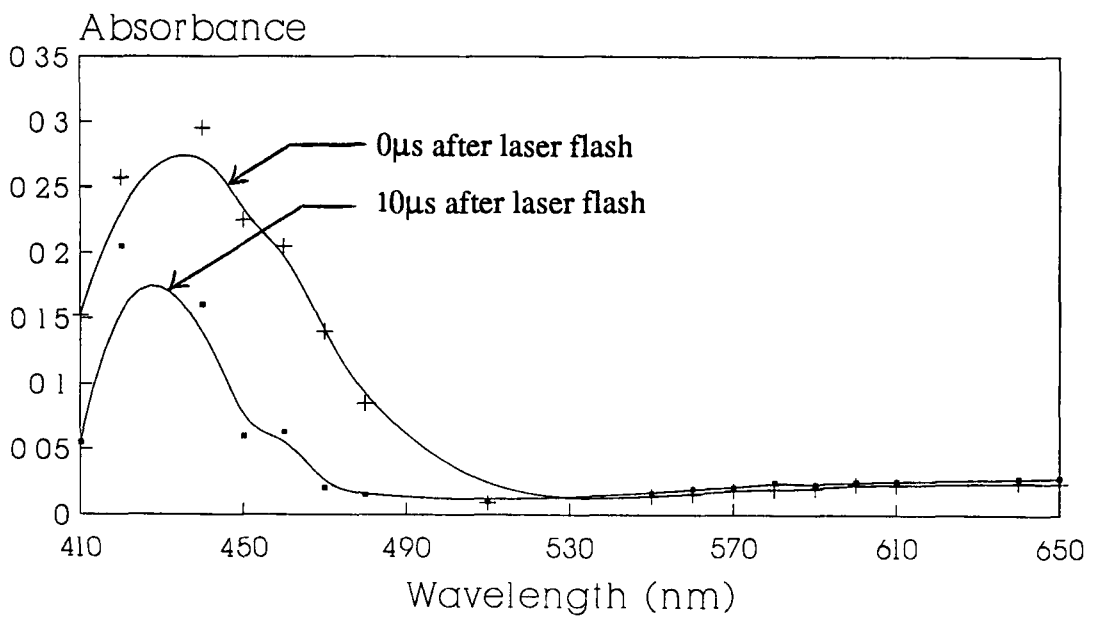

Figure 5.6.1.1 UV/vis difference spectra of the primary and secondary photoproducts recorded at 0μs and 10μs after the laser pulse under 0 5atm CO

5.6.2 Dependance of Secondary Photoproduct Decay Rate on [(η^5-C_5H_5)V(CO)$_4$]

The rate of decay of the secondary photoproduct at 440nm was observed to exhibit an approximate dependance on parent (η^5-C_5H_5)V(CO)$_4$ concentration; Figure 5 6 2 1, Table 5 6 2 1 The rate of reaction of this species was found to increase linearly with increasing (η^5-C_5H_5)V(CO)$_4$ concentration The second order rate constant for this reaction was calculated to be 3 54 x 10^6 dm^3 mol^{-1} s^{-1} This dependence indicates that the decay of this species involves a reaction with the parent molecule There is a large degree of scatter in these points as indicated by the correlation coefficient of only 0 903

Table 5.6.2.1 The rate constants (s^{-1}) for the decay of the secondary photoproduct at differing initial concentrations of (η^5-C_5H_5)V(CO)$_4$ (mol dm^{-3}) in cyclohexane

[(η^5-C_5H_5)V(CO)$_4$] mol dm^{-3}	k_{obs} s^{-1}
3 66 x 10^{-4}	818
5 34 x 10^{-4}	1568
5 60 x 10^{-4}	1745
6 62 x 10^{-4}	1948
6 88 x 10^{-4}	2467
7 72 x 10^{-4}	2820
8 92 x 10^{-4}	2415

^{k}[CpV(CO)$_4$] = 3 5 x 10^6 ± 0 8 x 10^6 dm^3 mol^{-1} s^{-1}

Intercept = -294 3 ± 316 1 s^{-1} Corr Coeff = 0 903

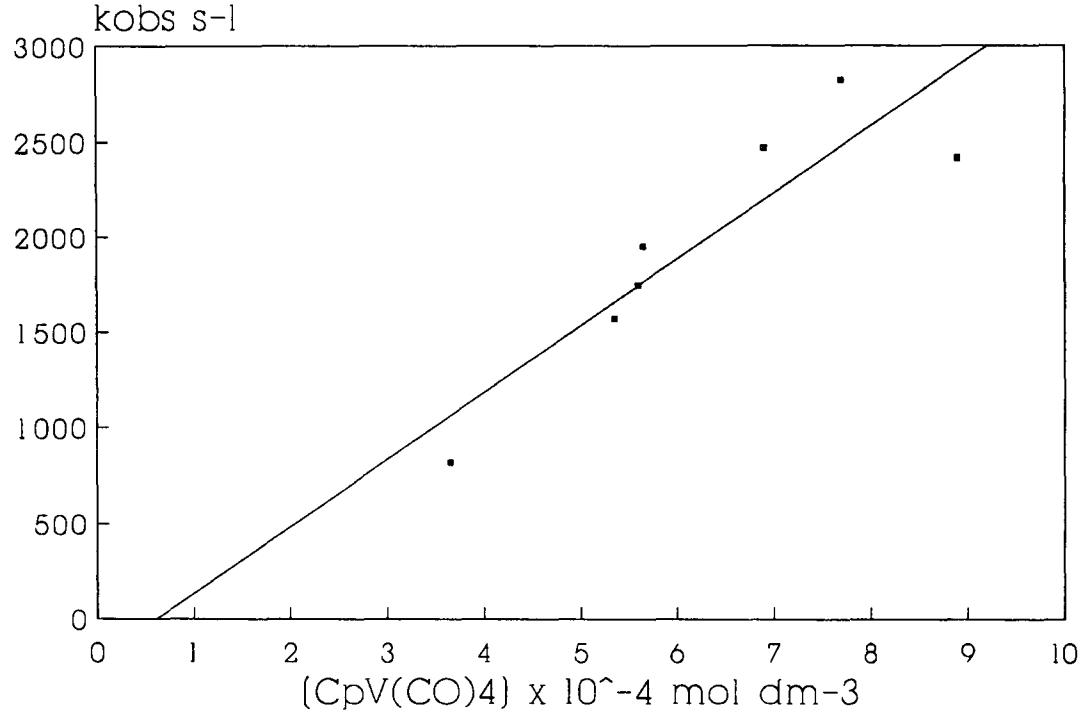

Figure 5.6.2.1 Plot of k_{obs} (s^{-1}) for the decay of the secondary photoproduct against the initial concentration of $(\eta^5\text{-}C_5H_5)V(CO)_4$ (mol dm^{-3}) in cyclohexane

5.7 Decomposition Studies

Frequently, $(\eta^5\text{-}C_5H_5)V(CO)_4$ samples prepared for laser flash photolysis decomposed prior to the 'freeze-thaw' degassing stage The UV/vis spectrum of samples which had not decomposed was monitored at regular intervals throughout the laser flash photolysis experiment It was observed that the system was not always fully reversible, even under CO atmosphere, i e the initial and final UV/vis spectra, recorded on commencement and completion of the experiment respectively, were not always identical Typical UV/vis spectral changes recorded thoughout the laser flash photolysis of a 8 47 x 10^{-4} mol dm^{-3} solution of $(\eta^5\text{-}C_5H_5)V(CO)_4$ in cyclohexane under 0 5atm CO are given in Figure 5 7 1 A gradual decrease in the absorbance of $(\eta^5\text{-}C_5H_5)V(CO)_4$ is observed with concomitant growth of a new species. The spectrum of the species formed is dominated by absorption bands centred at 280nm in the UV region and 448nm in the visible region, with a shoulder on the high energy absorption centred at *ca* 350nm, Figure 5 7 2 The long wavelength band could possibly be a d-->d transition Those bands at higher energy are likely to be V --> π^*CO CT transitions[11,15] In some decomposition studies isosbestic points at 420nm and 358nm were maintained throughout this transformation indicating that the process was uncomplicated by side or subsequent reactions A clear visual indication of this decomposition during the experiment was a change in colour of the sample solution from orange to green as the experiment progressed, indicating the production and build-up of a long-lived product in solution The UV/vis spectrum of this product appears to correspond to that of the secondary photoproduct observed earlier, the rate of production of which displayed a possible dependance on parent concentration

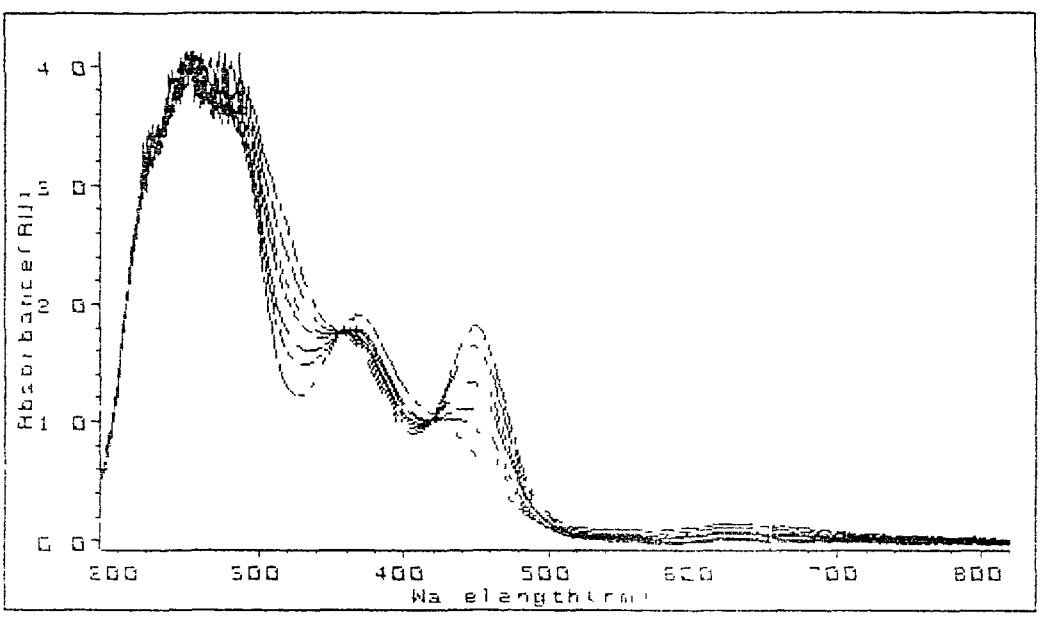

Figure 5.7.1 Typical UV/vis absorption spectral changes observed throughout the laser flash photolysis of a 7 68 x 10^{-4} mol dm^{-3} solution of $(\eta^5\text{-}C_5H_5)V(CO)_4$ in cyclohexane

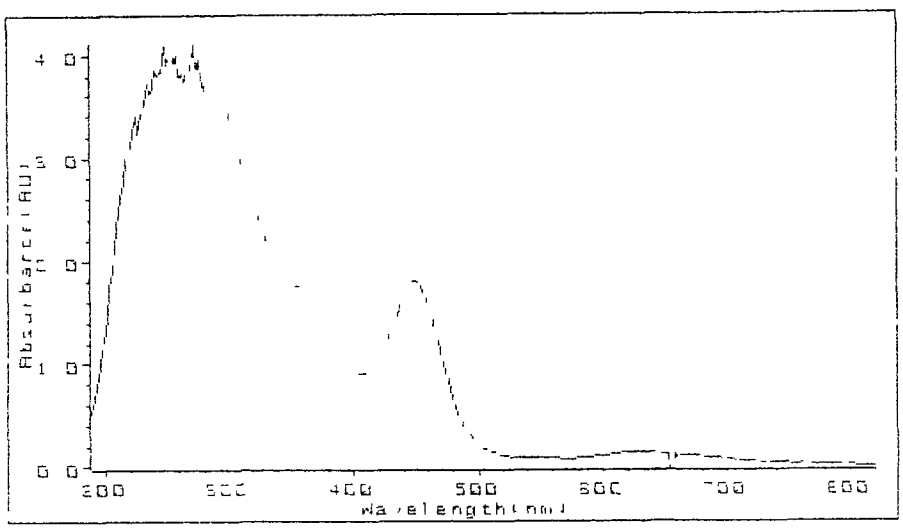

Figure 5.7.2 UV/vis absorption spectrum of the decomposition product in cyclohexane

5.8 Discussion

The results obtained from this series of experiments are plagued by irreproducibility, hence difficult to interpret Further studies were not undertaken because of the irreproducibility encountered There are a number of reasons which may be proposed to account for the experimental inconsistencies

(1) The interference of dissolved solvent impurities on the lifetimes of the transient species The effect of liquid pumping on the level of solvent impurities had not been investigated at the time these experiments were performed. The liquid-pumping stage may have been inadequate with a resultant inter-sample variation Experiments reported on the photochemistry of $(\eta^5\text{-}C_5H_5)V(CO)_4$ were performed in the presence of excess ligand[3-10,13] or in the stabilising influence of a matrix[11] Both these situations are less sensitive to trace amounts of impurities in the system

(2) The production of multiple primary photoproducts

Both a 'ring-slippage' and carbonyl loss product were reported in a previous study into the photochemistry of $(\eta^5\text{-}C_5H_5)V(CO)_4$[11]. On irradiation with light of wavelength 320nm to 390nm Rest *et al* noted the production of both the decarbonylation and ring-slipped species The 355nm Nd^{3+} YAG laser excitation used in the majority of these experiments lies in this wavelength range, consequently the formation of both species may be expected

(3) The formation of photosensitive dinuclear complexes in solution

Experimental studies performed by Lewis and Caulton have shown that $(\eta^5\text{-}C_5H_5)_2V_2(CO)_5$ is formed from the photochemistry of $(\eta^5\text{-}C_5H_5)V(CO)_4$ in THF[20]. Unfortunately, no UV/vis spectral data for this species is presented. $(\eta^5\text{-}C_5H_5)_2V_2(CO)_5$ is an isolable complex[21] and is itself photosensitive[20] Dissociation of CO is known to be the first step in the photoreactions of $(\eta^5\text{-}C_5H_5)_2V_2(CO)_5$ eventually leading to the reformation of $(\eta^5\text{-}C_5H_5)V(CO)_4$, reaction 5.8 1 [20]

$$Cp_2V_2(CO)_5 \xrightarrow{h\nu} Cp(OC)_3V{=}V(CO)_2Cp \longrightarrow 2CpV(CO)_3 \xrightarrow{+\,CO} 2CpV(CO)_4$$

(5 8 1)

(where $Cp = \eta^5\text{-}C_5H_5$)

$(\eta^5\text{-}C_5H_5)_2V_2(CO)_5$ also undergoes spontaneous thermal decomposition at 298K in alkane and donor solvents to regenerate $(\eta^5\text{-}C_5H_5)V(CO)_4$ ^{13}CO experiments have shown the pentacarbonyl to be in equilibrium with $(\eta^5\text{-}C_5H_5)_2V_2(CO)_4$ and CO in solution, reaction 5 8 2

$Cp_2V_2(CO)_5 \rightleftharpoons CO + Cp_2V_2(CO)_4$ ----------> products (5 8 2)

From the above observations it is apparent that the formation of $(\eta^5\text{-}C_5H_5)_2V_2(CO)_5$ in solution greatly complicates the number of possible photochemical pathways

Tentative assignments of the transient species were made based on the experimental results to date The first primary photoproduct observed is assigned to that of the $(\eta^5\text{-}C_5H_5)V(CO)_3(S)$ species The rate constant for the reaction of this species with carbon monoxide, $9\,2 \times 10^7$ dm^3 mol^{-1} s^{-1}, is very much faster than that measured for the reaction of substituted $(\eta^6\text{-arene})Cr(CO)_3$ with CO in cyclohexane, Table 5 8 1 The extreme reactivity of this species may perhaps explain the difficulties encountered with impurities in the system. Although extremely reactive, the second order rate constant for the reaction of this species with CO is not as fast as that recorded for the reaction of $Cr(CO)_5(S)$ with CO in perfluoromethylcyclohexane solvent[18], Table 5 8 1

Table 5.8.1 A comparison of the second order rate constants for the reaction of solvated carbonyl loss products with CO with that of the proposed $(\eta^5\text{-}C_5H_5)V(CO)_3(S)$ species [a]Reference 17 [b]Reference 18

Complex	Solvent	$k_{[CO]}$ dm^3 mol^{-1} s^{-1}
$(\eta^6$-benzene$)Cr(CO)_2(S)$	C_6H_6	$6.7 \times 10^6 \pm 0.6 \times 10^6$
$(\eta^6$-1,3,5-mesitylene$)Cr(CO)_3$	C_6H_6	$1.3 \times 10^7 \pm 0.7 \times 10^5$
$(\eta^6\text{-}C_6Et_6(\eta^6\text{-}Cr(CO)_2(S)$[a]	C_6H_6	$4.4 \times 10^7 \pm 5.0 \times 10^6$
$(\eta^5\text{-}C_5H_5)V(CO)_3(S)$ species	C_6H_6	$9.2 \times 10^7 \pm 1.0 \times 10^7$
$Cr(CO)_5(S)$[b]	C_7F_{14}	$3.0 \times 10^9 \pm 3.0 \times 10^8$

The secondary photoproduct formed by reaction of the above primary photoproduct is most plausibly assigned as the dinuclear complex $(\eta^5\text{-}C_5H_5)_2V_2(CO)_5$ Although Lewis and Caulton[20] have shown that formation of $(\eta^5\text{-}C_5H_5)_2V_2(CO)_5$ from $(\eta^5\text{-}C_5H_5)V(CO)_4$ in donor solvents requires two distinct photochemical steps, dimer formation may be accelerated in the absence of donor solvent to stabilise the photoreactive carbonyl loss product and the overall reaction sequence may differ markedly

The build-up in solution of a decomposition product of green colour may be attributed to the formation of one of two species, $(\eta^5\text{-}C_5H_5)V(CO)_3(S)$ or $(\eta^5\text{-}C_5H_5)_2V_2(CO)_5$ It is unlikely that this photodegradation product arises from the former species A green species identified as $(\eta^5\text{-}C_5H_5)V(CO)_3(THF)$ was produced in experiments performed by Lewis and Caulton, however, the absorption spectrum

of $(\eta^5\text{-}C_5H_5)V(CO)_3$(cyclohexane) would be expected to be shifted relative to this by virtue of the non-donating capacity of cyclohexane $(\eta^5\text{-}C_5H_5)V(CO)_3$(THF) was shown to revert to $(\eta^5\text{-}C_5H_5)V(CO)_4$ on addition of CO to the reaction cell, as all experiments described here were performed under CO atmosphere it is unlikely that a build-up of $(\eta^5\text{-}C_5H_5)V(CO)_3$(cyclohexane) would occur in solution. $(\eta^5\text{-}C_5H_5)_2V_2(CO)_5$ produces an emerald green solution and is the species most likely to be responsible for the colour change observed. This species is long-lived in solution, under N_2 atmosphere decomposition of $(\eta^5\text{-}C_5H_5)_2V_2(CO)_5$ in hexane began to be detectable within 10 minutes[20] Regrettably, an unequivocable assignment of this species is impossible as there is no reported absorption spectra of this species in the literature for comparison purposes On production of this species the system is no longer photochemically reversible on the time-scale of the flash photolysis experiment, as evidenced by the UV/vis spectra recorded periodically throughout the experiment Photochemical decomposition of this dinuclear species with reformation of $(\eta^5\text{-}C_5H_5)V(CO)_4$ would interfere severely with the photochemical observations of interest The level of interference would increase with increased initial concentration of parent tetracarbonyl complex and increased photolysis of the sample solution The secondary photoproduct species and the long-lived decomposition product may then be attributed to the same species, i e. $(\eta^5\text{-}C_5H_5)_2V_2(CO)_5$

Rest *et al* assigned the species formed on long wavelength photolysis of $(\eta^5\text{-}C_5H_5)V(CO)_4$ in all matrices as the $(\eta^3\text{-}C_5H_5)V(CO)_4$ species [11] This species coordinated CO present in the matrix to fill the vacant coordination site on the complex Hence, both a decarbonylation and ring slipped product may react with CO

and UV/vis spectra may reveal little structural information The primary photoproduct observed with a second order rate constant for reaction with CO in the range 2.4 x 10^4 to 2.2 x 10^3 dm^3 mol^{-1} s^{-1} may be attributed to this hapticity change product. On altering the laser excitation wavelength to 266nm it may be possible to induce either the production of a hapticity change or carbonyl loss product or to vary the relative amounts of either species produced, hence the observation that the photochemistry differed on altering the laser irradiation wavelength from 355nm to 266nm No experiments were carried out by Rest *et al* at wavelengths shorter than 320nm so no experimental comparisons may be drawn

5.9 Conclusions

Very little can be deduced conclusively from this series of experiments. The irreproducibility of the experimental results does not permit the proposal of a reaction scheme The irreproducibility may be accounted for by the presence of solvent impurities and/or the formation of multiple primary photoproducts and dinuclear species The results appear to confirm the proposed wavelength dependancy in the photochemistry of $(\eta^5\text{-}C_5H_5)V(CO)_4$ proposed by Rest *et al* The photochemical reactions are irreversible on the time-scale of the laser flash photolysis experiments as the build-up of a species assigned to the dinuclear complex $(\eta^5\text{-}C_5H_5)_2V_2(CO)_5$ is noted in solution

5.10 References

1 S Gambarotta, A Chiese-Villa, and C Guastini, *Inorg Chem* ,1988, **27**, 99

2 D Sellman, *Angew Chem* , 1972, **84**, 549

3 M Wrighton, *Chem Rev* , 1974, **74**, 401

4 A N Nesmeyanov, *Adv Organomet Chem* , 1972, **10**, 56

5 R Tsumura and N Nagihara, *Bull Chem Soc Jpn* , 1965, **38**, 1901

6 R J Kinney, W D Jones, and R G Bergman, *J Am Chem Soc* , 1978, **100**, 7902

7 E O Fischer and R J J Schneider, *Angew Chem , Int Ed Engl* , 1967, **6**, 569

8 E O Fischer, E Louis, and R J J Schneider, *Angew Chem , Int Ed Engl* , 1968, **7**, 136

9 D Rehder, L Dahlenburg, and I Muller, *J Organomet Chem* , 1976, **122**, 53

10 I Muller and D Rehder, *J Organomet Chem* , 1977, **139**, 293

11 R B Hitam and A J Rest, *Organometallics,* 1989, **8,** 1589

12 O Crichton, A J Rest, and D J Taylor, *J Chem Soc , Dalton Trans* , 1980, 167

13. M T Haward, M W George, S M Howdle, and M Poliakoff, *J Chem Soc , Chem Commun* , 1990, 913

14 F -R Grevels, personal communication

15 B S Creaven, personal communication

16 G L Geoffroy and M S Wrighton, *Organometallic Photochemistry,* Academic Press London, 1979

17 B S Creaven, M W George, A G Ginsburg, C Hughes, J M Kelly, C. Long, I.M M^{c} Grath, and M T Pryce, accepted for publication in *Organometallics,* 1993

18. J M Kelly, C Long, and R Bonneau, *J Phys Chem* , 1983, **87**, 3344.

19 J D Simon and X Xie, *J Phys Chem* , 1986, **90**, 6751

20 L N Lewis and K G Caulton, *Inorg Chem* , 1980, **19**, 1840

21. F A Cotton, B A Frenz, and L Kruczynski, *J Am Chem Soc* , 1973, **95**, 951

Chapter 6

Experimental Section

6.1 Materials

The following materials were used without further purification, (benzene)$Cr(CO)_3$, $Cr(CO)_6$ and $W(CO)_6$ (Strem Chemicals); C_6Me_6 (Aldrich Chemical Co), argon (air products Ltd), carbon monoxide (Irish Industrial Gasses Ltd., technical grade, B O C CP grade), cyclohexane and pentane (Aldrich Chemical Co , spectroscopic grade), p-xylene (Riedel de Haen), acetonitrile (Lab-Scan Analytical Ltd , HPLC grade), n-heptane (Aldrich Chemical Co , HPLC grade). $Mn(CO)_4$-η^3-C_3H_4-C_6H_5-$Cr(CO)_3$ and $Mn(CO)_4$-η^3-C_3H_4-C_6H_5 were obtained from Dr Anthony Wright, University of Nottingham, and used as received.

Toluene (Aldrich Chemical Co , analar grade) was boiled over $LiAlH_4$ for 3 hours, distilled and stored over sodium wire Mesitylene (Aldrich, gold label) was dried over sodium wire

6.2 Equipment

UV/vis spectra and absorbance readings were obtained on a Hewlett-Packard 8425a diode-array spectrometer using quartz cells of pathlength 1 0cm Peak positions are accurate to ± 2nm IR spectra were recorded on a Perkin Elmer 983G grating spectrometer Peak positions are accurate to ± $3cm^{-1}$ All infrared spectra were recorded in pentane unless otherwise stated Microanalyses were performed by University College Dublin Microanalysis Laboratory Preparative photolyses were performed using an Applied Photophysics 400W medium pressure mercury vapour lamp

6.3 Photolysis Apparatus

Preparative photolysis was carried out in a photoreactor as in Figure 6 3 1. An Applied Photophysics 400W medium pressure mercury vapour lamp was used as the irradiation source The lamp was housed in a double-walled quartz jacket through which water was circulated to cool the lamp and prevent heating of the photolysis solution The external vessel contained the solution to be irradiated The photolysis solution was 'purged' with argon for 15 minutes prior to photolysis to remove air from the solution Carbon monoxide liberated during the photolysis was removed by bubbling argon through the solution

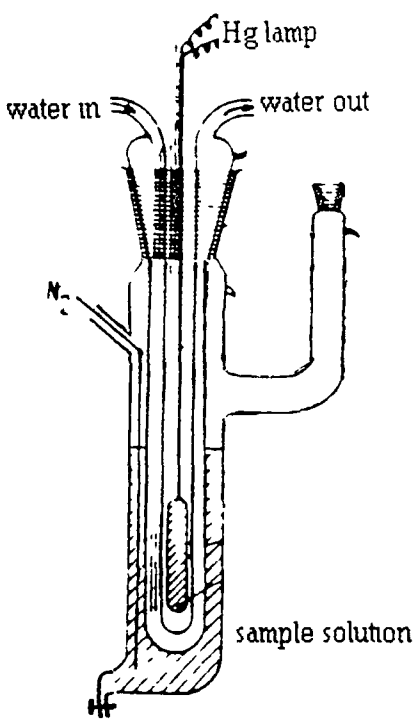

Figure 6.3.1 Photolysis apparatus used in the synthesis of substituted metal carbonyl complexes

6.4 Syntheses of (η^6-arene)$Cr(CO)_3$ Complexes

The (η^6-arene)$Cr(CO)_3$ complexes were prepared according to literature procedures[1] All manipulations were carried out under argon

6.4.1 Synthesis of (η^6-toluene)$Cr(CO)_3$

0 5g of $Cr(CO)_6$ was added to 100ml of degassed toluene in a round-bottomed flask and heated to reflux temperature for 94 hours On cooling, the excess toluene was removed under reduced pressure The impure (η^6-toluene)$Cr(CO)_3$ was recrystallised from petroleum spirit 60/80 at -20°C The purified material was air-stable in the crystalline form Compound purity was verified as satisfactory by microanalysis and infrared spectroscopy, calculated % (experimental %), C 52 64 (52 08) , H 3 53 (3 54) IR ν_{CO} in pentane, 1980(s), 1913(s) cm^{-1}

6.4.2 Synthesis of (η^6-p-xylene)$Cr(CO)_3$

0 5g of $Cr(CO)_6$ was added to 100ml of degassed p-xylene in a round-bottomed flask and heated to reflux temperature for 90 hours On cooling the excess p-xylene was removed under reduced pressure and the product crystallised out of solution The impure (η^6-p-xylene)$Cr(CO)_3$ was recrystallised from diethylether at -20°C The purified material was air-stable in the crystalline form Compound purity was verified as satisfactory by microanalysis and infrared spectroscopy, calculated % (experimental %), C 54 55 (54 05), H 4 16 (4 31) IR ν_{CO} in pentane, 1978(s), 1909(s) cm^{-1}

6.4.3 Synthesis of (η^6-1,3,5-mesitylene)$Cr(CO)_3$

0 2g of $Cr(CO)_6$ was added to 20ml of degassed dry mesitylene in a round-bottomed flask and heated to reflux temperature for 24 hours Some (η^6-1,3,5-

mesitylene)$Cr(CO)_3$ had sublimed at an outlet of the flask during this period, the yellow crystalline product was collected and did not require further purification The isolated material was air-stable in the crystalline form Compound purity was verified as satisfactory by microanalysis and infrared spectroscopy, calculated % (experimental %), C 56 25 (56 26), H 4 72 (4 56) IR ν_{CO} in pentane; 1972(s), 1904(s) cm^{-1}

6.4.4 Synthesis of (η^6-C_6Me_6)$Cr(CO)_3$

0 5g of $Cr(CO)_6$ was photolysed in 100ml of degassed acetonitrile for 22 hours. This solution was transferred to a round-bottomed flask and heated to reflux temperature for 52 hours On cooling, 0 5g of C_6Me_6 was added and the solution heated to reflux temperature foi a further 21 hours Excess solvent was removed under reduced pressure The impure (η^6-C_6Me_6)$Cr(CO)_3$ was recrystallised from diethylether at -20°C The purified material was air-stable in the crystalline form. Compound purity was verified as satisfactory by microanalysis and infrared spectroscopy, calculated % (experimental %), C 60 40 (60 88), H 6 08 (6.20) IR ν_{CO} in pentane, 1970(s), 1885(s) cm^{-1}

6.5 Sample Preparation

6.5.1 Laser Flash Photolysis with UV/vis Monitoring

Samples for flash photolysis were prepared in a fluorescence cuvette (d=10mm) attached to a degassing bulb The absorbance of the sample at the laser excitation wavelength was between 0 3 and 2 0 A U , the concentration of the carbonyl compound could then be calculated, by means of the Beer-Lambert Law, once the molar extinction coefficient of the compound at the laser wavelength was

known The sample solution was degassed by a minimum of three cycles of a freeze-pump-thaw procedure, to 10^{-3} Torr, followed by a substantial 'liquid-pumping' stage (if stated) to remove traces of water and carbon dioxide introduced in the degassing procedure A known pressure of either argon or carbon monoxide was then admitted to the solution cell to a pressure of 1 0 atmosphere The UV/vis absorption spectrum of the sample solution was monitored at regular intervals throughout each experiment. These spectra typically showed minimal variations and thus minimal decomposition of the sample solution (even in cases where a 'stable' product was observed over the time-domain of the flash photolysis experiment) indicating a satisfactory thermal reversibility of the photochemical processes

In the experiments to measure activation parameters the sample cell was immersed in a thermostated water bath and the temperature increased incrementally from approximately 281K to 313K in 3-5K intervals I_0 was measured at the monitoring wavelength and the system readied for analysis prior to the sample being heated so that transient data could be recorded immediately on removing the sample from the water bath At every analysis temperature, the sample solution was allowed to equilibrate for ten minutes The temperature range used was limited by the freezing point of the solvent (279K for cyclohexane) and the solubility of carbon monoxide in cyclohexane which could be expected to alter significantly as the temperature was raised greater than approximately 313K

6.5.2 Laser flash photolysis with TRIR detection

A quantity of carbonyl complex was weighed out, placed in the degassing vessel and 100ml of solvent added such that the final concentration of the solution was approximately 1 x 10^{-3} mol dm^{-3} The solution was degassed by continuous pumping on the solution under vacuum, it is estimated that, at most, 1-2mls of solvent is removed by this procedure and this does not greatly alter the concentration of the sample After degassing, argon or carbon monoxide, to a pressure of 2 0 atmospheres, was added to the cell

6.6 Laser Flash Photolysis System

A schematic diagram of the laser flash photolysis instrumentation in Dublin City University is given in Figure 6 6 1 The excitation source is a Q-switched Nd-YAG (neodinium doped yttrium aluminium garnet) laser (Spectron Laser Systems) with a fundamental wavelength output at 1064nm which can be doubled, tripled or quatrupled to generate a second, third or fourth harmonic wavelength at 532, 355 or 266nm respectively The power of the laser pulse can be varied by applying different voltages across the amplifier flash tube, typically the setting was maintained at 790V The maximum power output was 35mJ at 355nm and 45 mJ at 266nm excitation The pulse duration was 8-11ns

The monitoring light source was an air-cooled 275 watt Applied Photophysics xenon arc lamp, the monitoring and excitation beams were arranged in a cross-beam configuration The laser pulse was directed onto the sample cuvette *via* twin Pellin-Broca prisms A power meter, placed between the second prism and the sample, was used to trigger the oscilloscope At monitoring wavelengths greater than 350nm a UV

filter ($\lambda > 400$nm or $\lambda > 345$nm) was placed between the xenon arc source and the sample to minimise photolysis of the sample by the monitoring beam The beam passed through the sample and was focussed *via* a circular quartz lens onto the entrance slit of an Applied Photophysics f/3 4 monochromator containing a grating blazed at 300nm The light detector was a Hamamatzu 5-stage photomultiplier supplied by Applied Photophysics, which was operated at 850V The signals were captured either by a Phyllips PM 3311 storage oscilloscope, or a Hewlett-Packard 54510A digitising oscilloscope and the data reduction was performed on a 286/287 based computer system using software developed in-house Transient data were stored on disk for analysis, most measurements were the result of averaging 3-6 transient signals, in order to improve the signal-to-noise ratio

A laser flash photolysis experiment centres on the measurement of absorbance changes, a transient species is produced by the flash whose absorbance is recorded as a function of time As

$$Abs = I_0/I_t \qquad (6\ 6.1)$$

the amount of monitoring light being transmitted through the solution before the laser flash, i e I_0, is recorded initially This value is obtained by recording the voltage corresponding to the amount of light detected by the photomultiplier tube when the monitoring source shutter is open, less the voltage generated by stray light; this voltage is directly proportional to the I_0 value Transient kinetic data are obtained by opening the monitoring source shutter and firing the laser As the laser beam passes through the power meter it triggers the oscilloscope, the pulse then passes through the sample cuvette, producing a transient species The region of the cuvette through

which the excitation beam passes is traversed by the monitoring beam The change in voltage signal with time is detected by the photomultiplier tube at the particular monitoring wavelength and recorded by the oscilloscope The amount of light being transmitted at any time t (I_t) can be calculated from this information, and, as I_0 has been previously recorded, the values are readily converted to change in absorbance with time The transient signal recorded on the oscilloscope is stored on computer for future analysis, along with the timebase and voltage settings of the oscilloscope. Typical traces are given in Figure 6 6 2 By recording transient signals sequentially over a range of wavelengths, absorbance readings can be calculated at any time after the flash to generate a difference absorption spectrum of the transient species The term 'difference' implies that all absorbance readings are relative to the absorbance of parent material at a particular wavelength, hence the oscilloscope is set at a delay to enable the absorbance before the laser pulse to be determined

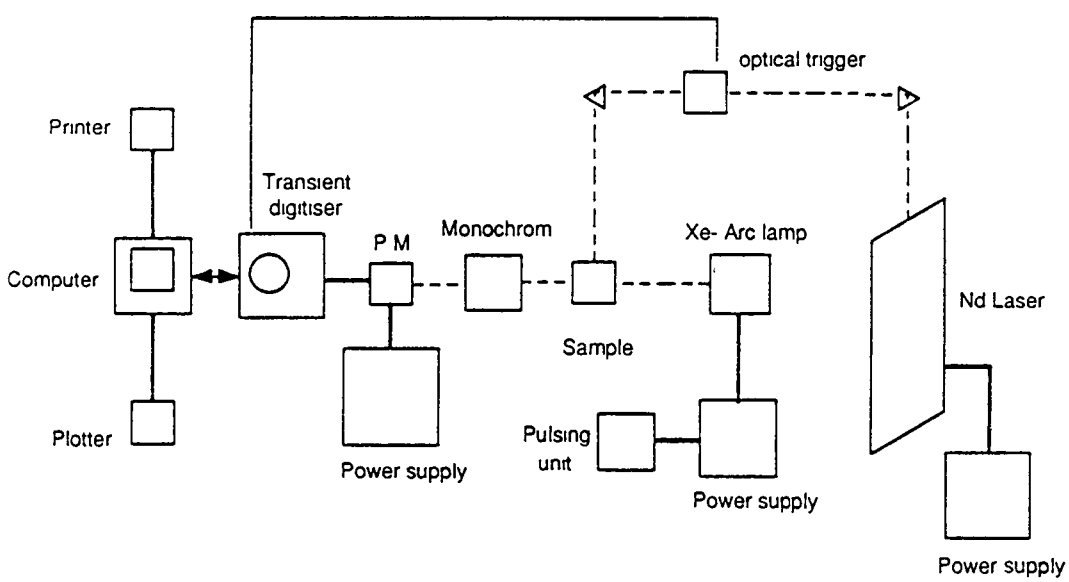

Figure 6.6.1 Schematic diagram of the laser flash photolysis instrumentation at Dublin City University

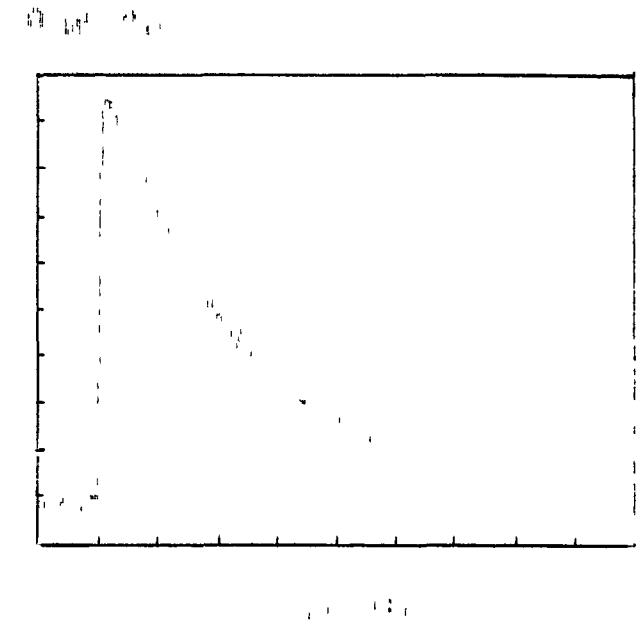

(a)

10 mV/Div

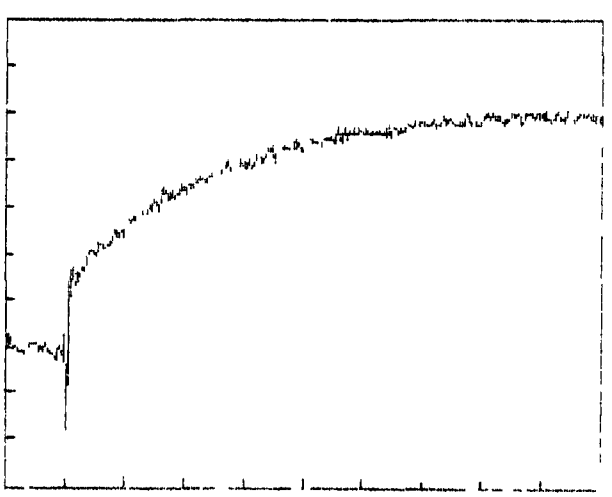

(b)

20 us/Div

Figure 6.6.2 Typical traces recorded by the oscilloscope corresponding to (a) the decay of a transient species and (b) the grow-in of a second transient species

6.7 TRIR Experimental System

A schematic diagram of the TRIR apparatus in Nottingham University, England is given in Figure 6 7 1[2] The excitation source is a Lumonics Hyperex-440 excimer laser operating on XeCl, 308nm output wavelength, 8-12ns pulse duration, 100mJ per pulse A flow-through cell is used, a conventional IR solution cell (CaF_2 windows, 1-4mm PTFE spacers) modified with short lengths of stainless-steel tubing This cell is connected to a vacuum pump and to the solution flow system made of glass and PTFE with manually operated greaseless taps The solution is changed between shots rather than flowing continuously The design of the IR cell means that the UV laser excitation beam and IR probe beam must necessarily be almost colinear The monitoring beam is a CO laser (Edinburgh Instruments PL3) cooled with isopentane and liquid nitrogen, line-tunable in $4cm^{-1}$ steps from 2020-1700 cm^{-1} A polished uncoated germanium beam-splitter is used to deflect part of the IR beam onto an IR spectiometer for wavenumber calibration (Perkin-Elmer 283B, single beam mode, accuracy $\pm$ 0 $5cm^{-1}$) A photoconductive HgCdTe detector (Infrared Associates Inc , HCT-100, area $1mm^2$, liquid nitrogen cooled) is used coupled to a home-built pre-amplifier (x68 amplification, rise-time <1μs). The IR laser beam is attenuated with an iris diaphragm which can be adjusted to compensate for solvent absorption Typical I_0 values are in the range 2 to 5V The kinetic traces were recorded using a transient digitiser triggered by the excimer laser pulse The data was transferred to a BBC microcomputer and stored on floppy disk, together with the wavenumber of the laser line and the I_0 value. With data points every $4cm^{-1}$

the resulting spectra have *ca* 8cm^{-1} resolution. All of the traces were recorded 'single-shot', i e with no signal averaging

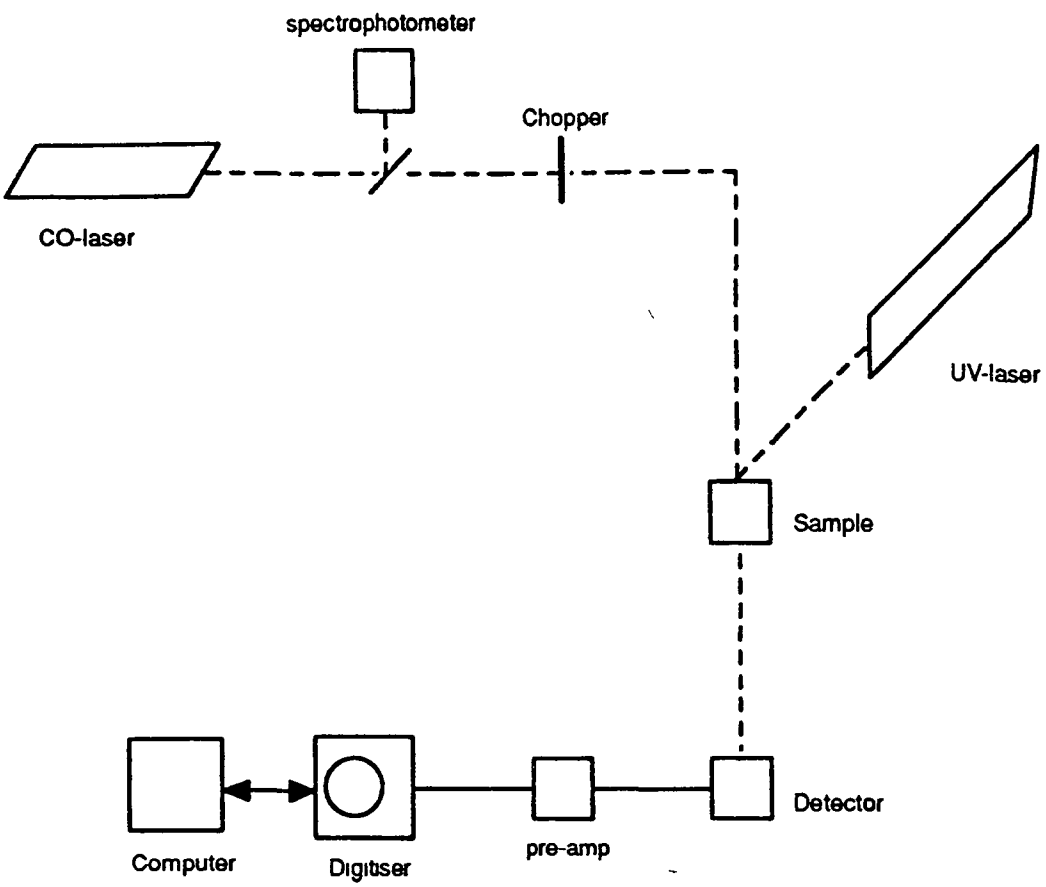

Figure 6.7.1 Schematic diagram of the time-resolved IR apparatus at Nottingham University, England

6.8 Transient deconvolution

A transient decay exhibiting characteristics of two first order decay processes is essentially a linear combination of two exponential decays The general equation for a double exponential-fit model is given in equation 6 8 1

$$Y = Ae^{\alpha x} + Be^{\beta x} \qquad (6\ 8.1)$$

The transient can be resolved into its individual components by fitting a double exponential curve function (equation 6 8 2) to the transient profile

$$Y = A_1e^{-k_1t} + A_2e^{-k_2t} \qquad (6\ 8\ 2)$$

The A_1 and A_2 terms in equation 6 8 2 are constants, k_1 and k_2 refer to the decay constants for the two components of the decay profile, t refers to time and Y to the value on the resultant decay curve This equation is similar to that for a single exponential decay, equation 6 8 3, the inverse log of this equation can be used to obtain a linear plot of lnY against time (t) to yield a slope of -k and an intercept of lnA

$$Y = Ae^{-kt} \qquad (6\ 8.3)$$

$$\ln Y = \ln A - kt \qquad (6\ 8\ 4)$$

6.9 Activation Parameter Determinations

The activation parameters were calculated from the Arrhenius and Eyring equations[3] The Arrhenius equation is given by

$$k_{obs} = A \exp(-E_a/RT) \qquad (6\ 9\ 1)$$

where A is called the frequency factor and E_a is the activation energy of the reaction in J mol^{-1} The Arrhenius equation is a good approximate representation of the

temperature dependance of k, a plot of ln k_{obs} versus 1/T should give a straight line of intercept lnA and slope $-E_a/R$,

$$\ln k_{obs} = \ln A - E_a/RT \qquad (6\ 9.2)$$

From transition-state theory expressed in thermodynamic terms the Eyring equation is obtained,

$$k_{obs} = kT/h \exp(-\Delta G /RT) \qquad (6\ 9\ 3)$$

where k is the Boltzmann constant and h is the Planck constant Since $\Delta G^{\neq} = \Delta H^{\neq} - T\Delta S^{\neq}$ this equation can be written as,

$$k_{obs} = kT/h \ (\exp \Delta S /R \ \exp -\Delta H /RT) \qquad (6\ 9\ 4)$$

The quantities $\Delta G^{\neq}$, $\Delta H^{\neq}$ and $\Delta S^{\neq}$ are called the Gibbs free energy of activation, the enthalpy of activation and the entropy of activation It follows from (6 9.4) that;

$$\ln k_{obs}/T = \ln k/h + \Delta S^{\neq}/R + (-\Delta H^{\neq}/RT) \qquad (5\ 9\ 5)$$

The values of $\Delta S^{\neq}$ and $\Delta H^{\neq}$ can be obtained from a plot of $\ln(k_{obs}/T)$ against 1/T, which should yield a straight line of slope $-\Delta H^{\neq}/R$ and intercept $\ln k/h + \Delta S^{\neq}/R$

6.10 Calculation of [CO] in Cyclohexane and n-Pentane

The concentration of CO in solution was determined by the pressure of CO admitted to the reaction cell after the degassing procedure Throughout this thesis the concentration of CO in cyclohexane solution was taken to be $1\ 2 \times 10^{-2}$ mol dm^{-3} under 1 0 atmosphere of CO at 298K[4], although literature brought to light towards the end of the manuscripts preparation revealed a value of $0\ 93 \times 10^{-2}$ mol dm^{-3} to be a more correct value[5] The concentration of CO in n-pentane solution under 1 0 atmosphere of CO at 298K was calculated from both mole fraction and Ostwald coefficient data[4,6] These sample calculations are given below The results obtained

using both methods of calculation are in close agreement It is assumed that the solubility of CO in cyclohexane remains constant over the temperature range used for activation parameter determinations, typically 280 to 320K Although data on the variation of [CO] with temperature are scarce it appears that this assumption is valid for cyclohexane[7]

6 10 1 Calculation of the [CO] in n-Pentane From Mole Fraction Data:

Solubility of CO in pentane at 298K expressed in mole fraction = $18\ 7 \times 10^{-4}$ moles^{-1}

1 litre of pentane = 626g

1 mole of pentane = 72 15g

=> 8 68 moles/litre

$$\frac{\#\text{ moles of CO}}{\#\text{ of moles of CO} + \#\text{ of moles of pentane}} = \text{Mole Fraction} = 18\ 7 \times 10^{-4}\ \text{moles}^{-1}$$

$$\#\text{ moles of CO} = x = (18\ 7 \times 10^{-4})x + (18\ 7 \times 10^{-4})(8\ 68)$$

$$= (18\ 7 \times 10^{-4})x + 1\ 62 \times 10^{-2}$$

$$\Rightarrow [x - (18\ 7 \times 10^{-4})x] = 1\ 62 \times 10^{-2}$$

$$\Rightarrow x(1 - 18\ 7 \times 10^{-4}) = 1\ 62 \times 10^{-2}$$

$$\Rightarrow x = 1\ 63 \times 10^{-2}$$ moles of CO/Litre of pentane at 1atms

6 10 2 Calculation of the [CO] in n-Pentane From the Ostwald coefficient:

$$\frac{22.4 \times 298}{273} = 24.4$$ = Molar Volume of a gas at 298K

Ostwald coefficient for pentane (C_5) = 0 395 ml CO / ml cyclohexane / atms

=> 0 395/24 4 = 1 62 x 10^{-2} moles of CO/Litre of pentane at 1atms

6.11 Experimental Errors

Simple linear regression analysis was used for all activation parameter plots and plots of rate dependance on parent or CO concentration Correlation coefficients are quoted only for plots consisting of four or more points The quoted error values are from this analysis, reflecting the statistical error in the calculation of the slope or intercept. Intrinsic experimental errors not taken into consideration in this value include the ± 0 5K variation in all temperature readings Individual rate constant readings are accurate to ± one standard deviation Variations in rate constant values may be attributed to alterations in base-line positioning and temperature A thermostatted sample holder was introduced after this work was completed in order to eliminate any variations in reaction rates caused by daily and seasonal temperature variations

6.12 References

1 B. Nicholls and M C Whiting, *J Chem Soc* , 1959, 551.

2. A J Dixon, M.A Healy, P M Hodges, B D Moore, M. Poliakoff, M.B. Simpson, J J Turner, and M A West, *J Chem Soc , Faraday Trans* , 1986, **82**, 2083

3 (a) Avery, *Basic Reaction Kinetics and Mechanisms,* Macmillan Education Ltd , London, 1986

(b) W J Moore, *Physical Chemistry*, Longman, New York, 1978

4. J.M. Kelly, C Long, and R Bonneau, *J Phys Chem* , 1983, **87**, 3344

5 (a) L Patyi, I E Furmer, J Makranczy, A S Sadilenko, Z G Stepanova, and M G Berengarten, *Zh Prikl Khim* , 1978, **51**, 1296

(b) E Wilhelm and R Battino, *J Chem Thermodyn* , 1973, **5**, 117

6. J Makranczy, K Megyery-Balog, L Rusz, and L Patyi, *Hung J Ind Chem* , 1976, **4**, 269

7. P.G T Fog and W Gerrard, *Solubility of Gases in Liquids,* Wiley, Chichester, 1990

Future Work

A number of experiments may be proposed to provide further information on the transient species described in this thesis TRIR studies are the ideal method of study of these photoreactions Photoproducts exhibiting suitably long lifetimes at ambient temperatures may be studied at cryogenic temperatures utilising a variable temperature IR cell (VTIR) The effect of different solvents should be further investigated as some reactive intermediates may appear non-solvated in cyclohexane but solvated in a different alkane solution

With respect to the photochemistry of (η^6-arene)$Cr(CO)_3$ complexes, a TRIR study of the (η^6-C_6Me_6)$Cr(CO)_3$ system would be extremely useful in clarifying the secondary photochemical products A spectrum of a (η^6-benzene)$Cr(CO)_2(H_2O)$ complex, recorded over a restricted ν_{CO} range, should be repeated over the entire carbonyl range for completion purposes

There are a number of possible experiments that may be conducted on the $Mn(CO)_4$-η^3-C_3H_4-C_6H_5 system A UV/vis difference spectrum of the first observed photoproduct should be recorded for comparison with the literature spectrum of $Mn(CO)_4$-η^1-C_3H_4-C_6H_5 This would conclusively implicate or eliminate this species as a primary photoproduct in the photochemical reactions. The rate of reaction of the first species with CO might be measured, although the lifetime of this species is very short and approaching the limit of resolution of the instrumentation Activation parameters might be determined for the decay of the second species to provide further information on the nature of the transition states in these photochemical reactions

The photoproducts produced on excitation of the hetero-bimetallic complex $Mn(CO)_4$-η^3-C_3H_4-η^6-C_6H_5-$Cr(CO)_3$ may be characterised using TRIR studies with isotopic labelling It may then be possible to conclusively assign the Cr or Mn metal centre as the source of the photoejected CO Future research projects might include the full characterisation of the nature of the third observed species in this system A study of a $Mn(CO)_4$-η^3-C_3H_5 complex may prove informative; in this case the formation of an acyclic pentadienyl group by means of an η^3 to η^5 rearrangement is impossible

It would be useful to obtain an IR spectrum of the decomposition product observed in the photochemistry of $(\eta^5$-$C_5H_5)V(CO)_4$ The absorption bands could then be compared to those of the dinuclear complex $(\eta^5$-$C_5H_5)_2V_2(CO)_5$ Alternatively, the dinuclear complex $(\eta^5$-$C_5H_5)_2V_2(CO)_5$ may be synthesised and its electronic spectrum recorded for comparison with that of the decomposition product No absorption spectrum of $(\eta^5$-$C_5H_5)_2V_2(CO)_5$ could be found in the literature.